About the Journal

Overview

Pertanika Journal of Science & Technology (JST) is the official journal of Universit Putra Malaysia published by UPM Press. It is an open-access online scientific journal which is free of charge. It publishes the scientific outputs. It neither accepts nor commissions third party content.

Recognized internationally as the leading peer-reviewed interdisciplinary journal devoted to the publication of original papers, it serves as a forum for practical approaches to improving quality in issues pertaining to science and engineering and its related fields.

JST is a **quarterly** (January, April, July and October) periodical that considers for publication original articles as per its scope. The journal publishes in **English** and it is open to authors around the world regardless of the nationality.

The Journal is available world-wide.

Aims and scope

Pertanika Journal of Science and Technology aims to provide a forum for high quality research related to science and engineering research. Areas relevant to the scope of the journal include: bioinformatics, bioscience, biotechnology and bio-molecular sciences, chemistry, computer science, ecology, engineering, engineering design, environmental control and management, mathematics and statistics, medicine and health sciences, nanotechnology, physics, safety and emergency management, and related fields of study.

History

Pertanika was founded in 1978. A decision was made in 1992 to streamline Pertanika into three journals as Journal of Tropical Agricultural Science, Journal of Science & Technology, and Journal of Social Sciences & Humanities to meet the need for specialised journals in areas of study aligned with the interdisciplinary strengths of the university.

After almost 25 years, as an interdisciplinary Journal of Science & Technology, the revamped journal now focuses on research in science and engineering and its related fields.

Goal of *Pertanika*

Our goal is to bring the highest quality research to the widest possible audience.

Quality

We aim for excellence, sustained by a responsible and professional approach to journal publishing. Submissions are guaranteed to receive a decision within 14 weeks. The elapsed time from submission to publication for the articles averages 5-6 months.

Abstracting and indexing of *Pertanika*

Pertanika is almost **40 years old**; this accumulated knowledge has resulted in Pertanika JST being abstracted and indexed in **SCOPUS** (Elsevier), Clarivate Analytics [*formerly known as Thomson (ISI)*] **Web of Science™ Core Collection** Emerging Sources Citation Index (ESCI). Web of Knowledge [BIOSIS & CAB Abstracts], **EBSCO** and EBSCOhost, **DOAJ**, **ERA**, **Google Scholar**, **TIB**, **MyCite**, Islamic World Science Citation Center (ISC), ASEAN Citation Index (ACI), **Cabell's Directories** & Journal Guide.

Future vision

We are continuously improving access to our journal archives, content, and research services. We have the drive to realise exciting new horizons that will benefit not only the academic community, but society itself.

Citing journal articles

The abbreviation for Pertanika Journal of Science & Technology is *Pertanika J. Sci. Technol.*

Publication policy

Pertanika policy prohibits an author from submitting the same manuscript for concurrent consideration by two or more publications. It prohibits as well publication of any manuscript that has already been published either in whole or substantial part elsewhere. It also does not permit publication of manuscript that has been published in full in Proceedings.

Code of Ethics

The Pertanika Journals and Universiti Putra Malaysia takes seriously the responsibility of all of its journal publications to reflect the highest in publication ethics. Thus all journals and journal editors are expected to abide by the Journal's codes of ethics. Refer to Pertanika's **Code of Ethics** for full details, or visit the Journal's web link at <u>http://www.pertanika.upm.edu.my/code_of_ethics.php</u>

International Standard Serial Number (ISSN)

An ISSN is an 8-digit code used to identify periodicals such as journals of all kinds and on all media–print and electronic. All Pertanika journals have ISSN as well as an e-ISSN.

Journal of Science & Technology: ISSN 0128-7680 (*Print*); ISSN 2231-8526 (*Online*).

Lag time

A decision on acceptance or rejection of a manuscript is reached in 3 to 4 months (average 14 weeks). The elapsed time from submission to publication for the articles averages 5-6 months.

Authorship

Authors are not permitted to add or remove any names from the authorship provided at the time of initial submission without the consent of the Journal's Chief Executive Editor.

Manuscript preparation

Refer to Pertanika's **Instructions to Authors** at the back of this journal.

Most scientific papers are prepared according to a format called IMRAD. The term represents the first letters of the words Introduction, Materials and Methods, Results, And, Discussion. IMRAD is simply a more 'defined' version of the "IBC" [Introduction, Body, Conclusion] format used for all academic writing. IMRAD indicates a pattern or format rather than a complete list of headings or components of research papers; the missing parts of a paper are: *Title, Authors, Keywords, Abstract, Conclusions*, and *References.* Additionally, some papers include Acknowledgments and Appendices.

The *Introduction* explains the scope and objective of the study in the light of current knowledge on the subject; the *Materials and Methods* describes how the study was conducted; the *Results* section reports what was found in the study; and the *Discussion* section explains meaning and significance of the results and provides suggestions for future directions of research. The manuscript must be prepared according to the Journal's **Instructions to Authors**.

Editorial process

Authors are notified with an acknowledgement containing a *Manuscript ID* on receipt of a manuscript, and upon the editorial decision regarding publication.

Pertanika follows a **double-blind peer-review** process. Manuscripts deemed suitable for publication are usually sent to reviewers. Authors are encouraged to suggest names of at least three potential reviewers at the time of submission of their manuscript to Pertanika, but the editors will make the final choice. The editors are not, however, bound by these suggestions.

Notification of the editorial decision is usually provided within ten to fourteen weeks from the receipt of manuscript. Publication of solicited manuscripts is not guaranteed. In most cases, manuscripts are accepted conditionally, pending an author's revision of the material.

As articles are double-blind reviewed, material that might identify authorship of the paper should be placed only on page 2 as described in the first-4 page format in Pertanika's **Instructions to Authors** given at the back of this journal.

The Journal's peer-review

In the peer-review process, three referees independently evaluate the scientific quality of the submitted manuscripts.

Peer reviewers are experts chosen by journal editors to provide written assessment of the **strengths** and **weaknesses** of written research, with the aim of improving the reporting of research and identifying the most appropriate and highest quality material for the journal.

Operating and review process

What happens to a manuscript once it is submitted to *Pertanika*? Typically, there are seven steps to the editorial review process:

1. The Journal's chief executive editor and the editorial board examine the paper to determine whether it is appropriate for the journal and should be reviewed. If not appropriate, the manuscript is rejected outright and the author is informed.

2. The chief executive editor sends the article-identifying information having been removed, to three reviewers. Typically, one of these is from the Journal's editorial board. Others are specialists in the subject matter represented by the article. The chief executive editor asks them to complete the review in three weeks.

   Comments to authors are about the appropriateness and adequacy of the theoretical or conceptual framework, literature review, method, results and discussion, and conclusions. Reviewers often include suggestions for strengthening of the manuscript. Comments to the editor are in the nature of the significance of the work and its potential contribution to the literature.

3. The chief executive editor, in consultation with the editor-in-chief, examines the reviews and decides whether to reject the manuscript, invite the author(s) to revise and resubmit the manuscript, or seek additional reviews. Final acceptance or rejection rests with the Edito-in-Chief, who reserves the right to refuse any material for publication. In rare instances, the manuscript is accepted with almost no revision. Almost without exception, reviewers' comments (to the author) are forwarded to the author. If a revision is indicated, the editor provides guidelines for attending to the reviewers' suggestions and perhaps additional advice about revising the manuscript.

4. The authors decide whether and how to address the reviewers' comments and criticisms and the editor's concerns. The authors return a revised version of the paper to the chief executive editor along with specific information describing how they have answered' the concerns of the reviewers and the editor, usually in a tabular form. The author(s) may also submit a rebuttal if there is a need especially when the author disagrees with certain comments provided by reviewer(s).

5. The chief executive editor sends the revised paper out for re-review. Typically, at least one of the original reviewers will be asked to examine the article.

6. When the reviewers have completed their work, the chief executive editor in consultation with the editorial board and the editor-in-chief examine their comments and decide whether the paper is ready to be published, needs another round of revisions, or should be rejected.

7. If the decision is to accept, an acceptance letter is sent to all the author(s), the paper is sent to the Press. The article should appear in print in approximately three months.

The Publisher ensures that the paper adheres to the correct style (in-text citations, the reference list, and tables are typical areas of concern, clarity, and grammar). The authors are asked to respond to any minor queries by the Publisher. Following these corrections, page proofs are mailed to the corresponding authors for their final approval. At this point, **only essential changes are accepted**. Finally, the article appears in the pages of the Journal and is posted on-line.

Pertanika Journal of

SCIENCE & TECHNOLOGY

A special issue devoted to
Advances in Science & Technology Research

Vol. 25 (S) Aug. 2017
(Special Edition)

ABSTRACTING/INDEXING

Pertanika is now over 40 years old; this accumulated knowledge has resulted the journals being indexed in abstracted in SCOPUS (Elsevier), Web of Science Core Collection (formerly ISI) [ESCI, BIOSIS & CAB Abstracts], EBSCO & EBSCOhost, ERA, DOAJ, AGRICOLA (National Agric. Library, USA), Cabell's Directories, Google Scholar, MyAIS, Islamic World Science Citation Center (ISC), ASEAN Citation Index (ACI) & Rubriq (Journal Guide).

Preface

We are very pleased to present this special issue, Volume 4, of the Pertanika Journal of Science and Technology (JST) which is a compilat on of selected papers that were presented at the 3rd Internat onal Conference on Science and Social Research (CSSR 2016). The CSSR 2016 was held from 6th-7th December 2016 in Putrajaya, Malaysia. The theme of the conference was "Waves of Interdisciplinary Research". The conference covered mult -disciplinary research areas, ranging from science and technology to social science and humanit es. The conference track was divided into three major areas: Track 1 - Engineering, Science & Technology; Track 2 - Clinical & Health Sciences and Track 3 - Arts, Humanit es & Social Sciences. All full papers submit ed to CSSR 2016 were subjected to a rigorous peer reviewing process to ensure quality and consistency of content before they were accepted for presentat on.

A total of 188 full papers in Track 1 (Engineering, Science & Technology) and Track 2 (Clinical & Health Sciences) were presented at the two-day conference, 19 of which were accepted for publicat on in this special issue, Volume 4. The theme of the special issue is "Advances in Science and Technology Research". In line with this theme, the research areas of full papers, which are included in this issue cover Mechanical and Industrial Engineering, Public Health, Environmental and Occupat onal Health and Safety, Manufacturing and Process Technologies, Coordinat on Chemistry, Biotechnology, Medical Biochemistry and Clinical Chemistry, Pathology, Nutrit on, Metals and Metal Alloy Materials, Architecture and Urban Environment, Remote Sensing, Optometry, Electrical & Electronic Engineering and Physiology.

We would like to thank the contributors as well as the reviewers for their support and commitment which made the publicat on of this special issue Volume 4 JST-CSSR2016 possible. It is hoped that this publicat on would encourage researchers from around the world to be more act ve in publishing their research output, in part cular, good quality science and technology papers, which would be useful for academics and pract t oners alike. Special thanks to Dr. Nayan Kanwal, the Chief Execut ve Editor, UPM Journals, and journal division staf for their hard work and dedicat on in the publicat on process of this issue. This has certainly mot vated us to become more prolif c and to do bet er in future.

Guest Editors:
Aidah Jumahat *(Assoc. Prof. Dr.)*
Saiful Izwan Suliman *(Dr.)*
Sharifah Aminah Syed Mohamad *(Assoc. Prof. Dr.)*

August 2017

Pertanika Journal of Science & Technology
Vol. 25 (S) Aug. 2017

Contents

Advances in Science & Technology Research

SCIENCE & TECHNOLOGY

An Ethnographic Survey of Culinary Students' Behaviours in the Implementation of Food Safety and Hygiene Practices

Mohammad Halim Jeinie[1,2], Norazmir Md Nor[2]*, Mazni Saad[3] and Mohd Shazali Md. Sharif[4]

[1]*Faculty of Food Science and Nutrition, Universiti Malaysia Sabah (UMS), 88400 Kota Kinabalu, Sabah, Malaysia*
[2]*Faculty of Health Sciences, Universiti Teknologi MARA (UiTM), 42300 Puncak Alam, Selangor, Malaysia*
[3]*School of Hospitality and Creative Arts (SHCA), Management & Science University (MSU), 40100 Shah Alam, Selangor, Malaysia*
[4]*Faculty of Hotel & Tourism Management, Universiti Teknologi MARA (UiTM), 42300 Puncak Alam, Selangor, Malaysia*

ABSTRACT

Suff cient knowledge on food safety and diligence during food handling are crucial to food safety and hygiene practices. A casual approach to handling food in the kitchen on a regular basis may link to foodborne pathogens, contaminations, and adverse health effects. The purpose of this study is to identify the right practices and behaviour among culinary students in terms of food hygiene practices and food safety perspectives. The methodology employed includes observations on 18 food culinary students in an actual kitchen setting. Effective food hygiene and food safety implementation are needed to improve the effectiveness of health education programmes for food handlers. The results suggest that transmission reduction of food pathogens, knowledge transfer and food safety training in selective industry criteria with proper guidelines should be introduced to produce a competent workforce.

Keywords: Culinary, culinary students, food safety, hygiene practices

INTRODUCTION

Food hygiene and food safety (FHS) is an important aspect of public health. Foodborne illness is a major health concern that can severely impact society and can incur a huge f nancial burden on our health care system. People have become increasingly aware of the food they consume and are more cautious about food safety considerations. Diarrheal

diseases have been found to be responsible for more than half of the global burden of foodborne disease annually, causing 550 million people to fall ill and 230,000 to die (World Health Day, 2015). More than 250 foodborne diseases are caused by various pathogens (bacteria, viruses, and parasites) and toxins (industrial chemical and biotoxins) of which, the most deaths are caused by diarrheal diseases worldwide (Fleury, Stratton, Tinga, Charron, & Aramini, 2008; Linscott, 2011).

Foodborne issues have been highlighted to indicate that access to safe food practices is crucial for community health (Saad, Poh, & Adil, 2013). In the United States of America, Scallan et al. (2011) estimated that 31 pathogens cause 228,744 hospitalisations every year, of which about 24% or 55,961 cases are due to the consumption of contaminated food. Of these, 64% were caused by bacteria, 25% by parasites, and 12% by viruses. Estimates of the overall number of episodes of food-borne illness are helpful for allocating resources and prioritising interventions.

Lack of knowledge of food safety and due diligence during preparation, processing, and storage of food can be considered a violation of food safety (Abdul-Mutalib et al., 2012). From the Malaysian perspective, Abdullah Sani and Siow (2014) revealed inadequate knowledge on food hygiene, poor hygiene practice, and poor attitude in sanitation and food safety among food handlers. Bolton, Meally, Blair, McDowell and Cowan (2008) said that previous researchers had emphasised effectiveness and that compulsory food safety training on a regular and ongoing basis should be conducted to eliminate possible misleading regards of food safety issues.

In relation to this, culinary school is one channel that actively provides theoretical and practical knowledge transfer in preventive measures to overcome FHS issues. Nevertheless, so far, the theoretical class, practical kitchen, and culinary internship have affected implementation of FHS among culinary students in Malaysia. The aim of this paper is to conduct an empirical study on student behaviours in hands-on activity during practical class. During the observation process, the student monitors his or her behaviour during food preparation at the workstation. Any behaviour which leads to FHS issues is reported in this study.

LITERATURE REVIEW

Food Hygiene and Food Safety Knowledge among Food Handlers

Foodborne illnesses are referred to as diseases, "usually either infectious or toxic in nature, caused by agents that enter the body through the ingestion of food" (World Health Day, 2015). Various foodborne pathogens have been identif ed for foodborne illness: *Campylobacter, Salmonella, Listeria Monocytogenes*, and *Escherichia Coli* O157:H7 have been found to be responsible for the majority of foodborne outbreaks (Alocilja & Radke, 2003; Chemburu, Wilkins, & Abdel-Hamid, 2005). Most of the earlier and recent food product recalls were also due to these pathogens (Belson & Fahim, 2007).

Accordingly, programmes and good practices are considered to reduce the pathogenic microorganisms in food at a signif cant level. Methodical programmes include good agricultural practices (Kay et al., 2008), good manufacturing practices, GMP (Jali, Ghani, & Nor, 2016), hazard analysis and critical control points, HACCP (Jin, Zhou, & Ye, 2008), and the food code

indicating approaches (Piatek & Ramaen, 2001). However, the role of human intervention remains vital, which is the key to prevention of problems related to health and safety. In the following section, human interventions when processing food that cause the transmission of various pathogens, their weaknesses, and the actions to be taken will be discussed.

Culinary Students

According to Saad, See, Abdullah and Nor (2013), the cooking process is intended to obliterate harmful microorganisms and ensures the food prepared is microbiologically safe for human consumption. This technique of safe food handling needs to be taught by competent instructors. The implied assumption is that continued education and training in food hygiene and safety could strengthen food handlers' knowledge (Seaman, 2010).

Despite the growth of culinary schools and the rise in the number of trained food handlers, food poisoning cases are still prevalent in commercial catering, mainly due to poor handling practices (Jeinie, Saad, Sharif, & Nor, 2016). Effective FHS implementation in culinary school can be strengthened through continued theoretical and practical food handling and safety learning. In the culinary programme, students are assigned to a culinary internship as part of the culinary syllabus.

With this training, it is expected that food handlers will adopt good hygiene practices, which will lead to the reduction of foodborne diseases (Zain & Naing, 2002). Therefore, future food handlers should master the knowledge and skills needed to ensure the safety of the food they provide. Effective FHS implementation is much needed to improve the effectiveness of health education programmes for food handlers.

MATERIALS AND METHOD

The ethnographic method uses two major tools which are applied in this research, that is, observations and photo-taking. Visual material is quoted as an integral part of the research process, be it as a form of data, a means for generating data, or a method of representing results (Knowles & Sweetman, 2004).

Participants

The participants for the study were culinary programme students of Culinary Art Management (HM245), Faculty of Hotel and Tourism Management (FHTM), Universiti Teknologi MARA (UiTM). A total of 18 culinary students were interviewed and observed via a mounted action camera to know their behavioural patterns in implementing food safety and hygiene practices at their workstations. The culinary students were selected because the respondents in this study were considered progressive, health and quality conscious and mentally competent to react to the implementation of food safety and hygiene practices. These students come from diverse pre-university backgrounds from both non-culinary programmes and culinary-related programmes. Some participants had undergone their culinary internship. The culinary internship varied, depending on the type of hotel, place of internship and star rating.

Setting for the Study

This study is set up at the workstation in an FHTM mock kitchen. During the process of observation, three action cameras (a unit of GoPro Hero4 Silver Edition, two units of SJCAM model M10) and a unit of the digital single-lens ref ex camera (Nikon DSLR model D90) were used to record their activities and tap real f eld experiences at the workstation. As such, equipment is one of the primary sources of ethnographic data collection.

RESULTS

Participant Characteristics

Participant are categorised into three characteristics: gender, postgraduate status, and Cumulative Grade Point Average (CGPA). For the interpretation, the group of participants is simplif ed and presented in Table 1.

Table 1
Participants' characteristics

Characteristics	Total Sample n = 18	
Gender		
Male	8	44.4
Female	10	66.6
CGPA		
2.00	0	0
2.01-2.50	2	11.1
2.51-2.00	5	27.8
3.01-3.50	7	38.9
3.51-4.00	4	22.2
Pre-university		
STPM	3	16.6
Matrix/ Foundation UiTM	3	16.6
Diploma from another institution of higher learning	1	5.6
Diploma UiTM	1	5.6
Final adoption of semester Diploma	10	55.6
Culinary internship		
Type of Hotel		
Resort	4	22.2
City Hotel	5	27.8
Boutique hotel	1	5.6
Hotel Star Rate		
3-star	3	16.6
4-star	5	27.8
5-star	2	11.1

Table 1 *(continue)*

Location of Internship		
Urban	5	27.8
Suburban	3	16.6
Island	2	11.1

Observation and Hands-on Activities

The process of observation took place once a week, for a four-hour session for each student, with a total of 72 hours of observation, which took six weeks to complete. Four themes of FHS were identif ed during the analysis of the footage and presented in Table 2.

Table 2
Themes of FHS

Themes	Never (0%)	Occasionally (1-50%)	Frequently (51-100%)
Wash theme			
a. Hands frequently			x
b. Knife before and after usage		x	
c. Test spoon before and after usage		x	
d. Food thermometer before and after usage		x	
e. Cooking utensils (spatula, thong) before and after usage		x	
f. Fruits and vegetables thoroughly			x
Clean theme			
a. Wear gloves	x		
b. Tabletops surface		x	
c. Chopping board		x	
d. Cap or scarf			x
e. Chef jacket			x
f. Kitchen pants			x
g. Apron			x
h. Kitchen towel			x
Use theme			
a. Different compartment for raw and cooked food			x
b. Color code chopping board		x	
c. Different knife for cutting raw and cooked food	x		
d. Thermometer when cooking meat, poultry and egg product		x	
e. Different kitchen towel to wipe dry especially wet surface		x	

Table 2 *(continue)*

Inspect theme		
a.	Smell raw meat, poultry, seafood and dairy products before use	x
b.	Raw items from foreign substances	x
c.	Expiry date	x
d.	Physical check on cans from dents and rust	x

FHS is usually associated with personal cleanliness and an eff cient workplace. The systematic organisation of a workplace can minimise the transmission of an organism from raw to cooked food through hands, utensils, and clothes. Figure 1 shows that the participant has organised his workplace through concrete FHS implementation.

Figure 1. Picture of nn organised workplace

Routine in the kitchen, can spread foodborne pathogen very eff ciently. This study identif es several negative FHS implementation habits. Figure 2 and Figure 3 show the contrary implementation of FHS, which may lead to foodborne illness.

Figure 2. Picture of a student handling of raw chicken

Figure 2 indicates the student's use of the wrong colour code chopping board in handling the raw chicken. Preparing raw chicken has long been recognised as an important source contaminant of *Salmonella* spp. and *Campylobacter* spp. Handling contaminated raw chicken disperses pathogens throughout the kitchen, not just onto work surfaces and hands (Cogan, Bloomf eld, & Humphrey, 1999).

Figure 3. Picture of a student handling of cooked product without gloves

DISCUSSION

Demographic Characteristics of Respondents

The demographic characteristics of 18 respondents are shown in Table 1. Most of the respondents were females (66.6%) compared to males (44.4%), with 61.1% of CPGA between 3.01 and 4.00. There were 10 (55.6%) respondents from culinary related programmes (private and government). It was learnt that 10 respondents (55.6%) had culinary internship experience, with half from city hotels and the rest from a 4-star urban hotel.

Food Safety and Hygiene Practice Implementation

This study presents insights into the implementation of FHS by monitoring culinary students' behaviours during a mock kitchen class. Food handlers and culinary students think that they know how to handle food safety, but their self-reported food handling behaviours do not support this assumption (Hassan & Dimassi, 2014; Saad, Abdullah, Jeinie, & Husain, 2016).

In eliminating the bias of students reacting abnormally because of the knowledge that they are being recorded, the researchers spent eight weeks on the site to make sure that the students involved in this study acted normally, as themselves. Based on the data from the study, it is found that students did not use gloves and only practised all purpose, single knife usage. Using gloves and having separate knife functions (vegetables, raw meat, seafood, and cooked food) may prevent cross contamination. Furthermore, using gloves and different knives for different purposes can avoid the transmission of foodborne pathogens, such as *E. coli, Listeria, Salmonella*, and others.

Meanwhile, this study also detected several potential activities that cause cross contamination. Even though 61.1% of the participants had a CGPA between 3.01 and 4.00, and 55.6% had a culinary internship with multi-background experience, the study indicated that students occasionally did not fully utilise or apply the knowledge they had learnt during theoretical classes, hands-on practical kitchen and industrial internship. Notably, these culinary interns had undergone the theoretical course of Food Safety Management (course code HTF533) in semester four. Abdullah Sani and Siow (2014) reported that there was a positive association between the level of knowledge, attitudes, and practices of food handlers; nevertheless, through the observations, it can be seen that many of them do not always apply the theoretical knowledge they have learnt in the actual practice of handling food.

Despite the numbers given above, the study ref ects that on the whole, culinary students do not practice the actual implementation of FHS. A total of 27.8% of the students with culinary internship experience showed a remarkable implementation of FHS. This study identif es hotel star rating, as well as the location and type of hotel, as a contributor to the shaping of student behaviour of being eff cient in FHS implementation. Hotels with a 5-star rating usually have well-developed FHS systems, such as the Halal certif cate, GMP, or HACCP system, to secure their investment.

Indeed, a culinary internship with an established FHS system tends to improve students' behaviour regarding FHS implementation. FHS knowledge gained from any form of knowledge transfer(theoretical class, hands-on practical kitchen, and industry internship) require the students to use all available resources and initiatives to improve the implementation of knowledge into practical application. Therefore, suff cient knowledge transfer and consistent training efforts are needed to produce the next generation of food handlers.

CONCLUSION

This study offers a signif cant understanding of the implication of FHS among culinary students. Culinary students who have knowledge of FHS and culinary experience are highly cautious about FHS implementation. The impact of culinary internship signif cantly changes students' behaviours in terms of FHS implementation. Nevertheless, the impact will be more signif cant if the place of internship implements and establishes HACCP system, GMP, Halal certif cate, or others related to FHS.

Therefore, effective FHS knowledge transfer and food safety training in selective industry criteria with proper guidelines should be introduced for all culinary schools to produce a competent workforce and to minimise the prevalence of foodborne hazards. Besides guidelines, this study recommends that a procedure be adopted to help students choose a suitable institution for their culinary internship. Indeed, hands-on activity needs intervention on rubric grading systems, which should include greater details of hygienic and safety practices to educate culinary interns.

It is acknowledged that there are also several limitations of this study. The data relied on the research setting, might have exhibited bias because the students may have reacted abnormally to the camera and picture taking during the process of observation. Attempts were made to compensate for this, and during the process of observation, the students were given

brief ng and orientation time of 15 to 60 minutes to become comfortable and familiar before recording took place.

Further research is needed to assess FHS implementation in the industry, in hotels in Malaysia that practise HACCP, GMP, Halal certif cate, or other FHS systems. Moreover, it would be worthwhile for future research to involve collaboration with government agencies such as the Ministry of Health or other related agencies as well as hotels to promote the effectiveness of the food safety study and identify suitable places for culinary internships. Indeed, by producing competent future chefs, such interventions will be game changing in reducing foodborne diseases.

ACKNOWLEDGEMENTS

REFERENCES

Abdul Mutalib, N. A., Abdul Rashid, M. F., Mustafa, S., Amin Nordin, S., Hamat, R. A., & Osman, M. (2012). Knowledge, attitude and practices regarding food hygiene and sanitation of food handlers in Kuala Pilah, Malaysia. *Food Control, 27*(2), 289–293.

Abdullah Sani, N., & Siow, O. N. (2014). Knowledge, attitudes and practices of food handlers on food safety in food service operations at the Universiti Kebangsaan Malaysia. *Food Control, 37*, 210–217.

Alocilja, E. C., & Radke, S. M. (2003). Market analysis of biosensors for food safety. *Biosensors and Bioelectronics, 18*(5), 841-846.

Bolton, D. J., Meally, A., Blair, I. S., McDowell, D. A., & Cowan, C. (2008). Food safety knowledge of head chefs and catering managers in Ireland. *Food Control, 19*(3), 291–300.

Chemburu, S., Wilkins, E., & Abdel Hamid, I. (2005). Detection of pathogenic bacteria in food samples using highly-dispersed carbon particles. *Biosensors and Bioelectronics, 21*(3), 491-499.

Cogan, T. A., Bloomf eld, S. F., & Humphrey, T. J. (1999). The effectiveness of hygiene procedures for prevention of cross-contamination from chicken carcases in the domestic kitchen. *Letters in Applied Microbiology, 29*(5), 354-358.

Fleury, M. D., Stratton, J., Tinga, C., Charron, D. F., & Aramini, J. (2008). A descriptive analysis of hospitalization due to acute gastrointestinal illness in Canada, 1995-2004. *Canadian Journal of Public Health/Revue Canadienne de Sante'ePublique*, 489-493.

Hassan, H. F., & Dimassi, H. (2014). Food safety and handling knowledge and practices of Lebanese university students. *Food Control, 40*, 127–133.

Jali, M. B., Ghani, M. A., & Nor, N. M. (2016). The confusion in complying with good manufacturing practice requirements in Malaysia. P*roceedings of the 2016 UKM FST Postgraduate Colloquium (pp. 30032-1 – 300032-6)*. AIP Publishing.

Jeinie, M. H., Saad, M., Sharif, M. S. M., & Nor, N. M. (2016). Hygiene practices and food safety knowledge for biological, chemical and physical hazards. *Social Sciences, 11*(19), 4633-4637.

Jin, S., Zhou, J., & Ye, J. (2008). Adoption of HACCP system in the Chinese food industry: A comparative analysis. *Food Control 19*(8), 823-828.

Kay, D., Crowther, J., Fewtrell, L., Francis, C. A., Hopkins, M., Kay, C., ... & Wyer, M. D. (2008). Quantification and control of microbial pollution from agriculture: a new policy challenge?. *Environmental Science and Policy, 11*(2), 171-184.

Knowles, C., & Sweetman, P. (2004). *Picturing the social landscape: Visual methods and the sociological imagination.* Routledge.

Linscott, A. J. (2011). Food-borne illnesses. *Clinical Microbiology Newsletter, 33*, 41-45.

Piatek, D. R., & Ramaen, D. L. J. (2001). Method for controlling the freshness of food products liable to pass an expiry date, uses a barcode reader device that reads in a conservation code when a product is opened and determines a new expiry date which is displayed. *Patent Number: FR2809519-A1*.

Saad, M., Abdullah, M. F. F., Jeinie, M. H., & Husain, R. (2016). *Ref ecting leadership effectiveness via food-hygiene practices* (pp. 268-278). National Taiwan University, Taipei, Taiwan: 7th Asian Conference on Environment-Behaviour Studies.

Saad, M., See, T. P., & Adil, M. A. M. (2013). Hygiene practices of food handlers at Malaysian government institutions training centers. *Procedia-Social and Behavioural Sciences, 85*, 118-127.

Scallan, E., Hoekstra, R. M., Angulo, F. J., Tauxe, R. V., Widdowson, M. A., Roy, S. L., ... & Griff n, P. M. (2011). Foodborne illness acquired in the United States—major pathogens. *Emerging Infectious Diseases, 17*(1), 7-15.

Seaman, P. (2010). Food hygiene training: Introducing the Food Hygiene Training Model. *Food Control, 21*(4), 381–387.

World Health Day (2015). *From farm to plate, make food safe. (37 000)*, 1–3. Retrieved from http://www.who.int/mediacentre/news/releases/2015/food-safety/en/

Zain, M. M., & Naing, N. N. (2002). Sociodemographic characteristics of food handlers and their knowledge, attitude and practice towards food sanitation: A preliminary report. *Southeast Asian Journal of Tropical Medicine and Public Health, 33*(2), 410-417.

Effect of Boronizing Medium on Boron Diffusion of Surface Modif ed 304 Stainless Steel

Mohd Noor Halmy[1], Siti Khadijah Alias[1]*, Radzi Abdul Rasih[1], Mohd Ghazali Mohd Hamami[1], Norhisyam Jenal[1] and Siti Aishah Taib[2]

[1]*Faculty of Mechanical Engineering, Universiti Teknologi MARA (UiTM) Johor, 81750, Masai, Johor, Malaysia*
[2]*Academy of Language Studies, Universiti Teknologi MARA (UiTM) Johor, 81750 Masai, Johor, Malaysia*

ABSTRACT

This study focuses on the effect of boronizing medium on the boride layer thickness of pack boronized 304 stainless steel after surface modif cation. Pack boronizing treatment was conducted in temperature of 900oC for a duration of eight hours. The treatment was performed using two different boronizing mediums which are powder and paste inside a tight box in an induction furnace. The characteristics of the samples were then observed using optical microscopy and XRD analyser. The thickness of boride layer was then measured using MPS digital image analysis software. The results showed that boronizing medium signif cantly affected the thickness of boride layer as paste boronized samples exhibited thicker boride layer thickness. The enhancement was mainly due to the size of boron particle in the paste medium which was smaller than powder medium that enabled better diffusion. It is expected that the enhancement of the boride layer thickness would result in further improvement of the mechanical and wear properties of this material.

Keywords: 304 stainless steel, boron diffusion, boronizing, boride layer thickness

INTRODUCTION

In boronizing, which combines both thermal and chemical reactions, boron atoms are diffused on the surface of steel and iron with the purpose of improving the properties such as hardness and wear resistance. The diffusion process will create boronized layers containing iron boride of FeB and Fe_2B phase (Jacuinde, Guerra, Rainforth, & Maldonado, 2015). The enhancement of hardness and wear properties are dependent on the thickness of

the boride layer formed on the surface of metal and alloy. Thicker boride layer will result in better surface protection, thus forming a material with superior hardness and wear resistance (Jacuinde et al., 2015). The formation of the boride layer is dependent on the boronizing medium (gas, liquid or solid), temperature and also time (Béjar & Henríquez, 2009; Kul, Oskay, Temizkan, Karaca, Kumruo lu, & Topçu, 2016; Mao, X. Wang, W. Wang, & Wei, 2012).

Pack boronizing is the most common type of boronizing method as it offers advantages such as low cost and simple operation. This process is conducted by immersing the sample in a box f lled with either powder or paste medium. The medium consists of boron compound, activator and diluents at a temperature of 750°C to 1100ºC for a duration of two to 10 hours (Alias, Abdullah, Latip, Roselina, Roseley, Jenal, & Kasolang, 2013a; Basir, Abdullah, & Alias, 2014). The variations of the medium result in different mechanical and wear properties of low alloyed steel and cast iron (Alias et al., 2013b; Dybkov, 2015). Generally, paste medium provides better boron diffusion thickness, thus acquiring better wear properties.

Other than pack boronizing, the treatment could also be conducted in liquid and gas states (Gunes, Ulker, & Taktak, 2011). A mixture of crystallised boraks and boric acid is often used in liquid boronizing while an inert gas such as argon is often used as carrier gas in gas boronizing. Using these methods, the improvement of wear resistance and mechanical properties could be achieved at a lower temperature and shorter time as compared to pack boronizing method. It is because more chemical reactions are activated during the treatment (Sahin, 2009). However, the restriction of this method is the requirement of removing the salt layers formed on the sample surface, which can be more complicated and expensive (Zepon, Nascimento, Kasama, Nogueira, Kiminami, & Botta, 2015). As the characteristic of boride layer thickness depends largely on the boronizing medium, this study focused on the effect of boronizing medium on the boron diffusion characteristic of 304 stainless steel.

MATERIALS AND METHOD

The characteristics of the samples were observed using Olympus B X 41 M microscopes. The thickness of boride layer was then measured using MPS digital image analysis software. The microstructures were prepared by mounting, cross-sectioning, and polishing according to ASTM E3 standard and etching according to ASTM E407 standard. 2% Nital was used as the chemical etchant. The phase structures were then conf rmed through Rigaku X-Ray Diffraction (XRD) diffractometer by means of CuK radiation with the 2 angle between 30 to 120. Table 1 shows the chemical composition of 304 stainless steel.

Table 1

Chemical composition of 304 stainless steel

Chemical composition	Weight percentage (%)
Carbon (C)	0.08
Silicon (Si)	0.8
Manganese (Mn)	1.8
Phosphorus (P)	0.045
Sulfur (S)	0.035
Nickel (Ni)	8.00
Chromium (Cr)	18.00

The surface modif cation process which was shot blasting was conducted on the surface of stainless steel in order to initiate boron diffusion using the Finimac shot blasting machine. The ceramic silicon carbide (SiC) ball with velocity between 150 to 200 m/s and a diameter of 2 mm was used as the steel shot. Figure 1 shows the surface modif cation process and the parameter implemented. The surface modif cation process helps initiate dislocation and vacancy, which allows better boron diffusion onto the surface of boronized stainless steel as the presence of alloying elements in high amount often restricted the boride layer formation.
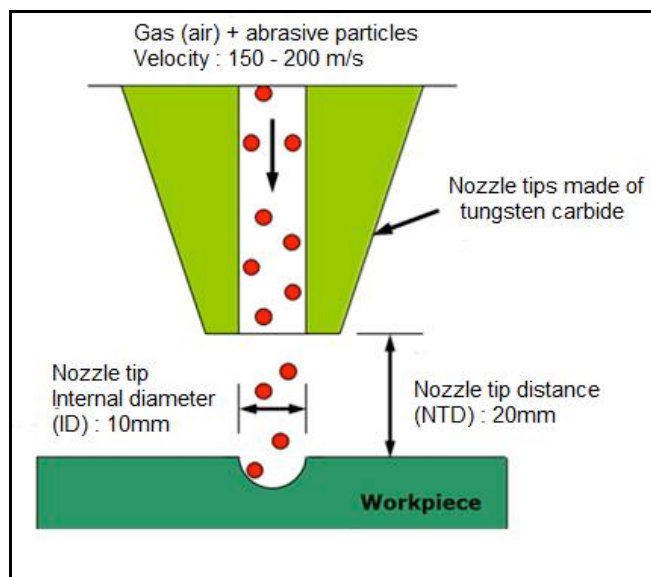
Figure 1. The schematic diagram of the mechanism for shot blasting process

RESULTS AND DISCUSSION

Microstructure Observation

The result of microstructure observation is shown in Figure 1. Figure 1(a) shows the microstructure of powder boronized sample while Figure 1(b) shows the microstructure of paste boronized sample. Both samples depicted the austenitic structure with sizes of 70 to 90 µm. There was a formation of boride layer consisting of iron boride I (FeB) and iron boride II (Fe_2B) in both samples. Iron boride I (FeB) exhibited more brittle manner with boron percentage of 16.23 wt% when compared to iron boride II (Fe_2B) which contained only 88 wt% of boron. The combination of these two layers, however, provided good strength and hardness to the surface of the material. The diffusion zone,which was a boron enriched area,was under the boride layer, while the substrate of the material was in the diffusion zone. Similarly, it was found that pack boronizing usually produce inter metallic phase containing FeB and Fe_2B phases when heated at a temperature between 800°C to 900°C for six to eight hours holding time (Alias et al., 2013a; Basir, Abdullah, & Alias, 2014).

(a)   (b)
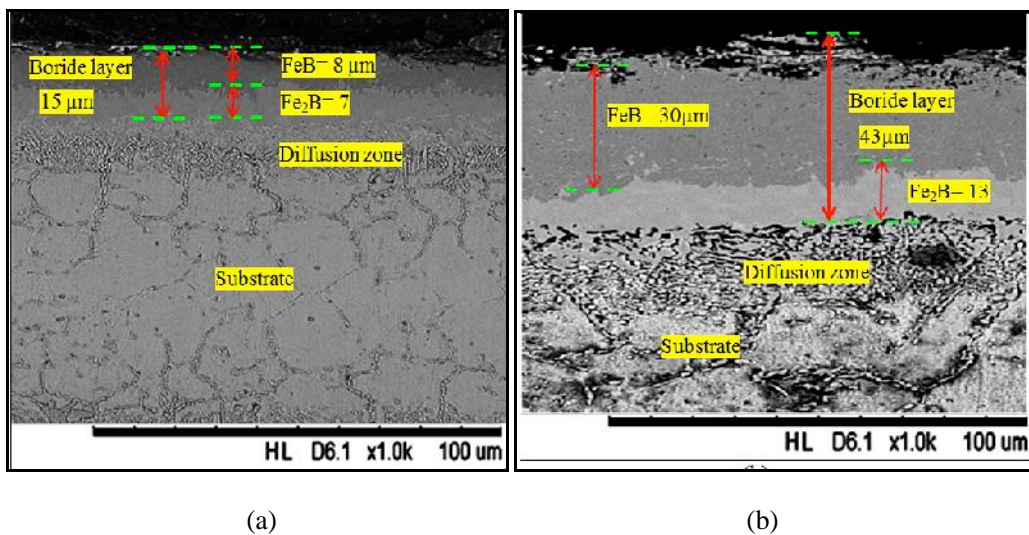
Figure 2. Microstructure of: (a) powder; and (b) paste boronized 304 stainless steel

The validation of FeB and Fe_2B phases is depicted in Figure 3. The formation of FeB and Fe_2B phases were conf rmed via XRD analysis at 2 Theta angles of 37°[1 1 9], 62°[4 3 4] and 80°[6 1 1] for FeB phase and 35°[2 0 8], 42°[0 1 1] and 82°[7 1 6] for Fe_2B phase.
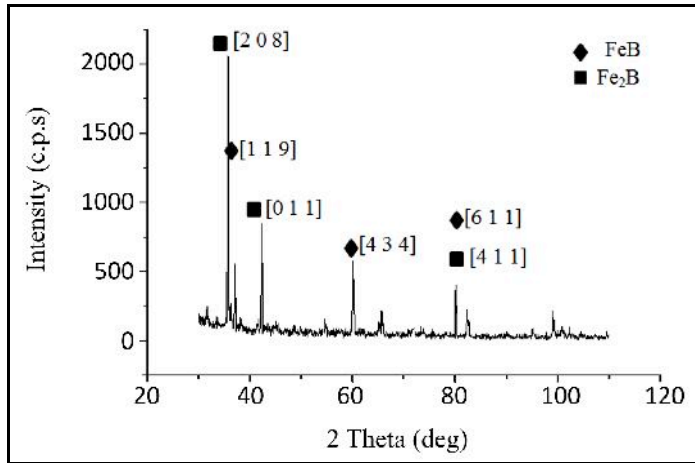
(a)
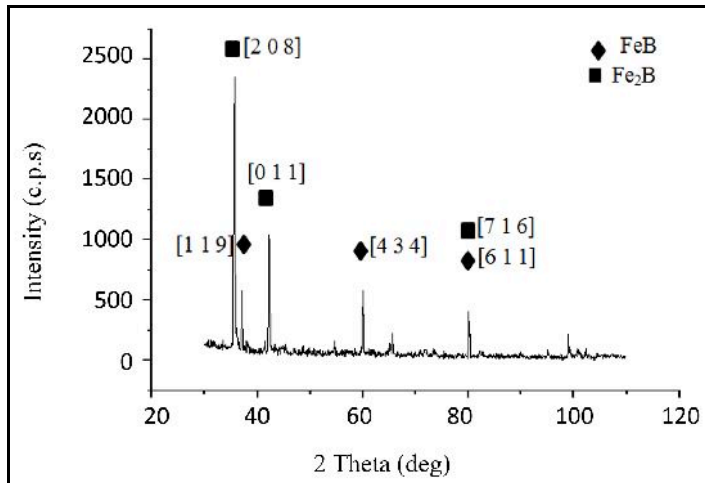
(b)

Figure 3. XRD Pattern of: (a) powder and (b) paste boronized stainless steel

Boride Layer Thickness

The result of the boride layer thickness is shown in Figure 4. It was observed that the overall thickness layer of powder boronized sample was 15 µm with a similar thickness of FeB and Fe_2B. However, paste boronized sample had successfully enhanced the boride layer thickness three times the value of the powder bronzed samples with the value of 43 µm. The thickness of FeB layer was more than twice the value of the Fe_2B layer as the value of the boron percentage in FeB was higher than Fe_2B. In paste medium, the particle size of the medium was smaller than the powder, which resulted in higher activation energy that enabled better diffusion at high

temperature. Similarly, it was found that the boride layer thickness of low alloyed steel was thicker when boronized using paste medium as compared to powder medium because more active boron ion, B^{+1} was diffused and reacted with Fe in the samples (Zepon et al., 2015).
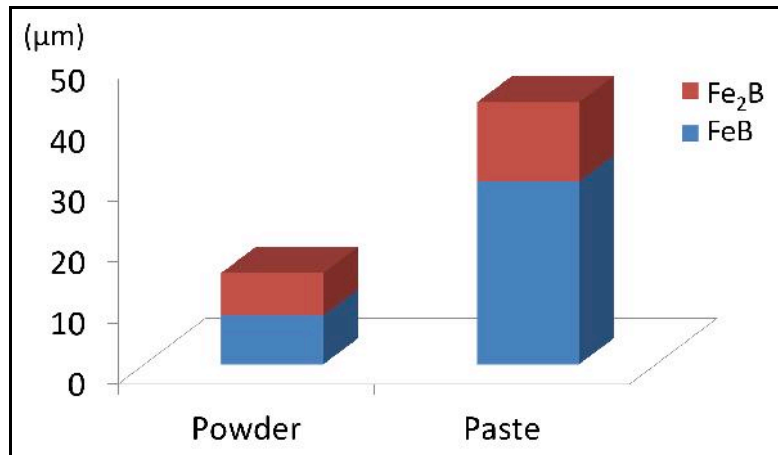
Figure 4. Boride layer thickness of power and paste boronized stainless steel

CONCLUSION

The main objective of this study which is to study the boronizing medium on boron diffusion of surface modif ed 304 stainless steel has been successfully achieved. It can be concluded that paste medium induced deeper boride layer with an improvement of almost three times as compared to powder medium due to smaller particle size that enabled higher citation energy during the boronizing process. This indicates that paste medium provides better protection to the surface of the material, thus leading to improvement of hardness and wear resistance of the material. It would be useful to study the kinetic energy of this method in the future to further improve this research.

ACKNOWLEDGEMENTS

REFERENCES

Alias, S. K., Abdullah, B., Latip, S. A., Roselina, N., Roseley, N., Jenal, N., & Kasolang, S. (2013a). Effect of temperature variations on wear properties of boronized stainless steel. *Applied Mechanics and Material, 393*, 217-221.

Alias, S. K., Abdullah, B., Latip, S. A., Roselina, N., Roseley, N., Jenal, N., & Kasolang, S. (2013a). Boron dispersion layer of paste boronized 304 stainless steel before and after shot blasting process. *Applied Mechanics and Material, 393*, 217-221.

Basir, M. H., Abdullah, B., & Alias, S. K. (2014). Wear properties of paste boronized 316 stainless steel before and after shot blasting process. *Scientif c Research Journal, 11*, 2.

Béjar, M. A., & Henríquez, R. (2009). Surface hardening of steel by plasma-electrolysis boronizing. *Materials and Design, 30*, 1726–1728.

Dybkov, I. (2015). Thermochemical Boriding of Iron-Chromium Alloys. *Chemistry Journal, 1*(3), 81-89.

Gunes, I., Ulker, S., & Taktak, S. (2011). Plasma paste boronizing of AISI 8620, 52100 and 440C steels. *Materials and Design, 32*, 2380–2386.

Jacuinde, A. B., Guerra, F. V., Rainforth, M. I., & Maldonado, C. (2015). Sliding wear behavior of austempered ductile iron microalloyed with boron. *Wear, 330-331*, 23–31.

Kul, M., Oskay, K. O., Temizkan, A., Karaca, B., Kumruo lu, L. C., & Topçu, B. (2016). Effect of boronizing composition on boride layer of boronized GGG-60 ductile cast iron. *Vacuum, 126*, 80–83.

Mao, D., Wang, X., Wang, W., & Wei, X. (2012). Effect of boronizing on the dry sliding wear behavior of DC53/0.45 mass% C steel pairs. *Surface and Coatings Technology, 207*, 190–195.

Sahin, S. (2009) Effects of boronizing process on the surface roughness and dimensions of AISI1020, AISI 1040 and AISI 2714. *Journal of Materials Processing Technology.* 1736-1741.

Zepon, G., Nascimento, A. R. C., Kasama, A. H., Nogueira, R. P., Kiminami, C. S., & Botta, W. J. (2015). Design of wear resistant boron-modif ed supermartensitic stainless steel by sprayforming process. *Materials and Design, 83*, 214-223.

Investigating the Effect of Different Weft Densities and Draw in Plan on Physical Properties and Seam Strength of Woven Plain Fabrics

Nurul Syazwani Abdul Latif* and Suzaini Abdul Ghani

Faculty of Applied Sciences, Universiti Teknologi MARA (UiTM), 40450 Shah Alam, Selangor, Malaysia

ABSTRACT

Weft density and draw in plan play an important role since they affect physical properties such as fabric weight, cloth cover factor as well as seam strength. Weft density refers to the amount of weft yarn in one inch. Meanwhile, draw in plan refers to the amount of heald shaft used and the order of warp yarn through the heald. In this study, plain woven fabrics were produced by using Sulzer Rapier Loom Machine. There were two different types of weft density used which were 15 and 20 weft per centimeter (wpcm) and four draws in plan: pointed, straight, broken and broken mirror. Seams were constructed by using plain seam of Ssa-1, four stitches of stitch density and 301 lockstitches for stitch type. Subsequently, the fabric samples were tested on seam strength by using Testometric tester. As a result of this study, it is proven that weft density and draw in plan of woven plain fabric are parameters that affect the seam strength and seam eff ciency. The highest increase in percentage of seam strength was obtained from straight draw in plan which increases up to 17.19% from 15wpcm to 20wpcm. Meanwhile, broken draw in plan has the lowest increase percentage for seam strength which is 6.46%. Furthermore, seam eff ciency also shows straight draw in plan gives good fabric durability compared to others. Lastly, it also shows broken draw in plan has no signif cant effect on fabric tensile strength and seam strength.

Keywords: Draw in plan, seam eff ciency, seam strength, stitch density, weft density

INTRODUCTION

In the apparel industry, in order to determine the quality and productivity of finished garments, the sewing process is one of the most critical processes (Sarhan, 2011; Bharani & Mahendra, 2012). The sewing process is important to produce a good functional end use, such as good seam strength and good durability of garments. Nowadays, seam

strength, seam puckering and seam eff ciency have become more important to the appearance and performance of garments (Anon, 1977). In order to produce good quality of sewn product, seam strength is one of the most important indicators which must be considered (Paul, Sanyal, Chowdhury, Mukhopadhyay, & Das, 2015). In addition, good quality garments must have good seam strength in order to meet customer satisfaction.

Seam strength is one of the alternative methods of measuring strength in which the material is stressed in warp or weft direction or both at the same time. In addition, seam strength also refers to the required force to break open the seam, either by breaking the sewn material or breaking the thread. There are two components in seam strength which are sewing thread and fabric. Therefore, seam strength will break either of fabric or thread or in other cases, it breaks simultaneously. It was found that the load required to break the unsewn material is more than to break the seam (Behera & Sharma, 1998; Choudhury, 2000).

From the previous studies (Behera & Chand, 1977; Behera & Shakun, 2000; Behera, Shakun & Snrabhi, 2000; Bhalerao, Budke, & Borkar, 1997; Midha, Mukhopadhyay, Chattopadhyay, & Kothari, 2010), it is conf rmed that there are many factors that affect the seam strength and seam appearance which include fabric parameters as well as sewing parameters. The examples of fabric parameters are type of fabric used and fabric properties which include fabric weight, fabric density and fabric structures. Meanwhile, the type of thread, seam type and stitch density are examples of sewing parameters. These parameters give effect to the seam strength as well as to the quality of end product (Megeid, Ezzat, & Ali, 2016; Paul et al., 2015). Fabric density can be divided into two groups which are warp density and weft density. Warp density is the amount of warp yarn in one inch square. Meanwhile, weft density refers to the amount of weft yarns in one inch square. From another previous study (Sarhan, 2011), it is known that that there are signif cant effects between seam strength and fabric weft density. Fabric weft density also gives positive correlation to seam strength. According to research conducted by Sarhan (2011), seam strength increases when weft density increases. This shows that the amount of fabric weft density used in garments is important to produce good seam strength.

In addition, fabric structure also plays an important role in fabric strength which affects seam strength performance. Based on the study by Gurarda (2008), plain fabric has lower breaking strength when compared to twill fabric. These different structures give effect to seam strength based on their fabric strength. Twill fabric has higher f oating yarn compared to plain yarn. So, it makes twill fabric not to easily break when exposed to stress. Moreover, from the research by Sarhan (2011), seam strength is also inf uenced by stitch density that was used. It means when stitch density increases, seam strength also increases. This may be due to the increase at the joining part between the sewing thread and fabric.

Nowadays, garments easily break especially at the joining part of the fabric. They easily break especially when a small amount of stress is applied to it especially during daily activities such as walking, sitting and squatting down. These activities can contribute to seam breakages. Therefore, seam strength is an important property to be considered when producing good quality garments. Therefore, it is important to study the seam strength with some fabric parameters in order to produce good quality garment and fulf ll customer satisfaction.

MATERIALS AND METHOD

Plain woven fabric with two different weft densities of 15 and 20 weft per centimeter (wpcm) and four different draw in plan - pointed, broken, broken mirror and straight were used as shown in Figure 1. These draw in plan was used to produce a plain woven fabric as the fabric sample. These woven fabric samples were produced on Sulzer Rapier Loom Machine with 1000rpm by using polyester yarn. Each fabric sample was sewn with Ssa^{-1} seam type. Sewing thread of 100 percent spun polyester with ticket number of 120 was used. The Lockstitch 301 was used for the type of stitch and for stitch density, 4 stitches cm^{-1} was used.

(a)   (b)

(c)   (d)
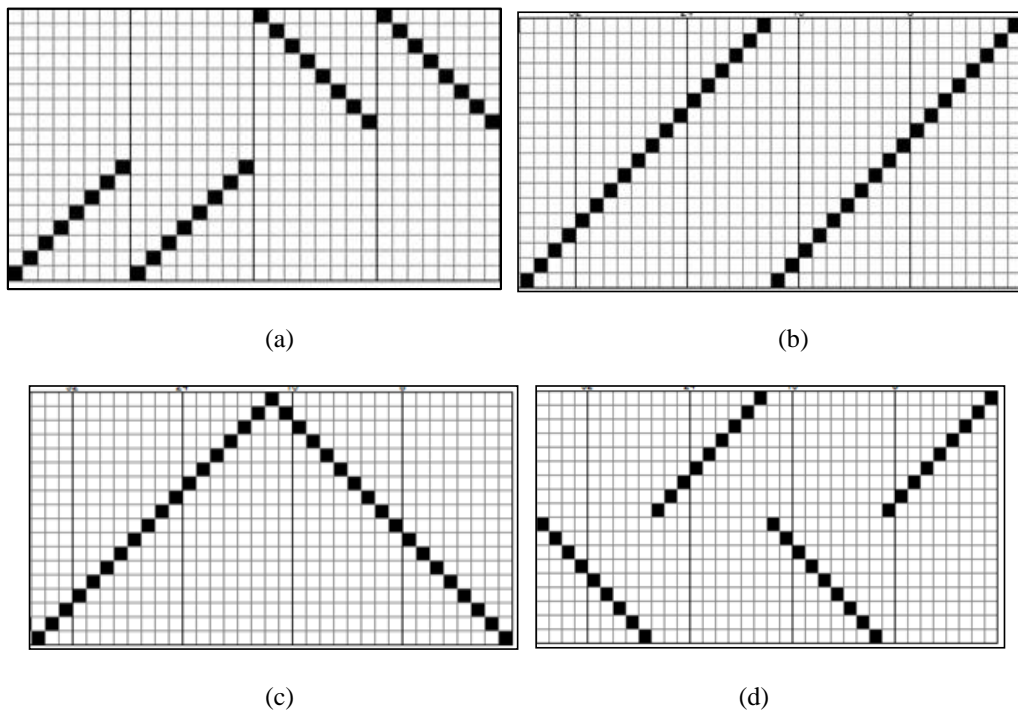
Figure 1. Structures of draw in plan: (a) broken mirror; (b) straight; (c) pointed; and (d) broken

Physical test and mechanical test of tensile strength were carried out in both warp and weft direction. Meanwhile, another mechanical test of seam strength was focused only on weft direction. This is because the amount of warp yarn was constant for this study. The fabric samples were tested for the following physical test - weight, thickness and cloth cover factor.

Seam strength was measured using Testometric Tensile machine with speed of 100mm/ min for three repeated readings in Newton ASTM D1683 standard. In the apparel industry, this method is widely used in order to evaluate the seam strength (Murugesu, Gowda, Rajashree, & Sarumathy, 2012). Several journals were referred to for this study, which used the same method to identify seam performance (Murugesu et al., 2012; Ali, Rehan, Ahmed, Memon, &

Hussain, 2014; Sular, Kefsiz, & Seki 2014). Seam eff ciency was also measured using formula as shown below. The samples were sewn in warp direction as shown in Figure 2 below.

$$\text{Seam Efficiency (\%)} = \frac{\text{Seam Tensile strength}}{\text{Fabric tensile strength}} \times 100$$
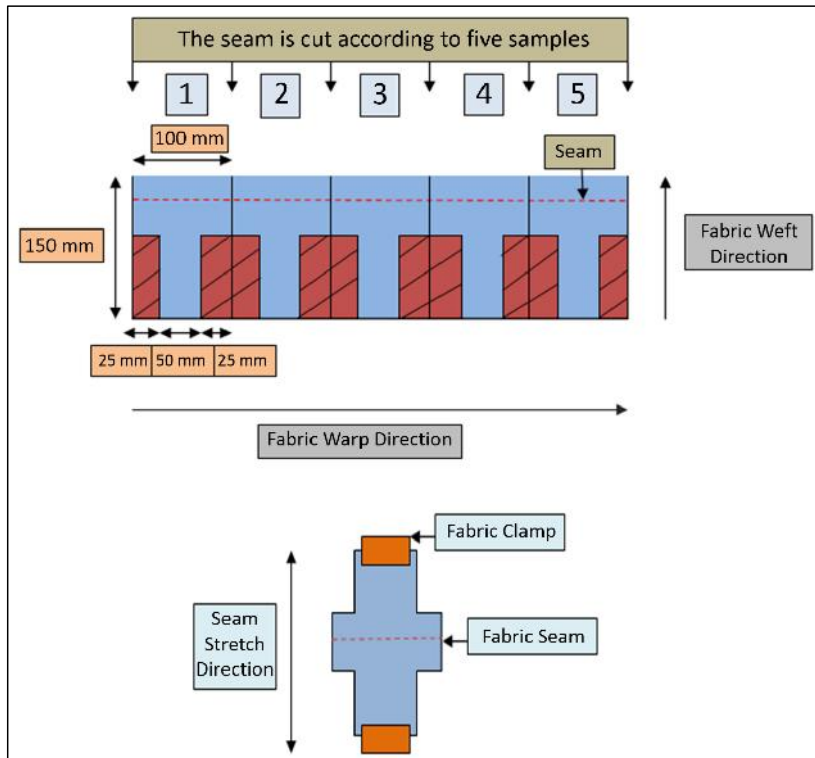
Figure 2. Preparation of sample for seam strength test

RESULTS AND DISCUSSION

Physical Testing

Table 1
Results for fabric testing of 15wpcm and 20wpcm

Fabric Weft Density	Draw in Plan Physical Testing	Pointed	Broken Mirror	Broken	Straight
15	Fabric Weight (g/m^2)	153.1	152.1	152.6	154.6
	Fabric Thickness (mm)	0.46	0.46	0.49	0.49
	Cloth Cover Factor	17.74	17.58	18.00	18.04
	Warp per inch	81	83	83	84
20	Fabric Weight (g/m^2)	174.7	171.4	171.7	176.0
	Fabric Thickness (mm)	0.449	0.451	0.470	0.462
	Cloth Cover Factor	18.33	18.68	18.66	18.42
	Warp per inch	75	78	77	78

Table 1 shows the results for woven plain fabric testing of 15wpcm and 20wpcm with different draw in plan. Based on the results, fabrics of 20wpcm have higher weight compared to 15wpcm, whereby the readings are between 171 g/m² to 176 g/m². Meanwhile, fabric of 15wpcm has lower weight compared to 20wpcm, whereby the readings are between 152 g/m² to 154 g/m². This is due to the higher amount of yarn per inch square in 20wpcm fabric compared to 15wpcm. Thus, it increases the fabric weight on 20wpcm. In addition, the amount of warp per inch for 15wpcm and 20wpcm also shows different readings. This is because the amount of warp yarn used in production was the same but it gives different amount per inch, due to the different draw in plan used.

MECHANICAL TESTING

Tensile Strength
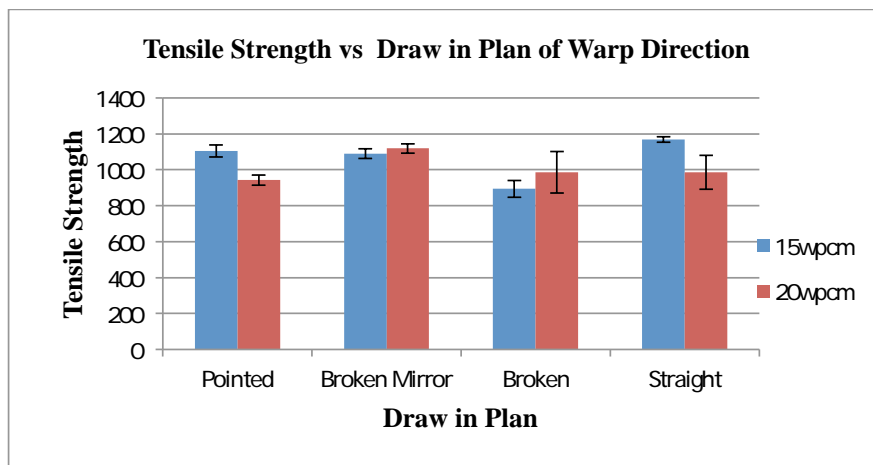
Figure 3. Tensile strength and draw in plan of warp direction for 15wpcm and 20wpcm

Figure 3 shows the bar chart of relationship between tensile strength and draw in plan of warp direction for 15wpcm and 20wpcm. According to the results, tensile strength for 15wpcm broken mirror and broken draw in plan shows an increased percentage to 1.30% and 4.88% respectively. Meanwhile, pointed and straight draw in plan have a decreased percentage for tensile strength from 15wpcm to 20wpcm which are 7.89% and 8.48% respectively. This means the highest increase in percentage are straight draw in plan. This may be due to the highest amount of warp per inch for straight draw in plan. Furthermore, there are statistically signif cant results for pointed and straight draw in plan based on the error bar shown in the graph.
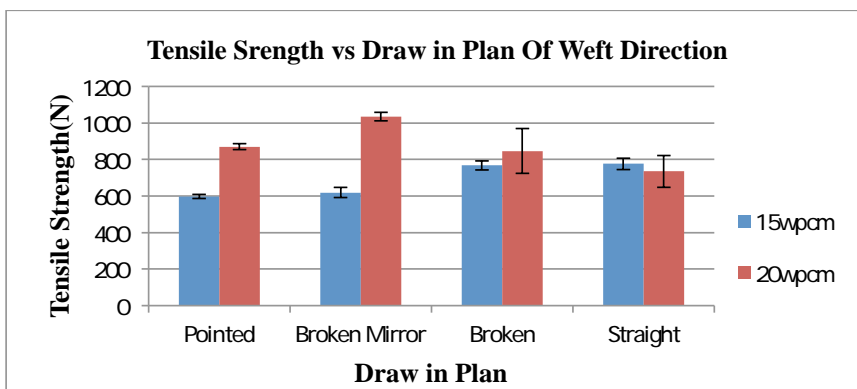
Figure 4. Tensile strength and draw in plan of warp direction for 15wpcm and 20wpcm

Figure 4 shows the bar chart of relationship between tensile strength and draw in plan of weft direction for 15wpcm and 20wpcm. According to the results of tensile strength on weft direction, broken mirror shows the highest percentage of increase, from 15wpcm to 20wpcm, which is up to 25%. Furthermore, only straight draw in plan shows decreased percentage from 15wpcm to 20wpcm, which is 2.7%. Meanwhile, for broken and straight draw in plan, the results are not signif cant for 15wpcm and 20wpcm. These different results may due to the different tension on the fabric during fabric production which gives effect to the performance tensile strength.

Seam Strength
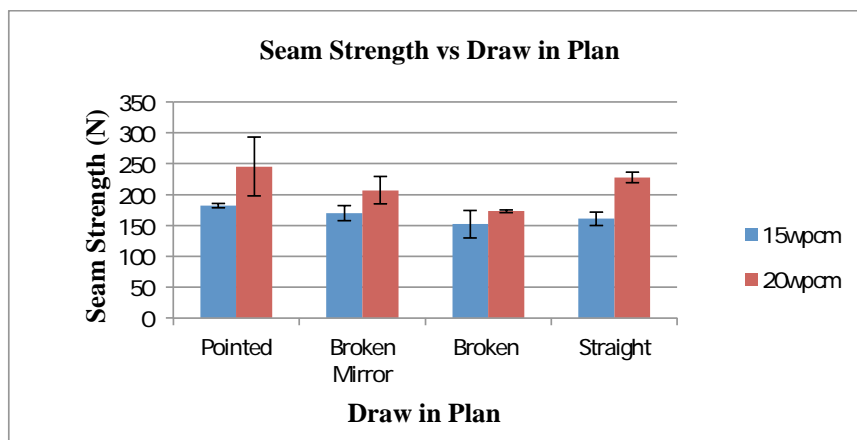
Figure 5. Seam strength and draw in plan of weft direction for 15wpcm and 20wpcm

Figure 5 indicates the bar chart of relationship between seam strength and draw in plan of 15wpcm and 20wpcm. The results show that all draw in plan have an increasing value of seam strength from 15wpcm to 20wpcm. The highest increase in percentage is from pointed draw in plan which increases until 17.19%. It means the increasing degree of weft density will increase

the seam strength. This is because fabric of 20wpcm have higher amount of weft yarn in one inch. So, it has good resistance to stress and does not easily break when stress is applied to it. Furthermore, from the error bar on the bar chart, it can be seen that the results are statistically signif cant for pointed and straight draw in plans. However, for broken draw in plan, it is not statistically signif cant between 15wpcm and 20wpcm.

Seam Eff ciency
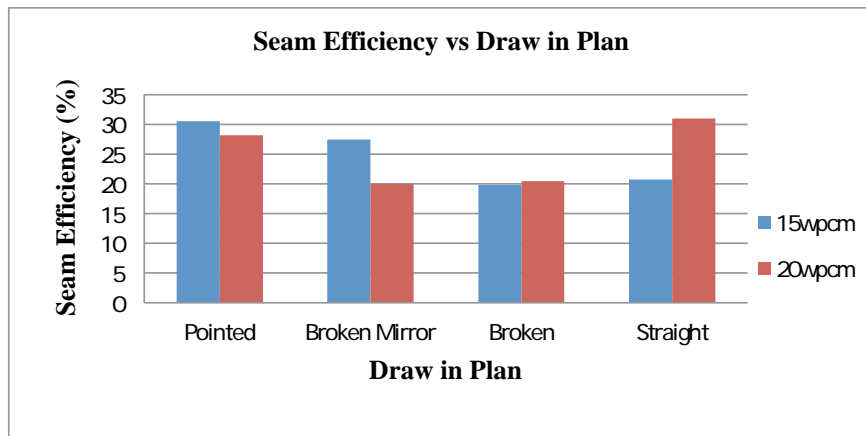
Figure 6. Seam eff ciency and draw in plan of weft direction for 15wpcm and 20wpcm

Figure 6 shows the percentage of seam eff ciency of different draw in plan for 15wpcm and 20wpcm. From the results obtained, it can be seen that the highest seam eff ciency is from straight draw in plan on 20wpcm. Meanwhile, the lowest is from broken draw in plan on 15wpcm. These differences may affected by the strength of the thread itself on different fabric samples. In addition, straight draw in plan has the highest percentage increase of seam eff ciency which increases up to 19.8% from 15wpcm to 20wpcm, compared to other draw in plan. This means that straight draw in plan has good durability compared to others.

CONCLUSION

It can be concluded that fabric weft density and draw in plan play an important role in order to produce good seam strength of garments. It is also a priority to ensure that garments do not easily tear, particularly at the joining part of the fabric when they are exposed to stress, especially during daily activities such as walking and sitting. The results conf rm that there is causal relationship between fabric parameters and seam strength performance. Furthermore, when the degree of weft density increases, the seam strength also increases the same way. However, the same cannot be applied for seam eff ciency. Finally, the highest fabric durability is found to be from straight draw in plan which has the highest percentage of 30.96% of seam eff ciency.

ACKNOWLEDGEMENTS

REFERENCES

Ali, N., Rehan, A. M., Ahmed, Z., Memon, H., & Hussain, A. (2014). Effect of different types of seam, stitch class and stitch density on seam performance. *Journal of Applied and Emerging Sciences, 5*(1), 32-43.

Anon. (1977). The problems of seam puckering. *DOB & Haka Praxis, 12*, 826.

Behera, B. K., & Chand, S. (1977). Sewability of denim. *International Journal of Clothing Sciences and Technology, 9*(2), 128-140.

Behera, B. K., & Shakun, S. (2000). Comparative assessment of low stress mechanical properties and sewability of cotton and cotton banana union fabrics. *Asian Textile Journal, 9*(5), 49-56.

Behera, B. K., & Sharma, S. (1998). Low stress behaviour and sewability of suiting and shirting fabrics. *Indian Journal of Fiber and Textile Research, 25*(4), 23-241

Behera, B. K., Shakun, S., & Snrabhi., S. (2000). Comparative assessment of low stress mechanical properties and sewability of cotton and cotton banana union fabric. *Asian Textile Journal, 23*(4), 49-56.

Bhalerao, S., Budke, A. S., & Borkar, P. (1997). Seam performance in suiting's. *Indian Textile Journal, 107*(11), 78-81.

Bharani, M., & Mahendra, G. R. V. (2012). Characterization of seam strength and seam slippage of PC blends fabric with plain woven structure and f nish. *Research Journal of Recent Sciences, 12*, 7-14.

Choudhury, P. K. (2000). Improvement in seam performance of jute bags. *Indian Journal of Fiber and Textile Research, 25*(3), 206-210.

Gurarda, A. (2008). Investigation of the seam performance of PET/Nylon-elastane woven fabrics. *Textile Research Journal, 78*(1), 21-27. Retrieved from http://www.dx.doi: 10.1177/0040517507082636

Megeid., Z. M. A., Ezzat, M. M., & Ali, R. M. (2016). Inf uence of some woven fabric constructional parameters on seam eff ciency. *International Journal of ChemTech Research, 9*(4), 27-34.

Midha, V. K., Mukhopadhyay, A., Chattopadhyay, R., & Kothari, V. K. (2010). Effect of process and machine parameters on changes in tensile properties of threads during high-speed industrial sewing. *Textile Research Journal, 80*(6), 491-507. Retrieved from http://dx.doi:10.1177/0040517509338311

Murugesan, B., Gowda, R. V. M., Rajashree, S., & Sarumathy, K. K. (2012). Characterization on sewability parameters of plain structures fabric with structurally modif ed trevira CS yarn for fefence application. *Chemical Sciences Review And Letters, 1*(2), 53-61.

Paul, P., Sanyal, P., Chowdhury, S., Mukhopadhyay, G., & Das, D. P. G. K. (2015). Relationship among seam strength, weft-wayy fabric strength and stitch density of B. Twill jute bag. *Indian Journal of Fibre and Textile Research (IJFTR), 40*, 195-199.

Sarhan, T. M. A. (2011). A study of seam performance of micro-polyester woven fabrics. *Journal of American Science, 7*(12), 41-46.

Sular, V. C. M., Kefsiz, H., & Seki, U. (2014). A comparative study on seam performance of cotton and polyester woven fabrics. *The Journal of The Textile Institute, 106*(1), 19-30.

Dinuclear Co(II) and Zn(II) Azomethine Complexes: Physicochemical and Antibacterial Studies

Hadariah Bahron[1]*, Siti Najihah Abu Bakar[1], Siti Solihah Khaidir[1] and Mastura Mohtar[2]

[1]*Faculty of Applied Sciences, Universiti Teknologi MARA (UiTM), 40450 Shah Alam, Selangor, Malaysia*
[2]*Natural Products Division, Forest Research Institute of Malaysia, 52109 Kepong, Selangor, Malaysia*

ABSTRACT

A symmetrical azomethine ligand L was synthesised from a reaction of *m*-phenylenediamine and *o*-vanillin in 1:2 molar ratio. Dinuclear complexes of Zn_2L_2 and Co_2L_2 have been successfully isolated and characterised through ^1H NMR, IR and magnetic moment. The x-ray crystal structure of Zn_2L_2 showed that the two Zn(II) nuclei were coordinated to two L moieties through the phenolic oxygen and imine nitrogen atoms, forming a slightly distorted tetrahedral geometry around the Zn(II) centres. When coordinated to metal centres, the signature n(C=N) of Lat 1616 cm^{-1} experienced a shift towards lower wave numbers of 1573-1613 cm^{-1}. The Zn(II) complex was diamagnetic whereas the Co_2L_2 complex was paramagnetic with 3 unpaired electrons having $\mu_{eff} = 4.07$ B.M. An antibacterial screening against methicillin resistant *Staphylococcus aureus* (MRSA) revealed that the activity of the complexes was more pronounced than that of the uncoordinated L. The complex Zn_2L_2 revealed the lowest MIC value of 0.56 µg/µl MIC, indicating that it was a better bactericides than Co_2L_2 and L, in that order.

Keywords: Antibacterial, azomethine, binuclear, X-Ray crystallography

INTRODUCTION

Azomethines, also known as Schiff bases, have imine-C=N- as the signature group in their structures. The synthesis is commonly performed through a facile condensation of primary amines with aldehydes or ketones. Their remarkable ability to coordinate with not just one metal centre but many, such as dinuclear (Clarke et al., 1998) and tetra nuclear metal complexes (Torayama, Nishide, Asada, Fujiwara, & Matsushita, 1997) has

triggered much interest in the coordination chemistry research fraternity due to the fascinating chemical structures and architecture of the metal complexes. This generates diverse exploration on the activities of the ligands as well as the complexes such as the study of anti-corrosion (Abdul Ghani, Bahron, Harun, & Kassim, 2014; Ramlee, Abu Bakar, Bahron, Harun, Kassim, & Yahya, 2010) and also bioactivity (Tajuddin, El Hassane, Ramasamy, Yamin, Alharthi, & Bahron, 2017) such as antibacterial and anti-cancer properties. It has been reported that Schiff base ligands exhibit numerous biological activities when coordinated to metals such as cobalt (Amirnasr, Schenk, Gorji, & Vafazadeh, 2001) and zinc (Shakir, Azim, & Parveen, 2006). The complexes are observed to be generally more biologically active than their parent ligands due to the presence of the metal moieties.

Of all the azomethine complexes, symmetrically coordinated salicylaldiimines have drawn wide attention as they are very versatile compounds resulting from the f exible synthetic procedures. Changes in their carbonyl and diamine moieties could lead to a radical alteration of behaviour. For example, when using *o*-vanillin as the carbonyl, the character of the metal salicylaldimine complexes as ligands is drastically changed, transforming them from bidentate to exceedingly effective tetradentate ligands (Torayama et al., 1997) that can form stable complexes where coordination takes place through N_2O_4 donor groups (Gaballa, Asker, Barakat, & Teleb, 2007). The use of tetradentate Schiff base complexes is increasingly signif cant for designing metal complexes related to synthetic and natural O_2 carriers.

Meta-phenylenediamine (MPD) has not been as commonly used as *ortho*-phenylenediamine (OPD) in the synthesis of azomethine ligands due to the distance between the nitrogen atoms of MPD and the molecule (Ramlee et al., 2010), hampering successful chelation to one metal centre within the same ligand. However, this feature enables the MPD derived salicylaldimines to obtain the formation of complexes containing two ligand moieties, that is, dimers, where the two azomethine moieties are bridged by two metal centres (El-Wahab, 2007; Hernández-Molina et al., 1997) forming dimeric dinuclear complexes. The distinctiveness of such behaviour however has rarely been applied and studied in the biological f eld, unlike complexes derived from the other two aromatic diamines namely, the *ortho-* and *para-* analogues. Dinuclear complexes are suggested to enhance biological activity when compared to mononuclear complexes due to the presence of double equivalence of metal ions (Kaczmarek, Pospieszna-Markiewicz, Kubicki, & Radecka-Paryzek, 2004), that are most often the active site.
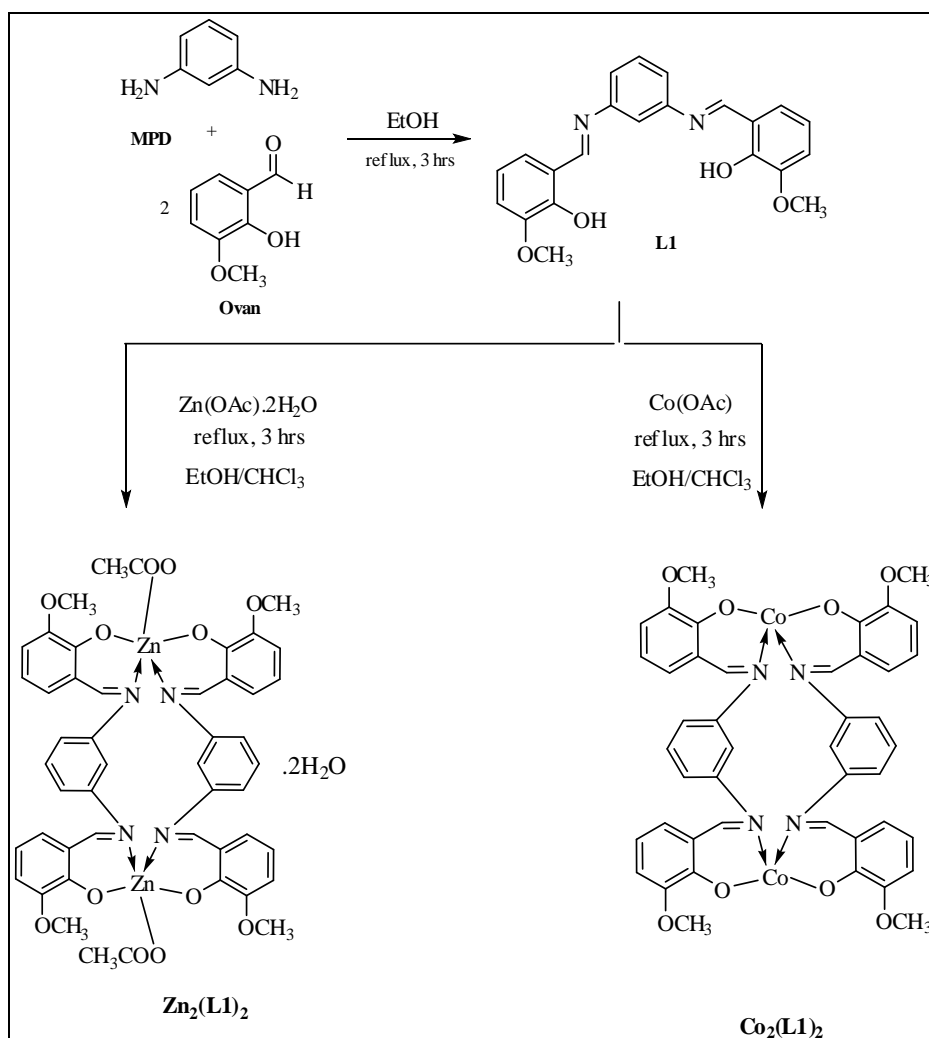
Figure 1. Reaction scheme for the synthesis of L and its dimeric dinuclear Zn(II) and Co(II) complexes

This paper reports the synthesis, characterisation and antibacterial studies of dinuclear Zn(II) and Co(II) complexes of symmetrical Schiff base ligand derived from *m*-phenylenediamine and *o*-vanillin, a salicylaldehyde derivative. The reaction scheme for the formation of the ligand L and its dimeric dinuclear Zn(II) and Co(II) complexes is illustrated in Figure 1.

MATERIALS AND METHODS

Materials

The solvents and reagents used in this research were ethanol, chloroform, dimethylsulfoxide (DMSO), *m*-phenylenediamine, *o*-vanillin (Ovan), cobalt(II) acetate tetrahydrate and zinc(II) acetate dihydrate. All chemicals were of analytical reagent grade purchased from Sigma Aldrich and used as received without prior purif cation.

Instrumentation

The microelemental analysis for C, H and N percentages were carried out on a Flash EA 110 Elemental Analyzer. Melting points of the ligand and complexes were determined in open capillary tubes using a BÜCHI Melting Point B-545 apparatus. ^{1}H NMR spectra for the free ligand and its diamagnetic zinc(II) complex were recorded on Bruker Avance 300 MHz as CDCl$_3$ solutions. Infrared (IR) spectra was recorded on Perkin Elmer 1600 Spectrometer in the 4000-400 cm^{-1} range. The magnetic susceptibility measurements of the complexes were performed using Sherwood Auto Magnetic Susceptibility Balance.

Synthesis

Synthesis of L ligand. *O*-vanillin and *m*-phenylenediamine were mixed in 2:1 in absolute ethanol, ref uxed and stirred under nitrogen for three hours. The orange precipitate which formed was f ltered off, rinsed with cold ethanol and dried in-vacuo over blue silica gel.

Synthesis of Co$_2$(L)$_2$ and Zn$_2$(L)$_2$ complexes. A reaction mixture containing a 1:1 molar ratio of the Co(II)/Zn(II) metal acetate salts with ligand L in chloroform was ref uxed and stirred under nirogen for three hours. The resulting precipitate of brick red Co$_2$(L)$_2$ and yellow Zn$_2$(L)$_2$ were f ltered off, washed with cold ethanol and dried under vacuum in a desiccator over blue silica gel. Recrystallisation was carried out from chloroform to afford reddish-brown and light yellow crystals, respectively. The air-sensitivity of Co$_2$(L)$_2$ hampered x-ray crystallography investigation at ambient conditions.

Antibacterial Study

An antibacterial screening against methicillin resistant *Staphylococcus aureus* (MRSA) was carried out using two methods.

Well diffusion method. The anti-bacterial property of L, Co$_2$(L)$_2$ and Zn$_2$(L)$_2$ was qualitatively evaluated using the well diffusion method as formerly reported by Gaballa Asker, Barakat and Teleb (2007). The samples were dissolved in DMSO with concentration of 10 µg/µl. Positive control experiments were carried out using commercially available standards, streptomycin and chloramphenicol.

Minimum inhibition concentration (MIC). The antibacterial activities of the ligand and complexes were investigated quantitatively using the minimum inhibitory concentration. A serial dilution method protocol was employed as described by Mohtar, Johari, Li, Isa, Mustafa, Ali and Basri. (2009) with slight modif cation where the microbial inoculums in the microtitre wells were directly exposed to the investigated compounds as pre-prepared solutions with serial concentrations of 4.5-0.04 ug/ulin DMSO. The lowest concentration which completely inhibited visible microbial growth was recorded as the minimum inhibition concentration. Streptomycin and chloramphenicol standards were used as positive controls.

RESULTS AND DISCUSSION

The condensation of the aromatic diamines m-phenylenediamine with o-vanillin resulted in the formation of the azomethineL: MPD(ovan)$_2$. Subsequently, the ligand L reactions with Co(II) and Zn(II) metal ions afforded the metal complexes $Co_2(L)_2$ and $Zn_2[(L)_2(OAc)_2].2H_2O$. The analytical data and the physical properties are shown in Table 1.

Table 1
Physical properties of L and Its metal complexes

Sample	Molecular formula	Molecular weight	Colour	Yield (%)	Melting point (°C)	Elemental analysis Found (Theoretical) (%)		
						C	H	N
L	$C_{22}H_{2}0N_2O_4$	376	Orange	72.2	129-131	69.95 (70.20)	5.61 (5.36)	7.42 (7.44)
$Co_2(L)_2$	$C_{44}H_{36}Co_2N_4O_8$	867	Brick red	29.2	>300	60.02 (60.98)	4.31 (4.19)	6.01 (6.46)
$Zn_2(L)_2$	$C_{48}H_{46}N_4O_{14}Zn_2$	1033	Yellow	16.6	>300	55.18 (55.77)	4.50 (4.49)	5.41 (5.42)

The elemental analysis results of $Co_2(L)_2$ and $Zn_2(L)_2$ indicate that both are dimeric dinuclear complexes.

^{1}H NMR Spectroscopy

The ^{1}H NMR spectroscopic data of the diamagnetic zinc complex is compared to that of the free L ligand as shown in Table 2.

The shifting of the azomethine carbon proton peaks in the complexes upon coordination indicates that the azomethine N is involved in bonding with Zn. The shift towards the upf eld region from 8.7 to 8.2 point out that the azomethine proton has become shielded with this coordination. The absence of the hydroxyl proton in the Zn(II) complex suggests that the hydroxyl groups underwent deprotonation in the complexation leaving the negatively charged oxygen to form ionic bonds with metal centres. Two new peaks are observed on the spectrum of the $Zn_2(L)_2$ complex, suggesting the existence of two acetate and two free water molecules (Silverstein & Webster, 1998) in the structure.

Table 2
^{1}H NMR data of L and its Zn(II) complexes

Sample	^{1}H NMR (ppm)					
	Azomethine proton (HC=N)	Hydroxyl proton (-OH)	Aromatic protons	Methoxyl protons (-OCH$_3$)	Free water proton (H$_2$O)	Acetate proton (CH$_3$COO)
L	8.7^s	13.5^s	7.5-6.9^m	3.9^s	-	-
Zn$_2$(L)$_2$	8.2^s	-	7.1-6.5^m	3.9^s	1.6^s	2.2^s

^{s}: singlet, ^{m}: multiplet

Infrared Spectroscopy

The mode of bonding between the ligands and the metal salts in complexes was examined by comparing the IR spectra of the complexes vs. that of the free ligand. Table 3 summarises the pertinent infrared peaks for the three compounds. L shows a strong band at 1616 cm^{-1} which is the characteristic peak for C=N, indicating successful formation of the azomethine. The peak shifted to lower frequencies of 1573-1613 cm^{-1} upon complexation with Co(II) and Zn(II), which means that the imine nitrogen atoms are involved in the chelation with the metal ions (Clarke et al., 1998), supporting the ^{1}H NMR data.

Similarly, the C-O stretching frequencies were observed to have shifted to lower frequencies from 1245 cm^{-1} in the ligand to a lower values of 12.44 and 1215 cm^{-1} in Zn$_2$(L)$_2$ and Co$_2$(L)$_2$, respectively. This indicates the participation of the oxygen atoms belonging to the phenolic hydroxyl group in the coordination to the metal ions (Golcu, Tumer, Demirelli, & Wheatley, 2005). However, the typically weak (M-N) and (M-O) peaks expected in the 600-400 cm^{-1} region (Tajuddin et al., 2017) were unable to be detected due to the presence of many f ngerprint peaks.

Table 3
Infrared and magnetic susceptibility data of L, Co$_2$(L)$_2$ and Zn$_2$(L)$_2$

Sample	Infrared peaks (cm^{-1})		u$_{eff}$ (B.M.)
	C=N stretch	C-O stretch	
L	1616	1245	-
Co$_2$(L)$_2$	1573	1215	4.07
Zn$_2$(L)$_2$	1606	1246	-

Magnetic Susceptibility

Co$_2$(L)$_2$ exhibited an effective magnetic moment, μ_{eff}, of 4.07B.M. (Table 3), slightly higher than that of the spin-only magnetic moment of three unpaired electrons (3.88 B.M.). The higher value suggested the presence of some orbital contribution to the magnetic moment values. There are two possibilities for the geometry of the 4-coordinate Co$_2$(L)$_2$ *viz*. tetrahedral or square planar. The presence of three unpaired electrons inferred by μeff value ruled out square planar geometry that would have only one unpaired electron as illustrated in the crystal f eld

splitting diagram shown in Figure 2. It is therefore suggested that the geometry of the Co(II) centres were tetrahedral.
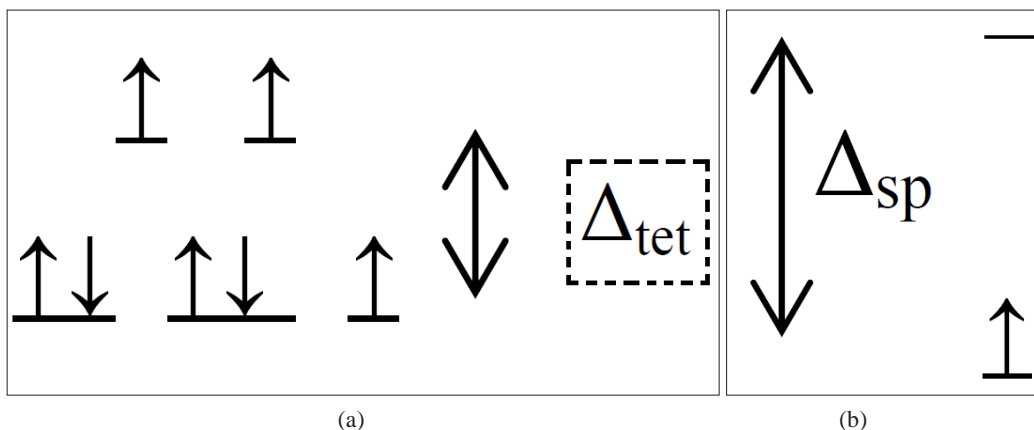
Figure 2. Crystal field splitting diagrams for Co(II) $3d7$ species in tetrahedral and square planar environments: (a) tetrahedral, 3 unpaired electrons; and (b) square planar, 1 unpaired electron

On the other hand, $Zn_2(L)_2$ showed diamagnetism, consistent with the 0 unpaired electrons of the d^{10} configuration.

Antibacterial Activity

The antibacterial screening against MRSA results revealed that the $Co_2(L)_2$ and $Zn_2(L)_2$ metal complexes were better bactericides than their parent ligand, L. The qualitative method indicated that the cobalt complex, with 15 mm inhibition zone, showed the highest activity (Table 4). However, quantitatively, with the lowest MIC of 0.56 µg/µl, the zinc complex exhibited a better antibacterial property than the cobalt complexes.

Table 4
Antibacterial activity of L, $Co_2(L)_2$ and $Zn_2(L)_2$ against methicillin resistant Staphylococcus Aureus (MRSA)

Compound	Antibacterial activity against MRSA	
	Inhibition Zone (mm)	MIC (µg/µl)
L	-	2.25
$Zn_2(L)_2$	12	0.56
$Co_2(L)_2$	15	1.13

Complexes are usually more bioactive than their parent ligand due to the presence of metal centres that are said to be the active sites for their bioactivity. Tweedy's chelation theory clarifies that in complexes, as opposed to plain inorganic salts, the polarity of the metal ion is reduced due to the overlapping of the ligand orbitals and partial sharing of positive charge of metal ion with the donor groups. This increases the delocalization of -electrons over the whole

chelate ring which in turn, augments the liphophilicity and improves the cell permeability of the complexes (Priya, Arunachalam, Manimaran, Muthupriya, & Jayabalakrishnan, 2009).

According to the same theory, once the complexes penetrate into the cells, they can restrict the normal cell processes by blocking the metal binding sites on enzymes of the microorganism or interrupt the respiration process of the cell and thus, stopping the synthesis of protein which retards further growth of the organism (Priya et al., 2009). There are also other contributing factors attributing to the increased bioactivity of metal complexes such as solubility, conductivity and dipole moment due to the presence of metal ions in the system (Emara, 2010).

CONCLUSION

Dinuclear Zn(II) and Co(II) complexes are successfully synthesised and characterised by elemental analysis, infrared spectroscopy, ^{1}H NMR spectroscopy, melting point and magnetic susceptibility measurements. The metal centres are indicated to adopt tetrahedral geometry, bridging two moieties of the ligand L. From the preliminary screening, it is observed that the Zn(II) complex exhibits better antibacterial properties against methicillin resistant *Staphylococcus Aureus* (MRSA) than its Co(II) analogue and the parent ligand.

ACKNOWLEDGMENTS

REFERENCES

Abdul Ghani, A., Bahron, H., Harun, M. K., & Kassim, K. (2014). Schiff bases derived from Isatin as mild steel corrosion inhibitors in 1 M HCl, *Malaysian Journal of Analytical Sciences, 18*(3), 507-513

Amirnasr, M., Schenk, K. J., Gorji, A., & Vafazadeh, R. (2001). Synthesis and spectroscopic characterization of [CoIII(salophen)(amine)$_2$]ClO$_4$ (amine = morpholine, pyrrolidine and piperidine) complexes. The crystal structures of [CoIII(salophen)(morpholine)$_2$]ClO$_4$ and [CoIII(salophen)(pyrrolidine)$_2$]ClO$_4$. *Polyhedron, 20*, 695-702.

Clarke, B., Clarke, N., Cunningham, D., Higgins, T., McArdle, P., Cholchúin, M. N., et al. (1998). Transition-metal schiff-base complexes as ligands in tin chemistry. Part 7. Reactions of organotin(IV) Lewis acids with [M(L)]$_2$ [M = Ni, Cu and Zn; H$_2$L = N, N'-bis (3-methoxysalicylidene) benzene-1,3-diamine and its -1,4-diamine analog]. *Journal of Organometallic Chemistry, 559*, 55-64.

El-Wahab, Z. H. A. (2007). Mononuclear metal complexes of organic carboxylic acid derivatives: Synthesis, spectroscopic characterization, thermal investigation and antimicrobial activity. *Spectrochimica Acta Part A: Molecular and Biomolecular Spectroscopy, 67*(1), 25-38.

Emara, A. A. A. (2010). Structural, spectral and biological studies of binuclear tetradentate metal complexes of N₃O Schiff base ligand synthesized from 4,6-diacetylresorcinol and diethylenetriamine. *Spectrochimica Acta Part A: Molecular and Biomolecular Spectroscopy, 77*, 117-125.

Gaballa, A. S., Asker, M. S., Barakat, A. S., & Teleb, S. M. (2007). Synthesis, characterization and biological activity of some platinum(II) complexes with Schiff bases derived from salicylaldehyde, 2-furaldehyde and phenylenediamine. *SpectrochimicaActa Part A: Molecular and Biomolecular Spectroscopy, 67*, 114-121.

Golcu, A., Tumer, M., Demirelli, H., & Wheatley, A. (2005). Cd(II) and Cu(II) complexes of polydentate Schiff base ligands: Synthesis, characterization, properties and biological activity. *Inorganica Chimica Acta, 358*, 1785-1797.

Hernández-Molina, R., Mederos, A., Gili, P., Domínguez, S., Lloret, F., Cano, J., ... & Solans, X. (1997). Dimer species in dimethyl sulfoxide–water (80: 20 w/w) solution of N, N -bis (salicylideneimine)-m-phenylenediamine (H 2 sal-m-phen) and similar Schiff bases with Cu II, Ni II, Co II and Zn II. Crystal structure of [Co2 (sal-m-phen) 2]· CHCl3. *Journal of the Chemical Society, Dalton Transactions, (22)*, 4327-4334.

Kaczmarek, M. T., Pospieszna-Markiewicz, I., Kubicki, M., & Radecka-Paryzek, (2004). Novel lanthanide salicylaldimine complexes with unusual coordination mode. *Inorganic Chemistry Communications, 7*, 1247-1249.

Mohtar, M., Johari, S. A., Li, A. R., Isa, M. M., Mustafa, S., Ali, A. M., & Basri, D. F. (2009). Inhibitory and resistance-modifying potential of plant-based alkaloids against methicillin-resistant Staphylococcus aureus (MRSA). *Current Microbiology, 59*(2), 181-186.

Priya, N. P., Arunachalam, S., Manimaran, A., Muthupriya, D., & Jayabalakrishnan, C. (2009). Mononuclear Ru(III) Schiff base complexes: Synthesis, spectral redox, catalytic and biological activity studies. *SpectrochimicaActa Part A: Molecular and Biomolecular Spectroscopy, 72*, 670-676.

Ramlee, N., Bakar, S. N. A., Bahron, H., Harun, M. K., Kassim, K., & Yahya, M. Z. A. (2010, December). Interaction of Schiff bases and their corresponding amines and aldehyde with mild steel surface in 1.0 M hydrochloric acid solution. In *Science and Social Research (CSSR), 2010 International Conference on* (pp. 451-456). IEEE.

Shakir, M., Azim, Y., & Parveen, S. (2006). Synthesis, characterization of complexes Co(II), Ni(II), Cu(II) and Zn(II) with 12-membered schiff base tetraazamacrocyclic ligand and the study of their antibacterial and reducing power. S*pectrochimicaActa Part A: Molecular and Biomolecular Spectroscopy, 65*, 490-496.

Silverstein, R. M., & Webster, F. X. (1998). *Spectrometric identif cation of organic compounds* (6th edition). John Wiley and Sons, Inc.

Tajuddin, A. M., El Hassane, A., Ramasamy, K., Yamin, B. M., Alharthi, A. I., & Bahron, H. (2017). DFT analysis and bioactivity of 2-((E)-(4-methoxybenzylimino) methyl) phenol and its Ni(II) and Pd(II) complexes, *Arabian Journal of Chemistry, 10*, 769-780.

Torayama, H., Nishide, T., Asada, H., Fujiwara, M. & Matsushita, T., (1997). Preparation and characterization of novel cyclic tetranuclearmanganese(III) complexes: MnIII4(X-salmphen)6 (X-salmphenH2 = N,N'-disubstituted-salicylidene-1,3-diaminobenzene (X=H, 5-Br)). *Polyhedron, 16* (21), 3787-3794.

Bioconversion of Leachate to Acetic and Butyric Acid by *Clostridium butyricum* NCIMB 7423 in Membrane Fermentor

Othman, M. F.[1], Tamat, M. R.[1], Wan Nadiah, W. A.[1], Serri, N. A.[1], Aziz, H. A.[2,3] and Tajarudin, H. A.[1,3]*

[1]*School of Industrial Technology, Universiti Sains Malaysia (USM), 11800 Minden, Pulau Pinang, Malaysia*
[2]*School of Civil Engineering, Engineering Campus, Universiti Sains Malaysia (USM), 14300 Nibong Tebal, Pulau Pinang, Malaysia*
[3]*Solid Waste Management Cluster, Engineering Campus, Universiti Sains Malaysia (USM), 14300 Nibong Tebal, Pulau Pinang, Malaysia*

ABSTRACT

Landf ll leachate imposes a huge problem to the environment and human beings. This work focused on bioconversion of leachate to acetic and butyric acids by *Clostridium butyricum* NCIMB 7423. A continuous stirred tank reactor (CSTR) was applied and connected to fabricate membrane module. The leachate was collected from Pulau Burung Landf ll Site (PBLS), Nibong Tebal, Penang. Prior to fermentation, leachate was treated to remove volatile fatty acid and adjusted to meet the minimum requirement of nutrients for anaerobic fermentation. Synthetic medium fermentation acts as a benchmark to the leachate fermentation. The outcomes indicated that the yield of acetic acid and butyric acid in synthetic medium fermentation was 0.70 g/L and 0.71 g/L, respectively. Meanwhile, leachate fermentation showed that the yield of acetic and butyric acid was 0.93 g/L and 1.86 g/L, respectively. High production of acetic and butyric acid showed that leachate fermentation is a green alternative to produce a cleaner product.

Keywords: Anaerobic, bioreactor, *C. butyricum*, fermentation, waste to wealth

INTRODUCTION

Equally, one of the aggressively developing countries in Asia, Malaysia faces the problem of solid waste disposal. A survey by the Malaysian government in 2013 shows that each day, a person produces 800 g of solid waste. On the other hand, those who dwell in the urban area produce 1.25 kg of waste per person daily. The government has estimated

that in 2013, Malaysian would be producing 30,000 to 33,000 tonnes of solid wastes a day. These amounts were alarming because, in the current situation, these had already exceeded the government's projection of 30,000 tonnes of solid waste daily for 2020 (Ismail, 2014). Waste disposal via landfll is the main method of disposal of municipal solid waste (MSW) in Malaysia (Abas & Wee, 2014).

Leachate is the main issue that links to the open landfll disposal. It is a percolated liquid from sanitary landfll (S. Q. Aziz, H. A. Aziz, Yusoff, Bashir, & Umar, 2010). It is reported that the leachate contains various contaminants such as organic materials, ammonia, heavy metals, phenol, nitrogen, and phosphorus. Various researchers constantly report that leachate contains these contaminant and imposes a great impact on an environment (Christensen et al., 2001; Kjeldsen et al., 2002; Ozturk, Altinbas, Koyuncu, Arikan, & Gomec-Yangin, 2003; Aziz, Adlan, Zahari, & Alias, 2004; Salem, Hamouri, Djemaa, & Allia, 2008; S. Q. Aziz, Yusoff, H. A. Aziz, Umar, & Bashir, 2009, Umar, Aziz, & Yusoff, 2010; Wang, Huang, Feng, Xie, & Liu, 2010; Kamaruddin, Yusoff, Aziz, & Basri, 2013; Raghab, Abd El Meguid, & Hegazi, 2013; S. Q. Aziz, H. A. Aziz, Bashir, & Mojiri, 2015). The issues on leachate treatment have existed for quite some time, but a universal solution has yet to be found (Wiszniowski, Robert, Surmacz-Gorska, Miksch, & Weber, 2006). Leachate treatment can be divided into aerobic treatment and anaerobic treatment. Aerobic treatment is a treatment of leachate in the presence of oxygen. In this process, the microorganisms will generate energy through enzyme-mediated electron transport using molecular oxygen as anelectron acceptor (Environmental Protection Agency, 2000). There are many types of aeration treatments, such as activated sludge reactor, rotating biological contactor (RBC) and aerated lagoons.

Anaerobic process is slightly different from the aerobic process where no oxygen is required. Electron acceptors in this process are inorganic compounds such as nitrate, sulphate and carbon dioxide (Environmental Protection Agency, 2000). The Environmental Protection Agency (2000) states that anaerobic process provides several benefts such as low sludge production, low energy demand (no oxygen required) and recovery of methane may provide energy. Anaerobic process is an effective process, but the remaining of BOD and COD are still high and at the end, leachate still needs to be treated with means of aerobic process to meet the effuent standard (Stegmann, Heyer, & Cossu, 2005).

The cost to treat leachate is a great barrier in the current situation. Leachate is not a proftable commodity, but the governments around the world need to spend a lot of annual expenditure to treat leachate. To date, lack of report has been published to turn the table around by making a proft from leachate, whilst at the same time attempting to treat this contaminant. The objective of this study is to implement membrane bioreactor in leachate treatment and at the same time produce a valuable product. This novelty treatment could solve a problem in leachate treatment and reduce the cost burden by the government.

Clostridium is a strictly anaerobic and gram-positive bacteria. Their morphology is cylindrical-shape (Szymanowska-Powalowska, Orczyk, & Leja, 2014). *Clostridium* is a spore-forming bacteria and strains can be isolated from soil, wastewater, animal digestive systems, and contaminated dairy products (Zigov & Sturdik, 2000). *Clostridium butyricum* can utilize a variety of carbohydrate from mono to disaccharides and complex polysaccharides which

include glucose, lactose from whey, sucrose from molasses, starch, potato wastes, wheat f our, cellulose or dextrose (Bahl & Dürre, 2001; Kong, He, Chen, & Ruan, 2006; Tracy, Jones, Fast, Indurthi, & Papoutsakis, 2012; Azan, Lovitt, Nur, & Azwa, 2013).

The novelty of this research lies in the fact, to date no research has been documented on the treatment of leachate by using *C. butyricum* and at the same time producing a valuable product. The result of this research enables the understanding in leachate treatment as well as opening more possibilities for green and sustainable practices.

MATERIALS AND METHOD

C. butyricum National Collection of Industrial, Food and Marine Bacteria (NCIMB) 7423 which was used in this study was purchased from NCIMB Ltd. (Aberdeen, Scotland, United Kingdom). The medium formulation for *C. butyricum* NCIMB 7423 culture consisted of 10 g/L of glucose, 10 g/L of yeast extract, 5 g/L of di-potassium hydrogen phosphate, 10 g/L of ammonium phosphate, and 1 ml/L of 0.05% resazurin (Azan, Lovitt, Nur, & Azwa, 2013). All chemicals used were of analytical grade. The medium was prepared and adjusted to pH 6.5 (pH 2700, Eutech Instruments, USA) before being transferred into 50 ml or 100 ml serum bottles. The serum bottle was prepared using Hungate Method (Wolfe, 2011).

Leachate was collected from Pulau Burung Landfill Site (PBLS), situated within Byram Forest Reserve at 5º 24' N Latitude, 100º 24' E Longitude in Nibong Tebal, Penang (Aghamohammadi et al., 2007). A total of 125 L leachate was collected from the site. Approximately, 200 ml of raw leachate was taken for analysis to check for Biological Oxygen Demand (BOD), Chemical Oxygen Demand (COD), total volatile acid, and total carbohydrate. Leachate was pre-treated in a perspex column (diameter: 142 mm, height: 1200 mm) with 5 kg of limestone to remove volatile fatty acid as *C. butyricum* growth is inhibited by volatile fatty acid. Then, leachate was adjusted by adding glucose (4.18 g/L) to meet the minimal requirement of C:N for anaerobic fermentation (250:5) (Ammary, 2004) prior to fermentation.

A 2.5 L bioreactor (Minifors, Infors HT, Switzerland) with working volume up to 1.7 L was used in this study. The reactor was connected to the ceramic membrane assembly. The ceramic membrane used in this study was supplied by National University of Singapore (NUS). The f at sheet membrane with a size of 30.34 cm × 11.00 cm, had a pore size of 0.22 µm and was encapsulated in a fabricated stainless steel container. The inoculum was 10 L and prepared in a 12 L vessel using the synthetic medium for both synthetic and leachate medium fermentation. The inoculum was f ltered using a membrane and the concentrated cell was used at the beginning of fermentation by adding fresh medium. For leachate fermentation, the medium used was only treated leachate with added glucose.

Sampling was carried out on an hourly basis. Sampling for both fermentations was the same. A total of 4 ml culture was removed from the sampling line and discarded, then 4 ml of culture was taken from the vessel. The sample was stored in the freezer at -20°C prior to analysis. Acetic and butyric acid content were measured using gas chromatography (GC). The method was carried out according to Standard Methods for the Examination of Water and Wastewater (American Public Health Association et al., 2005).

RESULTS AND DISCUSSION

The prof le for leachate taken from Pulau Burung Landf ll Site (PBLS) is tabulated in Table 1.

Table 1
Prof le for raw and pretreated leachate of Pulau Burung Landf ll Site (PBLS)

Analysis	Unit	Raw Leachate	Pretreated Leachate*
BOD	mg/L	N.D.	477.25
COD	mg/L	N.D.	794.00
Total volatile acid	mg/L	70.00	62.00
Total carbohydrate	g/L	0.16	0.16

N.D.: Not determined
*Treated by exposure to limestone for 30 minutes

From Table 1, the BOD of PBLS leachate after limestone pretreatment was 477.25 mg/L, exceeded the discharge limit. The leachate must undergo intensive treatment in order to surpass the stated discharge limit. The range of BOD measured by Aziz et al., (2009) for PBLS leachate was in the range of 67-93 mg/L, while a range of 252-730 mg/L was recorded earlier by Aghamohammadi et al. (2007).

The Chemical Oxygen Demand (COD) value for leachate after the pretreatment was 794 mg/L. The COD for PBLS leachate was reported to be in the range of 600-1300 mg/L by Aziz et al., (2010); the discharge limit is 100 mg/L (Ministry of Science and Environment, 1979). Again, the values reaff rmed that this leachate needed treatment before it could be discharged into the river. The BOD/COD ratio of the current leachate was 0.6. The values were in the range of 0.043-0.67 as reported by various researchers (Aziz et al., 2010). It was also stated that low BOD/COD value indicates that the leachate is stable and hard to treat biologically.

The volatile fatty acid (VFA) content in the current leachate was 70 mg/L. After subjected to limestone pretreatment, the VFA content reduced to 62 mg/L which accounted for 11.4% of reduction. *C. butyricum* NCIMB 7423 growth was inhibited by the VFA, including acetic and butyric acid, hence the VFA content needed to be lowered prior to fermentation. The f gure may not be much but it was capable of sustaining the growth of *C. butyricum* NCIMB 7423 while preserving all nutrients and organic material that was crucial for bacterial growth. The details of the adsorption study were not considered as part of the current research since the main focus was only to obtain leachate that could sustain the growth of *C. butyricum* NCIMB 7423.

The introduction of membrane separation to the fermentation vessel can theoretically solve the problem during downstream processing which is costly and not energy eff cient. To date, anaerobic membrane bioreactor is still in development and utilized particularly to treat low strength wastewater (Gao et al., 2010). The synthetic medium membrane fermentation was used as a benchmark to compare against leachate membrane fermentation. The membrane fermentation of *C. butyricum* NCIMB 7423 was achieved by connecting the membrane module to the stirred tank reactor. This set-up was reported by a researcher, but with different substrate (glycerol) (Szymanowska-Powałowska & Leja, 2014).

Figure 1(a) shows the growth curve of *C. butyricum* NCIMB 7423 on synthetic medium. From the f gure, it can be observed that the fermentation duration was long (23 h) before *C. butyricum* NCIMB 7423 biomass started to decline. The membrane fermentation did not experience lag phase, and biomass was accumulated from the instantaneous separation of cells from the acetic and butyric acid produced, preventing inhibition by the products formed. The maximum biomass achieved by current fermentation was 0.29 g/L with 0.05 h^{-1} of specif c growth rate. The biomass could be further increased, but the membrane had started to foul at biomass concentration of 0.29 g/L, resulting in membrane blockage.

Meanwhile, Figure 1(b) shows the membrane fermentation of altered-leachate. The fermentation condition was similar to that of the synthetic medium. The fermentation period was incredibly short compared to that of the synthetic medium fermentation. A specif c growth rate of 0.33 h^{-1} was obtained, and the highest biomass achieved was 0.29 g/L, after which the membrane started to foul. The results suggest that *C. butyricum* NCIMB 7423 grew far more favorably in altered-leachate compared to synthetic medium. The short fermentation time may be due to high nutrient content in leachate, carbohydrate supply from the added glucose, and continuous withdrawal of acetic and butyric acids from the fermentation vessel. The possibilities of membrane altered-leachate fermentation were broad because high biomass can be attained in a short period of time.

Foulant layer which consists of extracellular polymeric substances (EPS) and microbial cells contributes to membrane fouling. Gao et al. (2010) claim that the accumulation of EPS reduces the effective pore size in the membrane and increases proportional resistance to permeate f ux. In addition, they emphasize that the membrane fouling results in reducing membrane lifespan and membrane permeate f ux. Consequently, the accumulation of acetic and butyric acid resulted in inhibiting the growth of *C. butyricum* NCIMB 7423.
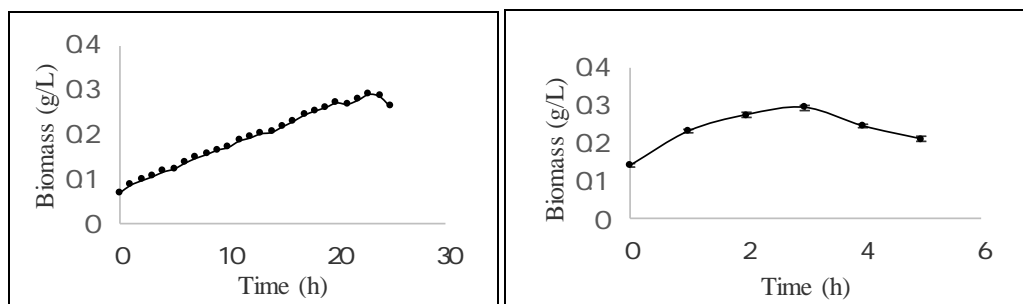
Figure 1. The growth curve of *C. butyricum* NCIMB 7423 in: (a) synthetic medium; and (b) altered-leachate. Data point are mean ± standard deviation (*n*=3)

For the acid production, Figure 2 shows the trends of acetic and butyric acid production throughout the 25 h fermentation using synthetic medium and altered-leachate medium.The concentrations of acetic and butyric acid were constant throughout fermentation. It should be noted that the fermentation sampling point was from the main vessel (level of acetic and butyric were maintained) and not from the permeate collection bottle (accumulation of acetic and butyric acid). The clear f uid could be observed at the permeate collection bottle which indicated that only product and liquid passed through.
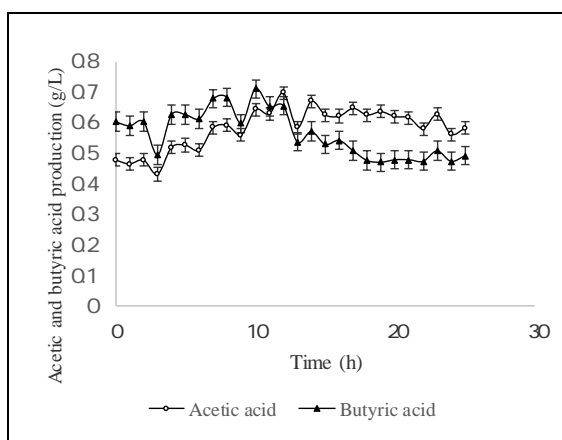
(a)
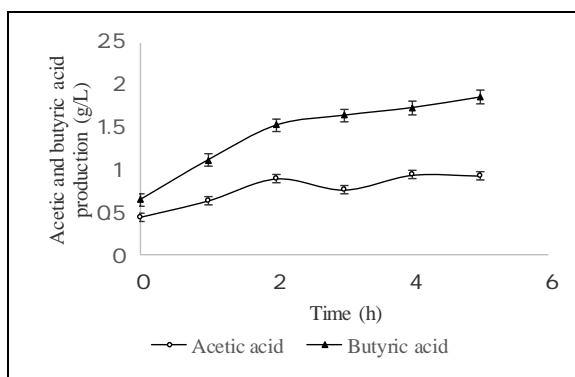
(b)

Figure 2. Acetic and butyric acid production by *C. butyricum* NCIMB 7423 in: (a) synthetic medium; (b) and altered-leachate medium

Using synthetic medium, for the f rst 11 h, the production of butyric acid exceeded the production of acetic acid (Figure 2(a)). This condition was favorable because of the high commercial value of butyric acid compared to acetic acid. From 12 h onwards, the production of butyric acid seemed to have reduced while production of acetic acid increased. According to Saint-Amans, Girbal, Andrade, Ahrenss and Soucaille (2001), the product of *C. butyricumis* not regulated at the genetic level, but at the enzyme level which is directly affected by the substrate concentration thus explaining the sudden changes in acid production. The highest production of acetic and butyric acid recorded in the fermentation vessel was 0.70 g/L and 0.71 g/L, respectively. It verif es that both acids were removed continuously from the fermentation vessel.

The highest productions of acetic and butyric acid by *C. butyricum* NCIMB 7423 in altered-leachate membrane fermentation were 0.93 g/L and 1.86 g/L, respectively (Figure 2(b)). The current production was higher compared to that produced during synthetic medium fermentation. Throughout the fermentation (from 0 h to 5 h), butyric acid production was higher than acetic acid. Figure 2(b) shows that the concentration of acetic and butyric acid

increased steadily, suggesting that the membrane was slowly starting to foul because of the high biomass of *C. butyricum* NCIMB 7423 resulting in accumulation of acetic and butyric acid in the fermentation vessel. The current f ndings are favorable as the production of both acids exceeded that produced in the synthetic medium at a faster rate.

CONCLUSION

The current study successfully demonstrates the production of acetic and butyric acid in leachate using membrane reactor. The results show acetic (0.93 g/L) and butyric acid (1.86 g/L) were highly produced in altered-leachate compared to acetic (0.70 g/L) and butyric acid (0.71 g/L) in synthetic medium. These f ndings open a revolutionary way to biologically treat landf ll leachate and at the same time, taking advantage of the treatment.

ACKNOWLEDGEMENTS

REFERENCES

Abas, M. A. & Wee, S. T (2014). Municipal Solid Waste Management in Malaysia: An Insight Towards Sustainability, in 4th International Conference on Human Habitat and Environment 2014. United Kingdom.

Aghamohammadi, N., Hamidi, A. A., Hasnain, I. M., Zinatizadeh, A. A., Nasrollahzadeh Saravi, H., & Ghafari, S.(2007). Performance of a Powdered Activated Carbon (PAC) Augmented Activated Sludge Process Treating Semi-Aerobic Leachate. *Int. J. Environ. Res. 1*, 96–103.

American Public Health Association, American Water Works Association, Water Environment Federation, American Public Health Association (APHA), A.W.W.A. (AWWA) & W.E.F. (WEF) (2005). *Standard Methods for the Examination of Water and Wastewater* 21st Edition, Standard Methods.

Ammary, B. Y. (2004). Nutrients Requirements in Biological Industrial Wastewater Treatment. *African J. Biotechnol. 3*, 236–238.

Azan, H. T., Lovitt, R. W., Nur, K. T., & Azwa, N. M. B. (2013). A Study of Fatty Acid Production in the Batch Reactor via the Carbohydrate Fermentation by *Int. J. Biol. Biomol. Agric. Food Biotechnol. Eng.7*, 828–833.

Aziz, H. A., Adlan, M. N., Zahari, M. S. M., & Alias, S. (2004). Removal of Ammoniacal Nitrogen (N-NH3) from Municipal Solid Waste Leachate by using Activated Carbon and Limestone. *Waste Manag. Res.22*, 371–375.doi:10.1177/0734242X04047661

Aziz, H. A., Yusoff, M. S., Aziz, S. Q., Umar, M., & Bashir, M. J. (2009). A leachate quality at Pulau Burung, Kuala Sepetang and Kulim landf lls-A comparative study. In *Proceedings Civil Engineering Conference (AWAM 09), ISBN* (pp. 978-983).

Aziz, S. Q., Aziz, H. A., Bashir, M. J. K., & Mojiri, A. (2015). Assessment of Various Tropical Municipal

Landfll Leachate Characteristics and Treatment Opportunities. *Glob. NEST J. 17*, 439–450.

Aziz, S. Q., Aziz, H. A., Yusoff, M. S., Bashir, M. J. K., & Umar, M., (2010). Leachate Characterization in Semi-Aerobic and Anaerobic Sanitary Landflls: A Comparative Study. *J. Environ. Manage. 91*, 2608–2614. doi:10.1016/j.jenvman.2010.07.042

Bahl, H., & Dürre, P., (2001). Clostridia: Biotechnology and Medical Applications. doi:10.1002/3527600108

Christensen, T. H., Kjeldsen, P., Bjerg, P. L., Jensen, D. L., Christensen, J. B., Baun, A., Albrechtsen, H., & Heron, G. (2001). Biogeochemistry of Land Leachate Plumes. *Appl. Geochemistry 16*, 659–718.

Environmental Protection Agency. (2000). Wastewater Technology Fact Sheet, Environmental Protection Agency. United States. doi:EPA 832-F-99-062

Gao, D. W., Zhang, T., Tang, C. Y. Y., Wu, W. M., Wong, C. Y., Lee, Y. H., Yeh, D. H., & Criddle, C. S. (2010). Membrane Fouling in an Anaerobic Membrane Bioreactor: Differences in Relative Abundance of Bacterial Species in the Membrane Foulant Layer and in Suspension. *J. Memb. Sci. 364*, 331–338. doi:10.1016/j.memsci.2010.08.031

Ismail, I. (2014). Malaysians Producing More Solid Waste than Before. Malay Mail Online.

Kamaruddin, M. A., Yusoff, M. S., Aziz, H. A., & Basri, N. K. (2013). Removal of COD, Ammoniacal Nitrogen and Colour from Stabilized Landfll Leachate by Anaerobic Organism. *Appl. Water Sci. 3*, 359–366. doi:10.1007/s13201-013-0086-1

Kjeldsen, P., Barlaz, M. A., Rooker, A. P., Baun, A., Ledin, A., & Christensen, T. H. (2002). Present and Long-Term Composition of MSW Landfll Leachate: A Review. *Crit. Rev. Environ. Sci. Technol. 32*, 297–336. doi:10.1080/10643380290813462

Kong, Q., He, G. Q., Chen, F., & Ruan, H., (2006). Studies on a Kinetic Model for Butyric Acid Bioproduction by *Clostridium butyricum.*Lett. *Appl. Microbiol. 43*, 71–77. doi:10.1111/j.1472-765X.2006.01902.x

Ministry of Science, Technology and Environment. (1979). Environmental Quality (Sewage and Industrial Effuents) Regulations, 1979, Environmental Quality Act. Malaysia.

Ozturk, I., Altinbas, M., Koyuncu, I., Arikan, O., & Gomec-Yangin, C. (2003). Advanced Physico-Chemical Treatment Experiences on Young Municipal Landfll Leachates. *Waste Manag. 23*, 441–446. doi:10.1016/S0956-053X(03)00061-8

Raghab, S. M., Abd El Meguid, A. M., & Hegazi, H. A. (2013). Treatment of Leachate from Municipal Solid Waste Landfll. *HBRC J. 9*(2), 187–192. doi:10.1016/j.hbrcj.2013.05.007

Saint-Amans, S., Girbal, L., Andrade, J., Ahrens, K., & Soucaille, P. (2001). Regulation of Carbon and Electron Flow in *Clostridium butyricum* VPI 3266 Grown on Glucose-Glycerol Mixtures. *J. Bacteriol. 183*, 1748–1754. doi:10.1128/JB.183.5.1748

Salem, Z., Hamouri, K., Djemaa, R., & Allia, K. (2008). Evaluation of Landfll Leachate Pollution and Treatment. *Desalination 220*, 108–114. doi:10.1016/j.desal.2007.01.026

Stegmann, R., Heyer, K., & Cossu, R.(2005). Leachate Treatment, in:Tenth International Waste Management and Landfll Symposium. CISA, Environmental Sanitary Engineering Centre, Italy, Cagliari.

Szymanowska-Powałowska, D., & Leja, K.(2014). An Increasing Of The Effciency Of Microbiological

Synthesis of 1,3-Propanediol from Crude Glycerol by the Concentration of Biomass. *Electron. J. Biotechnol. 17*, 72–78. doi:10.1016/j.ejbt.2013.12.010

Szymanowska-Powalowska, D., Orczyk, D., & Leja, K. (2014). Biotechnological Potential of *Clostridium butyricum* Bacteria. *Brazilian J. Microbiol. 45*, 892–901. doi:10.1590/S1517-83822014000300019

Tracy, B. P., Jones, S. W., Fast, A. G., Indurthi, D. C., & Papoutsakis, E. T. (2012). Clostridia: The Importance of Their Exceptional Substrate and Metabolite Diversity for Biofuel and Bioref nery Applications. *Curr. Opin. Biotechnol. 23*, 364–381. doi:10.1016/j.copbio.2011.10.008

Umar, M., Aziz, H. A. & Yusoff, M. S. (2010). Variability of Parameters Involved in Leachate Pollution Index and Determination of LPI from Four Landf lls in Malaysia 2010. doi:10.1155/2010/747953

Wang, Z. P., Huang, L. Z., Feng, X. N., Xie, P. C., & Liu, Z. Z. (2010). Removal of Phosphorus in Municipal Landf ll Leachate by Photochemical Oxidation Combined with Ferrate Pre-Treatment. *Desalin. Water Treat. 22*, 111–116 ST–Removal of phosphorus in municipal l. doi:10.5004/dwt.2010.1633

Wiszniowski, J., Robert, D., Surmacz-Gorska, J., Miksch, K., & Weber, J. V. (2006). Landf ll leachate Treatment Methods: A Review. *Environ. Chem. Lett. 4*, 51–61. doi:10.1007/s10311-005-0016-z

Wolfe, R. S. (2011). *Techniques for Cultivating Methanogens, 1st ed, Methods in Enzymology*. Elsevier Inc. doi:10.1016/B978-0-12-385112-3.00001-9

Zigova, J., & Šturdík, E. (2000). Advances in Biotechnological Production of Butyric Acid. *Journal of Industrial Microbiology and Biotechnology, 24*(3), 153-160.

Anti-inf ammatory Effects of High-Density Lipoprotein via Regulation of Nitric Oxide Synthase Expression and Nf- b Transcription in Activated Human Endothelial Cells

Wan Norhasanah Wan Yusoff¹, Yung-An Chua¹,
Gabriele Ruth Anisah Froemming¹,², Abdul Manaf Ali³ and Hapizah Nawawi¹*

¹Institute of Pathology, Laboratory and Forensic Medicine (I-PPerForM) and Faculty of Medicine,
Universiti Teknologi MARA (UiTM), Sungai Buloh Campus, 47000 Sungai Buloh, Selangor, Malaysia
²Faculty of Medicine and Health Sciences, Universiti Malaysia Sarawak (UNIMAS), 94300 Kota Samarahan,
Sarawak, Malaysia
³School of Agriculture Science and Biotechnology, Faculty of Biosources and Food Industry,
Universiti Sultan Zainal Abidin (UNISZA), Tembila Campus, 22200 Besut, Terengganu, Malaysia

ABSTRACT

Oxidation of low-density lipoprotein (LDL) and activation of the transcription factor nuclear factor kappa-light-chain-enhancer of activated B cells (NF- B) are critical for the inf ammatory response for endothelial dysfunction. The objective of this study is to investigate the effects of various doses of HDL on: (a) LDL susceptibility to oxidation; (b) expression of eNOS; and (c) expression of NF- B p50 and p65. Different concentrations of HDL were incubated in LDL. The reaction rates of LDL susceptibility to oxidation were obtained by kinetic modeling analysis. For determination of eNOS, NF- B p50 and p65 expression, different HDL concentrations were incubated in lipo polysacharides (LPS)-stimulated human umbilical vein endothelial cell line for 16 hours. Protein was extracted and analysed by western blot and nuclear transcription factor, for example, Co-incubation of LDL with increasing HDL concentrations showed longer lag time and lower reaction rate in a dose-dependent manner compared to controls ($p < 0.05$). The eNOS expression at higher HDL concentration was signif cantly increased when compared to controls ($p < 0.05$). HDL signif cantly decreased the expression of NF- B p65 but not that of NF- B p50. HDL protects LDL from oxidation, up regulates eNOS expression and down regulates the expression of NF- B p65. These in part contribute to the role of HDL in the prevention and retardation of atherogenesis and atherosclerosis-related complications.

Keywords: eNOS, NF- B, endothelial cells, HDL, LDL oxidation, protein expression

Wan Norhasanah Wan Yusoff, Yung-An Chua, Gabriele Ruth Anisah Froemming, Abdul Manaf Ali
and Hapizah Nawawi

INTRODUCTION

Coronary heart disease (CHD) is the major cause of premature death in most populations including Malaysia. It is an important source of disability and substantially contributes to the escalating costs of health care. The commonest underlying pathology is atherosclerosis, which is a major cause of morbidity and mortality in the world (Roger, et al., 2012). It develops insidiously over time and is usually already in advance stage by the time the cardiovascular symptoms occur. Currently, a lot of evidence points at oxidative stress and inf ammation as the precursor of atherogenesis (Hajjar & Gotto, 2013). High-density lipoprotein (HDL) plays an important role against the development of atherosclerosis and CHD. HDL is responsible in reverse cholesterol transport (Rothblat & Phillips, 2010), acts as an antioxidant (Kontush & Chapman, 2010), and regulates endothelial functions through its anti-inf ammatory property (Säemannet et al., 2010), promotes nitric oxide synthase (eNOS) and activation (Mineo & Shaul, 2012b).

Oxidative stress and low-density lipoprotein (LDL) cholesterol oxidation are key factors in the pathogenesis of atherosclerosis. Peroxidation of LDL is known to be the f rst step in the development of atherosclerosis (Bekkering et al., 2014; Esterbauer, Striegl, Puhl, & Rotheneder, 1993). It is postulated that in oxidative stress, the reactive oxygen species (ROS) is directly involved in the various mechanisms of atherogenesis such as endothelial dysfunction, monocyte migration, smooth muscle proliferation and LDL oxidation (Singh, Mengi, Xu, Arneja, & Dhalla, 2002). Oxidised LDL is highly atherogenic, which leads to foam cell formation that further develops into atheromatous plaque and ultimately, the hardening of the artery (Yu, Fu, Zhang, Yin, & Tang, 2013).

Endothelial cells maintain basal vascular tone and actively regulate vascular reactivity in physiological and pathological conditions. They respond to mechanical forces and a variety of neuro humoral mediators. Nitric oxide (NO) is one of the most important vasoactive substances released by the endothelium, which is not only used as a vasodilator (Förstermann & Sessa, 2012), but also inhibits cellular inf ammation (Kobayashi, 2010). In non-pathological conditions, NO is synthesised by enzymatic conversion of L-arginine, in the presence of molecular oxygen, by endothelial eNOS which is expressed constitutively in endothelial cells (Tousoulis, Kampoli, Tentolouris, & Stefanadis, 2012). Endotoxins, such as tumor lipopolysacharides (LPS) play a critical role in propagation of endothelial dysfunction by down regulating the expression of eNOS, resulting in decreased bio availability of nitric oxide (Wilson et al., 2000).

The ubiquitously expressed nuclear factor kappa-light-chain-enhancer of activated B cells (NF- B) is a transcription factor that regulates many cellular processes including cell proliferation, survival, adhesion, and immunity. NF- B is activated in the presence of stimuli such as in the event of oxidative stress, by cytokines or by bacterial LPS (Gupta, Sundaram, Reuter, & Aggarwal, 2010). Activated NF- B is an important regulator for inf ammatory mediators such as interleukin-1 and tumor necrosis factor (TNF) (Eda Shimada, Beidler, & Monahan, 2011). NF- B is retained and remains inactivated in the cytosol through sequestration by nuclear factor of kappa light polypeptide gene enhancer in B-cells inhibitor (I- B) proteins. NF- B is activated by I- B kinase (IKK) which degrades I- B through phosphorylation. A large

variety of stimuli potentially induce activation of NF- B which, in concert with transcriptional coactivators, lead to the induction of a multitude of target genes (Yamamoto & Gaynor, 2001).

The most prevalent active form of NF- B is a heterodimer composed of subunits p50 and p65. Def ciency of p65 is lethal due to its association with developmental abnormalities (Novack, 2011). Although p50 knockout mice can develop normally, B-cell proliferation is disrupted and antibody production is compromised (Franzoso et al., 1997). However, over-activation of NF- B is associated with various disorders. In auto-immune state, sustained activation of NF- B causes inf ammatory myopathies (Creus, De Paepe, & De Bleecker, 2009), while in the events of oxidative stress caused by hyperglycaemia or hypercholesterolaemia, sustained activation of NF- B is associated with atherosclerosis (Real et al., 2010; Vanessa Fiorentino, Prioletta, Zuo, & Folli, 2013).

To date, the mechanism HDL's antiatherosclerotic effect is still considered complex and its role as an antioxidant and anti-inf ammatory agent in terms of attenuating atherosclerosis is still not fully understood. The role of HDL in anti antherosclerosis was made even controversial when it was found that the HDL in people with coronary artery disease (CAD) does not upregulate NOS as in healthy people due to activation of endothelial protein kinase C II by the former that disrupts the eNOS activation pathway (Besler et al., 2011). However, since a lot of evidence has also indicated that HDL is inversely correlated with the incidence of CHD (Feig et al., 2011; Mackey et al., 2012; Vergeer, Holleboom, Kastelein, & Kuivenhoven, 2010), HDL may not simply exert its athero protective effect by a single pathway. Therefore, the objective of this study is to investigate whether the HDL can downregulate the expression of NF- B in human endothelial cells, which may in turn upregulate the expression of eNOS. The ability of HDL to reduce the susceptibility of LDL to oxidation is also investigated.

MATERIALS AND METHODS

Plasma Source

Approval from UiTM Board of Ethics Committee was obtained prior to the commencement of the study [reference number: 600-RMI (5/1/6/01)]. Pooled plasma was obtained from 20 healthy individuals from Faculty of Medicine, UiTM.

Lipoprotein Isolation

Plasma was adjusted to a density of 1.21 g/mL by adding 1.1 mL of pooled human plasma to 0.3270 g of potassium bromide and was mixed gently by vortex mixer. A discontinuous density gradient was made by overlaying the plasma solution with 2.2 mL of saline containing 0.1% ethylenediaminetetraacetic acid in ultracentrifuge tubes (d=1.006 g/mL). The ultracentrifuge tubes were sealed and centrifuged at 100,000 rpm at 4°C for 40 minutes using an ultracentrifuge (Optima TLX, Beckman Coulter, Palo Alto, CA). HDL fraction was placed in a nitrocellulose bag and was dialysed at 4°C for 24 hours. The total protein (TP) concentration was determined using a bio analyser (Cobas Integra 400 plus, Roche Diagnostics Limited, Rotkreuz, Switzerland).

Wan Norhasanah Wan Yusoff, Yung-An Chua, Gabriele Ruth Anisah Froemming, Abdul Manaf Ali
and Hapizah Nawawi

The Effects of HDL on LDL Susceptibility to Oxidation

Preparation of LDL and conjugated dienes formation was determined as described by Gieseg and Esterbauer (1994). Freshly prepared LDL (50 µg/mL) was incubated with different concentrations of HDL (20, 40, 60 and 80 µg/mL) which covered the lower and higher concentration than that of the LDL. The mixtures were oxidised with 0.5µM copper sulphate ($CuSO_4$) at 37°C for three hours. The conjugated dienes formation detected by the spectrophotometer (234 mm) represents the degree of lipid peroxidation in the sample, where the more conjugated dienes is detected, the more the LDL is susceptible to oxidation (Moore & Roberts, 1998). Lag time (min), which is the time interval between the addition of $CuSO_4$ and the beginning of the oxidation, represents how long the LDL is protected by the HDL before it is oxidised. The reaction rate (absorbance/minute) is the maximal rate of LDL oxidation detected in the kinetic curve and maximum absorbance of lipid peroxidation was obtained by kinetic modelling analysis (Esterbauer, Wäg, & Puhl, 1989).

HUVEC Isolation, Culture and Incubation Conditions

Human umbilical vein endothelial cell line (HUVEC) was purchased from Cambrex Bio Science Walkersville, USA. HUVEC (1 x 10^6 cells/mL) was cultured in 75 cm2 f ask in medium 199 containing 20% foetal calf serum, 10,000 U/mL penicillin/streptomycin, 100 mg/L heparin, 3 mmol/l L-glutamine and 15 mg/mL endothelial cell growth supplement. HUVEC was stimulated with LPS (1µg/mL) to induce inf ammatory response and different concentrations of HDL [20-80 µg/mL for LDL oxidation susceptibility study; 20-120 mg/dL for eNOS, NF- B p50 and p65 expression studies based on the optimum HDL concentration that supress cell apoptosis (Nofer et al., 2001) were added to the separated HUVEC cultures. Each HUVEC cultures with different HDL concentrations was prepared in triplicates. The HUVEC cultures were incubated in a humidif ed incubator (37°C, 5% CO_2) for 16 hours.

The Effects of HDL on eNOS Expression

Stimulated HUVEC was homogenised in celllysis buffer containing 10 mmol/L Tris (pH 7.4), 1 mmol/L sodium ortho-vanadate and 1% (w/v) sodium dodecyl sulfate. Protein concentrations in the lysates were measured using the bioanalyser. Proteins (50 µg) were analysed by western blot method according to the standard procedure. Monoclonal antibodies against human eNOS, were used as primary antibodies and horseradish peroxidise (HRP) goat anti-mouse antibody was used as secondary antibody. The bands were visualised and quantitated using the BioRad Gel system with Quantity One Quantitation Software (BioRad Laboratories, Hercules, CA, USA).

The Effects of HDL on NF- B p50 and p65 Expression

HUVEC was extracted using a nuclear extraction kit (Cayman Chemical, Ann Arbor, MI, USA). The cells were collected on ice-cold phosphate-buffered saline in the presence of phosphatase inhibitors. The pelleted cells were then re-suspended in ice-cold hypotonic buffer, followed by the addition of10% Nonidet-p40 and were centrifuged. Protein concentrations in the lysates (50 µg) were measured with NF- B (human p50 and p65) Transcription Factor

Assay kit (Cayman Chemical, Ann Arbor, MI, USA). The expression of NF- B was detected using the bioanalyser. NF- B was detected by addition of specif c primary antibody directed against NF- B. A secondary antibody conjugated to HRP was added to provide a sensitive colorimetric readout at 450 nm.

Statistical Analysis

Data were analysed using the Statistical Package for the Social Sciences (SPSS) version 22.0. Data are presented as mean ± SD. The effects of different concentrations of HDL were compared by analysis of variance. Comparison between two different groups was analysed using independent T-test. Signif cant level was set at $p < 0.05$.

RESULTS

The Effects of HDL on LDL Susceptibility to Oxidation

Co-incubations of LDL with HDL increased the mean lag time of diene formation and produced a slower rate of oxidation across all HDL concentration (Figure 1). On the contrary, the amounts of conjugated dienes generated by LDL during oxidation were signif cantly increased when co-incubated with 40 µg/mL of HDL and above.
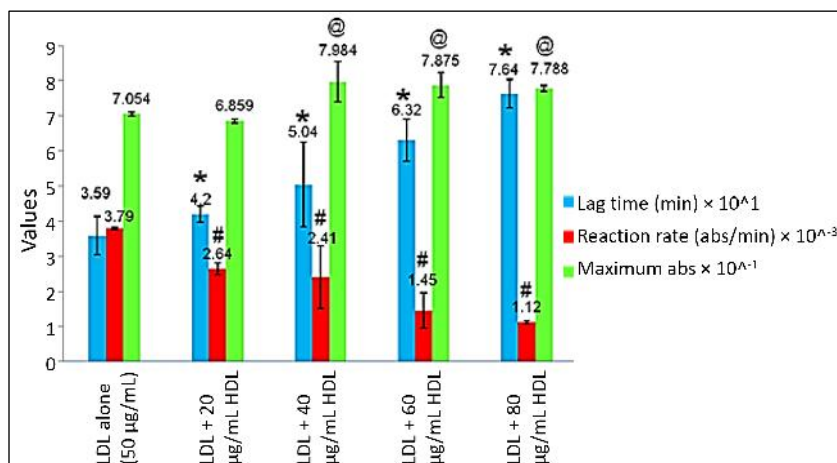
Figure 1. Mean lag time, oxidation reaction rate and amount of conjugated dienes formation by oxidised LDL (in the unit of maximum abs) with the presence of different concentrations of HDL

Mean lag times was gradually increased, while oxidation reaction rates were gradually decreased respective to the increase of co-incubated HDL concentration. *p<0.05 compared to LDL alone (Lag time), #p<0.05 compared to LDL alone (Reaction Rate), @p<0.05 compared to LDL alone (Maximum abs).

The Effects of HDL on Expression of eNOS

The eNOS was expressed as the 133 kDa band in the western blot shown in Figure 2. The changes in eNOS were determined after densitometric measurement of the western blots (Figure 3). Without addition of HDL or LPS, the endothelial cells in negative control expressed eNOS at normal rate. LPS successfully reduced the expression of eNOS by endothelial cells, demonstrated by the reduced band intensity in the positive control. HDL not only successfully mitigates the effect of LPS, but increased the expression of eNOS beyond its normal expression rate (negative control). At higher concentrations of HDL, (100 and 120 mg/dL) the expression of eNOS were signif cantly increased. At lower HDL concentrations (20-80 mg/dL), however, eNOS inductions were weaker and not signif cantly different when compared with the positive controls.
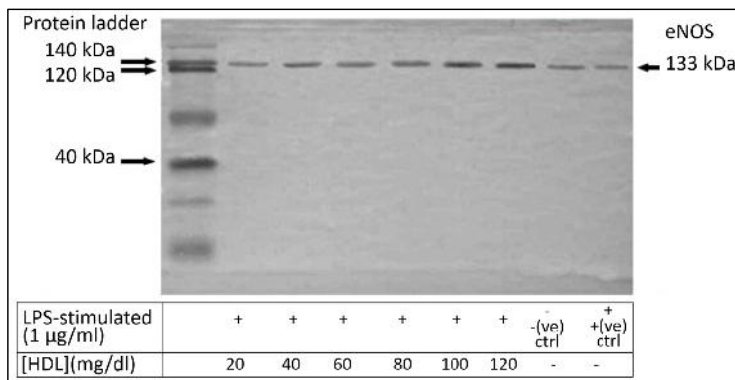
Figure 2. Western blot image of eNOS protein expression in HUVEC after stimulated with LPS and incubated with different concentrations of HDL for 16 hours

The band intensities were gradually increased from 20 to 120 mg/dL of HDL co-incubation. HUVEC incubated with LPS alone was used as positive control. Unstimulated HUVEC samples without HDL were used as negative controls.
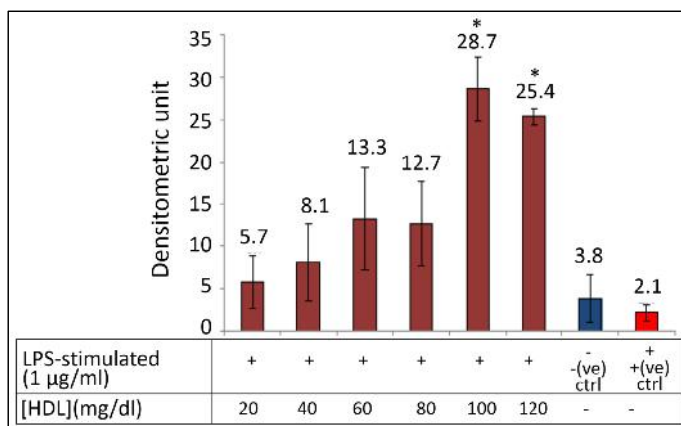
Figure 3. Western blot's quantitative result of eNOS protein expression in HUVEC after stimulated with LPS and incubated with different concentrations of HDL for 16 hours

HUVEC sample incubated with LPS alone was used as positive control. *p<0.05 when compared with positive control. Unstimulated HUVEC samples without HDL were used as negative controls.

The Effects of HDL on Expression of NF- B in LPS-Stimulated Endothelial Cell

Unlike the eNOS expression experiment, the expression of NF- Bp50 and p65 have to be down regulated in order to demonstrate the protective effect of HDL. After the LPS stimulation, the expression of NF- B p50 without co-incubation with HDL (positive control) was increased by 23% when compared with negative control (Figure 4). The expression of NF- B p50 after treatment with different concentrations of HDL, however, was not signif cantly different when compared with the positive control. On the other hand, the expressions of NF- B p65 signif cantly decreased across all the HDL concentrations when compared with the positive control (Figure 5).
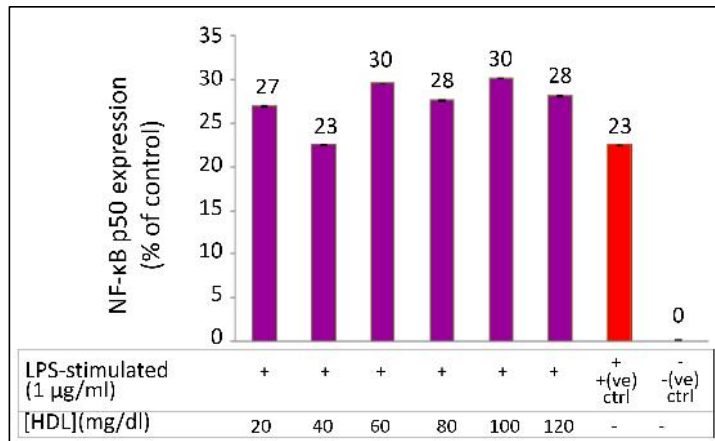
Figure 4. The effects of different concentrations of HDL on expression of NF- B p50

The expressions NF- B p50 were of not signif cantly different than that of positive control regardless of whether the HDL concentration was co-incubated with the LDL. HUVEC sample incubated with LPS alone was used as the positive control. Unstimulated HUVEC sample without HDL was used as negative control. Data are presented as % changes of NF- B versus unstimulated HUVEC samples.

Wan Norhasanah Wan Yusoff, Yung-An Chua, Gabriele Ruth Anisah Froemming, Abdul Manaf Ali and Hapizah Nawawi
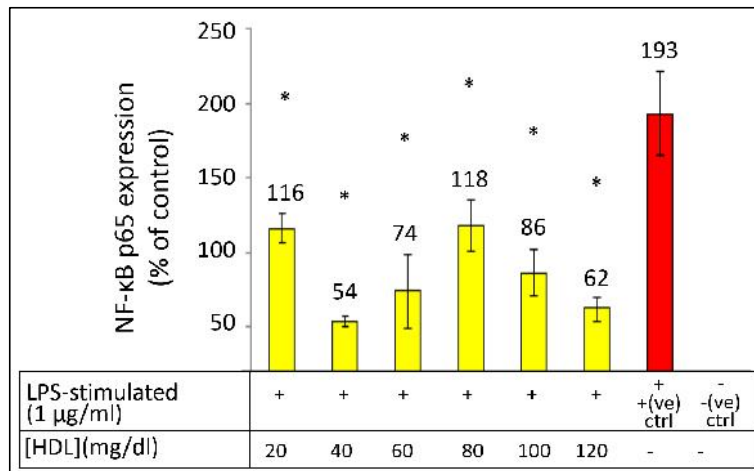
Figure 5. The effects of different concentration of HDL on expression of NF-kB p65

The expressions of NF-kB p65 were signif cantly downregulated in all LDL co-incubated with HDL. HUVEC sample incubated with LPS alone was used as positive control. Unstimulated HUVEC sample without HDL was used as negative control. Data are presented as % changes of NF-kB versus unstimulated HUVEC samples. $*p<0.05$ compared to positive controls.

DISCUSSION

This study demonstrated that HDL reduces LDL susceptibility to oxidation, evidenced by the increased oxidation lag time and reduced oxidation reaction rate, in proportion with the concentration of HDL co-incubated with the LDL. However, the maximum absorbance of conjugated dienes that represent the amount of oxidised LDL, are increased when co-incubated with HDL 40 µg/mL onwards. Thus, the optimum concentration of HDL to inhibit LDL oxidation appears to be only 20 µg/mL. These f ndings contradict with the previously elucidated reports on anti oxidative property of HDL. However, an *ex vivo* study conducted by Solakiviet et al. (2005) was in agreement with our f nding, which demonstrated that co-incubation of HDL in LDL samples not only increase the maximum dienes concentration, but also decrease the lag time and increase the rate of reaction of dienes formation (Solakiviet al., 2005). They hypothesised that HDL is even more susceptible to oxidation than LDL when a high concentration of Cu^{2+} (1.65 µM as used in their experiment) is used for induction of oxidation, suggesting that HDL only exerts its protective property in mildly oxidative environment, but not so in severe oxidative stress, probably due to the deactivation of serum paraoxonase 1 enzyme, which is usually associated with HDL to protect in from oxidation (Aviram et al., 1999). Nevertheless, the authors did not deny the contradicting f ndings of their study against several other studies (Bowry, Stanley, & Stocker, 1992; Ohmura et al., 1999; Schnitzer, Pinchuk, Fainaru, Schafer, & Lichtenberg, 1995; Suzukawa, Ishikawa, Yoshida, & Nakamura, 1995), were probably contributed by the non-standardised concentration of Cu^{2+} used in the studies and other potential individual intrinsic factors, such as size of the lipoproteins (Chait, Brazg, Tribble, & Krauss, 1993; Kontush, Chantepie, & Chapman, 2003) and blood glucose

level. Larger particle size of HDL is often associated with lower risk of cardiovascular disease (Kontush, 2015). Individuals with increased body mass index tend to have higher level of small particle size HDL (Williams et al., 1993). The standardisation of these purported intrinsic factors were not taken into account in this study, therefore might be responsible for producing this contradictory result. The increase of conjugated dienes formation at HDL 40 µg/mL and above also can be explained by the enhanced oxidation of HDL itself at higher concentration, particularly in a highly oxidative environment. Nevertheless, the f ndings of this study supports HDL as an inhibitor to LDL susceptibility to oxidation in terms of prolonged lag phase and diminished reaction rate.

The protective effect of HDL is contributed by multiple pathways, including moderating endotheliumapoptosis, proliferation and migration, acts as anti-inf ammatory agent and inhibits platelet aggregation (Mineo & Shaul, 2012b). In its antioxidative role, HDL re-stimulates eNOS, which has been repressed by oxidised LDL, through binding with scavenger receptor–B1 on cell membrane (Garcia-Cardena, Oh, Liu, Schnitzer, & Sessa, 1996; Stein & Stein, 1999). In this study, HDL not only mitigated the downregulation of eNOS caused by LPS, but also increased the eNOS expression beyond its normal rate, which was represented by the negative control that was not even suppressed by LPS in the beginning. However, the stimulation of eNOS by HDL is concentration-dependent. In this study, lower concentration of HDL (20 to 80 mg/dL), were not suff cient to exert signif cant increase in eNOS expression, even though the trend of gradual increase was still observable. The signif cant benef t effect of HDL was only exerted in high concentration (100 and 120 mg/dL).

This non-convincing f nding, however, does not discredit the potential benef ts of HDL. Pathologically increased activation of NF- B suppresses the eNOS expression (Lee, et al., 2014), therefore exacerbates the atherogenesis. HDL mitigates the downregulation of eNOS by suppressing the NF- B. The ability of HDL to suppress the activation of the readily expressed NF- B is well-documented, primarily studied by using electrophoretic mobility shift assay (Da Silveira Cruz   Machado, et al., 2010; Sanz, et al., 2010). The HDL prevents NF- B activation by neutralising the toxic effect of LPS (Wang, et al., 2008).

However, the effect of HDL on the expression of NF- B is not well-studied. A study conducted by Kastenbauer and Ziegler-Heitbrock (1999) demonstrated that the expression of both NF- B p50 and p65 sub units did not show similar response to LPS exposure, where the expression of p50 increased three-folds when compared with that of p65 after two to three days of LPS exposure. In this study, the expression of both NF- B p50 and p65 were upregulated in positive controls (Zhang et al., 2008). However, the enhanced expression of NF- B p50 were not as strong as that of p65. Co-incubation of HDL in NF- B p50 samples did not signif cantly reduce its expression either, probably because it was already very under expressed to be further suppressed by HDL. The different f ndings were probably due to the shorter sample incubation time used in this study (16 hours), compared to that by Kastenbauer and Ziegler (two to three days). The unsuppressed NF- B p50 are, in fact, benef cial for the reduction of inf ammatory mediator TNF. The increased amount of NF- B p50 forms p50 homodimers which competitively binds to the target gene with p50/p65 heterodimers (Kastenbauer & Ziegler-Heitbrock, 1999). The p50 does not activate the expression of the targeted gene because the protein terminal of p50 does not contain the transcription activation domain such in that of

p65, which is required for the gene activation (Ghosh & Hayden, 2012). The protective effect of HDL is demonstrated in this study as it does not downregulate the expression of NF-ᴋB p50, but signif cantly downregulates the expression of NF-ᴋB p65.

CONCLUSION

Overall, HDL protects the LDL from oxidation, but it may enhance LDL oxidation in highly oxidative environment. High concentration of HDL increases eNOS expression and inhibits NF-ᴋB expression, especially the p65 subunit, even in low concentrations. Hence, HDL has antioxidant and anti-inf ammatory properties, not only by prevention oxidation, but also by its roles in the eNOS and NF-ᴋB pathways. This may in part attribute to its role in reverse cholesterol transport. However, the mechanism of how HDL regulates the expression of NF-ᴋBis is still largely unknown. Future studies are warranted in addressing this issue.

ACKNOWLEDGEMENTS

REFERENCES

Aviram, M., Rosenblat, M., Billecke, S., Erogul, J., Sorenson, R., Bisgaier, C. L., ... & La Du, B. (1999). Human serum paraoxonase (PON 1) is inactivated by oxidized low density lipoprotein and preserved by antioxidants. *Free Radical Biology and Medicine, 26*(7), 892-904.

Bekkering, S., Quintin, J., Joosten, L. A. B., van der Meer, J. W. M., Netea, M. G., & Riksen, Niels P. (2014). Oxidized low-density lipoprotein induces long-term proinf ammatory cytokine production and foam cell formation via epigenetic reprogramming of monocytes. *Arteriosclerosis, Thrombosis, and Vascular Biology, 34*(8), 1731-1738.

Besler, C., Heinrich, K., Rohrer, L., Doerries, C., Riwanto, M., Shih, D. M., ... & Mueller, M. (2011). Mechanisms underlying adverse effects of HDL on eNOS-activating pathways in patients with coronary artery disease. *The Journal of Clinical Investigation, 121*(7), 2693-2708.

Bowry, V. W., Stanley, K. K., & Stocker, R. (1992). High density lipoprotein is the major carrier of lipid hydroperoxides in human blood plasma from fasting donors. *Proceedings of the National Academy of Sciences, 89*(21), 10316-10320.

Chait, A., Brazg, R. L, Tribble, D. L., & Krauss, R. M. (1993). Susceptibility of small, dense, low-density lipoproteins to oxidative modif cation in subjects with the atherogenic lipoprotein phenotype, pattern B. *The American Journal of Medicine, 94*(4), 350-356.

Creus, K. K., De Paepe, B., & De Bleecker, J. L. (2009). Idiopathic inf ammatory myopathies and the classical NF-ᴋB complex: Current insights and implications for therapy. *Autoimmunity Reviews, 8*(7), 627-631.

Da Silveira Cruz-Machado, S., Carvalho-Sousa, C. E., Tamura, E. K., Pinato, L., Cecon, E., Fernandes, P. A. C. M., ... & Markus, R. P. (2010). TLR4 and CD14 receptors expressed in rat pineal gland trigger NFKB pathway. *Journal of Pineal Research, 49*(2), 183-192.

Eda, H., Shimada, H., Beidler, D. R., & Monahan, J. B. (2011). Proinf ammatory cytokines, IL-1 and TNF- , induce expression of interleukin-34 mRNA via JNK-and p44/42 MAPK-NF- B pathway but not p38 pathway in osteoblasts. *Rheumatology International, 31*(11), 1525-1530.

Esterbauer, H., Striegl, G., Puhl, H., & Rotheneder, M. (1989). Continuous monitoring of in vztro oxidation of human low density lipoprotein. *Free Radical Research Communications, 6*(1), 67-75.

Esterbauer, H., Wäg, G., & Puhl, H. (1993). Lipid peroxidation and its role in atherosclerosis. *British Medical Bulletin, 49*(3), 566-576.

Feig, J. E., Rong, J. X., Shamir, R., Sanson, M., Vengrenyuk, Y., Liu, J., ... & Fisher, E. A. (2011). HDL promotes rapid atherosclerosis regression in mice and alters inf ammatory properties of plaque monocyte-derived cells. *Proceedings of the National Academy of Sciences, 108*(17), 7166-7171.

Förstermann, U., & Sessa, W. C. (2012). Nitric oxide synthases: regulation and function. *European Heart Journal, 33*(7), 829-837.

Franzoso, G., Carlson, L., Xing, L., Poljak, L., Shores, E. W., Brown, K. D., ... & Siebenlist, U. (1997). Requirement for NF- B in osteoclast and B-cell development. *Genes and development, 11*(24), 3482-3496.

Garcia-Cardena, G., Oh, P., Liu, J., Schnitzer, J. E., & Sessa, W. C. (1996). Targeting of nitric oxide synthase to endothelial cell caveolae via palmitoylation: Implications for nitric oxide signaling. *Proceedings of the National Academy of Sciences, 93*(13), 6448-6453.

Ghosh, S., & Hayden, M. S. (2012). Celebrating 25 years of NF- B research. *Immunological Reviews, 246*(1), 5-13.

Gieseg, S. P., & Esterbauer, H. (1994). Low density lipoprotein is saturable by pro-oxidant copper. *FEBS Letters, 343*(3), 188-194.

Gupta, S. C., Sundaram, C., Reuter, S., & Aggarwal, B. B. (2010). Inhibiting NF- B activation by small molecules as a therapeutic strategy. *Biochimica et Biophysica Acta (BBA)-Gene Regulatory Mechanisms, 1799*(10), 775-787.

Hajjar, D. P., & Gotto, A. M. (2013). Biological relevance of inf ammation and oxidative stress in the pathogenesis of arterial diseases. *The American Journal of Pathology, 182*(5), 1474-1481.

Kastenbauer, S., & Ziegler-Heitbrock, H. W. L. (1999). NF- B1 (p50) is upregulated in lipopolysaccharide tolerance and can block tumor necrosis factor gene expression. *Infection and Immunity, 67*(4), 1553-1559.

Kobayashi, Y. (2010). The regulatory role of nitric oxide in proinf ammatory cytokine expression during the induction and resolution of inf ammation. *Journal of Leukocyte Biology, 88*(6), 1157-1162.

Kontush, A. (2015). HDL particle number and size as predictors of cardiovascular disease. *Frontiers in Pharmacology, 6*.

Kontush, A., Chantepie, S., & Chapman, M. J. (2003). Small, dense HDL particles exert potent protection of atherogenic LDL against oxidative stress. *Arteriosclerosis, Thrombosis, and Vascular Biology, 23*(10), 1881-1888.

Kontush, A., & Chapman, M. J. (2010). Antiatherogenic function of HDL particle subpopulations: focus on antioxidative activities. *Current Opinion in Lipidology, 21*(4), 312-318.

Lee, K. S. K., Joohwan, K. S. N., Lee, K. S., Lee, D. K., Ha, K. S., ... & Kwon, Y. G. (2014). Functional role of NF- B in expression of human endothelial nitric oxide synthase. *Biochemical and Biophysical Research Communications, 448*(1), 101-107.

Mackey, R. H., Greenland, P., Goff, D. C., Lloyd-Jones, D., Sibley, C. T., & Mora, S. (2012). High-density lipoprotein cholesterol and particle concentrations, carotid atherosclerosis, and coronary events: MESA (multi-ethnic study of atherosclerosis). *Journal of the American College of Cardiology, 60*(6), 508-516.

Mineo, C., & Shaul, P. W. (2012a). Regulation of eNOS in caveolae. *Caveolins and Caveolae* (pp. 51-62): Springer.

Mineo, C., & Shaul, P. W. (2012b). Novel biological functions of high-density lipoprotein cholesterol. *Circulation Research, 111*(8), 1079-1090.

Moore, K., & Roberts, L. J. (1998). Measurement of lipid peroxidation. *Free Radical Research, 28*(6), 659-671.

Nofer, J. R., Levkau, B., Wolinska, I., Junker, R., Fobker, M., von Eckardstein, A., ... & Assmann, G. (2001). Suppression of endothelial cell apoptosis by high density lipoproteins (HDL) and HDL-associated lysosphingolipids. *Journal of Biological Chemistry, 276*(37), 34480-34485.

Novack, D. V. (2011). Role of NF- B in the skeleton. *Cell Research, 21*(1), 169-182.

Ohmura, H., Watanabe, Y., Hatsumi, C., Sato, H., Daida, H., Mokuno, H., & Yamaguchi, H. (1999). Possible role of high susceptibility of high-density lipoprotein to lipid peroxidative modif cation and oxidized high-density lipoprotein in genesis of coronary artery spasm. *Atherosclerosis, 142*(1), 179-184.

Real, J. T., Martínez-Hervás, S., García-García, A. B., Civera, M., Pallardó, F. V., Ascaso, J. F., ... & Carmena, R. (2010). Circulating mononuclear cells nuclear factor-kappa B activity, plasma xanthine oxidase, and low grade inf ammatory markers in adult patients with familial hypercholesterolaemia. *European Journal of Clinical Investigation, 40*(2), 89-94.

Roger, V. L., Go, A. S., Lloyd-Jones, D. M., Benjamin, E. J., Berry, J. D., Borden, W. B., ... & Fullerton, H. J. (2012). AHA statistical update. *Heart disease and stroke statistics–2012 Update. A report from the American Heart Association. Circulation, 125*, e2-e220.

Rothblat, G. H., & Phillips, M. C. (2010). High-density lipoprotein heterogeneity and function in reverse cholesterol transport. *Current Opinion in Lipidology, 21*(3), 229.

Säemann, M. D., Poglitsch, M., Kopecky, C., Haidinger, M., Hörl, W. H., & Weichhart, T. (2010). The versatility of HDL: a crucial anti-inf ammatory regulator. *European Journal of Clinical Investigation, 40*(12), 1131-1143.

Sanz, A. B., Sanchez-Niño, M. D., Ramos, A. M., Moreno, J. A., Santamaria, B., Ruiz-Ortega, M., ... & Ortiz, A. (2010). NF- B in renal inf ammation. *Journal of the American Society of Nephrology, 21*(8), 1254-1262.

Schnitzer, E., Pinchuk, I., Fainaru, M., Schafer, Z., & Lichtenberg, D. (1995). Copper-induced lipid oxidation in unfractionated plasma: the lag preceding oxidation as a measure of oxidation-resistance. *Biochemical and Biophysical Research Communications, 216*(3), 854-861.

Singh, R. B., Mengi, S. A., Xu, Y. J., Arneja, A. S., & Dhalla, N. S. (2002). Pathogenesis of atherosclerosis: A multifactorial process. *Experimental and Clinical Cardiology, 7*(1), 40.

Solakivi, T., Jaakkola, O., Salomäki, A., Peltonen, N., Metso, S., Lehtimäki, T., ... & Nikkari, S. T. (2005). HDL enhances oxidation of LDL in vitro in both men and women. *Lipids in Health and Disease, 4*(1), 25.

Stein, O., & Stein, Y. (1999). Atheroprotective mechanisms of HDL. *Atherosclerosis, 144*(2), 285-301.

Suzukawa, M., Ishikawa, T., Yoshida, H., & Nakamura, H. (1995). Effect of in-vivo supplementation with low-dose vitamin E on susceptibility of low-density lipoprotein and high-density lipoprotein to oxidative modif cation. *Journal of the American College of Nutrition, 14*(1), 46-52.

Tousoulis, D., Kampoli, A. M., Tentolouris N. P. C., & Stefanadis, C. (2012). The role of nitric oxide on endothelial function. *Current Vascular Pharmacology, 10*(1), 4-18.

Vanessa Fiorentino, T., Prioletta, A., Zuo, P., & Folli, F. (2013). Hyperglycemia-induced oxidative stress and its role in diabetes mellitus related cardiovascular diseases. *Current Pharmaceutical Design, 19*(32), 5695-5703.

Vergeer, M., Holleboom, A. G., Kastelein, J. J. P., & Kuivenhoven, J. A. (2010). The HDL hypothesis: Does high-density lipoprotein protect from atherosclerosis? *Journal of Lipid Research, 51*(8), 2058-2073.

Wang, Y., Zhu, X., Wu, G., Shen, L., & Chen, B. (2008). Effect of lipid-bound apoA-I cysteine mutants on lipopolysaccharide-induced endotoxemia in mice. *Journal of Lipid Research, 49*(8), 1640-1645.

Williams, P. T., Vranizan, K. M., Austin, M. A., & Krauss, R. M. (1993). Associations of age, adiposity, alcohol intake, menstrual status, and estrogen therapy with high-density lipoprotein subclasses. *Arteriosclerosis, Thrombosis, and Vascular Biology, 13*(11), 1654-1661.

Wilson, S. H., Caplice, N. M., Simari, R. D., Holmes, D. R., Carlson, P. J., & Lerman, A. (2000). Activated nuclear factor- B is present in the coronary vasculature in experimental hypercholesterolemia. *Atherosclerosis, 148*(1), 23-30.

Yamamoto, Y., & Gaynor, R. B. (2001). Role of the NF-kB pathway in the pathogenesis of human disease states. *Current Molecular Medicine, 1*(3), 287-296.

Yu, X. H., Fu, Y. C., Zhang, D. W., Yin, K., & Tang, C. K. (2013). Foam cells in atherosclerosis. *Clinica Chimica Acta, 424*, 245-252.

Zhang, X. T., Liu, J., Yu, X., Ning, Q., & Luo, X. P. (2008). Lipopolysaccharide and hyperoxia induce nuclear factor-kappa B expression in human embryo lung f broblasts *in vitro*. *Zhongguo dang dai er ke za zhi= Chinese Journal of Contemporary Pediatrics, 10*(5), 661-664.

Low Dose Palm Tocotrienol-Rich Fraction Reduces Aortic Tissue Endothelial Activation in Severely Atherosclerotic Rabbits

Razak, A. A.[1], Omar, E.[1,2], Muid, S.[1,2] and Nawawi, H.[1,2]*

[1]Institute of Pathology, Laboratory and Forensic Medicine (I-PPerForM) Universiti Teknologi MARA (UiTM), Sungai Buloh Campus, 47000 Sungai Buloh, Selangor, Malaysia
[2]Faculty of Medicine, Universiti Teknologi MARA (UiTM), Sungai Buloh Campus, 47000 Sungai Buloh, Selangor, Malaysia

ABSTRACT

Chronic inf ammation plays a pivotal role in atherogenesis. Antioxidants have a potential role in the prevention and treatment of atherosclerosis. The effects of palm oil-derived tocotrienol-rich fraction (TRF) supplementation on inf ammation are not well established. This study aims to investigate the effects of TRF supplementation on the inf ammatory biomarkers and adhesion molecules in severe atherosclerosis. A total of 28 New Zealand white rabbits were given 1% high-cholesterol diet (HCD) for f ve months and randomised from the second month onwards into one of f ve intervention groups: Placebo, TRF 15, 30, 60 and 90 mg/kg/day. Treatment was given for three months and the animals were fed HCD throughout the duration. At the end of the study, the aortas were obtained, stained with Sudan IV, f xed in formalin, embedded in paraff n and immunostained for tissue intracellular adhesion molecule-1 (ICAM-1), interleukin-6 (IL-6), E-selectin, smooth muscle actin (SMA), and nuclear factor- B (NF- B). The amount of atherosclerotic lesions was not signif cantly different between the groups and compared to placebo. Qualitative analysis showed lower trend of ICAM-1, IL-6, E-selectin and NF- B but higher trend of SMA tissue expression in TRF-treated groups especially at low dose of TRF (TRF-15) compared to placebo. Quantitative analysis showed lower ICAM-1 and E-select in positivity in TRF-15 compared to placebo group (25.1 ± 7.4 % vs. 3.8 ± 2.0 %, 23.2 ± 6.5 % vs. 4.2 ± 2.1 %, respectively, $p < 0.05$). In conclusion, low dose TRF is potentially benef cial in attenuating vascular endothelial activation in severe atherosclerosis.

Keywords: Aorta, atherosclerosis, inf ammation, tocotrienol-rich fraction

INTRODUCTION

Tocotrienol is a naturally-occurring form of vitamin E other than tocopherol, which exists in four isoforms: -, -, - and -tocotrienol

(Meganathan, et al., 2014). It differs from tocopherol in the structure of the isoprenoid side chain, where it has an unsaturated geranyl chain compared to the phytyl chain of tocopherol (Dörmann, 2007). This structural difference results in altered membrane distribution and improved interaction with free radicals making tocotrienol a more potent antioxidant than tocopherol (Theriault, Chao, & Gapor, 2002).

Inf ammation plays an important role in atherogenesis regardless of the initial cause of endothelial dysfunction (Rajendran et al., 2013). This process is typif ed by adhesion of circulating monocytes to stimulated endothelial cells, followed by exodus of the monocytes into the sub-endothelial space to form foam cells. The adhesion is aided by expression of endothelial adhesion molecules such as intercellular adhesion molecules-1 (ICAM-1), vascular cell adhesion molecule-1 (VCAM-1) and E-selectin (Muller, 2002). ICAM-1 which is regulated by nuclear factor- B (NF- B), serves as a ligand to the integrins found on leucocytes (Muller, 2002).

NF- B is a transcription factor involved in a number of cellular responses that are involved in various stimuli such as free radicals and oxidised low density lipoprotein (LDL) (Gilmore, 1999). In atherosclerosis, NF- B is expressed in all stages of disease (Berliner et al., 1996). NF- B regulates a few other molecules involved in atherosclerosis including ICAM-1. Alpha tocotrienol has been reported to reduce NF- B activation (Theriault, Chao, & Gapor, 2002). Therefore it has been postulated that alpha tocotrienol decreases expression of adhesion molecules as a result of blockage of NF- B activation (Theriault, et al., 2002).

Hypercholesterolemia is a major cause of atherosclerosis. Oxidised LDL, a potent inducer of inf ammation (Berliner et al., 1996), accumulates in the vascular wall, where it is cytotoxic and chemotactic for monocytes and lymphocytes. It also leads to increase in endothelial expression of adhesion molecules (Berliner et al., 1996). Monocyte activation leads to release of oxygen derived free radicals. These free radicals incur damage to the endothelium which in turn leads to recruitment of more monocytes and other cells to the atherosclerotic area, thus signifying the link between oxidative stress and inf ammation in atherogenesis. Therefore, the anti-oxidant properties of Vitamin E are of great interest in this condition.

Although epidemiological studies have reported the reduction of atherosclerosis related cardiovascular risk with administration of vitamin E (Rimm et al., 1993; Stampfer et al., 1993), large scale double blind intervention studies have failed to demonstrate consistent eff cacy of vitamin E against atherosclerosis (Tribble, 1999). In addition, majority of the studies used tocopherol as the vitamin E component (Miller et al., 2005). However current research in vitamin E is skewed towards tocopherol, where only 1% of the total literature on vitamin E deals with tocotrienol and the rest concentrates on tocopherol (Sen, Khanna, & Roy, 2007), including large scale intervention studies on eff cacy of vitamin E in atherosclerosis. This signif es an important gap in vitamin E research, one which precludes us the full benef ts of naturally-occurring vitamin E molecules. Hence, the effects of tocotrienol on plaque stability in both early and severe atherosclerosis and its optimal dose for inf ammatory inhibition in atherosclerosis are still not well established. This study aims to investigate the effects of tocotrienol-rich fraction (TRF) supplementation on aortic tissue inf ammatory biomarkers in severely atherosclerotic rabbits.

MATERIALS AND METHODS

Rabbits and High-cholesterol Diet

This study had been approved by the Institutional Animal Ethics Committee and conformed to the institutional and national guidelines on use of animals in research. A total of 28 New Zealand white rabbits were given 1% high-cholesterol diet (HCD) for two months to induce atherosclerosis and then randomised into f ve groups: Placebo (n=7), TRF 15 mg/kg (n=5), TRF 30 mg/kg (n=6), TRF 60 mg/kg (n=5) and TRF 90 mg/kg (n=5) daily. The treatment was given for three months and the animals were fed HCD throughout the duration. All the animals were housed in individual cages, with *ad libitum* access to food and water, maintained at a 12-hour dark/light cycle. The TRF supplements (Gold-Tri E 50® tocotrienol-enriched vitamin E) and placebo E were provided by Sime Darby BioganicSdn. Bhd., Malaysia.

Tissue Collection

At the end of the experiment, rabbits were sacrif ced and aortas were obtained. The proximal 5 mm of the aorta was used for immunohistochemistry analysis and the rest was immediately processed for Sudan IV staining.

Sudan IV Staining

For Sudan IV staining, the aortas were cut open longitudinally and f xed overnight with 10% neutral buffered formalin. Subsequently, they were washed with 70% ethanol, then immersed in Sudan IV stain for 15 minutes. After rinsing, the stained aortas were photographed (C-740 Ultra Zoom, Olympus, USA) and analysed for the percentage area of sudanophilia. The area was then calculated by an image analysis software (analySIS® FIVE, Olympus Soft Imaging Solutions, Olympus, USA).

Aortic Immunohistochemical Analysis

Immunohistochemistry to detect ICAM-1, E-selectin, IL-6 and NF- B, (Santa Cruz Biotechnology Inc., USA) and smooth muscle actin (SMA) (Dako, Denmark) was performed using a conventional streptavidin-biotin-peroxidase method (Santa Cruz Biotechnology Inc., USA). The tissue blocks were sectioned at 5 µm thickness and deparaff nised in xylene. After a few changes of graded concentration of alcohol, the sections underwent antigen retrieval process followed by endogenous peroxidase blocking (in 1% H_2O_2). They were then incubated for 60 minutes in the respective primary antibodies. This was followed by washing steps with phosphate buffer. Then biotinylated secondary antibody was administered, followed by streptavidin horseraddish peroxidase and f nally, 3,3'-diaminobenzidine substrate. Hematoxylin was used as counter stain.

    The immunostained specimens were scanned by a fully motorised microscope (Olympus BX61, USA). The endothelial lining of the aortic images for all biomarkers except SMA were selected for analysis. For SMA, the intima of the aortic images was chosen. Staining quantif cation were made based on def ned brown endothelial or intimal staining by using the

microscope proprietary software (analySIS® FIVE, Olympus Soft Imaging Solution Olympus, USA) and expressed as percentage area of positivity.

Statistical Analysis

The statistical analysis was performed using the Statistical Package for Social Sciences (SPSS version 22) software. For between-group differences, Student's t-test or Mann-Whitney test was used for variables with normal or non-normal distribution respectively. Within group pre and post treatment differences for each variable were analysed by paired t-test or Wilcoxon matched-pair test for those variables with normal distribution and non-normal distribution respectively. Normality was tested with Kolmogrov-Smirnov test. Probability value of p<0.05 was taken as signif cant.

RESULTS

Sudan Staining
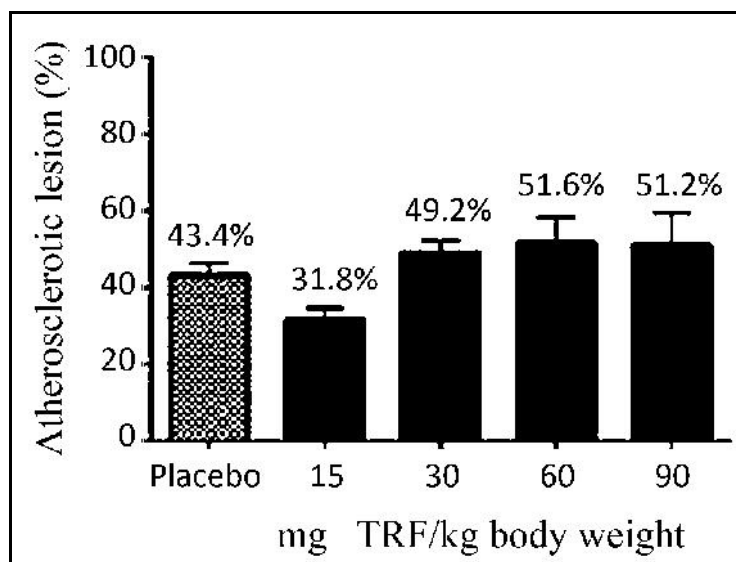
Figure 1. Percentage of atherosclerotic lesions in different treatment groups

All the rabbits developed atherosclerosis, with majority of lesion being of the severe type. The percentage of atherosclerotic lesion in TRF 15 group was the lowest among all the groups (Figure 1).

Immunostaining
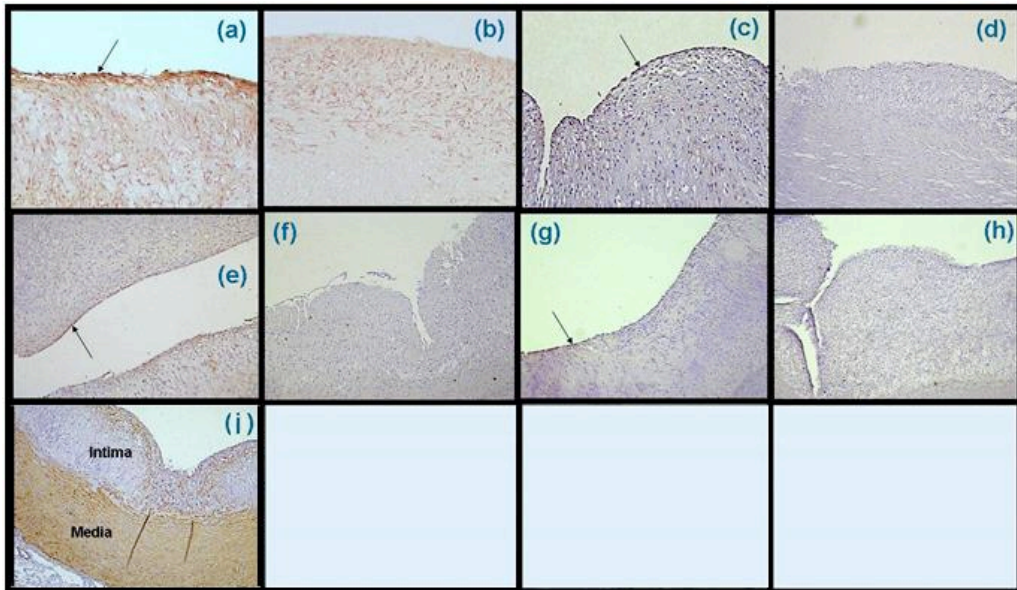
Figure 2. Endothelial and intimal immunohistochemical staining which showed: (a) Positive ICAM-1 (arrow); (b) Negative ICAM-1; (c) Positive NF- B (arrow); (d) Negative NF- B; (e) Positive E-selectin (arrow); (f) Negative E-selectin; (g) Positive IL-6 (arrow); (h) Negative IL-6; and (i) Positive intimal and medial SMA

Figure 2 (a – i) shows a typically positive and negative staining of all the immunohistochemical biomarkers.
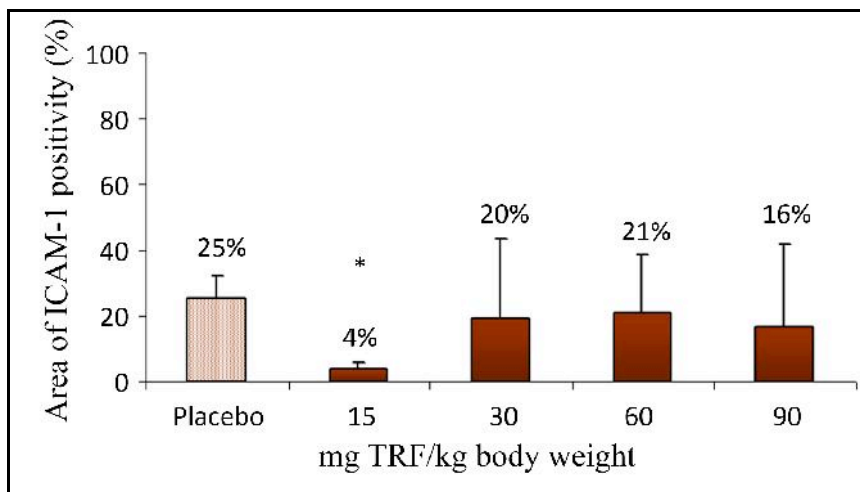
Figure 3. Quantitative Analysis of ICAM-1 immunostaining.* $p < 0.05$ compared to placebo; Data expressed as Mean ± SEM
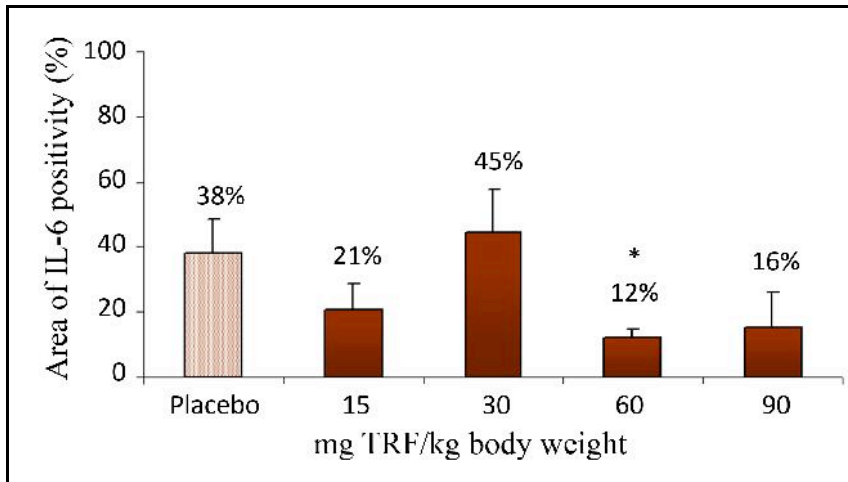
Figure 4. Quantitative analysis of IL-6 immunostaining.* $p<0.05$ compared to placebo; Data expressed as Mean ± SEM

ICAM-1 and IL-6 Expression

There was lower trend of ICAM-1 tissue expression in TRF-treated groups compared to placebo. Quantitative analysis showed lower % of ICAM-1 positivity in TRF-15 compared to placebo group (25 ± 7 % vs. 4 ± 2 % respectively, $p<0.05$) (Figure 3). There was a lower trend of IL-6 tissue expression in TRF-treated groups compared to placebo. The IL-6 expression was lower in the TRF-60 compared to placebo group (12.2 ± 3.1 % vs. 38.4 ± 11.5% respectively, $p<0.05$) (Figure 4).

E-selectin and NF-kB Expression
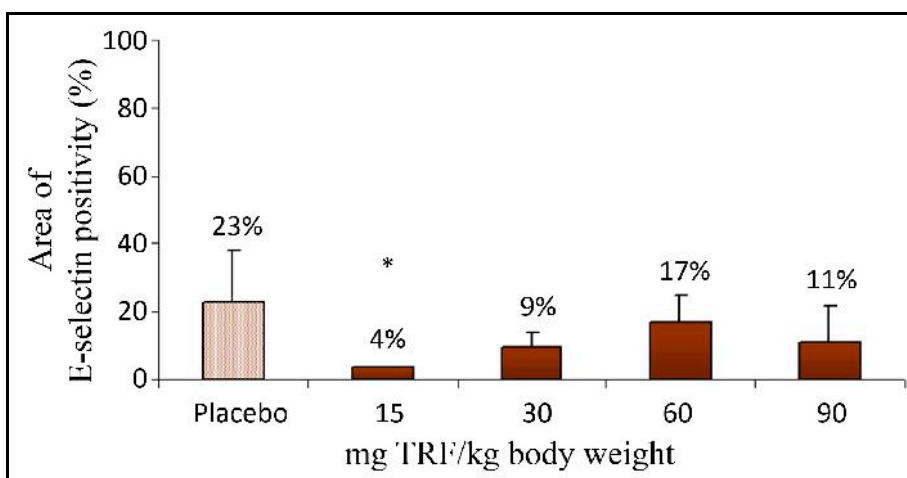
Figure 5. Quantitative analysis of E-selectin immunostaining; Data expressed as Mean ± SEM
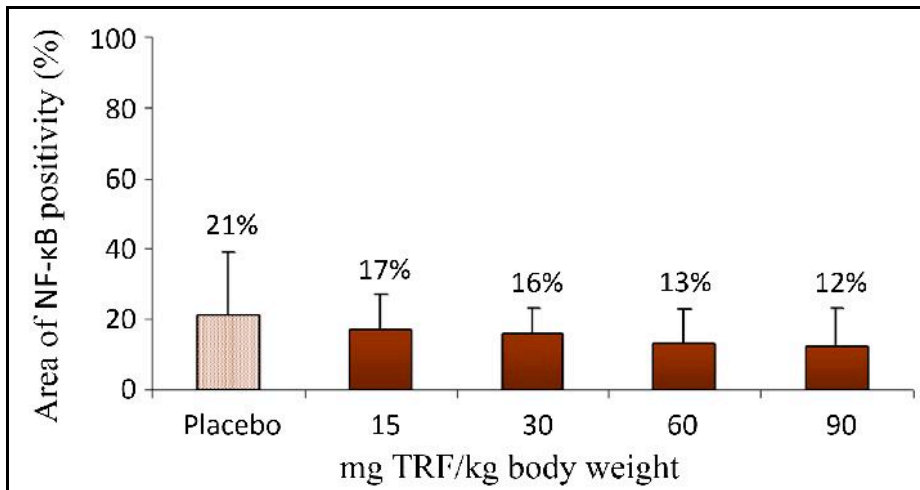
Figure 6. Quantitative analysis of NF- B immunostaining NF- B; Data expressed as Mean ± SEM

There was lower trend of E-selectin (Figure 5) and NF- B tissue expression (Figure 6) in TRF-treated groups compared to placebo. Quantitative analysis showed lower % of E-selectin positivity in TRF-15 compared to placebo group (23.2 ± 6.5 % vs. 4.2 ± 2.1 %, respectively, p<0.05).

Smooth Muscle Actin Expression
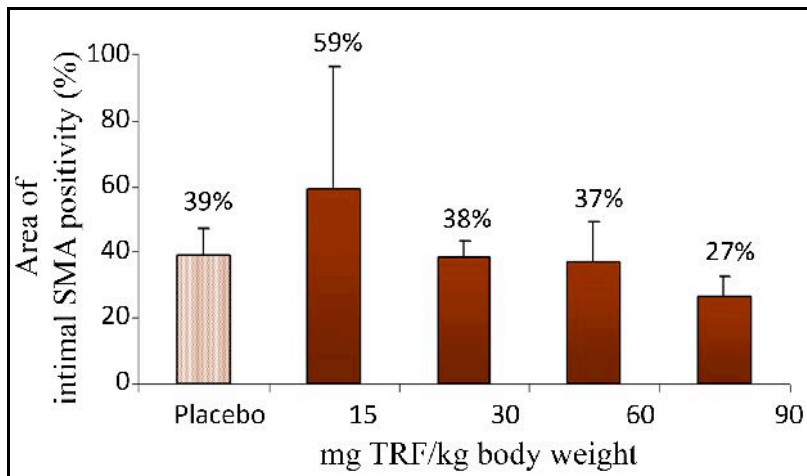
Figure 7. Quantitative analysis of SMA immunostaining; Data expressed as Mean ± SEM

SMA tissue expression (Figure 7) in TRF-treated groups compared to placebo.

DISCUSSION

As tocotrienol is a lipid-soluble antioxidant, the level of circulating biomarkers may not be suff cient to ref ect its action in the blood vessels. A tissue culture experiment showed that -tocotrienol accumulated in human umbilical vein endothelial cells to a level approximately 10-fold greater than that of -tocopherol (Noguchi, Hanyu, Nonaka, Okimoto, & Kodama, 2003). This result ref ects the importance of observing the *in situ* biomarker of atherosclerosis in determining the benef cial effect of tocotrienols. Hence, atherosclerotic lesions and vascular tissue biomarkers were selected to determine if there are anti-atherogenic effects of TRF supplementation, compared to higher doses.

This present study clearly demonstrates that TRF particularly at low dose (15 mg/kg), reduced in vivo aortic tissue endothelial activation and inf ammation in HCD induces severe atherosclerosis. In addition, it is clearly shown in the present study that the atherosclerotic lesions were maximally reduced at low dose of TRF (15 mg/kg) rather than at higher doses (30 to 90 mg/kg), compared to placebo. Furthermore, low dose TRF also maximally increased SMA expression, compared to other higher doses. This suggests a great potential of TRF at low dose in attenuating atherogenesis, enhancing plaque stability and subsequently leading to atherosclerotic plaque regression.

ICAM-1, IL-6, E-selectin and NF- B aortic tissue expression in TRF-treated groups were found to show lower trend compared to placebo. Furthermore, quantitative analysis showed signif cantly lower ICAM-1, E-selectin and IL-6 positivity in TRF-15 compared to placebo group (p<0.05). This suggests that TRF has the capability to inhibit the pro-inf ammatory states in severe progressive atherosclerosis. Further quantif cation analysis revealed TRF supplementation at dosage of 15 and 60 mg/kg body weight shows signif cant lower endothelial ICAM-1 and IL-6 expression respectively, as compared to placebo. This f nding suggests a probable inhibition in the development of atherosclerosis by pro-inf ammatory factor mediated by NF- B activation. This is consistent with the assumption that anti-atherogenic effects of antioxidants may in part be mediated by interference with oxidation-dependent intracellular signaling (Fruebis, Silvestre, Shelton, Napoli, & Palinski, 1999). It is also in agreement with the mechanistic studies on the role of -tocotrienol in atherogenesis through NF- B mediated inf ammation (Theriault, Chao, & Gapor, 2002). Furthermore, tocotrienols have been found to reduce endothelial expression of adhesion molecules, thus inhibiting the monocytic adherence to HUVEC (Naito et al., 2005).

The lowest dose of TRF (15 mg/kg body weight) which has inhibitory effect on ICAM-1 tissue expression is not supported by TRF intervention at high doses. It has been suggested that tocotrienol at high doses (micromolar concentrations) exert protective effect due to its antioxidant property, while tocotrienol at low doses (nanomolar concentrations) regulates specif c neurodegenerative signaling processes (Sen et al., 2007). There is even a study that has reported toxicity of TRF administration at higher tocotrienol dosage (Abd Manan, Mohamed, & Shuid, 2012). Similarly, the low dose used in this experimental atherosclerosis was probably capable of providing suff cient molecule signaling in reducing ICAM-1 tissue expression of the atherosclerotic tissues. A lower expression of NF- B in TRF-15 group also suggests that low dose tocotrienol may play a role in reducing the expression ICAM-1, E-selectin and IL-6via

the NF- B pathway. A more recent study on 31 hypercholesterolaemic patients supplemented with low dose delta-tocotrienol reported reduction in plasma inf ammatory and oxidative stress biomarkers compared to higher dose supplementation (Qureshi, Khan, Mahjabeen, Trias, Silswal, & Qureshi, 2015). This report is parallel with the f ndings of this present study.

CONCLUSION

TRF supplementation particularly at low dose decreases *in vivo* ICAM-1, IL-6, E-selectin and NF- B aortic tissue expression in HCD induced severe atherosclerotic lesions. This suggests that TRF has a potential benef t in attenuating vascular endothelial activation and inf ammation, as well as atherosclerotic plaque regression and possibly contributing to enhancing plaque stability. Hence, future studies investigating the therapeutic potential of TRF in reducing atherosclerosis-related complications such as coronary events are warranted.

ACKNOWLEDGEMENTS

REFERENCES

Abd Manan, N., Mohamed, N., & Shuid, A. N. (2012). Effects of low-dose versus high-dose -tocotrienol on the bone cells exposed to the hydrogen peroxide-induced oxidative stress and apoptosis. *Evidence-Based Complementary and Alternative Medicine, 2012*.

Berliner, J. A., Navab, M., Fogelman, A. M., Frank, J. S., Demer, L. L., Edwards, P. A., ... & Lusis, A. J. (1996). Atherosclerosis: Basic Mechanisms: Oxidation, Inf ammation, and Genetics. *ACC Current Journal Review, 3*(5), 37.

Dörmann, P. (2007). Functional diversity of tocochromanols in plants. *Planta, 225*(2), 269-276.

Fruebis, J., Silvestre, M., Shelton, D., Napoli, C., & Palinski, W. (1999). Inhibition of VCAM-1 expression in the arterial wall is shared by structurally different antioxidants that reduce early atherosclerosis in NZW rabbits. *Journal of Lipid Research, 40*(11), 1958-1966.

Gilmore, T. D. (1999). The Rel/NF-kappaB signal transduction pathway: Introduction. *Oncogene, 18*(49), 6842-6844.

Meganathan, P., Jabir, R. S., Fuang, H. G., Bhoo-Pathy, N., Choudhury, R. B., Taib, N. A., ... & Chik, Z. (2015). A new formulation of Gamma Delta Tocotrienol has superior bioavailability compared to existing Tocotrienol-Rich Fraction in healthy human subjects. *Scientif c Reports, 5*.

Miller, E. R., Pastor-Barriuso, R., Dalal, D., Riemersma, R. A., Appel, L. J., & Guallar, E. (2005). Meta-analysis: high-dosage vitamin E supplementation may increase all-cause mortality. *Annals of Internal Medicine, 142*(1), 37-46.

Muller, W. A. (2002). Leukocyte-endothelial cell interactions in the inf ammatory response. *Laboratory Investigation, 82*(5), 521.

Naito, Y., Shimozawa, M., Kuroda, M., Nakabe, N., Manabe, H., Katada, K., ... & Yoshikawa, T. (2005). Tocotrienols reduce 25-hydroxycholesterol-induced monocyte–endothelial cell interaction by inhibiting the surface expression of adhesion molecules. *Atherosclerosis, 180*(1), 19-25.

Noguchi, N., Hanyu, R., Nonaka, A., Okimoto, Y., & Kodama, T. (2003). Inhibition of THP-1 cell adhesion to endothelial cells by -tocopherol and -tocotrienol is dependent on intracellular concentration of the antioxidants. *Free Radical Biology and Medicine, 34*(12), 1614-1620.

Qureshi, A. A., Khan, D. A., Mahjabeen, W., Trias, A. M., Silswal, N., & Qureshi, N. (2015). Impact of delta-tocotrienol on inf ammatory biomarkers and oxidative stress in hypercholesterolemic subjects. *Journal of Clinical and Experimental Cardiology, 2015*.

Rajendran, P., Rengarajan, T., Thangavel, J., Nishigaki, Y., Sakthisekaran, D., Sethi, G., & Nishigaki, I. (2013). The vascular endothelium and human diseases. *International Journal of Biological Sciences, 9*(10), 1057-1069.

Rimm, E. B., Stampfer, M. J., Ascherio, A., Giovannucci, E., Colditz, G. A., & Willett, W. C. (1993). Vitamin E consumption and the risk of coronary heart disease in men. *New England Journal of Medicine, 328*(20), 1450-1456.

Sen, C. K., Khanna, S., & Roy, S. (2007). Tocotrienols in health and disease: the other half of the natural vitamin E family. *Molecular Aspects of Medicine, 28*(5), 692-728.

Stampfer, M. J., Hennekens, C. H., Manson, J. E., Colditz, G. A., Rosner, B., & Willett, W. C. (1993). Vitamin E consumption and the risk of coronary disease in women. *New England Journal of Medicine, 328*(20), 1444-1449.

Theriault, A., Chao, J. T., & Gapor, A. (2002). Tocotrienol is the most effective vitamin E for reducing endothelial expression of adhesion molecules and adhesion to monocytes. *Atherosclerosis, 160*(1), 21-30.

Tribble, D. L. (1999). Antioxidant consumption and risk of coronary heart disease: emphasis on vitamin C, vitamin E, and -carotene. *Circulation, 99*(4), 591-595.

Neutral Effects of Tocotrienol-rich Fraction Supplementation on Serum Lipids, C-reactive protein and Plasma Lipid Peroxidation in Rabbits with Severe Hypercholesterolaemia and Atherosclerosis

Azlina A. Razak[1], Effat Omar[1,2], Suhaila Muid[1,2] and Hapizah Nawawi[1,2]*

[1]*Institute of Pathology, Laboratory and Forensic Medicine (I-PPerForM), Universiti Teknologi MARA (UiTM), Sungai Buloh Campus, 47000 Sungai Buloh, Selangor, Malaysia*
[2]*Faculty of Medicine, Universiti Teknologi MARA (UiTM), Sungai Buloh Campus, 47000 Sungai Buloh, Selangor, Malaysia*

ABSTRACT

Tocotrienols have been reported to possess potent cholesterol lowering, anti-hypertensive, anti-inf ammatory and anti-oxidative properties which are superior to tocopherols. Emerging evidence suggests pure tocotrienols have anti-atherogenic properties. However, optimal doses of oftocotrienol-rich fraction (TRF) in progressive atherogenesis remain unclear. This animal model experiment was designed to investigate the effects of a range concentration of TRF supplementation on the extent of atherosclerosis and soluble lipids, inf ammatory and oxidative stress biomarkers in high-cholesterol diet (HCD) induced hypercholesterolaemic (HC) rabbits with atherosclerosis. A total of 28 New Zealand white rabbits were given 1% high-cholesterol diet (HCD) for two months and then randomised into f ve groups: Placebo (n=7), TRF 15 mg/kg (n=5), TRF 30 mg/kg (n=6), TRF 60 mg/kg (n=5) and TRF 90 mg/kg (n=5) daily. The treatment was given for three months and the animals were fed HCD throughout the duration. Aortic vessels were obtained to assess the extent of atherosclerotic lesions at the end of the study. Fasting serum lipids (FSL), C-reactive protein (CRP), malondialdehyde (MDA) and 8-isoprostane levels were measured at baseline, one and two months post-HCD, one, two, and three months post-intervention. There were no differences in the extent of the atherosclerotic lesions, percentage changes of FSL, MDA, 8-isoprostane and CRP levels between the placebo and TRF groups. In conclusion, TRF across all doses studied have neutral effects on atherosclerotic lesions, soluble lipids, biomarkers of oxidative stress, coronary risk and inf ammation in severely atherosclerotic rabbits with progressive and continuous insult by high cholesterol feeding.

Keywords: Atherosclerosis, inf ammation, lipids, oxidative stress, soluble biomarkers, tocotrienol-rich fraction

INTRODUCTION

Atherosclerosis is the main underlying pathology in coronary heart disease (CHD), leading to clinical events such as acute myocardial infarction and unstable angina. Therefore, most clinicians target to reduce atherosclerosis by treating cardiovascular risk factors (Roger et al., 2012). Amongst the cardiovascular risk factors, hypercholesterolaemia was recognised to play a central role in the initiation of atherosclerosis or fatty streak development. It is characterised by elevated low-density lipoprotein (LDL) levels in the blood. Since LDL is the major cholesterol-carrying lipoprotein in plasma, there is a higher chance for it to undergo modif cation such as oxidation, proteolysis and aggregation and subsequently get trapped in the vascular walls (Berliner et al., 1996; Stocker & Keaney, 2004).

Following initiation, atherosclerosis is then manifested in stages of early, developing and mature lesions. In general, atherosclerotic lesions are characterised by lipid deposition, f brosis, and calcif cation of lesions (Heistad, 2006). Lipid component of these lesions can be visualised using special staining such as Sudan IV (Tangirala, Rubin, & Palinski, 1995; Zhang et al., 2010). In hypercholesterolaemic rabbits induced severe atherosclerosis, a time-dependent increase in plasma CRP has been shown (Yu et al., 2012). This suggests a predominant systemic inf ammatory state in response to continuous high plasma cholesterol level. Cholesterol feeding in animal model of atherosclerosis also produced increased lipid peroxidation (Mahfouz & Kummerow, 2000). Therefore, measuring soluble biomarkers in blood such as circulating lipids, serum CRP and products of lipid peroxidation is useful to monitor the on-going process of atherosclerosis. Two relevant products of lipid peroxidation in experimental atherosclerosis are 8-iso-Prostaglandin F2 (or 8-Isoprostane) and malondialdehyde (MDA). 8-Isoprostane is a stable end-product from the peroxidation of arachidonic acid (Morrow et al., 1990), while MDA is a short chain aldehyde which arises from ROOH fragmentation of free radical generation.

Vitamin E in the form of tocotrienols are naturally synthesised only by plants and found concentrated in rice bran and palm oil (Ahsan, Ahad, Iqbal, & Siddiqui, 2014). The palm tocotrienol can be produced in the form of tocotrienol-rich fraction (TRF), which comprises 30% tocopherol and 70% tocotrienol (Sundram, Sambanthamurthi, & Tan, 2003). TRF is currently available in the market for human consumption. Tocotrienols differ from tocopherols by possessing three double bonds in the phytyl side chain. In general, the term vitamin E covers four isomers of tocopherols (, ,   and) and four isomers of tocotrienols (, ,   and), all of which are lipid-soluble and chain-breaking antioxidants (Brigelius-Flohe & Traber, 1999). Previously, the effectiveness of pure tocotrienols in reducing inf ammation and endothelial activation in human endothelial cells *in vitro* was reported (Muid, Froemming, Rahman, Ali, & Nawawi, 2016). Rahman et al. (2016) also reported that pure tocotrienols reduced aortic inf ammation, endothelial activation and proteolytic enzymes. Similarly, TRF was also found to exhibit anti-atherogenic properties in experimental atherosclerosis (Mohd. Ismail, Abdul Ghafar, Jaarin, Hla Khine, & Md. Top, 2000; Norsidah, Asmadi, Azizi, Faizah, & Kamisah, 2013) and patients with carotid stenosis (Tomeo, Geller, Watkins, Gapor, & Bierenbaum, 1995). However, the effect of TRF to modulate circulating lipids and systemic inf ammation and lipid peroxidation in progressive HCD-induced severe atherosclerosis is not known. Therefore, this experimental atherosclerosis study aimed to further examine the effects of TRF supplementation

on progressive atherosclerotic lesions and soluble biomarkers in f ve-month cholesterol-fed rabbits. The doses of TRF supplement used were based on previous literature reports (Ahmad, Khalid, Luke, & Ima Nirwana, 2005; Rahman et al., 2016).

MATERIALS AND METHODS

Rabbits and High-cholesterol Diet

This study had been approved by the Institutional Animal Ethics Committee and conformed to the institutional and national guidelines on use of animals in research. The researchers used 28 male New Zealand white rabbits weighing (2.0 - 3.0 kg) which given 1% high-cholesterol diet (HCD) for two months to induce hypercholesterolaemia and establish atherosclerosis, following which, they were randomised into one of f ve groups: Placebo (n=7), TRF 15 mg/kg (n=5), TRF 30 mg/kg (n=6), TRF 60 mg/kg (n=5) and TRF 90 mg/kg body weight (n=5) daily. The treatment was given for three months and the animals were fed HCD throughout the duration. All animals were housed in individual cages, with *ad libitum* access to food and water, maintained at a 12-hour dark/light cycle.

Diet and TRF Supplement

HCD was purchased from Bio-Serv, USA. The TRF supplement (Gold-Tri E 50®, Sime Darby Bioganic Sdn. Bhd., Malaysia) consisted of -tocotrienol: 174.2 mg/g, -tocotrienol: 145.6 mg/g, -tocotrienol: 128.2 mg/g, -tocotrienol: 11.4 mg/g and -tocopherol: 95.8 mg/g. The placebo group was treated with distilled water.

Blood and Tissue Collection

Blood was taken for serum lipids, C-reactive protein (CRP), malondialdehyde (MDA) and 8-isoprostane levels at baseline (BL), one and two months intra-HCD, one, two, and three months post-treatment. About 10 ml of fasting blood samples were collected into plain and ethylene diamine tetra acetic acid (EDTA) coated blood tubes as anticoagulant from middle arterial veins at baseline (BL), one and two post-HCD, one, two, and three months post-TRF treatment. At three months post-TRF treatment the rabbits were sacrif ced and aortic vessels were obtained. The blood tubes were centrifuged at $1400 \times g$ for 10 minutes. Serum and plasma EDTA were isolated and kept in -80°C until analysis. The aorta, from the bifurcation point of the left subclavian artery to the iliac bifurcation, were removed from each rabbit.

Sudan IV Staining

These aortic vessels were processed immediately for macroscopic Sudan IV staining, which was performed according to the method by Hamm, Kaplan, Clarkson and Bullock (1983). The aortas were gently rinsed with normal saline, then cut open longitudinally to expose the lumen and pinned f at on a wooden board in a stainless-steel tray (8×16 cm). The opened aortic vessels were then f xed with 10% neutral buffered formalin overnight. After the process, the aortic vessels were taken out from the immersion and washed with 70% ethanol, followed

by immersion in Herskhemers solution for 15 minutes at room temperature and destained under running tap water for one hour. The stained aortic vessels were put on smooth contrast background for imaging.

The areas of the entire aortic vessels were captured at ultra zoom by a digital camera (C-740 Ultra Zoom, Olympus, USA). The percentage area of dark red regions (the area of atherosclerotic lesions) was calculated within the total surface area of the aortic vessel by using soft imaging solution (analySIS® FIVE, Olympus, USA).

Fasting Serum Lipid Prof les

Fasting lipid prof les [total cholesterol (TC), triglycerides (TG), high-density lipoprotein (HDL-c) and low-density lipoprotein (LDL-c)] were measured by Cobas Integra 400 Plus automated chemistry analyser (Hoffman-La Roche Ltd., Switzerland), according to the manufacturer's protocol and using Roche's calibrator for automated system (cfas), a lyophilised calibrator based on human serum. The use of this method for measuring lipids in rabbit serum has also been reported elsewhere (Idris et al., 2014; Rahman et al., 2016). For TC, the within and between batch coeff cient of variations (CVs) at 5.3 mmol/L were 1.3% and 2.2%, respectively while that for TG at 1.6 mmol/L were 1.6% and 1.9%, respectively. For HDL-c, the within and between batch CVs at 1.2 mmol/L were 0.9% and 1.7%, respectively; while the CVs for LDL-c at 4.3 mmol/L were 1.1% and 1.8%, respectively (Method Manual Cobas Integra 03/2002, 2002).

C-reactive Protein (CRP)

Quantitative determinations of rabbit serum CRP were based on enzyme-linked immunosorbent assay (ELISA) using rabbit CRP E-15CRP-8 ELISA kits (ICL Inc., USA). A standard curve for each microplate assay was prepared. The tests were run according to manufacturer's manual by automated EIA analyser (CODA, Bio-Rad Laboratories, USA). The calculated limit of detection in this assay was 0.3 ng/mL. The within and between batch CVs of rabbit CRP at 3.2 µg/mL were 5.3% and 9.1%, respectively (Rabbit CRP Package Insert, 2006).

Oxidative Stress Biomarkers

The MDA content in serum was determined as thiobarbituric acid-reactive substances (TBARS) as described by Ledwo , Michalak, St pie and Kadziołka (1986), with slight modif cation. The within and between batch CVs of MDA at 7.2 nmol/g were variation that ranged from 1-6% and 5.2%, respectively (Ledwo et al., 1986). Results were expressed as TBARS nmol per gram serum protein (3.1), using 1,1,3,3,tetramethoxypropane (Sigma) as standard.

The measurement of 8-Isoprostane was performed by a validated method adapted from Bohnstedt and colleagues (2003) using liquid chromatography (Agilent 1100 Series, Agilent Technologies, USA) coupled to tandem mass spectrometry system with turbo ion spray (API 4000™ LC/MS/MS System, Applied Biosystems, USA). Bohnstedt et al.(2003) reported that the within and between batch CVs of 8-Isoprostane at 0.28 ng/mL were 7.0% and 7.8%,

respectively. In our laboratory, the within and between batch CVs of 8-Isoprostane at 0.5 ng/mL during the method development were 1.6% and 4.8%, respectively.

Statistical Analysis

For between group differences, student's t-test or Mann-Whitney test was used for variables with normal or non-normal distribution respectively. Within group pre- and post-treatment differences for each variable were analysed by paired t-test or Wilcoxon matched-pair test for those variables with normal distribution and non-normal distribution respectively. Normality was tested with Kolmogrov-Smirnov test. Probability value of $p<0.05$ was taken as signif cant. The statistical analysis was performed using the Statistical Package for Social Sciences (SPSS) version 22.

RESULTS

Percentage of Atherosclerotic Lesions

At the end of the experiment, atherosclerotic lesions were analysed in all the rabbits. There were no differences observed in the extent of atherosclerosis, as represented by the Sudan IV positive areas, between the placebo and treatment groups (Figure 1).
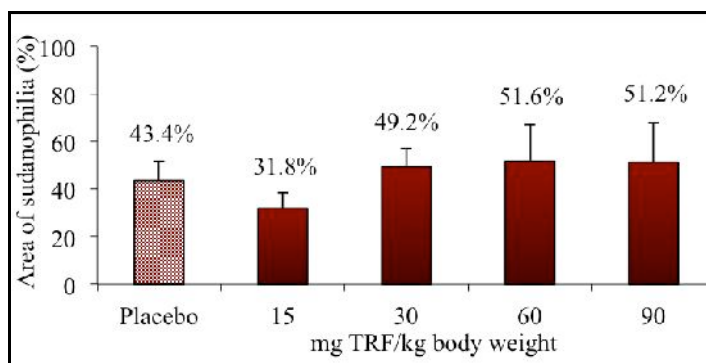
Figure 1. Extent of atherosclerosis def ned by percentage of sudanophilia area in all groups at 3 months post-intervention

Lipid Prof les

Total cholesterol, triglyceride, LDL-c and HDL-c levels signif cantly increased in all the groups at one and two months post HCD administration compared to baseline. The levels and percentage changes of the lipid prof les and baseline, one and two months post HCD are summarised in Table 1. Levels of all lipid parameters remained unaltered post-supplementation at 3 to 5 months compared to post HCD baseline (that is, at two months post HCD prior to randomisation) (Figure 2).

Table 1
Level of serum lipids in placebo and TEMF groups at baseline (BL), 1 month and 2 months post HCD (High cholesterol diet)

Groups	Time points	TC (mmol/L)	TG (mmol/L)	HDL-c (mmol/L)	LDL-c (mmol/L)
Placebo	BL	1.6 ± 0.2	0.6 ± 0.1	1.0 ± 0.2	0.4 ± 0.1
	1 month	12.9 ± 2.4*	0.6 ± 0.2	3.2 ± 0.4*	12.5 ± 2.8*
	2 months	16.7 ± 3.4*	0.6 ± 0.1	3.7 ± 0.7*	15.9 ± 2.8*
TEMF 15	BL	1.1 ± 0.1	0.6 ± 0.0	0.8 ± 0.1	0.2 ± 0.1
	1 month	23.0 ± 6.1*	1.6 ± 1.0	5.2 ± 0.5*	20.7 ± 5.3*
	2 months	25.5 ± 6.6*	1.6 ± 0.6	5.4 ± 1.0*	27.5 ± 7.3*
TEMF 30	BL	1.3 ± 0.2	0.7 ± 0.1	0.8 ± 0.1	0.4 ± 0.1
	1 month	19.6 ± 5.8*	1.5 ± 1.0	4.1 ± 0.7*	19.1 ± 6.4*
	2 months	15.5 ± 3.2*	1.4 ± 0.8	3.6 ± 0.7*	13.8 ± 2.7*
TEMF 60	BL	1.4 ± 0.2	0.7 ± 0.1	0.9 ± 0.2	0.2 ± 0.1
	1 month	20.4 ± 4.4*	0.7 ± 0.1	4.3 ± 1.0*	17.6 ± 5.4*
	2 months	18.9 ± 4.6*	0.9 ± 0.3	4.1 ± 1.0*	17.2 ± 4.4*
TEMF 90	BL	1.3 ± 0.2	0.9 ± 0.3	0.8 ± 0.2	0.4 ± 0.2
	1 month	22.4 ± 4.0*	1.1 ± 0.5	6.1 ± 0.4*	19.2 ± 4.2*
	2 months	12.4 ± 3.1*	1.7 ± 1.1	2.8 ± 0.5*	10.3 ± 2.5*

Note: Data are expressed as Mean ± SEM. * $p < 0.05$ when compared to BL in respective groups
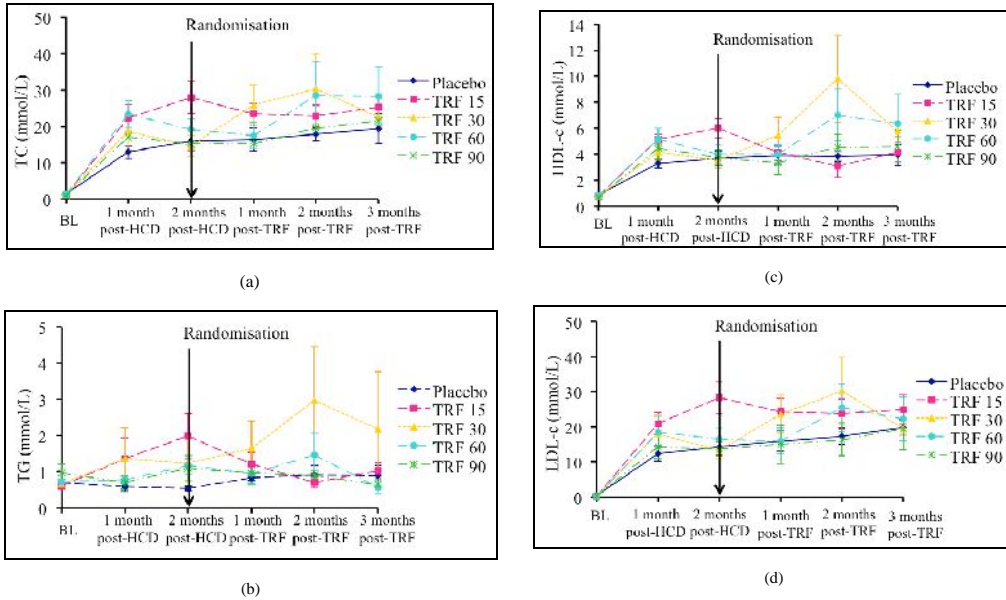
Figure 2. . Fasting lipid prof les: (a) TC; (b) TG; (c) HDL-c; and (d) LDL-c in all groups at BL, 1 and 2 Months Post-HCD, 1, 2 and 3 months post-treatment

Data are expressed as Mean ± SEM. No signif cant differences (p>0.05) in lipid prof les of TRF groups compared to placebo were observed. Different letters indicate signif cant differences compared to BL levels ([a] Placebo, [b] TRF 15, [c] TRF 30, [d] TRF 60, [e] TRF 90, p<0.05).

CRP, MDA and 8-isoprostane Levels

TRF treated groups, across all concentrations showed no signif cant changes in serum MDA, 8-isoprostane and CRP levels compared to the placebo groups (Figures 3 and 4).
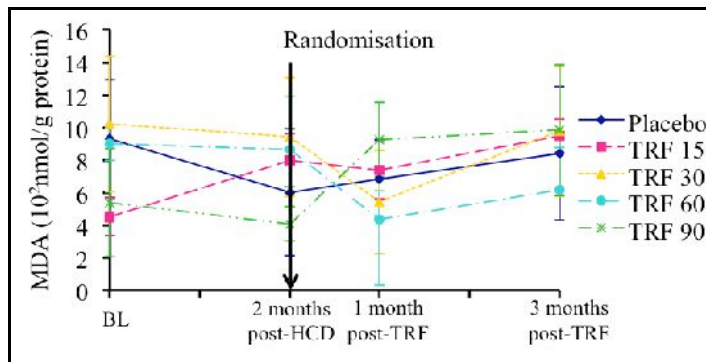
(a)
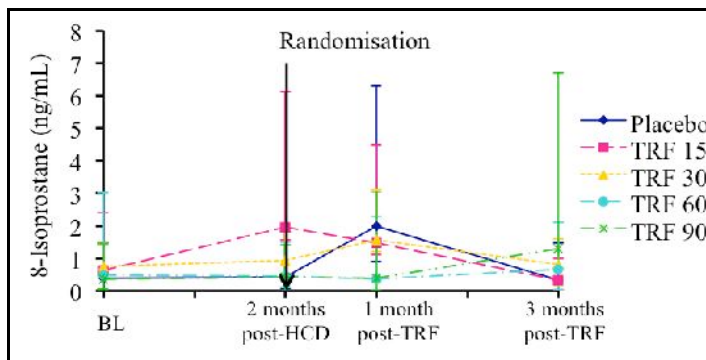
(b)

Figure 3. . Levels of: (a) Plasma MDA; and (b) 8-isoprostane, in all Groups at BL, 2 months post-HCD, 1 and 3 months post-treatment
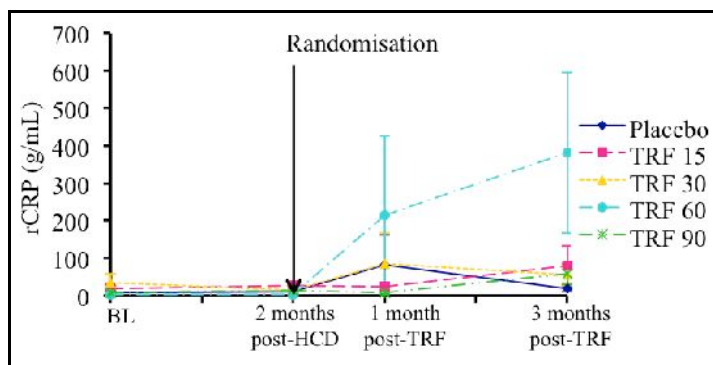
Figure 4. Serum CRP levels in all groups at BL, 2 months post-HCD, 1 and 3 months post-treatment

DISCUSSION

This study used 1% high cholesterol diet to induce hypercholesterolaemic state and severe atherosclerosis in a rabbit model experiment. Cholesterol-fed rabbits were used in investigating the effects of TRF because they are the established experimental model for research in hypercholesterolaemia-induced atherosclerosis (Finking & Hanke, 1997). Blood soluble biomarkers were used to determine the cholesterol lowering, anti-inf ammatory and anti-oxidative properties. Furthermore, inducement of hypercholesterolaemic state and severe atherosclerosis enable the investigation on the systemic hypolipidaemic action, antioxidant and anti-inf ammatory activities in active progression of severe atherosclerosis.

A previous study showed that hypercholesterolaemic-induced rabbits exhibited an increase in oxygen free radical production from one month of cholesterol feeding onward (Ohara, Peterson, & Harrison, 1993). Various percentages of dietary cholesterol were used to induce the hypocholesterolaemic status in other experimental atherosclerosis and vitamin E interventions (Mohd. Ismail et al., 2000; Norsidah et al., 2013; Prasad & Kalra, 1993). In this present study, 1% high cholesterol diet was given for two months prior to randomisation, followed by another three months of HC diet together with the treatment. Serum TC and LDL-c levels increased signif cantly before randomisation and remained high with or without tocotrienol-rich supplementation across all doses studied (15-90 mg/kg). This f nding suggests that the oral administration of TRF supplement does not suppress severe hypercholesterolaemia which may in turn indicate its lack of benef t in terms of cholesterol lowering in severe hypercholesterolaemic conditions such as familial hypercholesterolaemia.

Overall, this present study showed that the percentage of atheromatous lesion was not signif cantly reduced in TRF treated groups as compared to placebo group. However, low dose TRF at 15 mg/kg, had a trend of atherosclerotic regression but this did not indicate any statistical signif cance (p=0.06). It is also worth noting, however, that this study attempted to use TRF supplementation to inhibit the progressive atherogenesis in severe atherosclerosis, with a background of continuous insult by high cholesterol diet for a total period of f ve months. The design mirrored clinical trial on supplementation in patients with established atherosclerotic plaque progression such as tocotrienol trial in patients with carotid stenosis

(Tomeo et al., 1995). Investigation on this aspect is important, as it provides possible mechanistic value of TRF intervention in plaque formation and potentially its stability. Most anti-atherogenic properties of other investigated compounds are designed in the manner where there is regression of atherosclerosis. To study regression of lesions, it is suggested to induce the rabbits with 1.0 - 1.5% cholesterol or saturated fat and switch back to normal/basal diet at the point of intervention (Stein & Stein, 2001). Another experimental atherosclerosis design with positive effect of antioxidants is concurrent supplemental antioxidants and atherogenic diet. The antioxidants may be fed through oral gavage or incorporated with the atherogenic diet (Black, Wang, Maeda, & Coleman, 2000; Norsidah et al., 2013).

Although palm vitamin E enriched tocotrienols are found to have lipid lowering effects (Palau, Lightner, Brannon, & Krishnan, 2013; Parker, Pearce, Clark, Gordon, & Wright, 1993; Theriault, Chao, Wang, Gapor, & Adeli, 1999), the result in this experimental atherosclerosis utilising rabbits does not support the previous positive f nding. The previous rabbit model in investigating the effects of tocotrienols on cholesterol and atherosclerosis by Hasselwander et al. (2002) is in agreement with the outcome of this present study. However, the previous study employed dietary mixed tocotrienols supplementation rate of 500mg/kg diet which is equal to approximately 20 mg/kg body weight, while the current study uses slightly lower and higher doses (15-90 mg/kg).

In the present study, serum CRP levels are measured as a soluble biomarker as an indicator of systemic inf ammatory status. A time-course measurement of rabbit CRP sera indicated non-significant changes throughout the study in all groups. Limited original contributions have been found to indicate direct systemic anti-inf ammatory effect of TRF in experimental atherosclerosis, although tocotrienols have been found to reduce expression of aortic inf ammatory markers and increase plaque stability via reduction of vascular matrix metalloproteinases (Rahman et al., 2016).

The selected lipid peroxidation indices, MDA and 8-isoprostane, revealed non-signif cant changes throughout the study. Comparison among potent antioxidants on anti-atherosclerotic effect suggests that vitamin E may provide protective properties against hypercholesterolaemic atherosclerosis not linked to its antioxidant property (Özer & Azzi, 2000). For example, one of the probucol analogue, bis(3,5-di-*tert*-butyl-4-hydroxyphenylether) propane, failed to prevent atherosclerosis in rabbit despite its strong inhibition on LDL oxidation *in vitro* (Fruebis, Silvestre, Shelton, Napoli, & Palinski, 1999). It is also speculated that the undetectable anti-inf ammatory action by TRF may be due to its characteristic as a mixture of tocotrienols and tocopherols, as it is reported that tocopherol is capable in attenuating the hypocholesterolaemic activity of tocotrienols (Qureshi, Pearce, Nor, & Gapor, 1996). However, further study is necessary to clarify this possibility.

CONCLUSION

TRF has no *in vivo* effect on soluble biomarkers of coronary risk in severe HC and experimental atherosclerosis.

ACKNOWLEDGEMENTS

REFERENCES

Ahmad, N., Khalid, B., Luke, D., & Ima Nirwana, S. (2005). Tocotrienol offers better protection than tocopherol from free radical-induced damage of rat bone. *Clinical and Experimental Pharmacology and Physiology, 32*(9), 761-770.

Ahsan, H., Ahad, A., Iqbal, J., & Siddiqui, W. A. (2014). Pharmacological potential of tocotrienols: a review. *Nutrition and Metabolism, 11*(1), 52.

Berliner, J. A., Navab, M., Fogelman, A. M., Frank, J. S., Demer, L. L., Edwards, P. A., ... & Lusis, A. J. (1996). Atherosclerosis: Basic Mechanisms: Oxidation, Inf ammation, and Genetics. *ACC Current Journal Review, 3*(5), 37.

Black, T. M., Wang, P., Maeda, N., & Coleman, R. A. (2000). Palm tocotrienols protect ApoE+/− mice from diet-induced atheroma formation. *The Journal of Nutrition, 130*(10), 2420-2426.

Bohnstedt, K. C., Karlberg, B., Wahlund, L.-O., Jönhagen, M. E., Basun, H., & Schmidt, S. (2003). Determination of isoprostanes in urine samples from Alzheimer patients using porous graphitic carbon liquid chromatography–tandem mass spectrometry. *Journal of Chromatography B, 796*(1), 11-19.

Brigelius-Flohe, R., & Traber, M. G. (1999). Vitamin E: Function and metabolism. *The FASEB Journal, 13*(10), 1145-1155.

Finking, G., & Hanke, H. (1997). Nikolaj Nikolajewitsch Anitschkow (1885–1964) established the cholesterol-fed rabbit as a model for atherosclerosis research. *Atherosclerosis, 135*(1), 1-7.

Fruebis, J., Silvestre, M., Shelton, D., Napoli, C., & Palinski, W. (1999). Inhibition of VCAM-1 expression in the arterial wall is shared by structurally different antioxidants that reduce early atherosclerosis in NZW rabbits. *Journal of Lipid Research, 40*(11), 1958-1966.

Hamm, T., Kaplan, J., Clarkson, T., & Bullock, B. (1983). Effects of gender and social behavior on the development of coronary artery atherosclerosis in cynomolgus macaques. *Atherosclerosis, 48*(3), 221-233.

Hasselwander, O., Krämer, K., Hoppe, P. P., Oberfrank, U., Baldenius, K., Schröder, H., ... & Nowakowsky, B. (2002). Effects of feeding various tocotrienol sources on plasma lipids and aortic atherosclerotic lesions in cholesterol-fed rabbits. *Food Research International, 35*(2), 245-251.

Heistad, D. D. (2006). Oxidative stress and vascular disease. *Arteriosclerosis, Thrombosis, and Vascular Biology, 26*(4), 689-695.

Idris, C. A. C., Karupaiah, T., Sundram, K., Tan, Y. A., Balasundram, N., Leow, S. S., ... & Sambanthamurthi, R. (2014). Oil palm phenolics and vitamin E reduce atherosclerosis in rabbits. *Journal of Functional Foods, 7*, 541-550.

Ledwo , A., Michalak, J., St pie , A., & Kadziołka, A. (1986). The relationship between plasma triglycerides, cholesterol, total lipids and lipid peroxidation products during human atherosclerosis. *Clinica Chimica Acta, 155*(3), 275-283.

Mahfouz, M. M., & Kummerow, F. A. (2000). Cholesterol-rich diets have different effects on lipid peroxidation, cholesterol oxides, and antioxidant enzymes in rats and rabbits. *The Journal of Nutritional Biochemistry, 11*(5), 293-302.

Mohd. Ismail, N., Abdul Ghafar, N., Jaarin, K., Hla Khine, J., & Md. Top, G. (2000). Vitamin E and factors affecting atherosclerosis in rabbits fed a cholesterol-rich diet. *International Journal of Food Sciences and Nutrition, 51*(1), 79-94.

Morrow, J. D., Hill, K. E., Burk, R. F., Nammour, T. M., Badr, K. F., & Roberts, L. J. (1990). A series of prostaglandin F2-like compounds are produced in vivo in humans by a non-cyclooxygenase, free radical-catalyzed mechanism. *Proceedings of the National Academy of Sciences, 87*(23), 9383-9387.

Muid, S., Froemming, G. R. A., Rahman, T., Ali, A. M., & Nawawi, H. M. (2016). Delta-and gamma-tocotrienol isomers are potent in inhibiting inf ammation and endothelial activation in stimulated human endothelial cells. *Food and Nutrition Research, 60*(1), 31526.

Norsidah, K. Z., Asmadi, A. Y., Azizi, A., Faizah, O., & Kamisah, Y. (2013). Palm tocotrienol-rich fraction improves vascular proatherosclerotic changes in hyperhomocysteinemic rats. *Evidence-Based Complementary and Alternative Medicine, 2013*.

Ohara, Y., Peterson, T. E., & Harrison, D. G. (1993). Hypercholesterolemia increases endothelial superoxide anion production. *Journal of Clinical Investigation, 91*(6), 2546.

Özer, N. K., & Azzi, A. (2000). Effect of vitamin E on the development of atherosclerosis. *Toxicology, 148*(2), 179-185.

Palau, V., Lightner, J., Brannon, M., & Krishnan, K. (2013). Gamma-Tocotrienol and Simvastatin Synergistically Induce Cytotoxicity In Leukemia Cell Lines, K-562 and HL-60.

Parker, R. A., Pearce, B. C., Clark, R. W., Gordon, D. A., & Wright, J. (1993). Tocotrienols regulate cholesterol production in mammalian cells by post-transcriptional suppression of 3-hydroxy-3-methylglutaryl-coenzyme A reductase. *Journal of Biological Chemistry, 268*(15), 11230-11238.

Prasad, K., & Kalra, J. (1993). Oxygen free radicals and hypercholesterolemic atherosclerosis: Effect of vitamin E. *American Heart Journal, 125*(4), 958-973.

Qureshi, A. A., Pearce, B. C., Nor, R. M., & Gapor, A. (1996). Dietary alpha-tocopherol attenuates the impact of gamma-tocotrienol on hepatic 3-hydroxy-3-methylglutaryl coenzyme A reductase A activity in chickens. *The Journal of Nutrition, 126*(2), 389.

Rahman, T. A., Hassim, N. F., Zulkafli, N., Muid, S., Kornain, N. K., & Nawawi, H. (2016). Atheroprotective effects of pure tocotrienol supplementation in the treatment of rabbits with experimentally induced early and established atherosclerosis. *Food and Nutrition Research, 60*(1), 31525.

Roger, V. L., Go, A. S., Lloyd-Jones, D. M., Benjamin, E. J., Berry, J. D., Borden, W. B., ... & Fullerton, H. J. (2012). Heart disease and stroke statistics—2012 update. *Circulation, 125*(1), e2-e220.

Stein, Y., & Stein, O. (2001). Does therapeutic intervention achieve slowing of progression or bona f de regression of atherosclerotic lesions? *Arteriosclerosis, Thrombosis, and Vascular Biology, 21*(2), 183-188.

Stocker, R., & Keaney, J. F. (2004). Role of oxidative modif cations in atherosclerosis. *Physiological Reviews, 84*(4), 1381-1478.

Sundram, K., Sambanthamurthi, R., & Tan, Y.-A. (2003). Palm fruit chemistry and nutrition. *Asia Pacif c Journal of Clinical Nutrition, 12*(3).

Tangirala, R. K., Rubin, E. M., & Palinski, W. (1995). Quantitation of atherosclerosis in murine models: Correlation between lesions in the aortic origin and in the entire aorta, and differences in the extent of lesions between sexes in LDL receptor-def cient and apolipoprotein E-def cient mice. *Journal of Lipid Research, 36*(11), 2320-2328.

Theriault, A., Chao, J.-T., Wang, Q., Gapor, A., & Adeli, K. (1999). Tocotrienol: A review of its therapeutic potential. *Clinical Biochemistry, 32*(5), 309-319.

Tomeo, A., Geller, M., Watkins, T., Gapor, A., & Bierenbaum, M. (1995). Antioxidant effects of tocotrienols in patients with hyperlipidemia and carotid stenosis. *Lipids, 30*(12), 1179-1183.

Yu, Q., Li, Y., Waqar, A. B., Wang, Y., Huang, B., Chen, Y., ... & Liu, E. (2012). Temporal and quantitative analysis of atherosclerotic lesions in diet-induced hypercholesterolemic rabbits. *BioMed Research International, 2012*.

Zhang, C., Zheng, H., Yu, Q., Yang, P. G., Li, Y., Cheng, F., ... & Liu, E. (2010). A practical method for quantifying atherosclerotic lesions in rabbits. *Journal of Comparative Pathology, 142*(2), 122-128.

Aluminium Foam Sandwich Panel with Hybrid FRP Composite Face-Sheets: Flexural Properties

Mohd Fadzli Ismail[1], Aidah Jumahat[2]*, Ummu Raihanah Hashim[2] and Anizah Kalam[2]

[1]*Faculty of Mechanical Engineering, Universiti Teknologi MARA (UiTM) Terengganu, Kampus Bukit Besi, 23200 Dungun, Terengganu, Malaysia*
[2]*Faculty of Mechanical Engineering, Universiti Teknologi MARA (UiTM), 40450 Shah Alam, Selangor, Malaysia*

ABSTRACT

The increasing demand for high-strength light-weight f bre reinforced polymer (FRP) composite materials has driven the researchers to further innovate and introduce hybrid reinforcement materials. The usage of hybrid FRP composite and metal foam in the fabrication of sandwich panel in structural industries is still new and limited research has been reported in this area. In addition, there is limited research data on aluminium foam as a core material in sandwich panel and needs to be further studied. This research is aimed to determine the bending properties of closed-cell aluminium foam sandwich panel with hybrid FRP composite face-sheets. The three-point bending tests were carried out in order to determine mechanical properties of the material, such as Young's modulus and strength. The sandwich panels were prepared using FRP composite face-sheets, which consist of carbon and glass f bres and epoxy matrix, and closed-cell aluminium foam core material. The results show that aluminium foam sandwich panel with hybrid FRP composite face-sheets exhibit higher f exural strength and modulus compared to the neat closed-cell aluminium foam panel. It also has higher f exural strength and f exural modulus, by 338% and 136% respectively, as compared to the aluminium honeycomb sandwich panel.

Keywords: Aluminium foam, aluminium honeycomb, f exural strength, f exural modulus, hybrid FRP composite

INTRODUCTION

The invention and development of new materials have encouraged many researchers to investigate various types of high strength and lightweight materials that can be used in construction, automotive and aerospace industries. These investigations lead to porous

metal, such as aluminium foam, as one of the areas of interest by many researchers because of its excellent stiffness to weight ratio. Aluminium foam is a cellular structure which contains aluminium solid with a large volume fraction of gas-f lled pores. It has low density, high ductility, low thermal conductivity and competitive cost (Ismail, Jumahat, Abdullah, Hashim, & Ahmad, 2015).

Sandwich structure composite is a special class of composite materials, which is fabricated by attaching two thin stiff skins to a thick but lightweight core material. These structures are specif cally designed to achieve the requirement of least mass to carry optimum load capacity. The sandwich structures have higher specif c strength and stiffness compared to the pristine or constituent materials. The materials usually used as core are made up of honeycomb, foam, balsa wood and synthetic foam, and normally, these comprise polymeric and aluminium base (Crupi, Epasto, & Guglielmino, 2012; Sharma, Murthy, & Krishna, 2004). The selection of suitable core materials is crucial to maintaining the effectiveness of sandwich structure. Core materials must be strong enough to resist compressive and crushing loads as well as shear forces imposed on the panel.

Previous studies have been conducted and proved that hybrid reinforcement may contribute to better mechanical performance of the FRP composite structure (Ismail, Jumahat, Ahmad, & Ismail, 2015). Therefore, in this study the hybrid FRP composite will be used as a face sheet and will be combined with closed-cell aluminium foam in order to fabricate sandwich panel. Three-point bending tests will be conducted on the neat aluminium foam panel, hybrid FRP composite-aluminium foam and hybrid FRP composite-aluminium honeycomb sandwich panels in order to investigate the mechanical response of the panels under transverse loading. This research is aimed to determine the bending properties of closed-cell aluminium foam sandwich panel with hybrid FRP composite face-sheets. The mechanical behaviour of the panels concerning the f exural load-def ection curves and the failure deformation are also compared and discussed.

MATERIALS AND METHODS

The research was conducted using two types of core materials: commercial closed-cell aluminium foam and hexagonal aluminium honeycomb. Figure 1 shows the samples of core materials used in the experiment. The aluminium foam quality has an average density of 0.35 g/cm^3 and average pores size of 3.0 mm. Meanwhile, the hexagonal aluminium honeycomb has an average density of 0.07 ± 0.01 g/cm^3 and a 7.49 mm cells' diameter. Both these core materials have a thickness of 20 mm. These core materials were sandwiched with the hybrid FRP composite face-sheets. The hybrid FRP composite face-sheets consisted of carbon f bre reinforced polymer (CFRP) composite and glass f bre reinforced polymer (GFRP) composite. A 3K, 2×2 twill weave carbon and 7781 e-glass prepregs were used to create the hybrid FRP composite. These prepregs material is already impregnated with epoxy resin (27% to 33%) according to the data sheet given by the manufacturer ("Product data sheet - Prepreg 3K, 2x2 Twill Weave Carbon," 2010; "Product data sheet - Prepreg 7781 E-Glass," 2010). The prepregs were cut into 150 mm length and 50 mm width according to the sample of three-point bending

test. The carbon and glass prepregs were stacked together and placed in the hot press machine for the curing process. The temperature of the hot press machine was set at 154°C for one hour soaking time. The cured hybrid FRP composite was removed from the hot press machine once the temperature of the material dropped to less than 66°C.

(a)   (b)
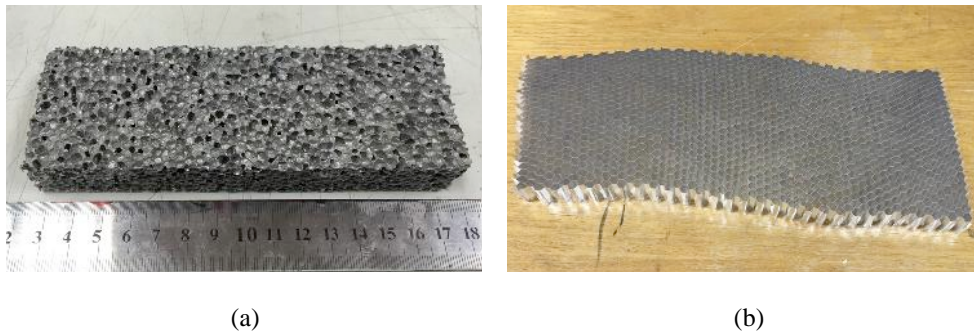
Figure 1. The core materials: (a) closed-cell aluminium foam; and (b) hexagonal aluminium honeycomb

The closed-cell aluminium foam and aluminium honeycomb were cut into a size of 150 mm length and 50 mm width. These materials were attached together with the hybrid FRP composite face-sheets at the top and the bottom side using Araldite glue. After curing the araldite glue adhered f rmly in between the materials and f lled up the empty hole space of the foam core, thus enhancing the bonding strength between the core and the face-sheet materials.

Three-point Bending Test

Three-point bending tests were performed to determine the bending properties for each of the structures of the panel. An Instron 3382 100 kN Floor Model Universal Testing machine as shown in Figure 2 was used to conduct the three-point bending test. Three types of different materials structure (neat closed-cell aluminium foams panels, aluminium foam sandwich panels with hybrid FRP composite face-sheets and aluminium honeycomb sandwich panels with hybrid FRP composite face-sheets) were tested according to the ASTM D7250/D7250M.

The specimens of 150 mm length $\times$ 50 mm width $\times$ 22 mm thickness (20 mm core and 1 mm face-sheets) as shown in Figure 3 were bent under three-point bending conf guration. The specimens were mounted on a steel cylinder of 10 mm diameter with a span length of 125 mm. Measurement of the specimens' thickness and width were done at three different points using a digital electronic Vernier calliper before commencing the experiment. The purpose of this measurement is to obtain the average value of width and thickness. These data were then recorded in the software of the machine. The three-point bending tests were conducted at a crosshead displacement rate of 1 mm/min at room temperature and load-displacement curves were recorded during the test.
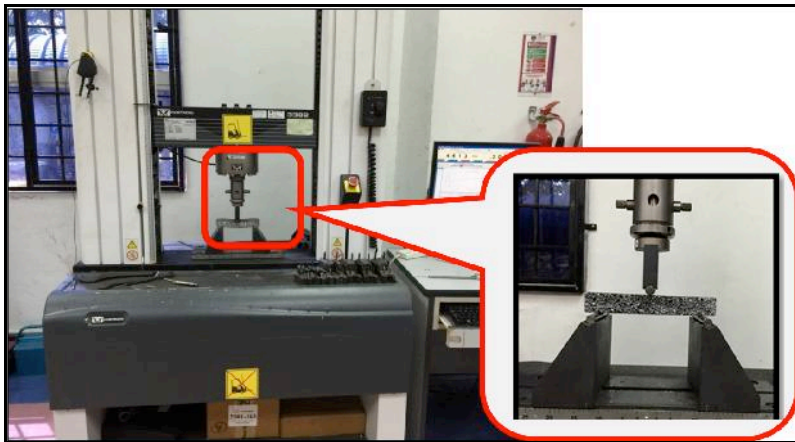
Figure 2. Instron 3382 100 kN f oor model universal testing machine with three-point bending test rig
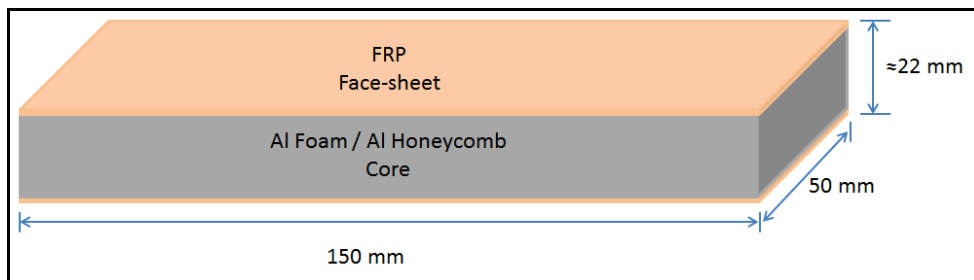
Figure 3. Dimension of specimen for three-point bending test

RESULTS AND DISCUSSION

Figure 4 shows the load-def ection curves of the neat closed-cell aluminium foam and hybrid FRP composite face-sheets sandwich panels subjected to the static three-point bending test. It is clear that that initially, all the panels have linear-elastic behaviour, followed by elasto-plastic phase until a peak value is reached. However, the neat closed-cell aluminium foam panel only has one peak load whereas the aluminium honeycomb and aluminium foam sandwich panels with hybrid FRP composite face-sheets have two peaks load, with the f rst peak higher than the second peak. The peak load of the neat closed-cell aluminium foam occurs just before it starts to fail at approximately 2 mm def ection. Subsequently, the f exural load decreases towards the x-axis. The loss load after the peak load is physically evident as illustrated in Figure 5 - crack load initiation exists. As the displacement increases, the bending failure is propagated towards the upper phase of aluminium foam panel until the f exural load becomes zero.
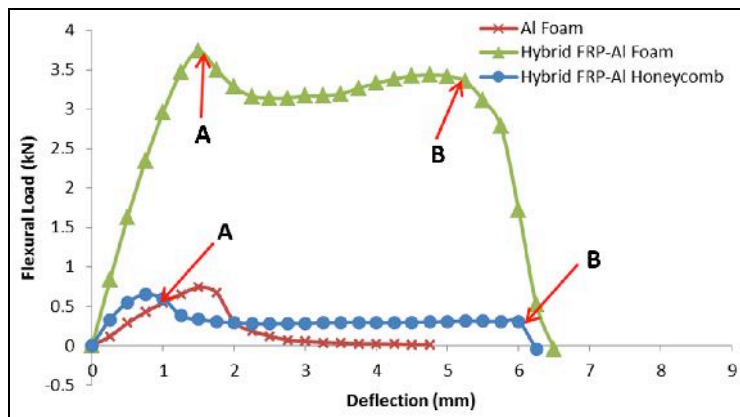
Figure 4. Load-def ection curves of the neat closed-cell aluminium foam and hybrid FRP composite face-sheets sandwich panels
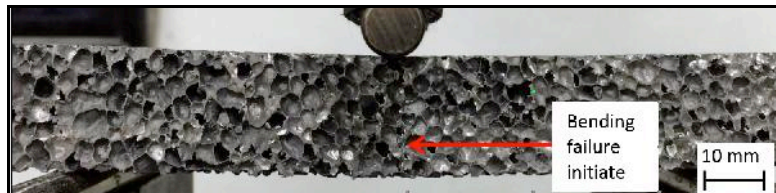
(a)
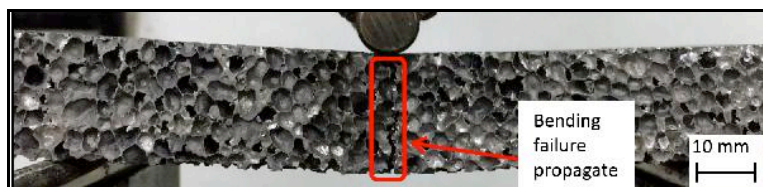
(b)

Figure 5. Failure deformation of the neat closed-cell aluminium foam panel

For the aluminium honeycomb and aluminium foam sandwich panels with hybrid FRP composite face-sheets, the f exural load-def ection curves experienced two loss load; identif ed as A and B in Figure 4. Point A in the aluminium honeycomb sandwich panel represents the face-sheets yield. As the displacement increases, the face-sheets yield also increases. The aluminium honeycomb sandwich panel displays a long plateau region owing to the uniformity of the cell size of the aluminium honeycomb. At the end of the plateau region, the panel experiencing debonding between the aluminium honeycomb of the core and the top face-sheets is indicated at point B. The failure deformation of aluminium honeycomb sandwich panel is shown in Figure 6.
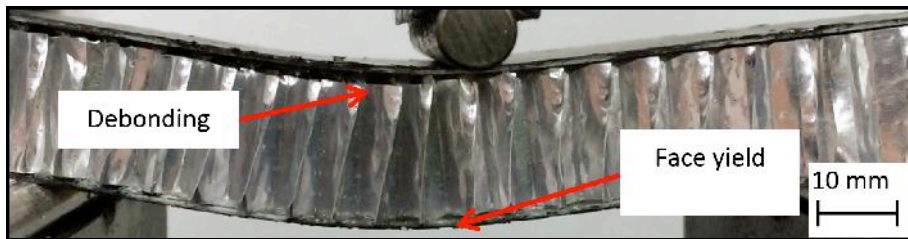
Figure 6. Failure deformation of the aluminium honeycomb sandwich panel with hybrid FRP composite face-sheets

In the aluminium foam sandwich panel, point A represents the failure of top face-sheet such as indentation and plastic hinge, and aluminium foam core failures, such as core crushing and core shear. The increase in displacement leads to an increase in core shear and core crushing as well. The entire core shear then connects with each other. The bottom face sheet is yielded during the load drop at point B. The debonding between core and bottom face-sheets is propagated due to the face sheet yielding. It has been identif ed that these failures occur when the core is thick enough (Yu, Wang, Li, & Zheng, 2008). The failure deformation of aluminium foam sandwich panel is shown in Figure 7.
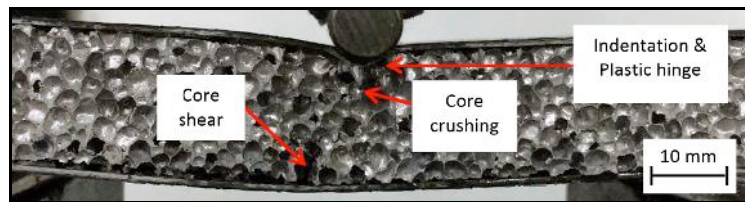
(a)
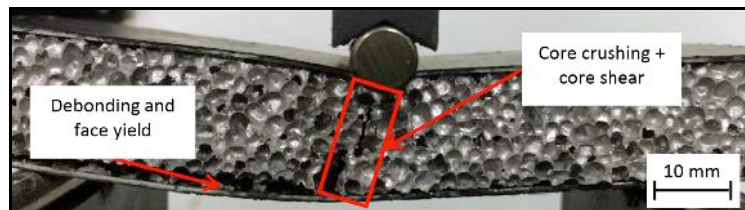
(b)

Figure 7. Failure deformation of the aluminium foam sandwich panel with hybrid FRP composite face-sheets

Figure 8 shows the graph of f exural strength and modulus value of the neat closed-cell aluminium foam panel and both aluminium honeycomb and aluminium foam sandwich panels with hybrid FRP composite face-sheets. The graph shows that the aluminium foam sandwich panel exhibits the highest f exural strength value of 23.7 MPa, followed by the aluminium honeycomb sandwich panel and the neat closed-cell aluminium foam panel, with f exural

strength value of 5.8 MPa and 5.4 MPa, respectively. The use of hybrid FRP composite face-sheets in the aluminium foam sandwich panel revealed a signif cant improvement in f exural strength of 309% compared to the neat closed-cell aluminium foam panel. However, the capability of the hybrid FRP composite face-sheets is limited when it is used in the aluminium honeycomb sandwich panel due to huge mismatch of stiffness; high stiffness of the hybrid FRP composite and low stiffness of the aluminium honeycomb (Shi, Sun, Hu, & Chen, 2014). The f exural strength of aluminium foam core sandwich panel is 338% higher than that of the aluminium honeycomb sandwich panel. This is because the aluminium foam is built from solid aluminium with gas-f lled pores, while aluminium honeycomb structure is a combination of corrugated aluminium sheets with an adhesive material. As a result, the aluminium foam has good material properties, is stronger and stiffer than the aluminium honeycomb. In addition, the aluminium foam has a closed-cell wall structure with larger bonding surface compared to the aluminium honeycomb.
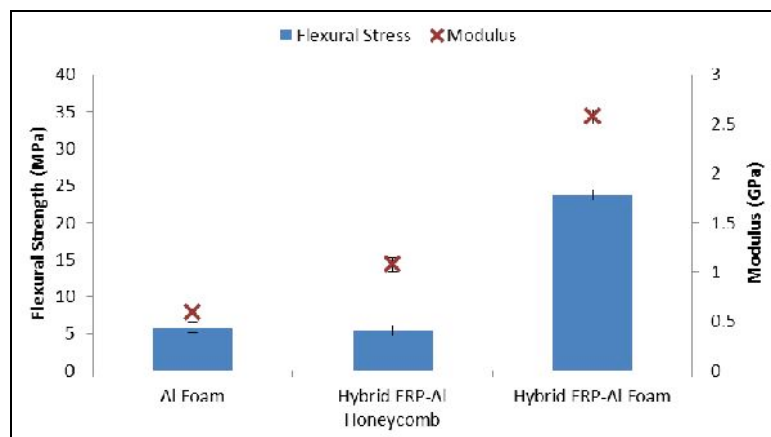
Figure 8. Flexural strength and modulus value of sandwich panels

The f exural modulus of the aluminium foam sandwich panel is the highest with 2.6 GPa, followed by the aluminium honeycomb sandwich panel with 1.1 GPa. On the other hand, the neat closed-cell aluminium foam panel exhibits the lowest f exural modulus of 0.6 GPa. The f exural modulus of the aluminium foam sandwich panel is 136% higher than the aluminium honeycomb sandwich panel and 333% higher than the neat closed-cell aluminium foam panel. This proves that the replacement of core material with aluminium foam enhanced the properties of the conventional (aluminium honeycomb core) sandwich panel. In addition, the presence of aluminium foam in sandwich panel improved the properties of the neat closed-cell aluminium foam panel. The aluminium honeycomb sandwich panel exhibits a higher f exural modulus of 83% than the neat closed-cell aluminium foam panel. Thus, from this study, it can be ascertained that the presence of hybrid FRP composite face-sheets on the aluminium honeycomb sandwich panel increases the stiffness of the whole structure of the sandwich panel.

CONCLUSION

A new sandwich panel consisted of closed-cell aluminium foam sandwich panel with hybrid FRP composite face-sheets was successfully developed in this research. The three-point bending tests were carried out to determine the f exural strength and f exural modulus (bending properties) of the aluminium foam sandwich panel with hybrid FRP composite face-sheets. The use of hybrid FRP composite face-sheets in the aluminium foam sandwich panel revealed a signif cant improvement in f exural strength and f exural modulus by 309% and 333%, respectively, compared to the neat closed-cell aluminium foam panel. The aluminium foam sandwich panel also exhibited higher f exural strength and f exural modulus by 338% and 136%, respectively, compared to the aluminium honeycomb sandwich panel by using the same face-sheets. The combination of the hybrid FRP composite face-sheets and aluminium foam core produced a superior sandwich panel by demonstrating high bending properties compared to the pristine material as well as the conventional sandwich panel. It can be concluded that the new developed closed-cell aluminium foam sandwich panel with hybrid FRP composite face-sheets is a promising advanced material and has high potential to be deployed in modern mechanical structures.

ACKNOWLEDGEMENTS

REFERENCES

Crupi, V., Epasto, G., & Guglielmino, E. (2012). Collapse modes in aluminium honeycomb sandwich panels under bending and impact loading. *International Journal of Impact Engineering, 43*, 6–15.

Ismail, M. F., Jumahat, A., Abdullah, B., Hashim, U. R., & Ahmad Aseri, S. E. (2015). Investigation on energy absorption of aluminium foam-CFRP sandwich panel subjected to impact loading. *Jurnal Teknologi (Sciences & Engineering), 75*(8), 113–116.

Ismail, M. F., Jumahat, A., Ahmad, N., & Ismail, M. H. (2015). Low-Velocity Impact of Aluminium Foam - Glass Fibre Reinforced Plastic Sandwich Panels. *Advanced Materials Research, 1113*, 74–79.

Product data sheet - Prepreg 3K, 2x2 Twill Weave Carbon. (2010). Fibre Glast Development Corporation.

Product data sheet - Prepreg 7781 E-Glass. (2010). Fibre Glast Development Corporation.

Sharma, S. C., Murthy, H. N. N., & Krishna, M. (2004). Low-velocity impact response of polyurethane foam composite sandwich structures. *Journal of Reinforced Plastics and Composites, 23*(17), 1869–1882.

Shi, S., Sun, Z., Hu, X., & Chen, H. (2014). Flexural strength and energy absorption of carbon-f ber–aluminum-honeycomb composite sandwich reinforced by the aluminium grid. *Thin-Walled Structures, 84,* 416–422.

Yu, J., Wang, E., Li, J., & Zheng, Z. (2008). Static and low-velocity impact behaviour of sandwich beams with closed-cell aluminum-foam core in three-point bending. *International Journal of Impact Engineering, 35*(8), 885–894.

The Role of Secondary Filler on Fracture Toughness and Impact Strength of HDPE/Clay Nanocomposites

Anizah Kalam*, Rahilah Kamarudzaman, Koay Mei Hyie, Aidah Jumahat and Noor Leha Abdul Rahman

Centre of Advanced Materials Research (CAMAR), Fakulti Kejuruteraan Mekanikal, Universiti Teknologi MARA (UiTM), 40450 Shah Alam, Selangor, Malaysia

ABSTRACT

In this study, oil palm fruit bunch fiber (OPEFB) was used as a secondary filler in HDPE/clay nanocomposites. The composites were prepared by melt compounding, containing high density polyethylene (HDPE), OPEFB f bers, Maleic anhydride grafted polyethylene (MAPE) and four different clay loading (3, 5, 7 and 10 PE nanoclay masterbatch pellets per hundred HDPE pellets). Four OPEFB sizes (180 µm, 250 µm, 300 µm and 355 µm) were added in the composites to investigate its effects on the fracture toughness and impact strength. Fracture toughness of the composites was determined according to ASTM D5045 and single edge notch bending (SENB) was employed during the test while impact tests were performed according to ASTM D256. The effects of alkali treatment were also investigated in this study. The result indicates that the fracture toughness slightly increased as clay loading increased. The highest value of fracture toughness was 0.47 and 1.06 MPa.m1/2 at 5 phr for both types of composites. The presence of OPEFB f ler as a secondary f ller in the matrix indicates signif cant enhancement of fracture toughness up to 133%. However, its impact strength seems to deteriorate with the presence of OPEFB f ber.

Keywords: Alkali treated, hybrid nanocomposite, oil palm empty fruit bunch (OPEFB) f ber, polyethylene, polymer

E-mail addresses:
anizahkalam@salam.uitm.edu.my (Anizah Kalam),
illacharl_2213@yahoo.com (Rahilah Kamarudzaman),
koay@salam.uitm.edu.my (Koay Mei Hyie),
aidahjumahat@salam.uitm.edu.my (Aidah Jumahat),
noorleha3585@salam.uitm.edu.my (Noor Leha Abdul Rahman)
*Corresponding Author

INTRODUCTION

Natural fibers have attracted the interest of material scientists, researchers, and industries to be used as reinforcement or f ller in composites because of their specif c advantages compared to conventional or synthetic f bers. Hence, a lot of research has been done to look into the potential of natural

f ber as a reinforcement in composite materials. However, its mechanical properties are still not comparable to the synthetic f ber, mainly due to lower ultimate tensile strength of the f ber itself and poor bonding between the f ber and matrix. Properties of the natural f ber depend mainly on the nature of the plant, location in which it is grown, age of the plant, and the extraction method used. Several attempts have been successfully made to enhance the mechanical properties of the composites by treating the f bers to improve the bonding between f bers and matrix.

Oil Palm Empty Fruit Bunch (OPEFB) f ber extracted from an empty fruit bunch which is abundantly available is one of the best types of potential f ber to combine with thermoplastic to produce natural f ber composites. Mechanical properties of OPEFB f ber composites have been quite extensively investigated by many researchers (Shinoj, Visvanathan, Panigrahiand, & Kochubabu, 2011). Previous research works of studying and developing thermoplastic reinforced oil palm fruit bunch f bres composites have successfully proven their capability in competing with other natural f bre f lled polymer composites (Kalam, Berhan, Ismail, & Razak, 2012) such as wood, kenaf, f ax, hemp, coconut husk, pineapple leaf, oil palm, and sisal. However, the major drawback of promoting the usage of OPEFB f bre as reinforcement in polymer composites is always its poor bonding with the matrix. So, the aim of this paper is to study the effect of OPEFB f ber size on the fracture toughness and impact strength of OPEFB f ber f lled polymer nanocomposites. This research also investigates the use of clay polymer nanocomposites as the matrix to improve the mechanical properties of composites, besides the adoption of f ber treatment.

MATERIALS AND METHODS

Oil palm fruit bunch f bers were supplied by Poly Region Sdn. Bhd. High density polyethylene (HDPE) was manufactured by Titan PP Polymers (M) Sdn. Bhd (melt f ow index of 2.16 and a density of 0.946 g/cm³, melting temperature between 120 - 130°C, processing temperature of 185°C). Polyethylene nanoclay (PE nanoclay) pellets were provided by Nanocor Inc. in the form of master batch, ready for injection moulding. Meanwhile, Maleic anhydride grafted polyethylene (MAPE) produced by Sigma Aldrich was used as a coupling agent.

Pulverised OPEFB f bres were sieved to separate the particles using the sieve shaker of 180 µm, 250 µm, 300 µm and 355 µm based on the previous study (Kamarudzaman, Kalam, Ahmad, Razak, & Salleh, 2014). The composite formulations consisted of 68 wt% HDPE/Clay nanocomposites as the matrix (the composition of HDPE/clay were similar as described by Kamarudzaman, Kalam, Fadzil, & Ahmad (2014), 30 wt% of OPEFB f bres as the secondary f ller and 2 wt% of maleic anhydride grafted polyethylene (MAPE) as the coupling agents. Details of the composite formulations are tabulated in Table 1. Some portions of OPEFB f bres were also treated with 5 % sodium hydroxide (NaOH) solution for 24 hours at room temperature to enhance the bonding between f bre and matrix. After treatment, OPEFB f bers were washed with distilled water to remove impurities and dried at 80°C for about eight hours.

Table 1
Composite formulations

OPEFB /Clay	180 µm	250 µm	300 µm	355 µm
3 phr	-	-	-	Untreated
5 phr	Untreated/treated	Untreated/treated	Untreated/treated	Untreated/treated
7 phr	-	-	-	Untreated
10 phr	-	-	-	Untreated

The compounding of HDPE/MAPE/PE nanoclay composites was performed in a sigma blade dispersion mixer at 185 °C and a rotor speed of 50 rpm for 30 minutes. After the compound was thoroughly mixed, OPEFB f bres were added and the compounding was continued for the next 30 minutes. The compound was removed from the mixer and allowed to cool at room temperature. The total mixing time was approximately one hour. The composite specimens were fabricated using injection moulding techniques into f at dog-bone shape specimens after the compounded material was crushed into granules. Notched Izod impact specimens were prepared and tested following the ASTM D256 to determine the impact strength of the composites.

On the other hand, fracture toughness of the composite was determined according to the ASTM D5045. Single edge notch bending (SENB) specimens were tested with a crosshead speed of 10 mm/min. The dimension of specimens were 52.8 mm × 12 mm × 6 mm (length × width × thickness) with a single notch 4 mm as shown in Figure 1. Five specimens were tested for each batch. The initial portion of the notch was machined with a V-blade at 4 mm and a starter crack was then introduced at the root of the notch by a razor blade, approximately at 2 mm. The ratio of crack length to width $(\frac{a}{w})$ was in the range 0.45 and 0.55.
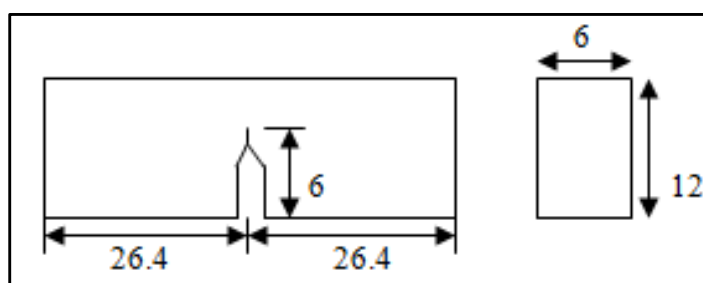
Figure 1. Sample specif cation of a Single Edge Notch Bend (SENB) specimen, all dimension (in mm)

Stress intensity (K_{1Q}) was calculated using the following equations:

$$K_{1Q} = \frac{P_Q S}{BW^{\frac{3}{2}}} \cdot f\left(\frac{a}{w}\right) \tag{1}$$

$$f\left(\frac{a}{w}\right) = \frac{3\left(\frac{a}{w}\right)^{\frac{1}{2}}\left[1.99 - \frac{a}{w}\left(1 - \frac{a}{w}\right)\left(2.15 - 3.93\left(\frac{a}{w}\right) + 2.7\left(\frac{a}{w}\right)^2\right)\right]}{2\left(1 + 2\frac{a}{w}\right)\left(1 - \frac{a}{w}\right)^{\frac{3}{2}}} \tag{2}$$

Validation of critical stress intensity K_{IC} valueor fracture toughness was done using equation 3.

$$B, \ W - a, \ a \geq 2.5\left(\frac{K_{1Q}}{\sigma_{ys}}\right)^2 \tag{3}$$

Where;

B   =   specimen thickness

W   =   specimen width

a =   the crack length

$W - a$ =   the ligament length

σ_{ys} =   the yield strength (Based on the data obtained from previous works by (Fadzil, Kalam, & Kamarudzaman, 2014)

RESULTS AND DISCUSSION

Load versus displacement curves of tested specimens are presented in Figure 2. The curves indicate that most of the specimens have similar trend, which is type I according to ASTM D 399. This trend of load-displacement graph is expected for polymer composites. A linear region can be observed at the beginning of the graph followed by slight nonlinearity before the maximum load is reached. The nonlinearity portion indicates that crack initiation is in progress. The presence of secondary f ller (OPEFB f bre) has signif cantly increased the maximum load of the Clay/HDPE nanocomposites. This trend signif es that the OPEFB f bres are good reinforcement for Clay/HDPE nanocomposites.
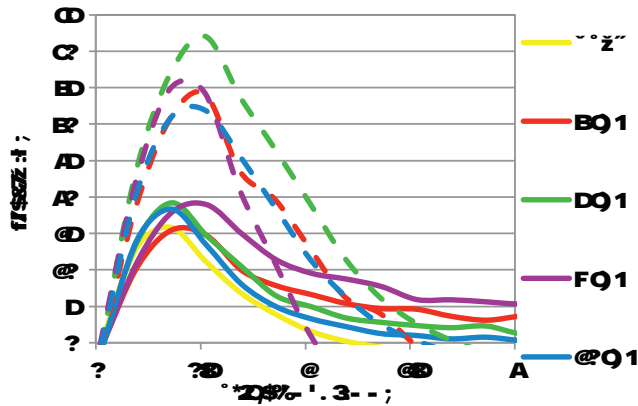
Figure 2. Load Versus displacement of tested specimens, solid curves indicate clay/HDPE and dashed curves indicate OPEFB/Clay/HDPE nanocomposites

Figure 3 shows the fracture toughness of pure HDPE, Clay/HDPE and OPEFB/Clay/HDPE nanocomposites. A slight increase occurs when various clay loadings are added into pure HDPE. The highest value of fracture toughness is 0.47 MPa.m$^{1/2}$ at 5 phr and the lowest value is 0.42 MPa.m$^{1/2}$ at 10 phr. The increase is about 1% to 4%, compared to the fracture toughness of pure HDPE which is 0.37 MPa.m$^{1/2}$. This behaviour is due to the presence of nanoclay which is conf rmed by XRD test reported elsewhere (Kamarudzaman et al., 2014).
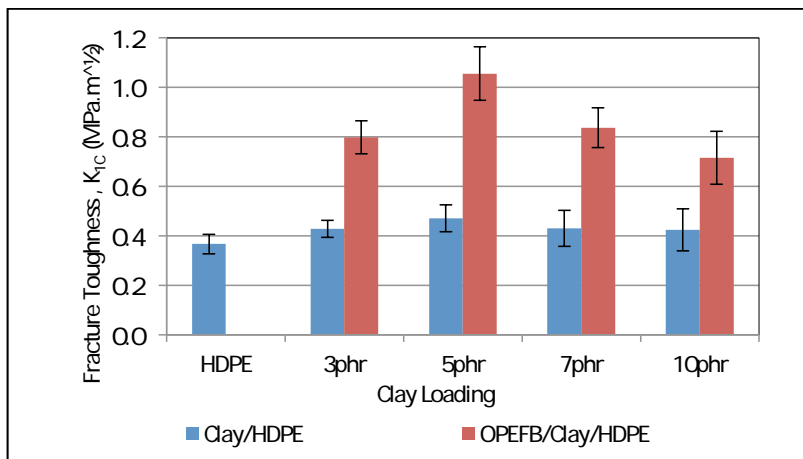
Figure 3. Fracture toughness of nanocomposites at various clay loadings

The addition of OPEFB f bre into Clay/HDPE nanocomposites has signif cantly increased the fracture toughness and the trend is also the same where it increases when there is an increase in the clay loading. The highest value of fracture toughness for OPEFB/Clay/HDPE is 1.06 MPa.m$^{1/2}$ at 5 phr while the lowest value is 0.72 MPa.m$^{1/2}$ at 10 phr. The covalent bonds between f ber and coupling agents which react with the hydroxyl groups of cellulose or hemicelluloses (two

main constituents in oil palm empty fruit bunch f bre) has improved their physical interlock, which consequently leads to fracture toughness enhancement of the composite (Suradi, Yunus, & Beg, 2011). However, beyond 5 phr clay loading, the fracture toughness decreases due to weak interfacial interaction between matrix and f ller, leading to weak interfacial bonding (Kamarudzaman et al, 2014). This is possibly due to insuff cient coupling agent as the clay loading increases.

The reinforcing ability of the f llers does not just depend upon the mechanical strength of the f llers, but also on many other features, such as polarity (types of functional group) of the f ller, surface characteristics and particle size of the f llers (Lewis & Nielsen, 1970). Hence, based on the highest fracture toughness recorded at 5 phr, further investigation was done on several sizes of OPFB f bres to investigate the effect of f bre size. The results are shown in Figure. 4, where the result of the alkali treated OPEFB f bre at 5% NaOH concentrations is also included. The f gure indicates that the fracture toughness has increased as the OPEFB f bre size increases towards maximum increase of about 40%. This trend is in line with the improvement of its mechanical properties that are reported in another article (Facile et al., 2014). Alkali treatment has a signif cant effect on the smaller OPEFB size (180 µm) showed by a 38 % increase in fracture toughness, compared to larger OPEFB f ber (355 µm), that shows insignif cant changes. This suggests insuff cient alkali concentration for larger OPEFB f bre drug during treatment.
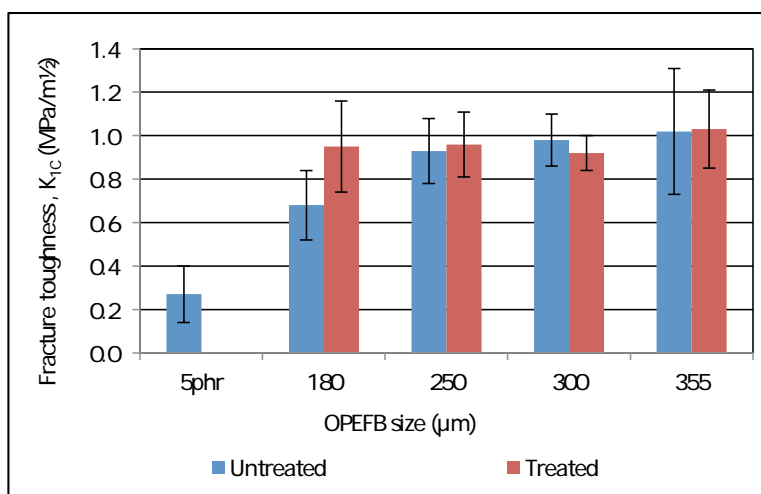
Figure 4. Fracture toughness of OPEFB/Clay/HDPE nanocomposites at various OPEFB f ber size

The addition of OPEFB f bers abruptly decreases the impact strength of composites as displayed in Figure 5. However, as the OPEFB f ber size increases, the impact strength of the nanocomposite also increases up to 27% at 300 µm, then it decreases again to 355 µm OPEFB f bers. It is also noted that alkali treatment on OPEFB f bres produce the same trend towards impact strength as well. For smaller OPEFB f ber size, the impact strength shows signif cant increase upon 5% alkali treatment. This evidence supports the suggestion that larger OPEFB f bre size needs higher alkali concentration as indicated in fracture toughness test.
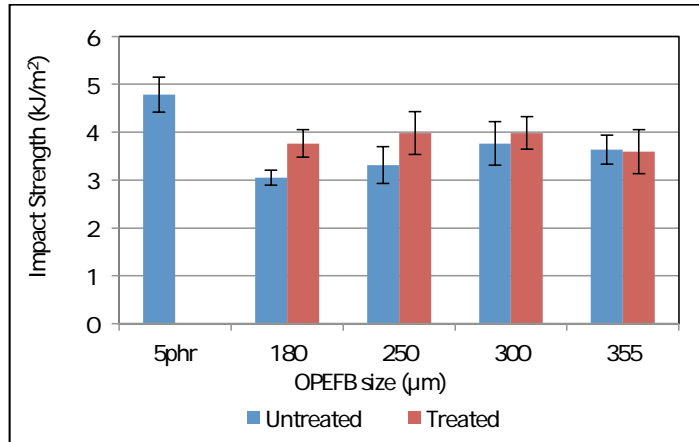
Figure 5. Impact Strength of OPEFB/Clay/HDPE Nanocomposites at Various OPEFB Fiber Size

The presence of clay in the composites is quite detrimental for high speed load, as indicated by the impact strength at various clay loadings shown in Figure 6. The addition of 3 phr of clay loading in HDPE has reduced the impact strength to about 7% and continues to decrease with the increase of clay loading. The same trend is seen by composites with OPEFB f bres as secondary f ller. Lower impact strength of composite as compared to pure HDPE is most probably due the brittleness of the composite, where the addition of f ller normally will transform the ductile polymer into brittle composite, which can be identif ed from their stress-strain curves reported in other work (Kamarudzaman et al., 2014). The impact resistance of ductile materials, is mostly contributed by shearing of polymer chain.
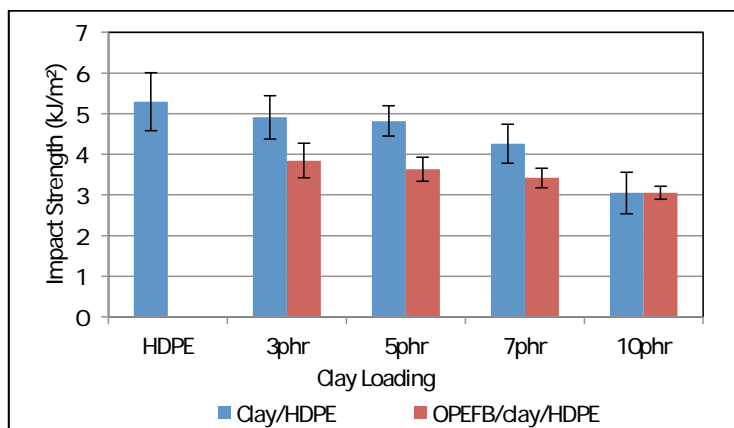
Figure 6. Impact strength of HDPE and its composites at various clay loadings

The improvement of mechanical properties by the addition of coupling agent and f llers is likely due to better bonding between f bre and the matrix. Some evidence of f bre debonding from the matrix that leaves empty holes, creates larger f aws and hence worsens the fracture

resistance ability, which can be observed from the FESEM micrograph is depicted in Figure 7(a). In Figure 7(b), it can be seen that the OPEFB f bre is nicely embedded in the matrix that supports the evidence of highest fracture toughness of nanocomposites with 5 phr clay loading. It is clearly shown that the interfacial region between f ller and the matrix is continuous, indicating a good interfacial bonding between the constituent phases.

(a)   (b)

(c)   (d)
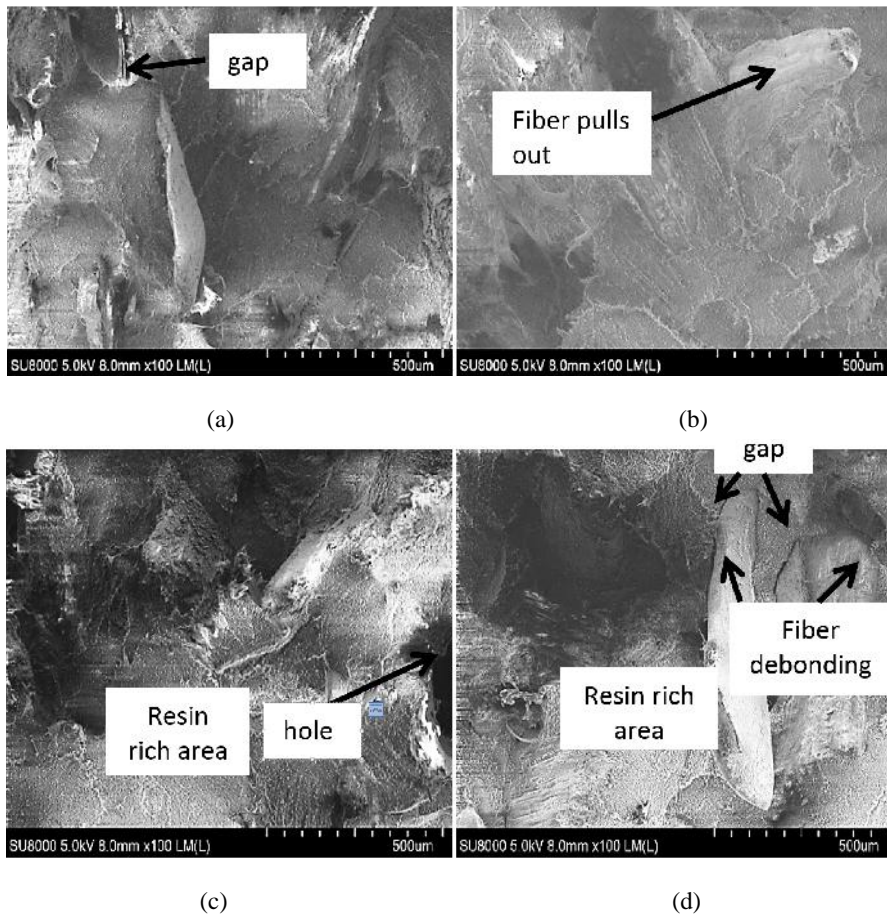
Figure 7. Fracture Surface of OPEFB/Clay/HDPE at various clay loadings: (a) 3 phr; (b) 5 phr; (c) 7 phr; and (d) 10 phr

A small hole as shown in Figure 7(c) due to air bubble during composites preparation also serves as a weak point during testing. A signif cant improvement can be achieved if the f bres are to be dispersed uniformly in the matrix (Ishak, Aminullah, Ismail, & Rozman, 1998), hence no resin rich areas are observed on the fracture surfaces. Some occurrences of OPEFB f ber debonding are visible, which is dominant on the fracture plane as illustrated in Figure 7(d). This is believed to be more detrimental to the mechanical performance of the composites.

CONCLUSION

The addition of OPEFB fiber as a secondary filler in the matrix indicates significant enhancement of fracture toughness of up to 133%. The highest fracture toughness, K_{1C} of clay/HDPE nanocomposites are found to be 0.47 MPa.m$^{1/2}$ at 5 phr clay loading. The addition of 355 μm OPEFB f bres in th eclay/HDPE nanocomposite has doubled the K_{1C} with the maximum value recorded at 1.15 MPa.m$^{1/2}$. Further investigation on the effect of OPEFB f bre size revealed that K_{1C} value increases in tandem with the increase in OPEFB f bre size. Fibre treatment with 5% NaOH solution appears to work well on the small OPEFB size, where it is proven to dramatically increase the K_{1C} value up to 40%. Further investigation is needed for higher concentration of NaOH and larger OPEFB size. However, its impact strength seems to deteriorate with the presence of OPEFB f ber concentration of NaOH and larger OPEFB size.

ACKNOWLEDGEMENTS

REFERENCES

Fadzil, N. A. M., Kalam, A., & Kamarudzaman, R. (2014). Mechanical properties of treated and untreated OPEFB f lled polymer nanocomposites at different OPEFB f ber size. *Advances in Environmental Biology, 8*(8), 2682-2688.

Ishak, Z. A. M., Aminullah, A., Ismail, H., & Rozman, H. D. (1998). Effect of silane-based coupling agents and acrylic acid based compatibilizers on mechanical properties of oil palm empty fruit bunch f lled high-density polyethylene composites. *Journal of Applied Polymer Science, 68*(13), 2189-2203.

Kalam, A., M. N., Berhan, Ismail, H., & Razak, N. W. A. (2012). The effects of oil palm fruit bunch f bre treatment on the performance of hybrid polypropylene nanocomposites. *8th Asian-Australasian Conference on Composite Materials (ACCM-8), 2*, 895-900.

Kamarudzaman, R., Kalam, A., Ahmad, N. N., Razak, N. W. A., & Salleh, Z. (2014). Effects of oil palm empty fruit bunch (OPEFB) f bre size on fracture toughness of OPEFB f lled polymer nanocomposite. *Advanced Materials Research, 871*, 189-193.

Kamarudzaman, R., Kalam, A., Fadzil, N. A. M., & Ahmad, N. N. (2014). Thermal degradation behaviour and tensile properties of OPEFB f bre f lled HDPE/Clay nanocomposites. *Advances in Environmental Biology, 8*(8), 2696-2702.

Lewis, T., & Nielsen, L. (1970). Dynamic mechanical properties of particulate-f lled composites. *Journal of Applied Polymer Science, 14*(6), 1449-1471.

Shinoj, S., Visvanathan, R., Panigrahi, S., & Kochubabu (2011). Oil palm f ber (OPF) and its composites: A review. *Industrial Crops and Products, 33*, 7-22.

Suradi, S. S., Yunus, R. M., & Beg, M. D. H. (2011). Oil palm bio-f ber-reinforced polypropylene composites: Effects of alkali f ber treatment and coupling agents. *Journal of Composite Materials, 45*(18), 1853-1861.

Improvement of Mechanical Properties and Fatigue Failure of Spot-Welded Joint through Pneumatic Impact Treatment (PIT)

Ghazali, F. A.[1]*, Salleh, Z.[2], Hyie, K. M.[3], Taib, Y. M.[4] and Nik Rozlin, N. M.[2]

[1]Fabrication and Joining Department, Universiti Kuala Lumpur Malaysia France, Institute (UniKL MFI), 43650 Bandar Baru Bangi, Selangor, Malaysia
[2]Faculty of Mechanical Engineering, Universiti Teknologi MARA (UiTM), 40000 Shah Alam, Selangor, Malaysia
[3]Faculty of Mechanical Engineering, Universiti Teknologi MARA (UiTM) Pulau Pinang, 13500 Permatang Pauh, Pulau Pinang, Malaysia
[4]Faculty of Mechanical Engineering, Universiti Teknologi MARA (UiTM) PasirGudang, 81750 Masai, Johor, Malaysia

ABSTRACT

This study focuses on examining the inf uence of post weld impact treatment (PWIT) using Pneumatic Impact Treatment (PIT) for spot welded joint on mechanical properties and fatigue failure. PWIT is one of the methods for improving mechanical properties and fatigue strength of welded joints. One of the versatile techniques of PWIT used for this study is PIT. The material investigated in this study was carbon steel with welded single lap shear joint with the constant thickness of 1.2mm. All the welded samples were later performing the tensile shear test, hardness test, and fatigue test. The tensile shear test was conducted on the spot welded both treated and untreated samples using crosshead speed of 2 mm/min, while hardness test was performed using 1kgf load via Vickers hardness indenter. Fatigue test was conducted using R=0.1 and frequency of 10 Hz. The effects of PIT on tensile-shear properties, hardness, and fatigue failure were evaluated. It was found that the implementation of PIT has increased tensile shear and hardness signif cantly and prolonged lifetime of spot welded joint.

Keywords: Fatigue failure, pneumatic impact treatment (PIT), post weld impact treatment, resistance spot weld, spot-welded

INTRODUCTION

Resistance spot welding (RSW) is widely used for producing a typical vehicle body-in-white (BIW), normally made of thin metal sheets that are connected together by clamping the sheets with two pincers while applying force

and transmitting current; eventually, a nugget develops and the interface locally disappears. The important changes occur in mechanical and metallurgical properties of the spot welds area is during the process of spot weld itself such as the weld fusion zone size, weld mechanical performance and failure mode (Charde, 2012). The investigation of this change is the most important for the safety and quality of the welded joints (Vural & Akkus, 2004). One single typical automotive car body contains about 300 sheet metal parts, joined by about thousand spot welds (Mali, Inamdar, Mali, & Inamdar, 2012). Due to this reason, quality, performance and failure characteristics of resistance spot welds are important to be evaluated for determining the durability and the safe design of the vehicles, as they transfer load through the structure during dynamical load and crash (Pouranvari & Marashi, 2013; Pouranvari, Mousavizadeh, Marashi, Goodarzi, & Ghorbani, 2011).

During the welding process, the steel is heated and segregated into several zones consist of base metal, heat affected zone (HAZ) and fusion zone. In HAZ, the cooling rate is different and comprises different regions of microstructure and often considered as a source of failure in welded joint (Srivastava, Tewari& Prakash, 2010; Xue, Benson, Meyers, Nesterenko, & Olevsky, 2003).

The enhancement of the static and fatigue resistance of welded joints is becoming increasingly signif cant in many areas such as the automotive, aerospace and railway industries. A recent method of enhancing the static and fatigue resistance of welded structures is to use modern post-weld treatment processes. Post–weld impact treatment (PWIT) is a process which was done after the welding process either the method of applied heat or impact used for stress relief. Improving the resistance of welded joints by conventional improvement methods such as grinding, shot peening, air hammer peening or tungsten inert gas (TIG) dressing are well established (Yildirim & Marquis, 2013). The purpose of stress relieving is to remove any internal or residual stresses that may be present from the welding operation. Stress relief after welding may be necessary in order to reduce the risk of brittle fracture, to avoid subsequent distortion or to eradicate the risk of stress corrosion. In parallel to the development of this treatment method, there have been an increasing number of publications dealing with high-frequency mechanical impact treatment (HFMI) technologies using Pneumatic Impact Treatment (PIT). The PIT is the versatile and modern technique used in modif ed the properties of welded joint. There are several researchers studied in this PIT area with a different f eld of welding.

Yildirim, Marquis and Sonsino (2015) studied on the fatigue strength improvement using PIT of longitudinal stiffeners of the steel grade S700. Experimental results perceived that the fatigue strength of improved welds increases with existing of weld modif cation through PIT. Mohamed, Manurung, Shah and Othman (2015) study presented an unconventional method to optimize the governing process parameters of Pneumatic Impact Treatment (PIT) and found that PIT treatment is a post weld treatment that can be used to signif cantly enhance the fatigue resistance level of FSW AA6061. However, the used of this kind of treatment towards the spot welded area still not yet established.

This study focuses on examining the inf uences of the application of post weld impact treatment (PWIT) using Pneumatic Impact Treatment (PIT) for spot welded joint through the tensile shear and fatigue failure. Regarding this concern, all the welded samples were later subjected by performing PIT to test the strength of the welded joint to fail or tear apart in terms

of its load and the properties through the failure modes to the energy-absorbing capacity of a weldment. Microhardness distribution from base metal (BM) to fusion zone (FZ) was measured. Fatigue failure was evaluated in order to predict the life of the welded joint.

MATERIALS AND METHOD

Resistance spot weld (RSW) joints may be exposed to stress under tensile-shear conditions. The experiment is designed to determine the shear load, hardness and fatigue failure of the welded zone.

Materials and Equipment

The material investigated in this study was low carbon steel grade JIS G3141 sheet. Lap shear samples were prepared according to AWS (American Welding Standard) standard which is D8.9M. The sheet metals were prepared in a rectangular shape with a size of the length (110 mm), width (45 mm) and thickness (1.2 mm) as shown in Figure 1. The welded joints were performed using the 75 KVA spot welding machine with electrode tips of 5 mm in diameter.
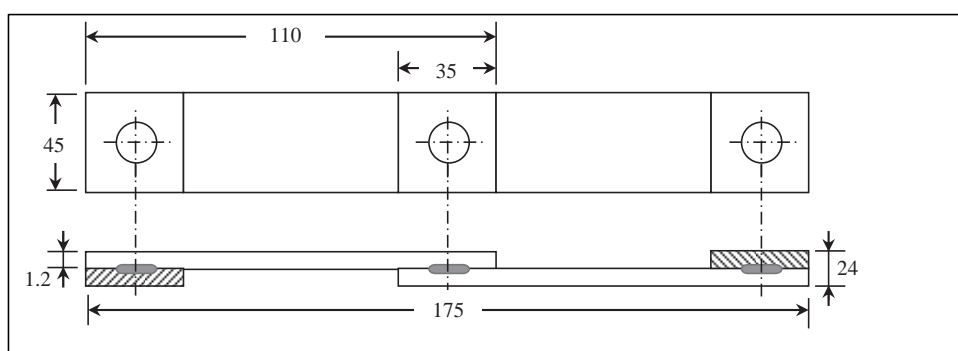
Figure 1. The spot welded sample (Ghazali, Manurung, Mohamed, Mohamed, & Abdullah, 2015)

Post Weld Impact Treatment

Treatment was performed using pneumatic impact treatment (PIT) on the spot welded samples. The PIT device operates with a hardened pin with a ball resting on the work piece with a diameter of 3 mm. The PIT device used in the PWIT process is depicted in Figure 2.

Figure 2. The PIT controller and handheld device (Mohamed, Manurung, Shah, & Othman (2015))

This pin was hammered with an adjustable intensity at 90 Hz at the welded zones and air pressure applied from the compressor is 4.5 bar. Local mechanical deformations occur in the form of a treatment track. The impact zone of the sample was analyzed using an optical 3D surface measurement device.

Testing Conditions

The tensile shear test was conducted with an Instron universal testing machine at a constant cross head displacement rate of 2 mm/min. The peak load was measured as the maximum point in the tensile-shear curve was extracted from the load–extension curve. An average tensile shear value of the 5 samples was recorded.

Vickers hardness with 5 repetitions of the joint is measured across the fusion zone, heat affected zone (HAZ) and base metal with the load of 1kgf acting on the samples surface. The dwell time of 15 seconds was used to 0.5 mm distance between the indents.

Fatigue testing of spot-welded samples was conducted under load-control with a load ratio of R = 0.1 and a sinusoidal waveform were applied with 10 Hz (Shen, Ding, Chen, & Gerlich, 2016). Final separation of coupons was considered as a failure. Tests were stopped after 10^7 cycles and considered run-outs. The numbers of cycles, as well as the failure modes, were recorded in all fatigue tests.

RESULTS AND DISCUSSION

The weld zone was deformed plastically and bonded due to impact from PIT which captures before and after the process as depicted in Figure 3.
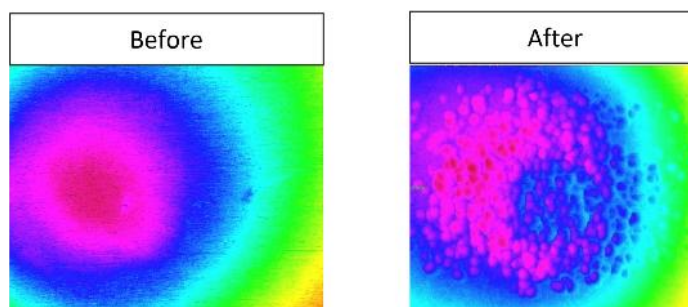
Figure 3. The impacted zones of spot welded joint

Table 1 gives the comparison between the tensile-shear results of the RSW PIT and RSW as-weld samples. The tensile-shear load force of RSW as-weld samples is increased as the treatment applied to the samples. Correspondingly, the average peak load increased due to the strong bond of base metal and the introduction of hardening precipitates, as well as the increment in pre-existing dislocations mainly, cause the increment in the tensile-shear load of the RSW PIT condition (Ghazanfari & Naderi, 2013)

Table 1
Comparison of shear-load of RSW PIT and RSW as-welded samples

Peak Load (kN)	RSW PIT	RSW as-weld
	8.81(0.07)	7.71(0.12)

Figure 4 shows the measured through-thickness hardness values for RSW PIT and RSW as-weld samples. As the result, the hardness is somewhat higher at the treated zone than near the untreated zone. This increase in hardness is clear which is from an average of 206 HV to 268 HV at the fusion zone. The hardness of thebase metal is about the same between 149 and 155 HV for both conditions. No phase transformation occurred because base metal (BM) of carbon steel was not affected during the pneumatic treatment (Joy-A-Ka et al., 2013). The hardness value for PIT samples experienced vast increased rather than as-welded samples. The hardness of base metal seemed to be lower than Heat Affected Zone (HAZ) and fusion zone (FZ) region due to the unaffected region during solidif cation process for both samples and also during the pneumatic treatment (Mikkola, Marquis, Lehto, Remes, & Hänninen, 2016).

For RSW PIT samples, it shows a huge difference in the range of FZ and HAZ. Both show higher difference value compared to RSW as weld samples. Hardness at fusion zone and HAZ were showed considerably higher values than that at base steel. Due to melting conditions during the welding process, re-solidify metal in fusion zone displayed relatively large volume fraction of ferrite morphologies which induced to softening of the zone. For the hardness properties, it can be stated that PIT samples were harder than as-weld samples.
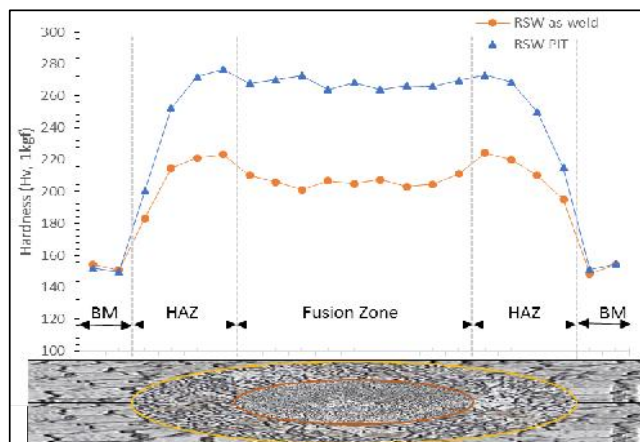
Figure 4. Hardness prof le for RSW PIT and RSW as-weld samples

It could be seen that the hardness of HAZ was higher than the fusion zone and base metal. The HAZ experienced solid state phase transformation but no melting induced during the welding process. The hardness of HAZ as moved toward the fusion zone experiences perceptible drop. The drop phenomenon observed was identif ed as HAZ softening which mainly caused by martensite tempering development (Zhao, Wang, Zhang, & Zhang, 2013; Liu, Zheng, He,

Wang, & Wei, 2016; Sun, Stephens, & Khaleel, 2008). Compared to the HAZ region, the effect of melting, the microstructure in fusion zone resolidif ed in RSW joints plays a major role in the elimination of strain hardening which signif cantly softens the weld zone (Pouranvari, Marashi, & Safanama, 2011). This, in turn, causes a decrement of the hardness values in the vicinity of the fusion zone.

For spot weld joint, results of fatigue tests are generally presented as load range vs. fatigue life (Hongyan et al., 2006; Spitsen, Kim, Flinn, Ramulu, & Easterbrook, 2005; Wang et al., 2008). The results of load-number of cycles containing RSW PIT and RSW as-welded joint were presented in L-N curves. The best-f t regression line depicted in Figure 5 shows a gradual decline in fatigue load with an increase in the number of fatigue life cycles. The load range was determined based on the maximum load applied. The maximum load of the RSW PIT and RSW as-weld sample is plotted on the curve at 1 cycle (log 1=0). RSW PIT exhibits higher fatigue strength than RSW as-weld in the entire applied load range. The regression line predicted endurance limit of about 2.4 kN (approximately 27% of maximum load) for the RSW PIT samples at 1 million cycles which corresponded to well with the experimental data as shown by an arrowhead. Hence a load level of up to 3 kN can be taken as a safe value for endurance limit for these RSW PIT sample. It should be noted that RSW PIT joints have different joining features due to the treatment applied from RSW as-weld joints, which resulted in the different crack initiation and growth behaviour between both joints.
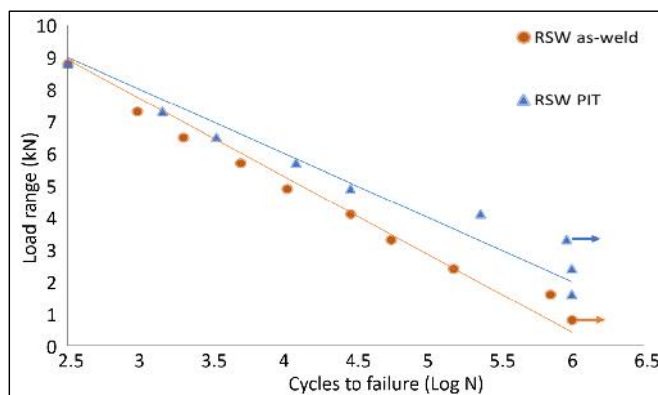
Figure 5. L-N curve for RSW PIT and RSW as-weld samples

In order to determine the fatigue sensitivity of the weld samples, it is more suitable to use normalized load versus cycles to failure curve. The L-N curve has been normalized with respect to the ultimate failure load of samples. The normalized load (maximum tensile load divided by shear load) versus cycles to failure curve is shown in Figure 6. The curve shows that the RSW PIT sample lost their static strength by almost 11.7% per decade of cycles, while the RSW as-weld, almost 15% static strength lost per decade.
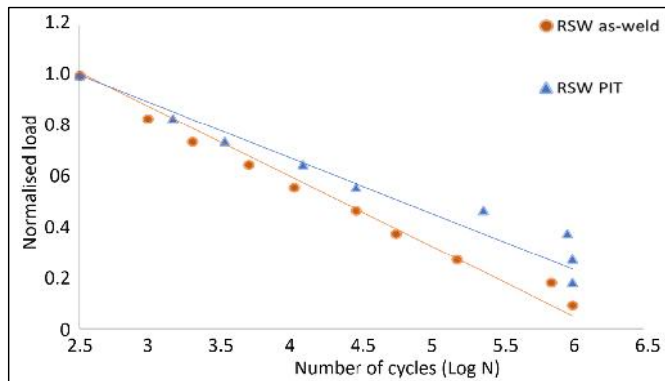
Figure 6. Normalised L-N curve for RSW PIT and RSW as-weld samples

The lower the percentage of lost value shows that the fatigue performance is better. Showing that, the fatigue performance for RSW PIT is better than RSW as-weld. A similar scatters trend for both RSW condition (RSW PIT and RSW as-weld) in term of reduction on normalized fatigue curves was also reported by Liu et al. (2013). These signif cance differences indicate that compressive residual stress relaxation as a consequence of local plastic deformation could have occurred in RSW PIT samples (Yildirim, Marquis, & Sonsino, 2015). Because the PIT impacted zone is highly cold worked, the true cyclic yield strength of the material in this region is probably much higher than for the RSW as-weld sample. This is explained by in pre-existing dislocations mainly, causes the increment in the fatigue failure of the RSW PIT condition (Mikkola, Marquis, Lehto, Remes, & Hänninen, 2016).

CONCLUSION

Alteration of local material properties changes existing in the post weld impact treatment spot weld sample was investigated by tensile shear test, hardness, and fatigue failure test. Two different spot weld samples conditions were studied: RSW PIT and RSW as-weld. The post weld impact treatment represents pneumatic impact treatment method was used to apply high-frequency mechanical impact on compressive residual stress existing in spot weld zone, meanwhile to improve the weld geometry and strain hardening the treated surface. The results showed that the treatment increased the tensile shear load of spot weld and also increase the hardness of the joint signif cantly. The pre-existing location due to treatment was lead to an increase in fatigue failure.

ACKNOWLEDGMENTS

REFERENCES

Charde, N. (2012). Characterization of spot weld growth on dissimilar joints with different thicknesses. *Journal of Mechanical Engineering and Sciences, 2*(unknown), 172-180.

Ghazali, F. A., Manurung, Y. H., Mohamed, M. A., Alias, S. K., & Abdullah, S. (2015). Effect of process parameters on the mechanical properties and failure behavior of spot welded low carbon steel. *Journal of Mechanical Engineering and Sciences, 8*, 1489-97.

Ghazanfari, H., & Naderi, M. (2013). Inf uence of welding parameters on microstructure and mechanical performance of resistance spot welded high strength steels. *Acta Metallurgica Sinica (English Letters), 26*(5), 635-640.

Joy-A-Ka, Hirano, T., Akebono, H., Kato, M., Sugeta, A., Fujii, H., & Sun,Y. F. (2013).3-Dimensional observation of the interior fatigue fracture mechanism on friction stir spot welded using 300 MPa-class automobile steel sheets, in *Proceedings of the 1st International Joint Symposium on Joining and Welding*, 6-8 November 2013.

Liu, C., Zheng, X., He, H., Wang, W., & Wei, X. (2016). Effect of work hardening on mechanical behavior of resistance spot welding joint during tension shear test. *Materials and Design, 100*, 188-197.

Liu, L., Xiao, L., Chen, D. L., Feng, J. C., Kim, S., & Zhou, Y. (2013). Microstructure and fatigue properties of Mg-to-steel dissimilar resistance spot welds. *Materials and Design, 45*, 336-342.

Mali, M. P., & Inamdar, K. H. (2012). Effect of spot weld position variation on quality of Automobile sheet metal parts. *International Journal of Mechanical and Materials Engineering, 2*, 23-27.

Mikkola, E., Marquis, G., Lehto, P., Remes, H., & Hänninen, H. (2016). Material characterization of high-frequency mechanical impact (HFMI)-treated high-strength steel. *Materials and Design, 89*, 205-214.

Mohamed, M. A., Manurung, Y. H., Shah, L. H. A., & Othman, N. H. Optimization of HFMI/PIT Parameters with Simultaneous Multiple Response Consideration using Multi-Objective Taguchi Method for Fatigue Life Enhancement of Friction Stir Welding. In *IIW International Conference High-Strength Materials - Challenges and Applications, 68*.DOI: 10.13140/RG.2.1.4115.5047

Pouranvari, M., & Marashi, S. P. H. (2011). Failure mode transition in AHSS resistance spot welds. Part I. Controlling factors. *Materials Science and Engineering: A, 528*(29-30), 8337-8343.

Pouranvari, M., & Marashi, S. P. H. (2013). Critical review of automotive steels spot welding: process, structure and properties. *Science and Technology of Welding and Joining, 18*(5), 361-403.

Pouranvari, M., Mousavizadeh, S. M., Marashi, S. P. H., Goodarzi, M., & Ghorbani, M. (2011). Inf uence of fusion zone size and failure mode on mechanical performance of dissimilar resistance spot welds of AISI 1008 low carbon steel and DP600 advanced high strength steel. *Materials and Design, 32*(3), 1390-1398.

Shen, Z., Ding, Y., Chen, J., & Gerlich, A. P. (2016). Comparison of fatigue behavior in Mg/Mg similar and Mg/steel dissimilar ref ll friction stir spot welds. *International Journal of Fatigue, 92*, 78-86.

Spitsen, R., Kim, D., Flinn, B., Ramulu, M., & Easterbrook, E. T. (2005). The effects of post-weld cold working processes on the fatigue strength of low carbon steel resistance spot welds. *Journal of Manufacturing Science and Engineering, 127*(4), 718-723.

Srivastava, B. K., Tewari, S. P., & Prakash, J. (2010). A review on effect of preheating and/or post weld heat treatment (PWHT) on mechanical behavior of ferrous metals. *International Journal of Engineering Science and Technology, 2*(4), 625-631.

Sun, X., Stephens, E. V., & Khaleel, M. A. (2008). Effects of fusion zone size and failure mode on peak load and energy absorption of advanced high strength steel spot welds under lap shear loading conditions. *Engineering Failure Analysis, 15*(4), 356-367.

Vural, M., & Akkus, A. (2004). On the resistance spot weldability of galvanized interstitial free steel sheets with austenitic stainless steel sheets. *Journal of Materials Processing Technology, 153*, 1-6.

Wang, B., Duan, Q. Q., Yao, G., Pang, J. C., Li, X. W., Wang, L., & Zhang, Z. F. (2014). Investigation on fatigue fracture behaviors of spot welded Q&P980 steel. *International Journal of Fatigue, 66*, 20-28.

Xue, Q., Benson, D., Meyers, M. A., Nesterenko, V. F., & Olevsky, E. A. (2003). Constitutive response of welded HSLA 100 steel. *Materials Science and Engineering: A, 354*(1-2), 166-179.

Yildirim, H. C., & Marquis, G. B. (2013). A round robin study of high-frequency mechanical impact (HFMI)-treated welded joints subjected to variable amplitude loading. *Welding in the World, 57*(3), 437-447.

Yıldırım, H. C., Marquis, G., & Sonsino, C. M. (2015). Lightweight potential of welded high-strength steel joints from S700 under constant and variable amplitude loading by high-frequency mechanical impact (HFMI) treatment. *Procedia Engineering, 101*, 467-475.

Zhao, D. W., Wang, Y. X., Zhang, L., & Zhang, P. (2013). Effects of electrode force on microstructure and mechanical behavior of the resistance spot welded DP600 joint. *Materials and Design, 50*, 72-77.

Effect of Low Blow Impact Treatment on Fatigue and Mechanical Properties of Spot-Welded Joints

Farizah Adliza Ghazali[1]*, Zuraidah Salleh[2], Ya'kub Md Taib[2], Koay Mei Hyie[3] and Nik Rozlin Nik Mohd Masdek[2]

[1]*Fabrication and Joining Department, Universiti Kuala Lumpur Malaysia France Institute (UniKL MFI), 43650 Bandar Baru Bangi, Selangor, Malaysia*
[2]*Faculty of Mechanical Engineering, Universiti Teknologi MARA (UiTM), 40000 Shah Alam, Selangor, Malaysia*
[3]*Faculty of Mechanical Engineering, Universiti Teknologi MARA (UiTM) Pulau Pinang, 13500 Permatang Pauh, Pulau Pinang, Malaysia*

ABSTRACT

Post Weld Impact Treatment (PWIT) is necessary in order to improve the tensile shear and hardness strengths on the welded joints of spot welding process. PWIT can be performed via Low Blow Impact Treatment (LBIT), which is the main focus in this research. In this present study, two plates of low carbon steel (LCS) with dimensions of 110 mm × 45 mm × 1.2 mm underwent a resistance spot welding. All welded samples were later tested for their mechanical properties by performing the tensile-shear, hardness test and qualitative analysis. Tensile shear test was conducted on the spot welded area for both treated and untreated samples using crosshead speed of 2 mm/min, while hardness test was performed using 1 kgf load Vickers hardness indenter. The effects of LBIT on tensile-shear properties, hardness and fatigue strength were evaluated and it was found that the implementation of LBIT increased the tensile shear strength, fatigue strength and hardness on the welded joint signif cantly.

Keywords: Hardness test, LBIT, LCS, PWIT, tensile-shear test

INTRODUCTION

Resistance spot welding (RSW) has been employed for a long time by the automotive industries. The weld regions are formed by the combination of pressure, heat and time elements. The resistance to a current f ow of materials to be welded causes a localised heating in the materials in order to achieve a complete coalescence (Vural & Akkus, 2004).

Quality and strength of weld are def ned by the weld joints. In RSW, the stress distribution occurs inside the material, which in turn affects the mechanical properties of the joined metals. For spot welding, the mechanical properties that are usually observed after a load is applied to the spot welded joint includes the tensile strength, hardness, and microstructure. However, the mechanical properties of the resistance spot welding are diff cult to measure and quantif ed because of the small size of the weld region.

During the welding process, the steel is heated and segregated into several zones, which consist of base metal, heat affected zone (HAZ) and fusion zone (FZ). In HAZ, the cooling rate is different and comprises different regions of microstructure and is often considered as a source of failure in welded joint (Mali & Inamdar, 2012; Pouranvari & Marashi, 2013). Hence, post-weld treatment is implemented to improve the properties at the welded joint. There are a few techniques used in post-weld treatment such as Post-Weld Heat Treatment (PWHT) and Post Weld Impact Treatment (PWIT). PWHT, also known as artif cial aging and solution treatment is performed on the welding specimen after the welding process has been carried out. This treatment helps in improving the mechanical properties and modif es the microstructure of the joint (Pouranvari, Mousavizadeh, Marashi, Goodarzi, & Ghorbani, 2011). PWIT consists of several processes, such as shot-peening, hammer-peening, and impact.

Many works have been cited on various post weld treatments. Ma, Qin, Geng and Fu (2015) studied the different heat treatment effects on the mechanical properties and microstructure of the dissimilar sheet steels (1045 carbon steel and 304 stainless steel) friction spot welded samples. The joint was heat treated at different post-weld heat treatment (PWHT) temperature. Tensile strength and elongation of the joint were improved substantially after PWHT at 400°C, attaining the equivalent strength of stainless steel and elongation of carbon steel. This occurs as the microstructure became homogeneous to some extent and a number of chromium carbides barely increased. The joint was heat treated at different post-weld heat treatment (PWHT) temperature. Tensile strength and elongation of the joint were improved substantially after PWHT at 400°C, which could reach up to the equivalent strength of stainless steel and elongation of carbon steel as the microstructure became homogeneous to some extent and a number of chromium carbides barely increased.

Xue, Benson, Meyers, Nesterenko and Olevsky (2003) examined the inf uences of post-weld heat treatment on Q235 steel resistance spot weld. The effect of cross-current on the nugget shape, microstructure, and mechanical properties were investigated. It was found that the cross-current PWHT enhances the eff ciency of PWHT and improves the mechanical performance of nugget. The quasi-equiaxed grains of martensite due to the heat applied during PWHT in the weld nugget drastically increase the microhardness of weld nugget and the tensile-shear force of the weld joint.

The effects of second pulse current in RSW on the microstructure changes and mechanical behavior of transformation-induced plasticity (TRIP) steel were studied (Baltazar, Okita, & Zhou, 2013). The local post weld heat treatments through the second impulse current were applied to the RSW TRIP steel in order to alter the fusion zone microstructure and consequently, the mechanical performance. The most important result of this study is the ability in improving

the mechanical properties with desirable pullout failure mode. It is accomplished when the FZ microstructure consists of a recrystallised structure of martensite achieved in the medium level of the second pulse current PWHT.

This present research focuses on evaluating low blow impact treatment (LBIT) as application in post weld impact treatment (PWIT) on spot welded joint. All the welded samples were subjected to LBIT prior to the tensile shear, hardness and fatigue tests. The energy-absorbing capacity of weldment was identif ed and the microhardness was determined within base metal (BM) to fusion zone (FZ).

MATERIALS AND METHOD

Material and Equipment

Low carbon steel (LCS) grades of JIS G3141 sheets were used in this research. Lap shear samples were prepared according to AWS (American Welding Standard) standard, which is D8.9M. The sheet metals were prepared in rectangular shape of equal size (110 mm x 45 mm x1.2 mm) as shown in Figure 1. The welded joints were performed using the 75 KVA of spot welding machine with electrode tips of 5 mm in diameter.
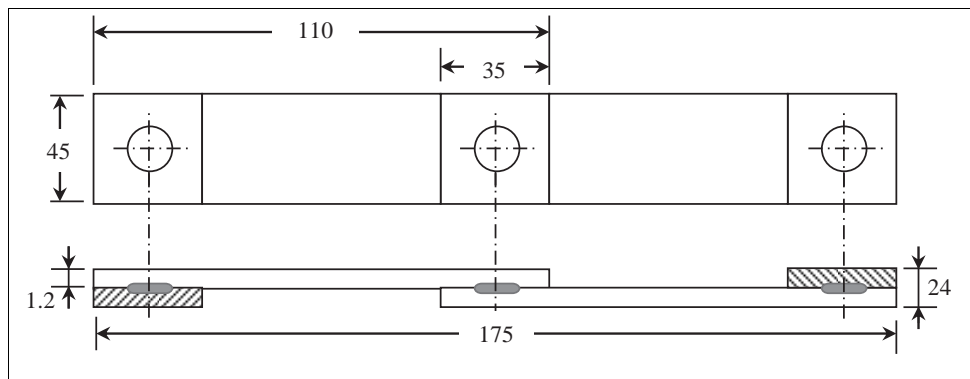
Figure 1. The spot welded sample (Ghazali, Manurung, Mohamed, & Abdullah, 2015)

Post-Weld Impact Treatment

Low blow impact treatment (LBIT) was performed manually using a specially built mini falling weight impact tester as shown in Figure 2. The samples were clamped between two steel plates that had 18 mm diameter hole at the center. A falling weight or impactor then impinged at the predetermined location on the sample. Steel weights were subsequently added on the impactor in order to obtain the required impact energy.
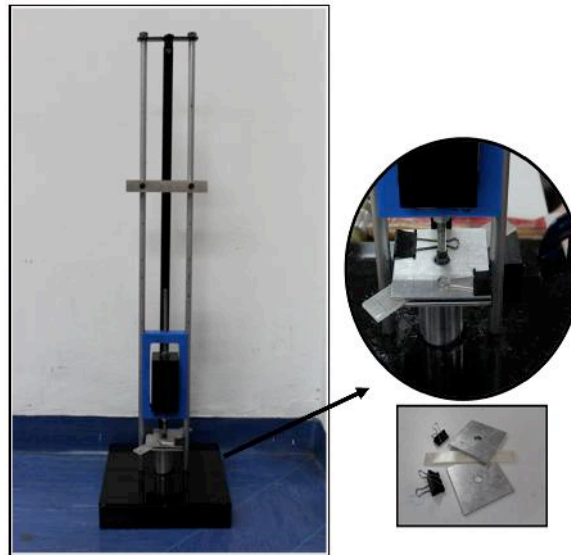
Figure 2. Mini falling weight impact tester

Experimental Set Up

The tensile shear test was conducted on a universal testing machine at a constant cross head displacement rate of 2 mm/min. The peak load was taken as the maximum tensile-shear load, from the load–extension curve. An average maximum tensile shear value of the f ve samples was recorded.

Vickers hardness with f ve repetitions of the joint was measured across the fusion zone, heat affected zone (HAZ) and base metal with the load of 1 kgf acting on the sample surface, as shown in Figure 3. The dwell time of 15 seconds was used for 0.5 mm distance between the indents.
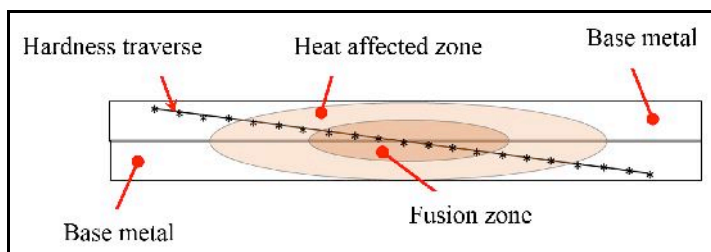
Figure 3. Cross-sectioned hardness traverse

Fatigue testing of spot-welded samples using f at coupon specimen type was conducted under load-control with a load ratio R = 0.1. A sinusoidal waveform was applied at 10 Hz. Final separation of coupons was considered as a failure. Tests were stopped after 1×10^7 cycles if there was no separation and considered as run-out. The number of cycles to failure was noted in these tests.

RESULTS AND DISCUSSION

The tensile-shear of RSW samples improved when the low blow impact treatment was conducted on the samples. The tensile-shear description on load of RSW LBIT and RSW as-weld are provided in Table 1. The RSW LBIT samples show a signif cant increase of 3% in tensile-shear load compared to the as-welded sample. The strong bond of the treated welded joint mainly contributed to the increase in the tensile-shear load of the RSW LBIT and introduction of plastic deformation during the compressive stress applied by low blow impact, reducing the residual stress existing in spot weld joint.

Table 1
Comparison of shear-load of RSW PIT and RSW as-welded samples

No	Description of tensile specimen condition	Load (N)
1	RSW LBIT	8420
2	RSW as-welded	8203

There were some changes in hardness of spot-welded joint due to the impact treatment. Figure 4 shows the hardness prof le of spot-welded joint with acting loading of 1 kgf. Points of the indentation were primarily taken in the FZ in order to analyse treated region of the samples.

It was found that the hardness of base metal material for both RSW as-welded and LBIT treated samples was about the same (~ 149 and 155 HV). It was observed that the hardness of HAZ was higher than the fusion zone and base metal. The HAZ experienced solid state phase transformation but no melting was induced during the welding process. In addition, the area closer to the fusion zone revealed a def nite drop. This phenomenon is identif ed as HAZ softening, mainly caused by martensite tempering development (Mali & Inamdar, 2012; Pouranvari, Marashi, & Safanama, 2011; Zhao, Wang, Zhang, & Zhang, 2013). Compared to the HAZ region, the effect of melting the microstructure in fusion zone resolidif ed in RSW joints plays a major role in the elimination of strain hardening which signif cantly softens the weld zone (Yildirim & Marquis, 2013). This in turn, causes a decrease of the hardness values in the vicinity of the fusion zone. The mean hardness value of the fusion zone in the as-welded condition is recorded at 211 HV compared to the average value of 229 HV obtained for the LBIT treated.
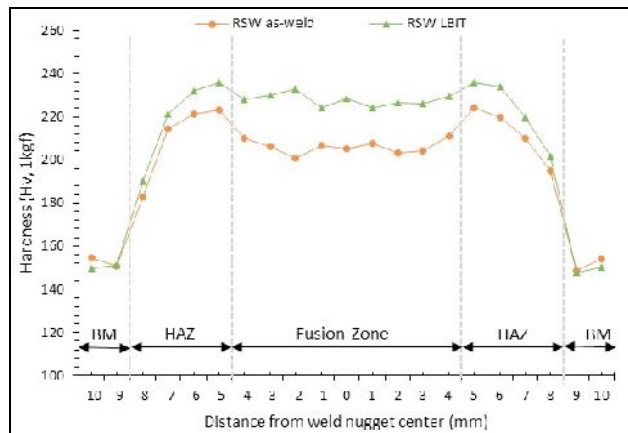
Figure 4. Hardness prof le for RSW LBIT and RSW as-weld samples

The hardness value for LBIT samples is generally higher at both FZ and HAZ than as-welded samples. The hardness of base metal is lower than HAZ and FZ due to the unaffected region during solidif cation process for both samples and also during the low blow impact treatment. For LBIT samples, there is signif cant difference in the range of FZ and HAZ. No phase transformation occurred because the base metal of carbon steel was not affected during the low blow impact treatment. Hardness at fusion zone and HAZ showed considerably higher values than that at the base steel. It is envisaged that melting and during re-solidif cation of the welding process displayed relatively large volume fraction of ferrite morphologies, which induced softening of the zone. The average hardness value for three different zones in RSW LBIT spot welded joint is shown in Figure 5. These hardness results are partially in good agreement with the literature (Liu, Zheng, He, Wang, & Wei, 2016).
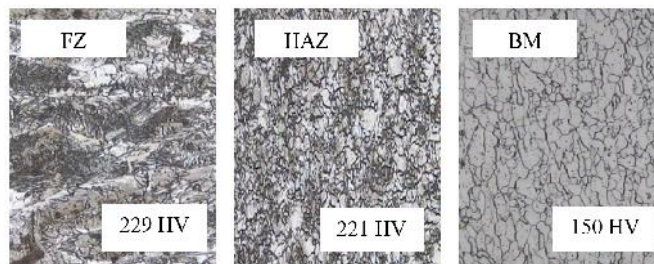
Figure 5. Hardness of the RSW LBIT sample zones

The L-N curve of RSW LBIT and as-welded joint presented in this study are shown in Figure 5. A total 45specimens were tested at nine different stress levels, that is, f ve specimens were tested at each load level, with the maximum load tested at 7.3 kN. It is noted that all specimens were tested until failure and no run-outs were recorded. As expected, the fatigue strength of the LBIT samples were higher than as–welded samples.

Fatigue test was conducted with ten percent increase of load level. The static load of the RSW LBIT and RSW as-weld samples is plotted on the curve at 1 cycle (log 1=0). RSW LBIT exhibits higher fatigue strength than RSW as-weld in the entire applied load range. The regression line predicted endurance limit of about 2.4 kN for the RSW PIT samples at 1 million cycles that corresponded well with the experimental data as shown by an arrowhead. Hence, it can be deduced that a load level of up to 2 kN can be taken as a safe value for endurance limit for this RSW LBIT sample.

It should be noted that RSW LBIT joints have different joining features due to the treatment applied compared to RSW as-weld joints. From the treatments, the RSW LBIT joint is improved as the propagation of existence in any crack tends to slow and decelerate. This results in different crack initiation and growth behaviour between both joints.
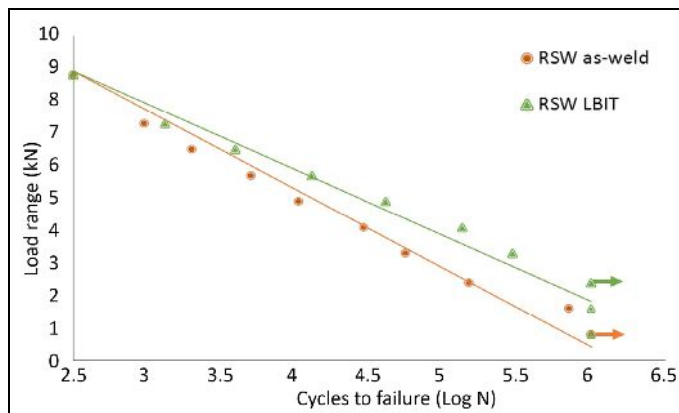
Figure 6. L-N curve for RSW LBIT and RSW as-weld samples

In order to determine the fatigue sensitivity of the LBIT weld samples, it is more suitable to use normalised load versus cycles to failure curve. For spot weld joint, results of fatigue tests are generally presented as load range vs. fatigue life (Hongyan & Senkara, 2006; Spitsen, Kim, Flinn, Ramulu, & Easterbrook, 2005; Wang et al., 2014). The normalised load (maximum tensile load divided by shear load) versus cycles to failure curve is shown in Figure 7. The curve shows that the RSW LBIT sample lost their static strength by almost 11.9% per decade of cycles, while for the RSW as-weld, almost 15% static strength was lost per decade. Lower percentage of lost value shows that the fatigue performance is better. Showing that, the fatigue performance for RSW LBIT is better than RSW as-weld. This may be due to the treatment that is applied to the joints which shows that the residual stress of RSW LBIT sample is improved. As noticed, signif cant improvement in the fatigue life can be obtained by modifying the residual stress levels in the material. There is a similar scatters trend for both RSW condition (RSW LBIT and RSW as-weld) in terms of reduction on normalised fatigue curves (Liu et al., 2013).

The scatter in fatigue life is large even under controllable and repeated testing conditions. Imprecision in testing equipment, loose tolerance in sample dimensions and large variations in environmental conditions may lead to unacceptably large scatter in presenting the data. For this

reason, one should ensure that the scatter in experimental data is within the acceptable range and tests are conducted under controllable and repeated conditions. This requires a statistical analysis of data collection. One of the methods to estimate the scatter in fatigue number of cycles is to calculate the fatigue sensitivity coeff cient.
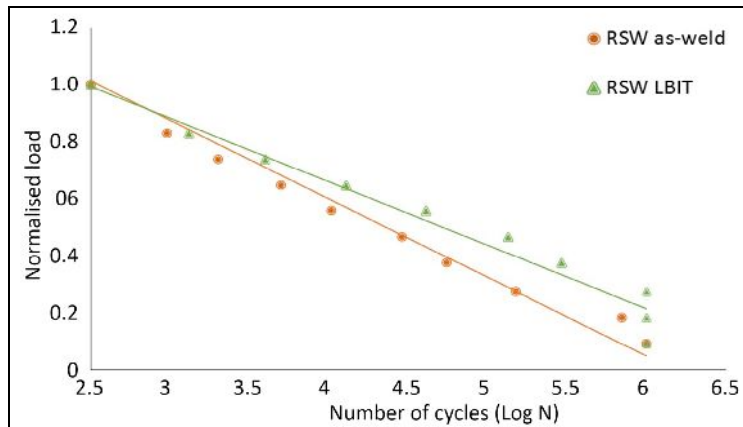
Figure 7. Normalised L-N curve for RSW LBIT and RSW as-weld samples

Typical values for fatigue sensitivity of mild steel are in the range from 0.10 to 0.50. However, the fatigue sensitivity for welded joints is even higher. In order to judge whether the scatter is within the acceptable range, one may also examine the regression coeff cients obtained through regression analysis of the experimental data. It is known that fatigue life data can typically be f tted to a power-law. The fatigue sensitivity coeff cient and coeff cient of determination (R^2) of the as-weld sample are shown in Table 2. The fatigue sensitivity coeff cient for as-weld sample exhibits the value of 0.14, which falls in the typical value range. The determination coeff cient (R2) value for RSW LBIT is 0.9530, which is close to 1 indicating that the linear line is a good f t for the data, and the predictability of the regression is quite high (Sun, Stephens, & Khaleel, 2008).

Table 2
Fatigue sensitivity coeff cient and determination coeff cient of RSW LBIT and RSW as-weld sample

Weld conf guration	Fatigue sensitivity coeff cient	Determination coeff cient
RSW LBIT	0.142	0.9530
RSW as-weld	0.262	0.9717

CONCLUSION

LBIT treatment is a post weld impact treatment that can be applied and used to signif cantly enhance the tensile shear load and hardness of RSW joint. LBIT helps in strengthening the metals through cold work that may increase the surface hardness and provide increased resistance to failure. As a whole, it has been proven through the experimental analysis that the

treatment of LBIT increases the strength for the low carbon steel spot weld joining that could substantially reduce the material cost for loading structures in industries.

Effects of modif cation of local material properties in the post weld impact treatment of spot weld sample were investigated through tensile shear test, hardness, and fatigue failure tests. Two different spot weld samples conditions were studied: RSW LBIT and RSW as-weld. The results showed that the treatment increased the tensile shear load of spot weld and also increased the hardness of the joint signif cantly. However, the modif cation of spot welded surface due to LBIT treatment led to an increase in fatigue failure.

ACKNOWLEDGEMENTS

REFERENCES

Baltazar-Hernandez, V. H., Okita Y., & Zhou, Y. (2013). Second pulse current in resistance spot welded TRIP steel - Effects on the microstructure and mechanical behavior. *Welding Journal, 91*(10), 278s-285s.

Ghazali, F. A., Manurung, Y. H., Mohamed, M. A., Alias, S. K., & Abdullah, S. (2015). Effect of process parameters on the mechanical properties and failure behavior of spot welded low carbon steel. *Journal of Mechanical Engineering and Sciences, 8*, 1489-97.

Liu, C., Zheng, X., He, H., Wang, W., & Wei, X. (2016). Effect of work hardening on mechanical behavior of resistance spot welding joint during tension shear test. *Materials and Design, 100*, 188–197.

Liu, L., Xiao, L., Chen, D. L., Feng, J. C., Kim, S., & Zhou, Y. (2013). Microstructure and fatigue properties of Mg-to-steel dissimilar resistance spot welds. *Materials and Design, 45*(0), 336–342.

Ma, H., Qin, G., Geng, P., & Fu, B. (2015). Effect of post-weld heat treatment on friction welded joint of carbon steel to stainless steel. *Journal of Materials Processing Technology, 227*, 24-33.

Mali, M. P., & Inamdar, K. H. (2012). Effect of spot weld position variation on quality of automobile sheet metal parts. *International Journal on Applied Research in Mechanical Engineering, 2*(2).

Pouranvari M., & Marashi, S. P. H. (2013). Critical review of automotive steels spot welding: process, structure and properties. *Science and Technology of Welding and Joining, 18*, 42.

Pouranvari, M., Marashi, S. P. H., & Safanama, D. S. (2011). Failure mode transition in AHSS resistance spot welds. Part II: Experimental investigation and model validation. *Materials Science and Engineering: A, 528*, 8.

Pouranvari, M., Mousavizadeh, S. M., Marashi, S. P. H., Goodarzi, M., & Ghorbani, M. (2011). Inf uence of fusion zone size and failure mode on mechanical performance of dissimilar resistance spot welds of AISI 1008 low carbon steel and DP600 advanced high strength steel. *Materials and Design, 32*(3), 1390–1398.

Spitsen, R., Kim, D., Flinn, B., Ramulu, M., & Easterbrook, E. T. (2005). The effects of post-weld cold working processes on the fatigue strength of low carbon steel resistance spot welds. *Journal of Manufacturing Science and Engineering, 127*(4), 718–723.

Sun, X., Stephens, E. V., & Khaleel, M. A. (2008). Effects of fusion zone size and failure mode on peak load and energy absorption of advanced high strength steel spot welds under lap shear loading conditions, *Engineering Failure Analysis, 15*, 11.

Vural, M., & Akkus, A. (2004). On the resistance spot weldability of galvanized interstitial free steel sheets with austenitic stainless steel sheets. *Journal of Materials Processing Technology, 153*, 1-6.

Wang, B., Duan, Q. Q., Yao, G., Pang, J. C., Li, X. W.,Wang, L., & Zhang, Z. F. (2014). Investigation on fatigue fracture behaviors of spot welded Q&P980 steel. *International Journal of Fatigue, 66*, 20–28.

Xue, Q., Benson, D., Meyers, M. A., Nesterenko, V. F., & Olevsky, E. A. (2003). Constitutive response of welded HSLA 100 steel. *Materials Science and Engineering: A, 354*(1–2), 166–179.

Yildirim, H. C., & Marquis, G. B. (2013). A round robin study of high-frequency mechanical impact (HFMI)-treated welded joints subjected to variable amplitude loading. *Welding World Association, 57*(3), 437-447.

Zhang, H., & Senkara, J. (2011). *Resistance welding: fundamentals and applications.* CRC press.

Zhao, D. W., Wang, Y. X., Zhang, L., & Zhang, P. (2013). Effects of electrode force on microstructure and mechanical behavior of the resistance spot welded DP600 joint. *Materials and Design, 50*, 6.

Aerosol Radiative Forcing Estimation Using Moderate Resolution Imaging Spectroradiometer (MODIS) in Kuching, Sarawak

Asmat, A.[1]*, Jalal, K. A.[1] and Ahmad, N.[2]

[1]*Faculty of Applied Sciences, Universiti Teknologi MARA (UiTM), 40450 Shah Alam, Selangor, Malaysia*
[2]*National Space Agency, 62100 Putrajaya, Malaysia*

ABSTRACT

High uncertainties in aerosol radiative forcing (ARF) arise from inaccurate estimation for aerosol optical depth (AOD) as an input parameter into Santa Barbara Discrete Ordinate Radiative Transfer (SBDART) model. Inf uence of AOD in ARF at the top of atmosphere (TOA) and surface over Kuching from 2011 until 2015 was investigated using Moderate Resolution Imaging Spectroradiometer (MODIS). Multi plane regression technique was used to retrieve AOD from MODIS (AOD_{MODIS}) by using different statistics (mean and standard deviation ($MODIS_{\mu\pm}$) and relative absolute error ($MODIS_{RAE}$) for accuracy assessment in spatial averaging and compared with Aerosol Robotic Network (AERONET). The relationship between AOD_{MODIS} and AOD from AERONET ($AOD_{AERONET}$) showed R^2 value for $MODIS_{\mu\pm}$ and $MODIS_{RAE}$ is 0.906 and 0.932, respectively. AOD_{MODIS} over Kuching tends to underestimate AOD during low variations and overestimate AOD when aerosol loading is higher. The retrieval of AOD_{MODIS} was used as an input parameter into SBDART for ARF estimation and compared with ARF from AERONET. When using AOD_{MODIS} from $MODIS_{\mu\pm}$, the ARF at TOA was between -5.95 Wm^{-2} and 0.89 Wm^{-2} and at the surface was from -389.7 Wm^{-2} and -31.4 Wm^{-2} while for $MODIS_{RAE}$, ARF value at the surface was from -392.3 Wm^{-2} and -27.3 Wm^{-2} while at TOA was between -5.89 Wm^{-2} and 0.98 Wm^{-2}. Average ARF value within the atmosphere for both $MODIS_{\mu\pm}$ and $MODIS_{RAE}$ were 151.6 Wm^{-2} and 130.4 Wm^{-2}, respectively. There is a poor relationship between the SBDART and AERONET for $MODIS_{\mu\pm}$, where R^2 is 0.33, while strong relationship is observed for $MODIS_{RAE}$ with R^2 value at 0.724.

Keywords: Aerosol optical depth, aerosol radiative forcing, AERONET, MODIS

INTRODUCTION

Atmospheric aerosols are one of the largest sources of uncertainty in assessing climate change and cause the quantif cation of aerosol

effects to become very challenging for many researchers. There are two effects of aerosols as stated by Charlson et al. (1992): (1) direct effect leads to scattering; and (2) absorption mechanisms while indirect effects modify the properties of clouds. The effects of aerosol can be quantifed through the estimation of aerosol radiative forcing (ARF) in unit Wm^{-2} by using radiative transfer models (RTM) with aerosol optical properties such as aerosol optical depth (AOD) and single scattering albedo (SSA) as an input parameter (Dhar et al., 2017). Unfortunately, high uncertainties in modelling ARF may arise from the input parameters for RTM (McComiskey et al., 2008). Santa Barbara Discrete Ordinate Atmospheric Radiative Transfer (SBDART) model is mostly used by researchers to estimate ARF. An example study was by Dhar et al. (2017) who observed good agreement with the slopes at 1.45 and 1.26, with and without aerosol respectively, and indicated that surface net shortwave fuxes estimated by SBDART model are slightly lower than obtained from CNR4 radiometer due to uncertainties in the input parameters such as AOD, SSA and asymmetry factor (ASY). The AOD was being measured as a unitless parameter and defned as extinction coeffcients of aerosol loading that was measured in vertical column of the atmosphere (Alam, Trautmann, Blaschke, & Majid, 2012). Dhar et al. (2017) explained changes in AOD and surface ARF during the observation period in Tripura which showed surface ARF primarily governed by the magnitude of AOD values. Higher AOD value (0.71) causes the ARF value during winter and pre monsoon to have comparable values of 32 Wm^{-2} and 33.45 Wm^{-2} respectively, and ARF value decreased in the monsoon due to lower SSA value (0.94) as well as AOD value.

Satellite data monitors global aerosol budget and their radiative effects on climate such as Moderate Resolution Imaging Spectroradiometer (MODIS) which has spatial data at 10 km twice a day (Remer et al., 2005). Ground based data like Aerosol Robotic Network (AERONET) is useful in estimating continuous microphysical and optical properties for aerosol in real time monitoring and can be used to validate satellite data (Holben et al., 1998). Validation between satellite and ground based data is necessary to develop a long term database for climatological studies and to improve the accuracy and coverage achievable with a single sensor (Prasad & Singh, 2007). More, Pradeep Kumar, Gupta, Devara, and Aher (2013) studied the comparison of aerosol products retrieved from AERONET, MICROTOPS Sunphotometer and MODIS over a tropical urban city and found the result which showed R^2 values ranging from 0.62 to 0.93. For MODIS, it was inclined to predict smaller AOD value as compared to actual AOD value derived from AERONET especially during winter, possibly due to improper assumptions of surface refectance and the incorrect selection of aerosol type.

The aim of this study is to retrieve AOD from MODIS (AOD_{MODIS}) by multiple plane regression technique using two different statistics which are mean and standard deviation ($MODIS_{\mu\pm}$) (Tripathi et al., 2005) and the usage of relative absolute error ($MODIS_{RAE}$) (Collopy & Armstrong, 2000), which is introduced for accuracy assessment in spatial averaging and compared with AERONET ($AOD_{AERONET}$). Collopy and Armstrong (2000) stated the relative absolute error (RAE) is a useful measure especially when making comparisons across a small set of time series data. However, RAE has not been used in retrieval of AOD study. Next, the impact of AOD_{MODIS} using $MODIS_{\mu\pm}$ and $MODIS_{RAE}$ daily variations are evaluated for conducting quantitative estimation of ARF as an input parameter into SBDART model over Kuching area. To date, there is no documented study regarding ARF estimation in Malaysia

even though it is very much needed since Malaysia receives considerable amount of smoke aerosols almost every year during the haze phenomenon. Therefore, it is important to understand whether the radiative force due to biomass smoke burning and other aerosol types cause positive or negative climatic implications.

MATERIALS AND METHODS

The experimental site for this study is Kuching, Sarawak with tropical rainforest climate, which is moderately hot and humid. The average annual rainfall is approximately 4200 mm with an average of 247 rainy days per year. Two types of data used were MODIS and AERONET from 2011 until 2015. For AERONET, AOD at 500 nm Level 2 (quality assured) data with the uncertainty under cloud free conditions was $<\pm0.01$ for >440 nm and $<\pm0.02$ for shorter wavelengths (Holben et al., 1998). MODIS data was capable of retrieving AOD under cloud free conditions with an accuracy of $\pm0.05\pm0.20$ over land and $\pm0.04\pm0.10$ over the ocean at mid-visible wavelength (Chu et al., 2002). AOD at 550 nm obtained from Terra MODIS Level 2 (MOD04) was categorised as processed data where the geophysical satellite derived information on both qualitative and quantitative analysis (Engel-cox, Holloman, Coutant, & Hoff, 2004) with spatial resolution of 10 km $\times$ 10 km.

Spatial and temporal averaging were conducted, with ±20 min as the time window with respect to MODIS overpass, then compared with the time availability for AERONET. Minimum distance technique was performed for MODIS data to calculate the closest pixel of latitude and longitude to the AERONET site with evaluation of 11×11 window size. The spatial average for MODIS over the AERONET was collocated from pixels lying in $\pm(1/4°)$ of latitude (1.491°) and longitude (110.349°) of AERONET station. The 53 points extracted from MODIS data were corresponding to latitude, longitude and AOD value using Matlab software.

Five nearest values of latitude and longitude data lying within the $\mu\pm$ and the lowest RAE were chosen to reduce error during ARF estimation using SBDART model. These two methods were compared. Then, multiple regression plane technique was analysed to predict AOD value based on the latitude and longitude to locate optimum value for AOD based on regression equation. The results were plotted in scatter plot with independent variables, latitude and longitude, on the X and Y axes and dependent variable, AOD, on the Z axis (Tripathi et al., 2005). Next, AOD data was interpolated by using power of law shown in Equation 1, as suggested by Prasad and Singh (2007), to convert AOD from different wavelength range for both data to the same wavelength range for easy comparison and validation.

$$AOD_{550nm} = AOD_{500nm} \left(\frac{550}{500}\right)^{-\alpha} \tag{1}$$

is the angstrom exponent at wavelength 440/870 nm obtained from AERONET data. The AOD_{MODIS} was validated by using $AOD_{AERONET}$ to understand errors in retrieval of AOD, so that retrieval algorithm can be corrected (More et al., 2013). The statistics obtained in this analysis are correlation coeffcient (R^2), root mean square error (RMSE) and mean absolute percentage error (MAPE). Finally, AOD derived from $MODIS_{\mu\pm}$ and $MODIS_{RAE}$ used as input parameter into SBDART for ARF estimation (Ricchiazzi, Yang, Gautier, & Sowle, 1998). The net fux

at the top of atmosphere (TOA) and surface were computed separately, within the wavelength range from 0.2 to 4.0 μm over 24 h with one hour time interval. The outcome from SBDART model is the value of instantaneous irradiance which is downward and upward solar f uxes (Ricchiazzi, Yang, Gautier, & Sowle, 1998) and calculated into ARF value. Calculation of ARF can be estimated by using Equation 2 with negative values of ARF which correspond to cooling effect while positive values of ARF correspond to warming effect, either at the surface or at TOA (Alam, Trautmann, Blaschke, & Majid, 2012).

$$\Delta F = (F_a \downarrow - F_a \uparrow) - (F_n \downarrow - F_n \uparrow) \tag{2}$$

Where F_a and F_a are downward and upward solar f uxes at the surface in the presence of aerosols and F_n and F_n are the same quantity but without aerosols and F is the ARF value. The difference between the TOA and surface gives the atmospheric forcing (F_{atm}) which represents the energy absorbed in the atmosphere.

RESULTS AND DISCUSSION

From the interpolation results, comparison between AOD_{MODIS} and $AOD_{AERONET}$ were made based on Julian Days. Figure 1 shows the daily average for AOD_{MODIS} and $AOD_{AERONET}$ over Kuching from 2011 until 2015 by using $MODIS_{\mu\pm}$.

Figure 1. Daily average AOD at 550 nm wavelength retrieved from AOD_{MODIS} and $AOD_{AERONET}$ Using $MODIS_{\mu\pm}$

Based on Figure 1, the range value for AOD_{MODIS} was -1.56 to 5.3 while for $AOD_{AERONET}$ the minimum and maximum values were 0.04 and 2.95, respectively. The high AOD value on certain Julian Days was due to the high concentration of aerosol loading at Kuching area as a result of dry season which usually occurs from June to September every year, as well as due to the presence of haze. Overestimation of AOD_{MODIS} occurred at Julian Day 253 in 2015 when extremely high AOD_{MODIS} was observed, at 5.3, while $AOD_{AERONET}$ was only 2.9. During the dry season, the surface is dry and causes the surface ref ectance to be high, which may cause the

overestimation of AOD. An error of ±0.006 in measuring the surface ref ectance yields an error of ±0.06 in retrieval of AOD (Tripathi et al., 2005). Extremely low AOD value was obtained during the wettest seasons from November to March. There was a large underestimation for AOD_{MODIS} on Julian Day 245 in 2011 where predicted AOD_{MODIS} was -1.6 as compared with the actual value from $AOD_{AERONET}$ which was only 0.15. The inconsistency between aerosol microphysical and optical properties and surface ref ectance used in the MODIS were possible reasons for the underestimation of AOD during the wet season (More et al., 2013). Figure 2 presents daily average for AOD_{MODIS} and $AOD_{AERONET}$ by using $MODIS_{RAE}$ from 2011 until 2015.
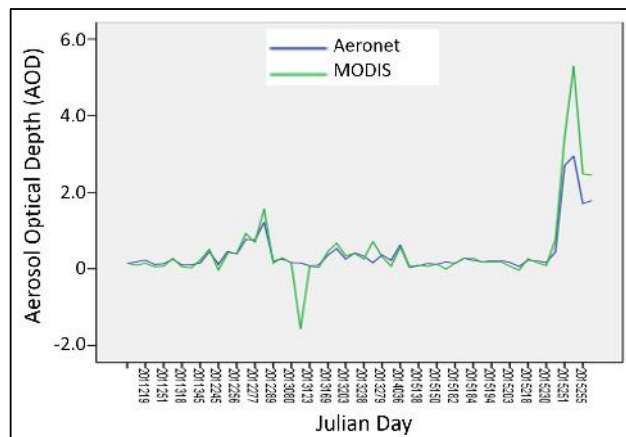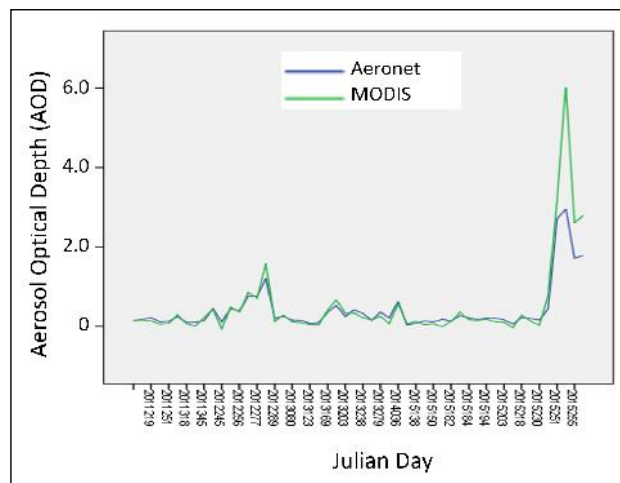

Figure 2. Daily average AOD at 550 nm wavelength retrieved from AOD_{MODIS} and $AOD_{AERONET}$ using $MODIS_{RAE}$

As presented in Figure 2, the range value for AOD_{MODIS} was -0.06 to 6.0 while for $AOD_{AERONET}$ the minimum and maximum values were 0.04 and 2.95 respectively. Overestimation of AOD_{MODIS} occurred on Julian Day 253 in 2015 when extremely high AOD_{MODIS} was observed with 6.0 and only 2.9 for $AOD_{AERONET}$. The variations of AOD at Kuching is the same where high concentration of AOD is observed during dry seasons (June to September). On the contrary, during wet seasons from November to March, the aerosol loading was monitored at low AOD. Therefore, it can be said that the spectral variations of AOD at Kuching are based on the seasonal distinctive features. Similar results were also obtained by Salinas, Chew, Mohamad, Mahmud and Liew (2013) at Kuching area but data was available only for 2011, where there was low aerosol loading for most of the period except for the months of August and September which examined high AOD values from regional episodes of biomass burning and f re activity during these particular months. Linear regression technique between AOD_{MODIS} and $AOD_{AERONET}$ are displayed in Figure 3.

(a)

(b)
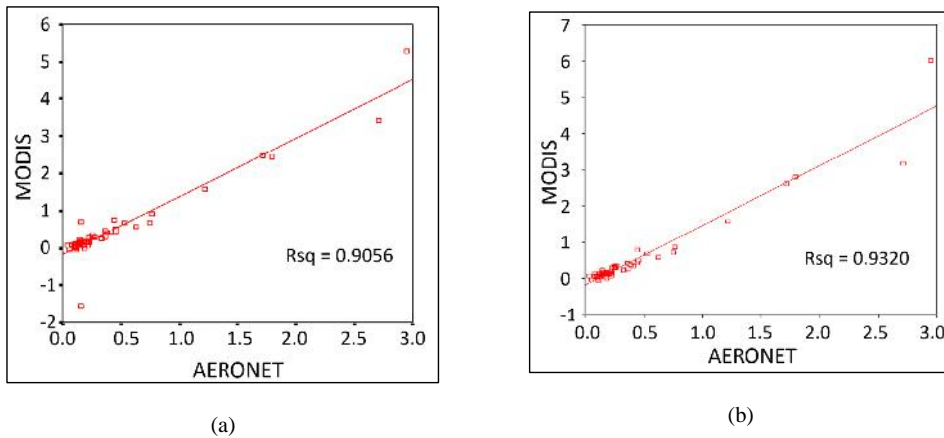
Figure 3. Linear regression for AOD_{MODIS} and $AOD_{AERONET}$ using: (a) $MODIS_{\mu\pm}$; and (b) $MODIS_{RAE}$

Based on Figure 3, the retrieval algorithm performance is validated from the resulting statistical parameters of the linear regression which are intercept (A), slope (B) and correlation coeff cient (R^2).

$$AOD_{MODIS} = A + B * AOD_{AERONET} \qquad (3)$$

Here non zero intercepts (A= - 0.1762 and – 0.1181) for $MODIS_{\mu\pm}$ and $MODIS_{RAE}$, respectively show that the retrieval algorithm is biased at low AOD value due to association with a sensor calibration error or incorrect assumption on ground surface ref ectance (Zhao et al., 2002). Chu et al. (2002) stated large errors in surface ref ection estimation could lead to larger intercept values. Lanzaco, Olcese, Palancar, and Toselli (2016) studied the comparison of AOD using MODIS and AERONET where the underestimation of AOD was probably due to incorrect characterisation of the local aerosols and the predominantly low AOD values observed. A slope that is different from unity indicates inconsistency between aerosol microphysical and optical properties used in the retrieval algorithm (Zhao et al., 2002) and represents systematic biases in the MODIS retrievals (More et al., 2013). Slope higher than unity at 1.5609 for $MODIS_{\mu\pm}$ and for $MODIS_{RAE}$ at 1.6469, indicates an overestimation of AOD by MODIS with respect to AERONET retrieval. The R^2 obtained for $MODIS_{\mu\pm}$ was 0.9056 and using $MODIS_{RAE}$ was 0.932, showing strong relationship between AOD_{MODIS} and $AOD_{AERONET}$. For $MODIS_{\mu\pm}$, the MAPE was found to be 24% and RMSE value was 0.45 while for $MODIS_{RAE}$, the MAPE was around 12% and RMSE was 0.47. There was only little difference between RMSE for $MODIS_{\mu\pm}$ and $MODIS_{RAE}$ while for MAPE, the value for $MODIS_{\mu\pm}$ was quite higher of 24%, as compared to $MODIS_{RAE}$, with only 12%. Based on that, it shows that the selection method using $MODIS_{RAE}$ can also be used to retrieve true value of AOD.

The assessments of ARF conducted by using SBDART model with AOD value retrieved from $MODIS_{\mu\pm}$ and $MODIS_{RAE}$ as input parameter are shown in Figure 4 and 5.
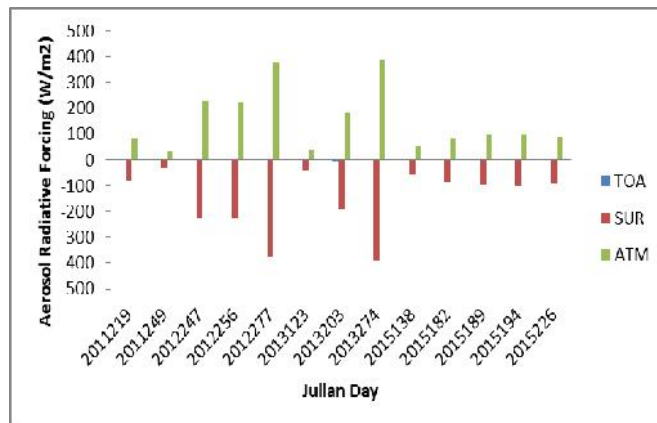
Figure 4. Daily variations of ARF at TOA surface and within the atmosphere using MODIS$_{\mu\pm}$

In Figure 4, the range value for ARF at TOA for AOD$_{MODIS}$ derived using MODIS$_{\mu\pm}$ was between -5.95 Wm^{-2} and 0.89 Wm^{-2} and at the surface, was from -389.7 Wm^{-2} to -31.4 Wm^{-2}. The ARF value at TOA was quite low compared with the surface ARF which could reach around -389.7 Wm^{-2}. The daily average ARF value within the atmosphere was at 151.6 Wm^{-2}, which is quite large. Results obtained by Kalluri et al. (2016) stated that atmospheric force was found to be around 36.8 Wm^{-2} during summer due to the combination of dust and carbon aerosols, producing very high AOD value. Thus, high atmospheric force values indicated maximum absorption might be attributed to the mixing of absorbing black carbon with moderately absorbing dust.
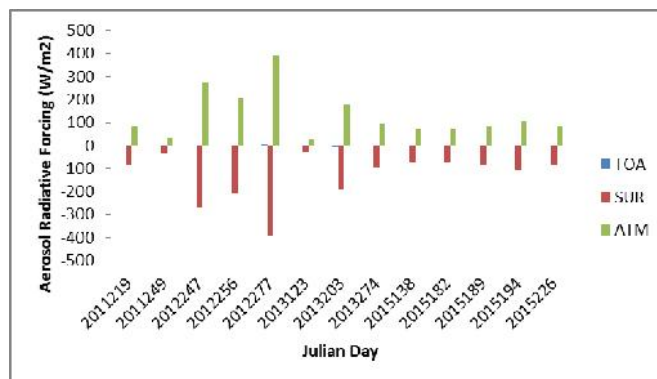
Figure 5. Daily variations of ARF at TOA, surface and within the atmosphere using MODIS$_{RAE}$

Based on Figure 5, ARF value using MODIS$_{RAE}$ at the surface was within -392.3 Wm^{-2} and -27.3 Wm^{-2} and TOA was between -5.89 Wm^{-2} and 0.98 Wm^{-2}. The ARF value within the atmosphere can be estimated by the difference of ARF at surface and TOA and the average value was 130.4 Wm^{-2}. The results obtained from this study did not show pattern of variations for AOD towards changes in ARF value, causing diff culties in observing the relationship between ARF and aerosol loading. It can still be proven that the slight changes for AOD value as derived from

using $MODIS_{\mu\pm}$ and $MODIS_{RAE}$ resulted in different values of ARF. As an example, AOD_{MODIS} derived using $MODIS_{\mu\pm}$ was 0.4, while for $MODIS_{RAE}$ the value of AOD was 0.36 causing ARF estimation at TOA at -2.31 Wm^{-2} and -2.19 Wm^{-2}, respectively. Extremely high negative value at surface which can reach -392.3 Wm^{-2} was probably due to improper retrieval of AOD or when estimating ARF value using SBDART model (Alam et al., 2012).

Theoretically, high negative value at surface aerosol signif cantly reduced the solar radiation producing a large surface cooling (Kalluri et al., 2016). The difference between ARF value at surface and TOA was a greater absorption of solar radiation within the atmosphere with high positive values in ARF, as a consequence, warming the atmosphere and cooling the surface area (Alam et al., 2012). Research by Wu, Zhu, Che, Xia, and Zhang (2015) showed negative ARF gradually increased with increasing AOD, both at the surface and TOA because of the increase in light scattering and absorption induced by aerosol particles.

On the other hand, linear regression between SBDART and AERONET for $MODIS_{\mu\pm}$ and $MODIS_{RAE}$ was also analysed. It showed poor relationship between SBDART and AERONET for $MODIS_{\mu\pm}$ with R^2 value at 0.33, compared to $MODIS_{RAE}$, where the R^2 was 0.724. The $MODIS_{RAE}$ demonstrated signif cant results, which might be due to high accuracy assessment in terms of statistical method during spatial and temporal averaging. The differences in ARF estimation by using these two statistical methods could be contributed from the variations in AOD value (Alam et al., 2012).

CONCLUSION

As a conclusion, one of the reasons towards the changes in the estimation of ARF value by using radiative transfer model comes from input parameters for aerosol optical properties such as AOD. This is because when there are slight changes for AOD value from using $MODIS_{\mu\pm}$ and $MODIS_{RAE}$, different values for ARF estimation are derived. These problems may arise due to lack of appropriate aerosol models in the MODIS aerosol retrieval algorithm, or as a result of other factors such as temporal and spatial variability of aerosols. Therefore, it is essential to improve the MODIS retrieval algorithm because radiative transfer simulations should consider uncertainties in the output. Thus, the uncertainty in retrieval of input parameter in radiative transfer model should be improved in obtaining accurate ARF values. For further study of the surface ref ectance, ozone concentration and other meteorological parameters can be used as input parameter into SBDART to provide better understanding of the regional and local behaviour and improve the estimation of ARF value.

ACKNOWLEDGEMENTS

REFERENCES

Alam, K., Trautmann, T., Blaschke, T., & Majid, H. (2012). Aerosol optical and radiative properties during summer and winter seasons over Lahore and Karachi. *Atmospheric Environment, 50*, 234–245. https://doi.org/10.1016/j.atmosenv.2011.12.027

Armstrong, J. S., & Collopy, F. (2000). Another Error Measure for Selection of the Best Forecasting Method: The Unbiased Absolute Percentage Error. *International Journal of Forecasting, 8*(2), 69-80.

Charlson, R. J., Schwartz, S. E., Hales, J. M., Cess, R. D., Coakley, J. A., Hansen, J. E., et al. (1992). Climate forcing by anthropogenic aerosols. *Science, 255*, 423-430.

Chu, D. A., Kaufman, Y. J., Ichoku, C., Remer, L. A., Tanre, D., & Holben, B. N. (2002). Validation of MODIS aerosol optical depth retrieval over land. *Geophysical Research Letters, 29*(12), 8007. Retrieved from https://dx.doi.org/10.1029/2001GL013205

Dhar, P., De, B. K., Banik, T., Gogoi, M. M., Babu, S. S., & Guha, A. (2017). Atmospheric aerosol radiative forcing over a semi-continental location Tripura in North-East India: Model results and ground observations. *Science of the Total Environment, 580*, 499–508. Retreived from https://dx.doi.org/http://dx.doi.org/10.1016/j.scitotenv.2016.11.200

Engel-cox, J. A., Holloman, C. H., Coutant, B. W., & Hoff, R. M. (2004). Qualitative and quantitative evaluation of MODIS satellite sensor data for regional and urban scale air quality, *38*, 2495–2509. Retrieved from https://dx.doi.org/10.1016/j.atmosenv.2004.01.039

Holben, B. N., Eck, T. F., Slutsker, I., Tanre, D., Buis, J. P., Setzer, A., ... & Lavenu, F. (1998). AERONET—A federated instrument network and data archive for aerosol characterization. *Remote Sensing of Environment, 66*(1), 1-16. Retrieved from https://dx.doi.org/10.1016/S0034-4257(98)00031-5

Kalluri, R. O. R., Gugamsetty, B., Kotalo, R. G., Nagireddy, S. K. R., Tandule, C. R., Thotli, L. R., ... & Surendranair, S. B. (2016). Direct radiative forcing properties of atmospheric aerosols over semi-arid region, Anantapur in India. *Science of the Total Environment, 566*, 1002-1013. Retrieved from https://dx.doi.org/10.1016/j.scitotenv.2016.05.056

Lanzaco, B. L., Olcese, L. E., Palancar, G. G., & Toselli, B. M. (2016). A method to improve MODIS AOD Values: Application to South America, 1509-522. Retrieved from https://dx.doi.org/10.4209/aaqr.2015.05.0375

McComiskey, A., Schwartz, S. E., Schmid, B., Guan, H., Lewis, E. R., Ricchiazzi, P., & Ogren, J. A. (2008). Direct aerosol forcing: Calculation from observables and sensitivities to inputs. *Journal of Geophysical Research: Atmospheres, 113*(D9), 1–16. Retrieved from https://dx.doi.org/10.1029/2007JD009170

More, S., Pradeep Kumar, P., Gupta, P., Devara, P. C. S., & Aher, G. R. (2013). Comparison of aerosol products retrieved from AERONET, MICROTOPS and MODIS over a tropical urban city, Pune, India. *Aerosol and Air Quality Research, 13*(1), 107–121. Retrieved from https://dx.doi.org/10.4209/aaqr.2012.04.0102

Prasad, A. K., & Singh, R. P. (2007). Comparison of MISR-MODIS aerosol optical depth over the Indo-Gangetic basin during the winter and summer seasons (2000 – 2005), *107*, 109–119. Retrieved from https://dx.doi.org/10.1016/j.rse.2006.09.026

Remer, L. A., Kaufman, Y. J., Tanré, D., Mattoo, S., Chu, D. A., Martins, J. V., ... & Eck, T. F. (2005). The MODIS aerosol algorithm, products, and validation. *Journal of the Atmospheric Sciences, 62*(4), 947-973.

Ricchiazzi, P., Yang, S., Gautier, C., & Sowle, D. (1998). SBDART: A research and teaching software tool for plane-parallel rRadiative transfer in the earth's atmosphere. *Bulletin of the American Meteorological Society, 79*(10), 2101–2114.

Salinas, S. V., Chew, B. N., Mohamad, M., Mahmud, M., & Liew, S. C. (2013). First measurements of aerosol optical depth and Angstrom exponent number from AERONET's Kuching site. *Atmospheric Environment, 78*, 231–241. Retrieved from https://dx.doi.org/10.1016/j.atmosenv.2013.02.016

Tripathi, S. N., Dey, S., Chandel, A., Srivastava, S., Singh, R. P., & Holben, B. N. (2005, June). Comparison of MODIS and AERONET derived aerosol optical depth over the Ganga Basin, India. In *Annales Geophysicae* (Vol. 23, No. 4, pp. 1093-1101).

Wu, Y., Zhu, J., Che, H., Xia, X., & Zhang, R. (2015). Column-integrated aerosol optical properties and direct radiative forcing based on sun photometer measurements at a semi-arid rural site in Northeast China. *Atmospheric Research, 157*, 56–65. Retrieved from https://dx.doi.org/10.1016/j.atmosres.2015.01.021

Xu, H., Guo, J., Ceamanos, X., Roujean, J. L., Min, M., & Carrer, D. (2016). On the inf uence of the diurnal variations of aerosol content to estimate direct aerosol radiative forcing using MODIS data. *Atmospheric Environment, 141*, 186–196. Retrieved from https://dx.doi.org/10.1016/j.atmosenv.2016.06.067

Zhao, T. X. P., Stowe, L. L., Smirnov, A., Crosby, D., Sapper, J., & McClain, C. R. (2002). Development of a global validation package for satellite oceanic aerosol optical thickness retrieval based on AERONET observations and its application to NOAA / NESDIS operational aerosol retrievals. *American Meteorological Society, 59*, 294–312.

Buari-Chen Malay Reading Chart (BCMRC): Contextual Sentence and Random Words 2-in-1 Design in Malay Language

Buari, N. H. and Chen, A. H.*

Faculty of Health Sciences, Universiti Teknologi MARA (UiTM), 42300 Puncak Alam, Selangor, Malaysia

ABSTRACT

A full description of a new reading chart in Malay language, the Buari-Chen Malay Reading Chart (BCMRC) is described. Internal and external comparisons of BCMRC are also reported. BCMRC comprised four reading sets with contextual sentence (CS1 and CS2) and random words (RW1 and RW2) designs. A total of 14 prints, ranging from 1.3LogMAR to 0.0LogMAR in 0.1LogMAR steps (equivalent to 8 M to 0.4 M) were printed in high contrast Arial font. CS1, CS2, RW1 and RW2 were presented in random order to the participants for internal comparison. The reading was evaluated aloud with clear pronunciation (errors were recorded). Maximum reading speed (MRS) was reported in words per minute. The external comparison involved two standard English reading charts [MNread acuity chart (MNread) and Bailey-Lovie words reading chart (Bailey-Lovie)]. The internal and external comparisons were analysed using the intra-class correlation coeff cient (ICC) and Cronbach's alpha ( ) respectively. Contextual sentence set (ICC=0.82) and random word set (ICC=0.85) exhibited good reliability in our internal comparison. The external comparison showed acceptable reliability for both MNread (=0.76) and Bailey-Lovie (=0.80). BCMRC sets with similar features could be used interchangeably to monitor clinical progress in visual rehabilitation. BCMRC was comparable with MNread and Bailey-Lovie reading charts.

Keywords: Malay reading chart, reading, reading chart, reading speed

INTRODUCTION

The reading assessment in an eye examination was evaluated using reading charts. Standardized reading charts are usually equipped with its validity and reliability. Contextual sentences and random words are the options for text design. The contextual sentence comprises continuous and meaningful text. The random words design

uses string of words that are independent of semantic and syntactic cues. The contextual sentence reading charts available are MNread acuity chart (MNread)(Mansf eld, Ahn, Legge, & Luebker, 1993), Radner reading chart (Radner) (Radner et al., 1998) and International reading speed test (IReST) (Hahn et al., 2006). The random words reading charts include Bailey-Lovie word acuity chart (Bailey-Lovie) (Bailey & Lovie, 1980), practical near acuity chart (PNAC) (Wolffsohn & Cochrane, 2000), Pepper Visual Skill for Reading Test (VSRT) (Watson, Whittaker, & Steciw, 2010) and Rate of Reading Test (RRT) (Wilkins, Jeanes, Pumfrey, & Laskier, 1996). The majority of random words reading charts contain string of words that are arranged to mimic sentences. Some are translated into different languages for the clinical evaluation of reading (Alio et al., 2008; Buari, Azizan, & Chen, 2015; Buari, Chen, & Musa, 2014; Calossi, Boccardo, Fossetti, & Radner, 2014; Castro, Kallie, & Salomao, 2005; Hahn et al., 2006; d l et al., 2011; Maaijwee, Mulder, Radner, Van Meurs, & Meurs, 2008; Mataftsi et al., 2013; Trauzettel-Klosinski & Dietz, 2012).

The need for standardised reading charts in local language is undisputable. Language barrier should be eliminated during reading assessment by adapting to native language. Factors that should be considered in developing and designing the reading chart include the notation, number of words for every print size, number of lines for every print size, font type and the arrangement on the chart. The majority employed LogMAR notation for reading acuity scoring because it gives similar geometric progression (Bailey, 2006). Other notations are "M" notation and "N" notation (Colenbrander, 2001). The number of words and lines for every print size vary for different reading charts. Some charts have a constant number of words throughout the print sizes (Radner et al., 1998; Wilkins et al., 1996; Wolffsohn & Cochrane, 2000) while others have different number of words for each print size (Bailey & Lovie, 1980; Buari et al., 2015; Buariet al., 2014; Hahn et al., 2006; Mansf eld et al., 1993). The variations in the number of words per print size might affect the duration of reading for each print size (Jufri, Buari, & Chen, 2016). The number of lines may vary according to different charts ranging from a single line up to 13 lines. The alignment is either centre alignment or left alignment in the reading chart. *Times New Roman* is the most common font typeface used in reading charts to relate to the common print size used for newspapers and books (Wolffsohn & Cochrane, 2000). Font choice is crucial to reduce the visual noise and crowding effect especially among people with special needs (Spinelli, De Luca, Judica, & Zoccolotti, 2002).

Most reading charts establish its reliability before being used in the clinical setting or as a research tool. The MNread displays good reliability on normal vision (adults: r = 0.82; children: r = 0.95 to 0.94) (Castro et al., 2005; d l et al., 2011; Legge, Pelli, Rubin, & Schleske, 1985; Legge, Rubin, Pelli, & Schleske, 1985; Mansf eld et al., 1993; Mansf eld, Legge, & Bane, 1996; Virgili et al., 2004) and low vision (Subramanian & Pardhan, 2006, 2009). The PNAC

is highly correlated with Bailey-Lovie (r = 0.99) (Wolffsohn & Cochrane, 2000), Radner had has good inter-chart reliability (reliability = 0.88 – 0.98) (Burggraaff, van Nispen, Hoek, Knol, & van Rens, 2010; Maaijwee et al., 2008; Radner et al., 1998; Stifter et al., 2004), UiTM-Mrw and UiTM-Muw had has good reliability (0.85) in repeated measurement of the reading speed (Buari, Yusof, Mohd-Satali, & Chen, 2014). Contextual sentence design ref ects daily reading activities, but random word design dedicates visual aspect in reading (Lüdtke & Kaup, 2006; Van Petten & Kutas, 1990). Having both designs in a single reading chart might be an advantage. Internal and external comparisons of Buari-Chen Malay Reading Chart are reported in our study.

MATERIALS AND METHODS

Buari-Chen Malay Reading Chart (BCMRC)

The chart in this study is referred as Carta Membaca Bahasa Melayu Buari-Chen (in Malay) or Buari-Chen Malay Reading Chart (in English). BCMRC comprises four reading sets with contextual sentences (CS1 and CS2) and random words (RW1 and RW2) designs (Figure 1). The fundamental characteristics and features in each set design are identical except for the text itself (sentences and words). Contextual sentences and random words are organised to form the reading text. Both the materials used are approved under the Ministry of Education, Malaysia. The contextual sentences are selected from Malay language primary school textbooks from Grade 3 to Grade 6. The random words consist of a string of words that do not represent any contextual meaning. The words are selected randomly from Word Registry of Primary School (Daftar Kata Bahasa Melayu Sekolah Kebangsaan) for primary school students from Grade 1 to Grade 6. A total of 28 sets of contextual sentences and 28 sets of random words are constructed to develop the BCMRC. The appropriateness of the Malay contextual sentences were examined, f nalised, and conf rmed through formal consultation with experienced Malay language school educators. It was done manually within the scope of grammar, composition and arrangement of contextual sentences. Subsequently, 14 print sizes ranging from 1.3LogMAR to 0.0LogMAR in 0.1LogMAR steps were printed in high contrast Arial font. Each print size comprise six Malay words and is arranged into two lines. Four notations are incorporated in the design namely the M notation, N notation, Snellen ratio and LogMAR. The M notation and Snellen ratio range from 8 M to 0.4 M and 20/400 to 20/20, respectively. The N notation is from N64 to N3. The sentences are set at left alignment. The BCMRC is printed on A4 size white matte surface material, double sided with high contrast of black print on white background.
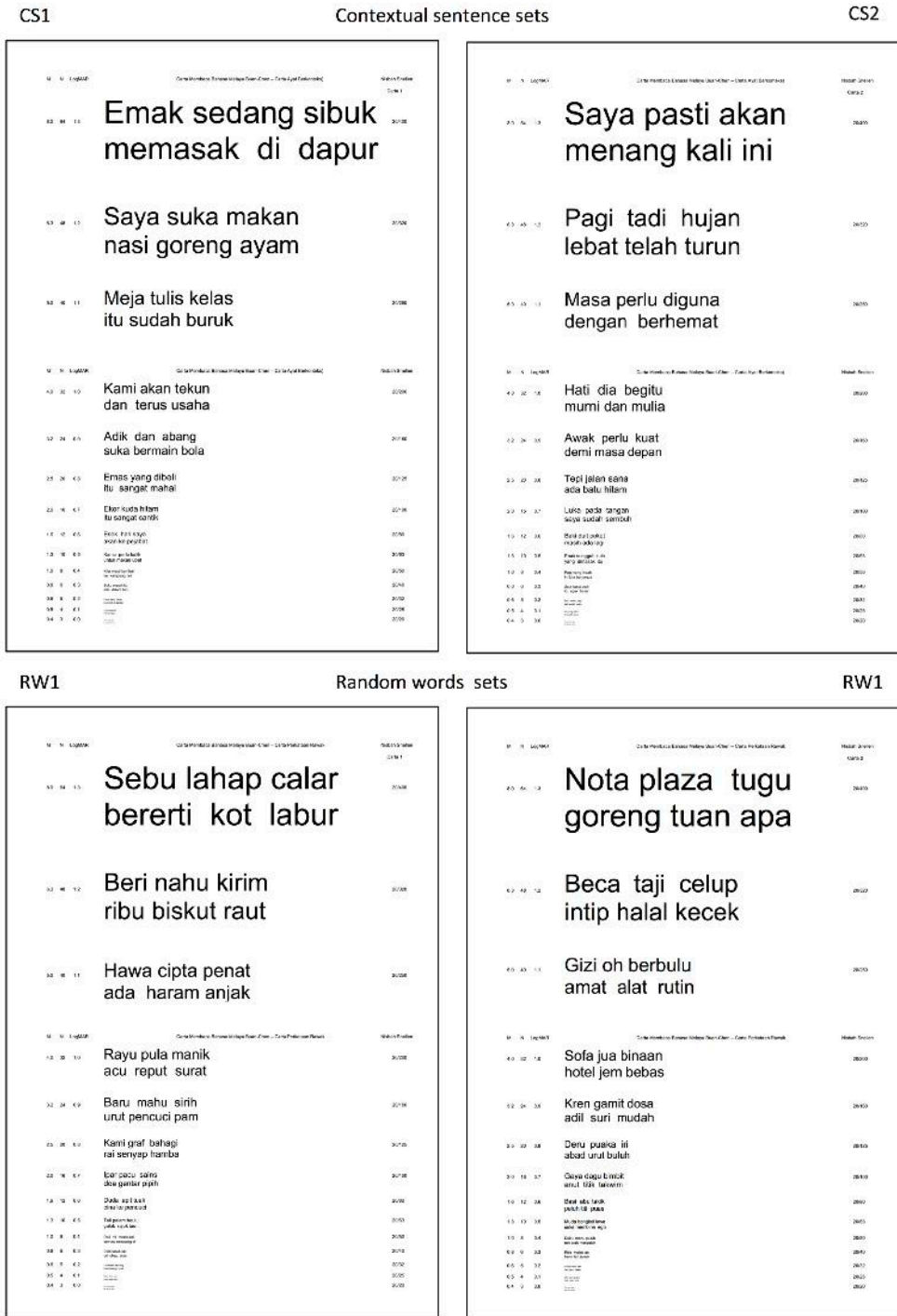
Figure 1. Buari-Chen Malay reading chart

Internal Comparison of BCMRC

The internal comparison between sets was evaluated by comparing the maximum reading speed (MRS) for both BCMRC contextual sentence sets (CS1 vs CS2) and BCMRC random words sets (RW1 vs RW2). The reading speed of each sentence was calculated as number of correct words read in a minute (wpm). The reading speed was plotted against the print sizes to obtain the critical print size (CPS). The CPS was the smallest print size that gave the maximum reading speed before it plateaued within 1.96 standard deviation of the mean reading speed (Stifter et al., 2004). The maximum reading speed (MRS) was then determined as the maximum number of words that could be read by the participants in a minute, that is, the words per minute. The MRS was calculated as the mean reading speed from the print size of 1.1LogMAR (5M) to the critical print size (Maaijwee et al., 2008). The two largest and smallest print sizes were excluded as the reading speed was deviated from the constant rate (Legge, et al., 1985). Ethical approval and informed consent was obtained to examine 31 young adults with normal vision (mean age: 22.17±1.71 years). The sample size was calculated using G power version 3.1.9.2 based on reading outcome from previous f ndings (Alio et al., 2008). The alpha error of probability was set at 0.05; the effect size (d) was 0.71 and this gave the power of study of 0.87.

The inclusion criteria: habitual distance visual acuity (6/9 binocularly or better), remote near point of convergence (5±2.5cm) and amplitude of accommodation (18–1/3(age)±2D). The participants were asked to read from the largest to smallest prints of the sets. The testing distance was set at 40 cm. The sets were read binocularly under the illumination of 80-90 cd/m² with their habitual refractive error correction at random order. An inclined reading stand with a 45-degree angle was used to hold the chart. A blank card was used to cover before the reading speed evaluation to avoid pre-reading. The participants were asked to read the charts at normal speed aloud, with clear and precise pronunciation. The time taken to read until the smallest print size was recorded. The end point was more than 50% incorrect words of the smallest print size. Errors such as incorrect, substitution, reversal and omission were noted. The reading evaluation was recorded on audio tape.

External Comparison of BCMRC

The external comparison involved two standard English reading charts [MNread acuity chart (MNread) and Bailey-Lovie words reading chart (Bailey-Lovie)]. The reliability test was performed between the contextual sentence set of BCMRC and MNread. The MNread was chosen because the contextual sentence reading chart was widely used in clinical setting and in research (Subramanian & Pardhan, 2006, 2009). The random words set of BCMRC was compared with Bailey-Lovie because the Bailey-Lovie was the standardised random word chart. Similar participants from the previous section continued reading the MNread and Bailey-Lovie at random. The testing distance was at 40 cm except for Bailey-Lovie, which was set at 25 cm as to comply with the recommended testing distance of each reading chart.

RESULTS

Internal Comparison of BCMRC

The internal comparison of MRS was examined between CS1 vs CS2 and RW1 vs RW2 using the independent sample t-test and intra class correlation coeff cient (ICC). The signif cant level was set at 0.05(Kottner et al., 2011). ICC ranged between 0 and 1. The following rules of thumb were used in the interpretation of ICC values: > 0.9 – Excellent, > 0.8 – Good, > 0.7 – Acceptable, > 0.6 – Questionable, > 0.5 – Poor, and < 0.5 – Unacceptable (Gliem & Gliem, 2003). The agreements between charts were plotted using Bland and Altman plot (Bland & Altman, 1986; Bland & Altman, 1995). The mean difference between two variables and 95% limits of agreement as the mean difference of 1.96 standard deviation were calculated. The presentation of the 95% limits of agreement was for the visual judgement of how well the two variables agreed (Sedgwick, 2013). The reading speed for each print size was charted against the print size to obtain the critical print size (CPS) and maximum reading speed (MRS) of every set. MRS was 201.64 ± 32.95 wpm for CS1 and 202.29 ± 34.71 wpm for CS2. The difference in MRS was not statistically signif cant $[t(60) = -0.08, p>0.05]$. CPS was 0.3LogMAR (0.8M) for both CS1 and CS2. The agreement between CS1 and CS2 was well distributed within the lines of lower and upper limits of agreement in Bland and Altman plot [Figure 2(a)]. The mean difference was -0.66 ± 22.26 wpm (95% CI: -17.85 to 16.54 wpm). The lower and upper limits of agreement ranged from -44.97 wpm (95% CI: -30.61 to -59.33 wpm) to 42.97wpm (95% CI: 57.33 – 28.61 wpm). The intra class correlation coeff cient between CS1 and CS2 was found to be good (ICC=0.88). Good agreement and intra class correlation coeff cient suggested that the two contextual sentence sets of BCMRC were homogeneous in evaluating the reading speed among young adults. The CPS for random words set of BCMRC was at 0.3LogMAR, which was equivalent to 0.8M or N6. The MRS for RW1 and RW2 were 156.30 ± 24.92wpm and 147.63 ± 20.08wpm respectively. The difference was not signif cant $[t(60) = 1.51, p>0.05]$. The agreement between RW1 and RW2 was also good with the mean difference of 8.67 ± 12.10 wpm and 95% of conf dent interval range between -2.83 to 20.17 wpm [Figure 2(b)]. The lower limit of agreement was at -15.05 wpm (95% CI: -7.24 to -22.86 wpm) while the upper limit of agreement fell at 32.40 wpm (95% CI: 40.21 to 24.59 wpm). RW1 and RW2 showed good intra class correlation coeff cient (ICC = 0.92).
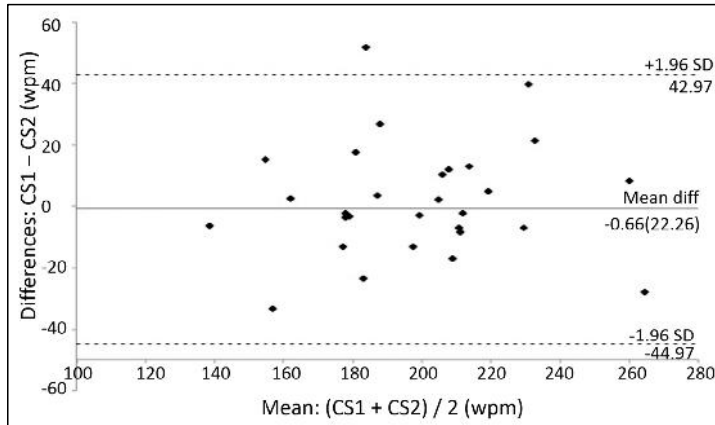
(a)
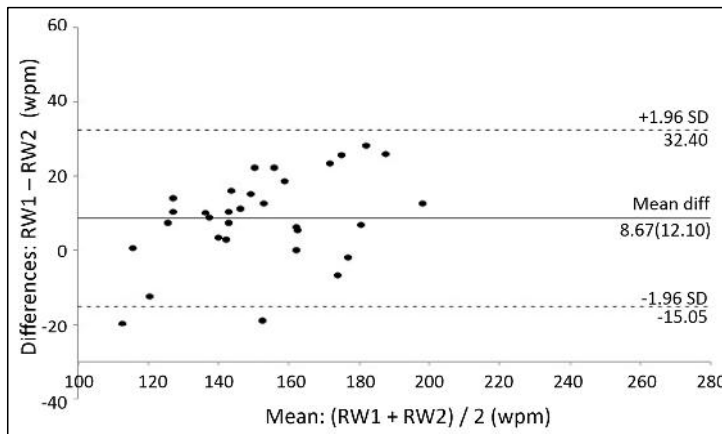
(b)

Figure 2. The Bland and Altman plot for internal comparison of BCMRC: (a) CS1 versus CS2; and (b) RW1 versus RW2

The differences of MRS were charted against the mean of MRS between two sets of BCMRC. The middle black line represent the mean difference in measurement of MRS between the two charts. The dashed-lines illustrated the upper limit of agreement (+1.96 SD) and lower limit of agreement (-1.96 SD).

External Comparison of BCMRC

The external comparison of BCMRC was tested with Cronbach's alpha ( ). The MRS for BCMRC and MNread were 201.64±32.95wpm and 205.71±26.41wpm, respectively. Most of the data in Bland and Altman agreement plot between BCMRC and MNRead was fell within

the lower limit of agreement and upper limit of agreement that ranged from -55.78 (95% CI: -38.77 to -72.79 wpm) wpm to 47.64 wpm (95% CI: 30.63 to 64.65 wpm) with a narrow mean difference, -4.07 wpm and 95% of CI ranged between -19.25 to 11.10 wpm [Figure 3(A)]. This indicated a good agreement between BCMRC and MNread. BCMRC had a good reliability with MNread (= 0.76). Good reliability (= 0.80) and good agreement [Figure 3(B)] between BCMRC and Bailey-Lovie was also demonstrated. The MRS was 156.30±24.92 wpm and 117.30±16.89 wpm for BCMRC and Bailey-Lovie respectively. The lower limit of agreement was 4.83 wpm (95% CI: -6.41 to 16.07 wpm) and upper limit of agreement was 73.17 wpm (95% CI: 61.93 to 84.41 wpm).
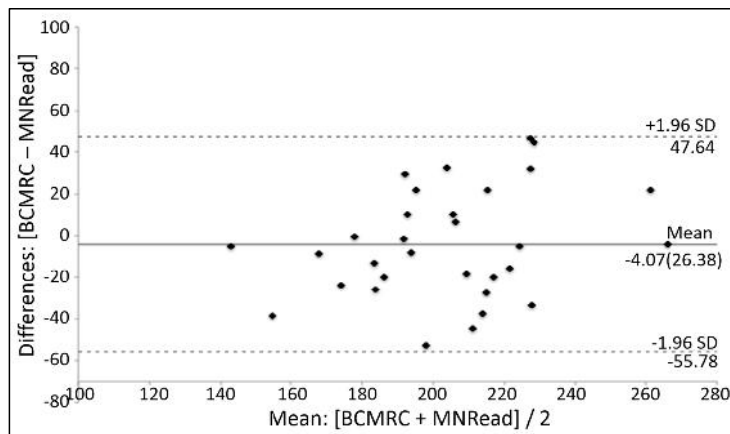
(a)

(b)

Figure 3. The Bland and Altman plot for external comparison of BCMRC: (a) BCMRC versus MNread; and (b) BCMRC versus Bailey-Lovie

The differences of MRS were plotted against the mean of MRS between two charts. The middle black line presents the mean of differences of measurement of MRS between two charts. The dashed-lines indicate the upper limit of agreement (+1.96 SD) and lower limit of agreement (-1.96 SD).

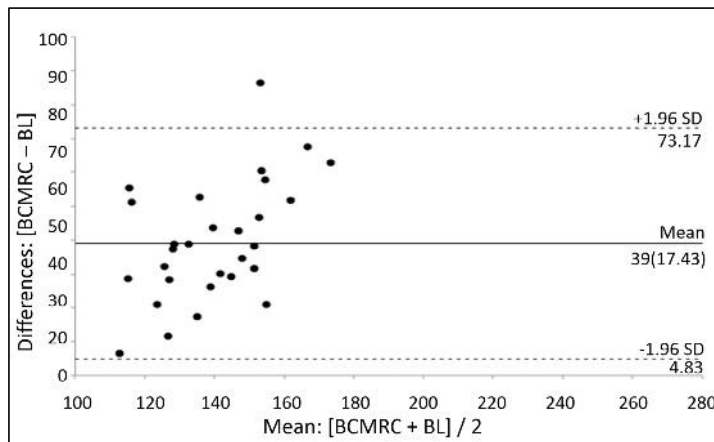## DISCUSSIONS

Internal Comparison of BCMRC

The internal comparison of contextual sentence sets of BCMRC found that the CS1 and CS2 provided similar agreement between each other with a good ICC. The contextual sets of BCMRC used meaningful sentence to test the reading acuity and reading speed simultaneously. Reading charts that employed meaningful or contextual sentence were the MNread, Radner, IReST and UiTM-Mrw (Buari et al., 2014; Hahn et al., 2006; Mansfeld et al., 1993; Radner et al., 1998). Among the mentioned contextual reading charts, MNread, Radner and IReST had more than one set of charts. Similar with internal comparison of CS1 and C2 in our study, MNread, Radner and IReST also showed good reliability between sets. Excellent reliability score was obtained in both MNread and Radner with Cronbach Alpha of 0.95 (Virgili et al., 2004) and 0.98 (Burggraaff et al., 2010; Maaijwee et al., 2008; Radner et al., 1998) respectively. Apart from reliability test, some other charts tested its inter-chart comparison with Pearson's correlation coefficient. Highly significant correlation coefficient was found in MNread (r=0.86 to 0.88) (Ahn et al., 1995; dl et al., 2011; Legge et al., 1989), Radner (r=0.98) (Burggraaff et al., 2010; Maaijwee et al., 2008; Radner et al., 1998) and also between sets in IReST texts (0.77 to 0.93) (Trauzettel-Klosinski & Dietz, 2012). Similar with BCMRC, MNread also had two sets of chart (dl et al., 2011; Mataftsi et al., 2013; Subramanian & Pardhan, 2006) and Radner had three sets of chart (Burggraaff et al., 2010). The earlier version of IReST had 10 sets of text for each of the four European languages and it was found that seven out of 10 texts were comparable (Hahn et al., 2006). The second version of IReST also consisted of 10 sets of text, but the choice of language was expanded up to 17 languages (Trauzettel-Klosinski & Dietz, 2012). Usually more than one set is available in the existing reading charts, so that they can be used interchangeably. The multiple sets are beneficial for the repeated measurements and rehabilitation sessions. Therefore, learning bias could be ruled out in the clinical setting.

The MRS outcome of CS1 and CS2 were 201 wpm and 202 wpm respectively. In comparison to the same construction of text design, that is, the contextual sentence, the MNread, Radner, IReST and UiTM-Mrw gave approximately similar outcome of MRS. The MRS was found to be 215 wpm in MNread (Legge et al., 1985), 211 wpm for Radner (Radner et al., 1998), 228 wpm for English IReST (Trauzettel-Klosinski & Dietz, 2012) and 200 wpm for UiTM-Mrw (Buari et al., 2014). Similar finding might be due to similar text choices, that is, contextual sentence. The construction of designs of BCMRC and UiTM-Mrw are different in the number of lines per print size despite using the same Malay language. UiTM-Mrw has varied number of lines. There are two lines of sentence for six print sizes (1.4LogMAR to 0.8LogMAR) and single line for the rest of the print sizes. In comparison, BCMRC has two lines for every print size available in the set. The varied number of lines in UiTM-Mrw is because it has varied number of words, that is, maximum of 10 words and minimum of six words for

some of the print sizes. Standardisation has been made in BCMRC as in other established English reading charts (Mansf eld et al., 1993; Radner et al., 1998) where a similar number word for every print size is chosen.

The random word sets of BCMRC also show no signif cant difference in MRS between RW1 and RW2. The sets are in agreement and have good intra-class correlation coeff cient. The random words set available reading charts are the Bailey-Lovie (Bailey & Lovie, 1980), PNAC (Wolffsohn & Cochrane, 2000), UiTM-Muw (Buari et al., 2015), VSRT (Watson et al., 2010) and RRT (Wilkins et al., 1996). Among the published random words reading charts, only Bailey-Lovie, VSRT and RRT have more than one set. The Bailey-Lovie is among the pioneer random words set of progressive log-scale reading chart that is designed in f ve sets. The comparison between sets is not published elsewhere, but the features have been described in a previous study (Bailey & Lovie, 1980). The VSRT has three sets, which contain f ve print sizes from 4M to 1M. The VSRT is a combination of single letter, short word (two to three letters per word) and compound words for every print sizes (Watson et al., 2010). The RRT has two sets with the highest number of words, which is, 150 words in comparison with other types of charts. It is a non-progressive logarithmic random words chart that contains single print size. The correlation coeff cient is good between these 2 sets (r=0.83) (Wilkins et al., 1996). As comparison in our random words sets of BCMRC, it is designed as a progressive logarithmic chart from largest print size to the near acuity threshold print size. The BCMRC in this study controlled the number of words and the number of lines to make it similar between every print size. The outcome of MRS by RW1 and RW2 of BCMRC were 156 WPM and 147 wpm respectively. These outcomes are a bit higher than RRT as they found the reading speed of 99 wpm (Wilkins et al., 1996). The differences might be due to different sample size, which this study investigated among normally sighted young adults, but Wilkins et al. (1996) tested the RRT among school children of grade 4 to 6. The reading speed of children was proven to be lower than young adults. Furthermore, BCMRC was is short sentence reading chart while the RRT is a long passage reading chart. The reading speed for random words was found to be within 69 to 135 wpm among Malay native speakers (Buari et al., 2015; Omar & Mohammed, 2005).

Having more than one chart would be an advantage to minimise the learning effect during repeated measurements. However, both charts should offer similar outcomes, thus, the evaluation of reading speed is reliable.

External Comparison of BCMRC

The MRS of BCMRC was compared with the standardised English version of reading charts. Each contextual sentence and random words set of BCMRC was selected in this external comparison. The contextual sentence of BCMRC was compared with contextual sentence reading chart (MNread). The BCMRC had a good reliability and agreed with MNread. The random words of BCMRC was also reliable and was in agreement with Bailey-Lovie. A comparison between newly developed reading charts with published reading charts was done in several previous studies (Buari et al., 2015; Buari et al., 2014; Wolffsohn & Cochrane, 2000). The limits of the agreement were calculated based on d± 1.96s, whereby, d was the

mean difference and s was the standard deviation of the mean difference. From the calculation, the limits of the agreement were between 1.96 of ±26.38 wpm and ±17.43 wpm for contextual sentence set and random words set respectively. Previous study recommended calculating the CI of both limits of agreement, as the limit was only estimation (McAlinden et al., 2011). When the limit is wide, it may be due to small sample size (McAlinden et al., 2015). The conf dent interval for mean difference, lower limit of agreement and upper limit of agreement indicated a possible error in estimation (Giavarina, 2015). However, 95% of conf dence interval that was calculated from standard error and t value for degree of freedom was found to be ±17.01 wpm for contextual sentence set and ±11.24 wpm for random word set in the study. Inter-chart comparison of MNread for young adults and low vision patient showed the mean difference of 8.6 wpm and 2 wpm respectively (Patel et al., 2011; Subramanian & Pardhan, 2006). Both studies did not mention the 95% of CI for upper and lower limits of agreement. However, it was stated that when the bias falls within the limit of the agreement, then a good agreement is achieved (Subramanian & Pardhan, 2006). Other studies that measured the agreement between two charts showed the limits of agreement ranged between -46.5 wpm to 58.3 wpm (Buari et al., 2014). The agreement of 3 Radner charts were ranged between -16.11 wpm to 32.17 wpm (Stifter et al., 2004). Although the mean difference is not zero, the 95% conf dence interval contains zero, thus no practice effect exists.

The PNAC was compared with Bailey-Lovie (Wolffsohn & Cochrane, 2000), the UiTM-Mrw and UiTM-Muw were compared with MNread and Colenbrander reading chart (Buari et al., 2015; Buari et al., 2014). The PNAC was found to be highly correlated with Bailey-Lovie. However, the time to measure the near acuity was found faster with PNAC as compared with Bailey-Lovie. This might be because PNAC employs short words which contain three words per print size. In comparison, Bailey-Lovie, comprises two words (1.6 LogMAR to 1.4LogMAR), three words (1.3LogMAR to 1.1LogMAR) and six words (1.0LogMAR toward 0.00LogMAR) (Bailey & Lovie, 1980). The UiTM-Mrw was found to be comparable and highly agreeable with MNread and Colenbrander because all tested charts use contextual sentence reading charts.

The reading speed of UiTM-Mrw differ and have weak agreement with MNread and also Colenbrander (Buari et al., 2015). The differences in reading speed could be due to different text construction; the UiTM-Mrw is designed with low syntactic and semantic cues, but both MNread and Colenbrander use contextual sentences. Comparing the reading speed between the contextual sentences and random words reading chart might give different outcomes of the reading speed. A different brain processing image pattern is shown in reading poor lexico-semantic f t words in both strong and weak constraint sentences (Hoeks et al., 2004). The message-level and lexico-semantic information is the main component of the reading process to understand the meaning of sentences that may lead to an increase in the reading time and comprehension. Increased reading time might be due to the increase of preview duration that happen in low contextual constraints of target words (Li et al., 2017).

External comparison of the newly developed and established reading chart might give an overview of design and its application in relation to established reading charts. It might be benef cial to have a standardised and good construction of reading chart with the language that can be used among the native speakers of that language. The f uency of reading with different languages might be biased in the evaluation of the reading speed. Several established reading

charts have also been constructed with different languages to serve patients with different preferable speaking or reading language.

In conclusion, the Buari-Chen Malay reading charts display good internal and external comparisons and is recommended for the clinical evaluation of reading performance for Malay language native speakers.

ACKNOWLEDGEMENTS

REFERENCES

Ahn, S. J., Legge, G. E., & Luebker, A. (1995). Printed cards for measuring low-vision reading speed. *Vision Research, 35*(13), 1939–1944.

Alió, J. L., Radner, W., Plaza-Puche, A. B., Ortiz, D., Neipp, M. C., Quiles, M. J., & Rodríguez-Marín, J. (2008). Design of short Spanish sentences for measuring reading performance: Radner-Vissum test. *Journal of Cataract and Refractive Surgery, 34*(4), 638-642.

Bailey, I. L. (2006). Visual acuity. In W. J. Benjamin & I. M. Borish (Eds.), *Borish's clinical refraction* (2nd Edition) pp. 217–246. Saint Louis: Butterworth-Heinemann. Retrieved from http://dx.doi.org/ http://dx.doi.org/10.1016/B978-0-7506-7524-6.50012-0

Bailey, I. L., & Lovie, J. E. (1980). The design and use of a new near-vision chart. *American Journal of Optometry and Physiological Optics, 57*(6), 378–387. Retrieved from http://europepmc.org/abstract/ MED/7406006

Bland, J. M., & Altman, D. G. (1986). Statistical methods for assessing agreement between two methods of clinical measurement. *Lancet, 1*(8476), 307–10.

Bland, J. M., & Altman, D. G. (1995). Comparing two methods of clinical measurement: A personal history. *International Journal of Epidemiology, 24*(Supplement 1), S7–S14.

Buari, N. H., Azizan, M. F., & Chen, A.-H. (2015). Comparison of reading speed using Malay unrelated word reading chart with standardised English reading charts. *International Journal of Medical and Health Sciences Research, 2*(3), 55–61.

Buari, N. H., Chen, A.-H., & Musa, N. (2014). Comparison of reading speed with 3 different log-scaled reading charts. *Journal of Optometry, 7*(4), 210–216.

Buari, N. H., Yusof, N. H., Mohd-Satali, A., & Chen, A. H. (2014). Repeatability of the Universiti Teknologi MARA reading charts. *Bangladesh Journal of Medical Science, 14*(3), 236-240. Retrieved from http://dx.doi.org/10.1111/j.1463-1326.2011.01375.x

Burggraaff, M. C., van Nispen, R. M. A., Hoek, S., Knol, D. L., & van Rens, G. H. M. B. (2010). Feasibility of the Radner Reading Charts in low-vision patients. *Graefe's Archive for Clinical and Experimental Ophthalmology, 248*, 1631–1637.

Calossi, A., Boccardo, L., Fossetti, A., & Radner, W. (2014). Design of short Italian sentences to assess near vision performance. *Journal of Optometry, 7*(4), 203–9. Retrieved from http://dx.doi.org/10.1016/j.optom.2014.05.001

Castro, C., Kallie, C., & Salomao, S. (2005). Development and validation of the MNREAD reading acuity chart in Portuguese. *Brazilian Archives of Ophthalmology, 68*(6), 777–783.

Colenbrander, A. (2001). Measuring vision and vision loss. In T. D. Duane, W. Tasman, & E. A. Jaeger (Eds.), *Duane's Clinical Ophthalmology* (Revised, Vol. 5, pp. 1–42). Philadelphia: Lippincott Williams & Wilkins.

Gliem, J. A., & Gliem, R. R. (2003). Calculating , interpreting , and reporting Cronbach's Alpha reliability coeff cient for Likert-type scales. In *Midwest Research-to-Practice Conference in Adult, Continuing, and Community Education* (pp. 82–88). The Ohio State University, Columbus.

Hahn, G. A., Penka, D., Gehrlich, C., Messias, A., Weismann, M., Hyvärinen, L., ... & Vital-Durand, F. (2006). New standardised texts for assessing reading performance in four European languages. *British Journal of Ophthalmology, 90*(4), 480-484.

Hoeks, J. C. J., Stowe, L. A., & Doedens, G. (2004). Seeing words in context: The interaction of lexical and sentence level information during reading. Brain Research. *Cognitive Brain Research, 19*(1), 59–73. Retrieved from http://dx.doi.org/10.1016/j.cogbrainres.2003.10.022

 d l, . A., Çali kan, D., d l, N. B., dil, . A., Çaliskan, D., & dil, N. B. (2011). Development and validation of the Turkish version of the MNREAD visual acuity charts. *Turk J Med Sci, 41*(4), 565–570. Retrieved from http://dx.doi.org/10.3906/sag-1008-1

Jufri, S., Buari, N. H., & Chen, A. H. (2016). Text structures affect reading speed. *Social and Management Research Journal, 13*(1), 117–127.

Kottner, J., Audigé, L., Brorson, S., Donner, A., Gajewski, B. J., Hróbjartsson, A., ... & Streiner, D. L. (2011). Guidelines for reporting reliability and agreement studies (GRRAS) were proposed. *Journal of Clinical Epidemiology, 64*(1), 96–106.

Legge, G. E., Pelli, D. G., Rubin, G. S., & Schleske, M. M. (1985). Psychophysics of reading--I. Normal vision. *Vision Research, 25*(2), 239–252.

Legge, G. E., Ross, J. A., Luebker, A., & LaMay, J. M. (1989). Psychophysics of reading. VIII. The Minnesota low-vision reading test. *Optom Vis Sci, 66*(12), 843–853.

Legge, G. E., Rubin, G. S., Pelli, D. G., & Schleske, M. M. (1985). Psychophysics of reading—II. Low vision. *Vision Research, 25*(2), 253–265.

Li, N., Wang, S., Mo, L., & Kliegl, R. (2017). Contextual constraint and preview time modulate the semantic preview effect: Evidence from Chinese sentence reading. *The Quarterly Journal of Experimental Psychology*, 1–32. Retrieved from http://dx.doi.org/10.1080/17470218.2017.1310914

Lüdtke, J., & Kaup, B. (2006). Context effects when reading negative and aff rmative sentences. In *Proceedings of the 28th Annual Conference of the Cognitive Science* (Vol. 29, pp. 1735–1740). City, State: Publisher.

Maaijwee, K., Mulder, P., Radner, W., Van Meurs, J. A. N. C., & Meurs, J. C. (2008). Reliability testing of the Dutch version of the Radner Reading Charts. *Optometry and Vision Science, 85*(5), 353–358.

Mansf eld, J. S., Ahn, S. J., Legge, G. E., & Luebker, A. (1993). A new reading-acuity chart for normal and low vision. *Ophthalmic and Visual Optics/Noninvasive Assessment of the Visual System Technical Digest, 3*, 232–235.

Mansf eld, J. S., Legge, G. E., & Bane, M. C. (1996). Psychophysics of reading. XV: Font effects in normal and low vision. *Investigative Ophthalmology and Visual Science, 37*(8), 1492–1501. Retrieved from http://www.ncbi.nlm.nih.gov/pubmed/8675391

Mataftsi, A., Bourtoulamaiou, A., Haidich, A. B., Antoniadis, A., Kilintzis, V., Tsinopoulos, I. T., & Dimitrakos, S. (2013). Development and validation of the Greek version of the MNREAD acuity chart. *Clinical and Experimental Optometry, 96*(1), 25-31.

Omar, R., & Mohammed, Z. (2005). Relationship between vision and reading performance among low vision students. *International Congress Series, 1282*, 679–683. Retrieved from http://dx.doi.org/10.1016/j.ics.2005.05.063

Radner, W., Willinger, U., Obermayer, W., Mudrich, C., Velikay-Parel, M., & Eisenwort, B. (1998). A new reading chart for simultaneous determination of reading vision and reading speed. *Klinische Monatsblatter fur Augenheilkunde, 213*(3), 174–181. Retrieved from http://europepmc.org/abstract/MED/9793916

Sedgwick, P. (2013). Limits of agreement (Bland-Altman method). BMJ: *British Medical Journal (Online)*, 346.

Spinelli, D., De Luca, M., Judica, A., & Zoccolotti, P. (2002). Crowding effects on word identif cation in developmental dyslexia. *Cortex, 38*(2), 179–200. Retrieved from http://dx.doi.org/http://dx.doi.org/10.1016/S0010-9452(08)70649-X

Stifter, E., König, F., Lang, T., Bauer, P., Richter-Müksch, S., Velikay-Parel, M., & Radner, W. (2004). Reliability of a standardized reading chart system: variance component analysis, test-retest and inter-chart reliability. *Graefe's Archive for Clinical and Experimental Ophthalmology, 242*(1), 31-39. Retrieved from http://dx.doi.org/10.1007/s00417-003-0776-8

Subramanian, A., & Pardhan, S. (2006). The repeatability of MNREAD acuity charts and variability at different test distance. *Optom and Vision Science, 83*(8), 572–576.

Subramanian, A., & Pardhan, S. (2009). Repeatability of reading ability indices in subjects with impaired vision. Investigative *Ophthalmology and Visual Science, 50*(8), 3643–7.

Trauzettel-Klosinski, S., & Dietz, K. (2012). Standardized assessment of reading performance: The new international reading speed texts IReST. *Investigative Ophthalmology and Visual Science, 53*(9), 5452–5461. http://dx.doi.org/10.1167/iovs.11-8284

Van Petten, C., & Kutas, M. (1990). Interactions between sentence context and word frequency in event-related brain potentials. *Memory and Cognition, 18*(4), 380–93. Retrieved from http://www.ncbi.nlm.nih.gov/pubmed/2381317

Virgili, G., Cordaro, C., Bigoni, A., Crovato, S., Cecchini, P., & Menchini, U. (2004). Reading acuity in children: evaluation and reliability using MNREAD charts. *Investigative Ophthalmology and Visual Science, 45*(9), 3349–3354. Retrieved from http://dx.doi.org/10.1167/iovs.03-1304

Watson, G. R., Whittaker, S., & Steciw, M. (2010). *Visual skills for reading test.* (G. R. Watson, M. E. Flax, & O. M. Weisser-Pike (Eds.) (10th ed.). Madison: Fork in the Road Vision Rehabilitation Services LLC.

Wilkins, A. J., Jeanes, R. J., Pumfrey, P. D., & Laskier, M. (1996). Rate of reading test: Its reliability, and its validity in the assessment of the effects of coloured overlays. *Ophthalmic and Physiological Optics, 16*(6), 491–497.

Wolffsohn, J. S., & Cochrane, A. L. (2000). The practical near acuity chart (PNAC) and prediction of visual ability at near1. *Ophthalmic and Physiological Optics, 20*(2), 90–97.

Colour Discrimination Ability under Fluorescent and Light Emitting Diode

Ai-Hong Chen*, Fazrin Mazlan and Saiful-Azlan Rosli

Optometry, Faculty of Health Sciences, Universiti Teknologi MARA (UiTM), 42300 Puncak Alam, Selangor Malaysia

ABSTRACT

This article aims to quantify the colour discrimination ability by using Total error scores (TES) to categorise colour discrimination level into superior, average or inferior levels under three different types of light sources, with different spectral power distribution. Colour discrimination was investigated using Farnsworth-Munsell 100 hues and compared upon three light sources: compact f uorescent light (CFL), f uorescent light (FL) and light emitting diode (LED). Total error score calculated and pattern of colour caps misplacement plotted used the web-based scoring method (http://www.torok.info/colorvision/fm100.htm). Total error score (TES) for three types of light sources (TES for LED 58.00 ± 18.67, FL 80.00 ± 19.27 and CFL 127.25 ± 28.02) were signif cantly different [One-way ANOVA (F=9.98, P<0.05)]. Tukey post hoc analysis showed that there was signif cant difference between compact f uorescent light & f uorescent light, and between compact f uorescent light & light emitting diodes. Variation of the mid-point cap was smaller for both types of f uorescent lights but higher under light emitting diodes. Fluorescent light and light emitting diode with 4000K correlated colour temperature showed average colour discrimination with mean total error score range between 20 to 100, while compact f uorescent light showed inferior colour discrimination with mean total error score of more than 100. Different light sources with different spectral power distributions affected the colour discrimination differently. This cross-over study design using the same subjects, the same testing tool and the same examiner suggested that subject responded differently towards f uorescent light and light emitting diode light source in the total error score of the Farnsworth-Munsell 100 hues.

Keywords: Colour discrimination, Farnsworth-Munsell 100 hues, f uorescent, light emitting diode, light source

INTRODUCTION

An important aspect of lighting design is obligatory to minimise the amount of

electricity consumed, for both f nancial and environmental reasons (Bridger, 2003). The vast growing innovation and technology today emphasises lighting that enhances the productivity of task performance and cost eff ciency. Light emitting diodes (LED) light has gradually substituted the conventional f uorescent light (FL) for its cost eff ciency and longer lifespan, but its visual impact remains inconclusive. Due to the close link between lighting and visual ergonomic, a comprehensive strategy for lighting design is essential to protect signif cant benef ts, money and human resources (SLL CIBSE, 2009). Despite the variation in lighting application under different circumstances such as industrial, off ce, hospital, and retail settings, all share three similar objectives in different situations including to facilitate quick and accurate work, to contribute to the safety of those doing the work and to create a comfortable visual environment (The Society of Light and Lighting, 2012). Retail lighting emphasises a balance between general lighting, accent lighting and display lighting to convey the important business message to consumers if the business aims for budget or highly exclusive customers. Lighting for industry depends on the nature of visual information required to undertake work in different industries (Faulkner & Murphy, 1973). Similarly, lighting in the hospital is also functional based (Dalke et al., 2006). The most important function is to meet the task requirements in each area of the hospital. Some of the tasks require high levels of visual performance for the safety of patients. Light can inf uence human emotions and feelings of well-being. Appropriate lighting in the hospital can increase harmony and competency within the hospital (SLL CIBSE, 2009).

The effect of lightings on colour perception is undisputable. Illuminants A, B, and C were introduced in 1931 by the International Commission on Illumination (CIE), with the intention of respectively representing average incandescent light, direct sunlight, and average daylight (Schanda, 2015). Illuminant D represents phases of daylight, Illuminant E is the equal-energy Illuminant, while Illuminants F represents f uorescent lamps of various compositions. Daylight illumination or Illuminant C is recommended for all colour vision tests. The replacement of LED light source from the conventional light source may have an impact on the quality of life (Ryckaert, Smet, Roelandts, Van Gils, & Hanselaer, 2012). Light source plays an important role in colour discrimination ability, performance and comfort (Boyce & Simons, 1977). Due to its broad spectral characteristics, natural daylight can be used in any visual tasks that need precise colour discrimination ability (Birch, 2001).

The aim of the study was to compare the effect of three types of light with different spectral power distribution (SPD) on colour discrimination. The Farnsworth-Munsell 100 hue test (F-M 100 Hue) was originally designed to test hue discrimination among people with normal colour vision and to measure the areas of colour confusion in colour-defective observers (Farnsworth, 1957). Caps for the centre of confusion zones were used to characterise the major axis of congenital colour defects (Farnsworth, 1943, 1957; Verriest, 1963). The F-M 100-hue test is a chromatic discrimination where the total error score is correlated with the matching range on the anomaloscope and with the wavelength discrimination function a test of the wavelength difference is needed for an observer to detect colour difference (Lakowski, 1971). The F-M 100-hue test was not designed for the screening of colour defect (Birch, 2001). Error scores
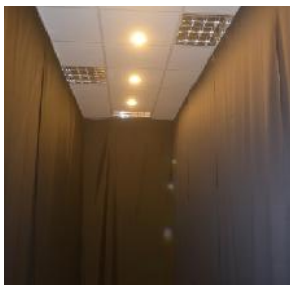
for normal observers should be classif ed only in three categories (superior, average, and inferior) (Farnsworth, 1957) and can be compared to population statistics (Aspinall, 1974; Kinnear, 1970). A change in score is signif cant at 0.05 level if the difference of the square roots exceeds 2.27 and at 0.01 level, if the difference exceeds 2.99 (Aspinall, 1974). Therefore, F-M 100-hue test was used in our study to quantify the colour discrimination ability by using error scores to categorise the colour perception as superior, average or inferior level under three different lightings.

MATERIALS AND METHOD

The study was carried out in a windowless $6.0 \times 4.5 \times 3.0$ m room dimension at Optometry and Visual Science Research Centre (iROViS) UiTM Selangor, Malaysia. The room was separated into three partitions using black coloured curtains, as in Figure 1, to minimise the interference from the surrounding surface colour. Due to the wavelength absorption properties of black that might result in dimmer surroundings, the researchers ensured the level of light was maintained within the range of illumination recommended for libraries and residential reading (Schwartz, 2010). Black curtain helped to reduce the surface ref ectance to minimise glaring effect. Each partition was installed with different light source: partition 1 had compact f uorescent light (CFL), partition 2 had tubular f uorescent light (FL), and partition 3 was installed with tubular light emitting diode (LED). The characteristics of these light sources are shown in Table 1. Each light source was measured for their illumination and spectral power distribution (SPD) using Lutron LX 101-A and Konica Minolta CL-500A respectively. Illuminance meter (Lutron LX 101-A) and illuminance spectrophotometer (Konica Minolta CL-500A) were positioned in the middle of the working plane which was 2.33 m from the light source. Three readings were taken and averaged from each light source illumination. Meanwhile, the illuminance spectrophotometer (Konica Minolta CL-500A) was connected to a personal laptop. The spectral power distribution graph was automatically tabulated using Konica Minolta CL-S10w software once the readings were taken. FL sources showed similar SPD pattern compared to LED, but the peak wavelengths were different. Correlated colour temperature (CCT) was one of the characteristics of light. CFL was categorised as warm white (2927K). Both FL and LED were grouped as natural white (4000K). The spectral power distribution (SPD) pattern for both CFL and FL peaked at three dominant wavelengths, while LED displayed two dominant wavelengths. Fluorescent lights recorded three highest peaks at 544, 611 and 436 nm, in sequence, respectively, with the spiked bandwidth around 434 to 444 nm, 531 to 558 nm and 603 to 634 nm. For the LED, there were two broad wavelength peaks, 595 and 451 nm, with the broader bandwidth around 431 to 468 nm and 488 to 726 nm as in Figure 2.

Table 1
Summary of the three light source characteristics

Light source	Compact fuorescent light (CFL)	Fluorescent light (FL)	Light emitting diode (LED)
Brand	SYLVANIA	SYLVANIA	GE
Model	E27	T8 4FT Fluorescent	T8 4FT LED
Watt	25W	36W	16W
Correlated colour temperature (CCT)	2927K	4000K	4000K
Colour Rendering Index (CRI)	80	82	84
Peak wave-length	512.0 nm	545.0 nm	577.5 nm
Illumination	220 Lux	440 Lux	319 Lux

(a) Compact fuorescent light (CFL)

(b) Fluorescent light (FL)

(c) Light emitting diodes (LED)

Figure 1. Three Types of Lighting Set Up in the Experimental room: (a) Compact fuorescent light (2927K); (b) Fluorescent light (4000K); and (c) Light emitting diode (4000K)
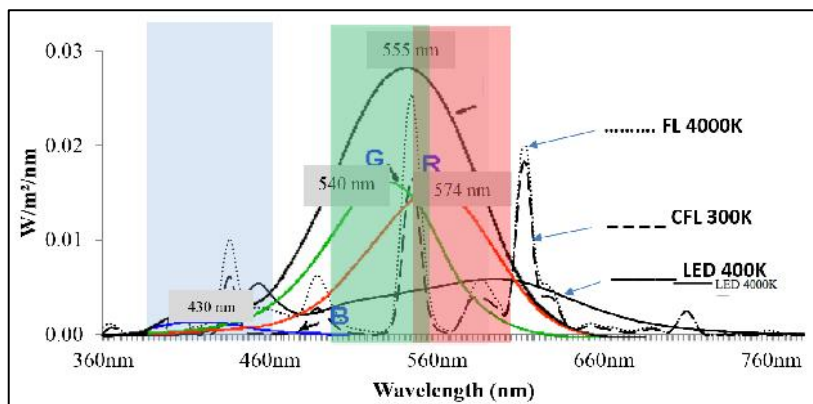

Figure 2. Spectral power distribution of three light sources: 3000K compact fuorescent light (CFL), 4000K fuorescent light (FL) and 4000K light emitting diodes (LED)

These light sources were embedded with relative human spectral sensitivity on cone (555 nm), blue (430 nm), green (540 nm) and red photoreceptor (575 nm) sensitivity. Blue tint area was for blue sensitivity, green tint area was for green sensitivity, red tint area was for red sensitivity, and green and red for photopic sensitivity (Adapted from (Mann, 2011).

Ethical approval was obtained (reference number 600-FSK(PT5/2) from the UiTM ethical committee. To quantify the colour discrimination ability using the different light source, four subjects with mean age of 28±2.27 years were recruited. A preliminary assessment was conducted to ensure that the subject met the selection criteria (age range of 19 to 38 years old, with distance and near visual acuity of 6/6 or better, no known ocular disease and colour vision defect). D-15 colour vision screening was used to rule out any colour def ciency. Informed consent was obtained before participation. Each subject was exposed to three lighting conditions in one visit and f ve minutes of dark and light adaptation were allocated in between lighting conditions. In order to stabilise the rod and cones photoreceptor sensitivity from previous lighting, light adaptations denoted the wash off period in between the tests. These were evidenced in previous studies that applied at least f ve to 10 minutes of light adaptation or resting. Bernecker, Davis, Webster, and Webster (1993) tested the effects of several task lighting on visual comfort and f ve minutes of resting was allocated. Boyce, Akashi, Hunter, and Bullough (2003) allocated 10 minutes of adaptation in their study on the effect of four lighting conditions near visual acuity. Five minutes of adaptation was allocated by Berman, Navvab, Martin, Sheedy and Tithof (2006) in their investigation on near visual acuity under three lighting conditions. Zahiruddin, Banu, Dharmarajan and Kulothungan (2010) also examined the effect of two lighting illumination on colour vision with f ve to 10 minutes of resting in between the test. Thus, the 10 minutes total of lighting adaptation should be suff cient as wash out period for eye sensitivity to stabilise and at the same time providing time for subject to rest. The testing procedure began with f ve minutes of dark adaptation and followed by f ve minutes of light adaptation, before the administration of F-M 100 Hue, as the washing period. Colour discrimination was tested at different light source using F-M 100Hue at random sequence. F-M 100 Hue consists of 85 movable colour testers with a diameter of 1.2 cm arranged in a sequential hue in four boxes of 21 or 22 colours each. The testers were chosen to represent perceptually equal steps of hue and to form a natural hue circle. The colours were set in plastic caps and subtend 1.5° at 50 cm. They were numbered on the back according to the correct colour order of the hue circle. Two referenced colours were f xed at either end of each box. The results obtained were recorded and the total error score (TES) colour cap misplacements were calculated and plotted in F-M 100 Hue online software (http://www.torok.info/colorvision/fm100.htm). The number of colour caps were arranged in sequential circular form in the middle of the recording sheet, as in Figure 3, while middle six colours (red, yellow, green, cyan, blue and purple) were the colour transitions between colour caps. Each line indicated the colour caps wavelength, written outside the recording sheet in nanometres (nm). The dotted lines showed three distinct main rings that classif ed the colour discrimination scoring - the further the pattern away from the middle ring (higher spikes) showed lower discrimination ability. The graphic representation of colour vision defect f ndings for protanomaly, deuteranomaly and tritanomaly were also illustrated in Figure 2. The mid-points colour caps range for protanomaly, deuteranomaly, and tritanomaly were 62-70, 56-61,

and 46-52 respectively (Farnsworth, 1957). Each type of colour defect showed a similar trend of colour cap confusion arrangement according to the mid-point, an arrow represented in the circle. The TES pattern was interpreted and analysed to determine which light source showed more superior colour discrimination ability, average or inferior discrimination ability. The total duration required for each subject was approximately 50 minutes. SPSS Version 21.0 software was used to analyse all the descriptive and comparison data.
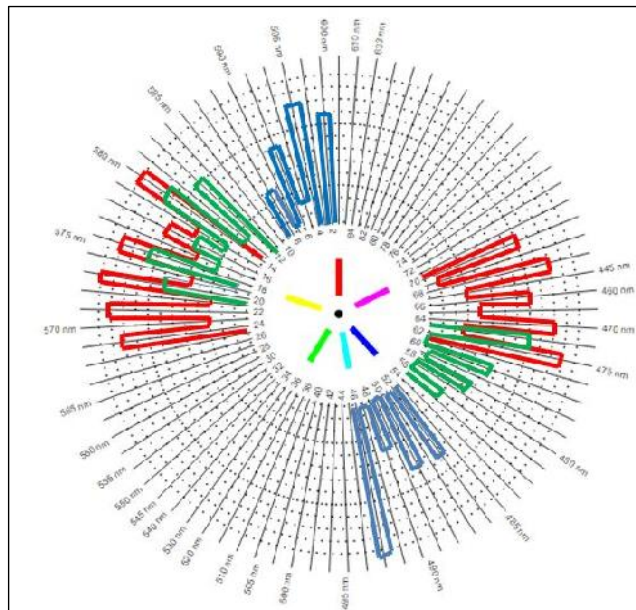

Figure 3. Graphical interpretation of colour def ciency conditions

Protanomaly is represented by red line, deuteranomaly is represented by green line, while tritanomaly is represented by blue line.

RESULTS

One-way ANOVA revealed a signif cant difference in the total error score for three different light types [F (2, 9) = 9.98, p<0.05)]. LED demonstrated the best total error score 58.00 ± 18.67, followed by FL with 80.00 ± 19.27 TES. CFL showed the worst TES (127.25 ± 28.02). Tukey post hoc analysis revealed signif cant mean differences of TES between CFL and LED [(69.25 TES), 95% CI (25.30 to 113.470)] and between CFL and FL [(47.25 TES), 95% CI (3.03 to 91.47)]. The trend of mid-point colour caps was found to be different between FL and LED. Mid-point position was related to the type of colour defect. No major axis of congenital colour defects was detected that mimicked the pattern of protanomaly, deuteranomaly and tritanomaly. Even though there was no specif c colour def cient pattern, the trend of colour caps confusion variation was similar in CFL and FL, but different in LED. The variation of the mid-point cap was higher for both types of f uorescent lights [colour cap in of F-M 100 hues ranged from 29 to 34 (500 nm-574 nm)]. More square opaque was found in Figure 4(a)

and 4(b). High calculated TES represented more colour confusion. Lower variation was found among the same subjects under LED [colour cap ranged from 8 to 76 [(400-499nm) & (573-634nm)], with less square opaque as in Figure 4(c). Low calculated TES represented least colour confusion. A normal colour vision perception may differentiate between primary colours (red, green, and blue) but individual colour discrimination may vary at different saturation, as in Figure 5. Thus, the range of variation in the mid-point caps at different light source may predict the pattern of colour confusion among normal.
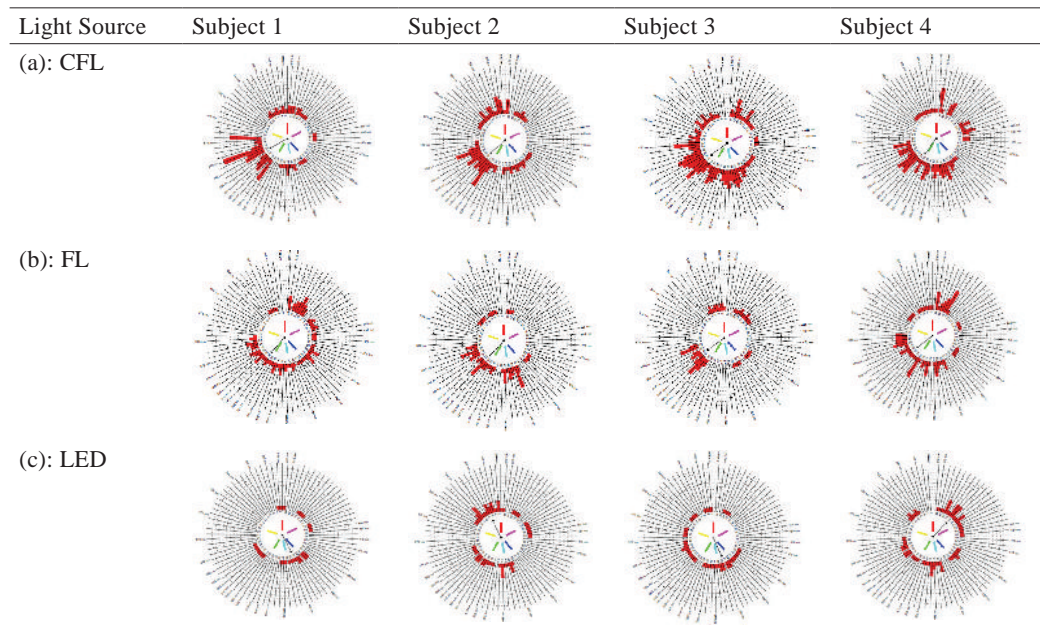
Light Source	Subject 1	Subject 2	Subject 3	Subject 4
(a): CFL				
(b): FL				
(c): LED				

Figure 4. Graphical interpretation of colour vision using: (a) Compact f uorescent light (CFL); (b) Fluorescent light (FL); and (c) Light emitting diodes (LED) (http://www.torok.info/colorvision/fm100.htm)
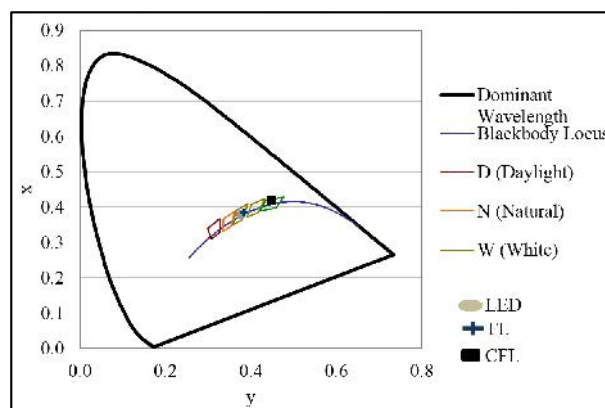

Figure 5. Chromaticity coordinates of compact f uorescent light (CFL), f uorescent light (FL), and light emitting diodes (LED)

The f gure above was plotted according to the 1931 CIE Chromaticity Diagram. Each coloured box was classif ed according to the light source correlated colour temperature of daylight (red), natural (orange), white (light green) and warm white (green).

DISCUSSIONS

The eye can discriminate several wavelengths for its adjustment towards photopic, mesopic and scotopic, which is controlled by photoreceptors cones and rods (Taylor, 2000). Cones actively respond to colour because they receive three types of photoreceptor cone cells and have high-resolution ability. It is 564 nm for red, 533 nm for green and 437 nm for blue and have the highest sensitivity towards the wavelength (Wyszecki & Stiles, 1982). These three distinct values are called tristimulus values which are def ned by the CIE 1931 colour space, in which they are denoted X, Y, and Z (Schanda, 2007). This trichromacy is reported to provide an accurate description of surface colour, which ref ect under most lighting conditions, through non-opponent achromatic system and two opponent chromatic systems in human colour vision physiology (Lennie & D'Zmura, 1987). It is considered metameric since an endless assortment of potential SPD in the scene can produce the same colour response in the three integrated channels (Fairchild et al., 2001). Humans seem to distinguish colour differently under dissimilar lighting conditions. This study used the perceived, matched and arranged performance in F-M 100 hues to investigate the cone sensitivity performance in relation to different SPD and CCT. It was found that LED gave higher metamerism effect (less TES and less variation in mid-point caps), in which the nature of spectrum was wider within shorter to longer wavelength compared to FL and CFL. Colour confusion occurred mostly on the green to yellow range for both f uorescent lights in the study. One possible explanation is the SPD difference as difference in peak and bandwidth wavelength may cast different metamerism effect on colour discrimination performance. A previous study shared similar f nding, where structured SPDs successfully increased gamut area or TES (Royer, Houser, & Wilkerson, 2012).

The subjects' mood, time to complete F-M 100 hues and cognitive task performance were previously reported to improve with increasing CCT without any signif cant differences found in TES between FL and LED (Hawes, Brunyé, Mahoney, Sullivan, & Aall, 2012). Similarly visual comfort, task performance and alertness were also reported to increase under daylight (CCT 6500K) (Shamsul, Sia, Ng, & Karmegan, 2013), while reduction in pupil size was found to lessen the chromatic aberration effect that might lead to enhanced colour discrimination (Berman et al., 1987). The contribution of shorter wavelength also amplif ed with increasing CCT compared to longer wavelength due to changes of SPD (Fotios, 2001). A study compared colour discrimination between f uorescent and LED with a range of CCT of 2618K to 2715K. The colour discrimination was reported to deteriorate under LED compared to f uorescent lighting (Royer et al., 2012). Lower total errors were found in colour discrimination for LED compared to FL and CFL in this study. The discrepancy may suggest a complex interaction between SPD and CCT when the characteristics of light shift from natural white to warm white. The f nding implies that the effect of SPD pattern may over-ride the effect of CCT on colour discrimination task. However, this speculation requires further investigation to explore the interaction between SPD and CCT.

The relationship between lights (different SPD & CCT) and colour discrimination ability is important in our daily life. Fewer high-pressure sodium lamps than deluxe f uorescent lamps are installed in department stores for commodity lighting, mainly because the commodities under illumination from high-pressure sodium usually appear in dull yellow shades while the same commodities under deluxe f uorescent, at the same light level, display variation of colours. Consumer preference is prioritised instead of function accuracy (Xu, 2012) and some public areas require excellent colour discrimination. The characteristic of the light source should at least have high colour discrimination index of 80 and above to perceive actual colour, which also applies to textile premises (textile material should render the same colour as they render under the reference light) and hospital (risk of fault among medical practitioners and nurses in performing delicate colour discrimination task) (Boyce, 2014).

CONCLUSION

Different light spectrum result in different colour discrimination ability using F-M 100 Hue. The value of F-M 100 Hues to quantify the colour discrimination ability for lighting application as well as the possible complex interaction between SPD and CCT should be explored further.

ACKNOWLEDGEMENTS

REFERENCES

Aspinall, P. A. (1974). Inter-eye comparison on the 100 hue test. *Acta Ophthalmologica, 52*(3), 307–316. Retrieved from http://dx.doi.org/10.1111/j.1755-3768.1974.tb00382.x

Berman, S., Navvab, M., Martin, M. J., Sheedy, J., & Tithof, W. (2006). A comparison of traditional and high colour temperature lighting on the near acuity of elementary school children. *Lighting Research and Technology, 1*(38), 41–52.

Berman, S. M., Jewett, D. L., Bingham, L. R., Nahass, R. M., Perry, F., & Fein, G. (1987). Pupillary size differences under incandescent and high pressure sodium lamps. *Journal of the Illuminating Engineering Society, 16*(1), 3–20.

Bernecker, C. A., Davis, R. G., Webster, M. P., & Webster, J. P. (1993). Task lighting in the open off ce: A visual comfort perspective. *Journal of the Illuminating Engineering Society, 22*(1), 18–25. Retrieved from http://dx.doi.org/10.1080/00994480.1993.10748013

Birch, J. (2001). *Diagnosis of defective color vision* (2nd edition). London: Butterworth Heinemann.

Boyce, P., Akashi, Y., Hunter, C., & Bullough, J. (2003). The impact of spectral power distribution on the performance of an achromatic visual task. *Lighting Research and Technology, 35*(2), 141–161. Retrieved from http://dx.doi.org/10.1191/1477153503li075oa

Boyce, P. R. (2014). *Human factors in lighting* (3rd edition). CRC Press.

Boyce, P. R., & Simons, R. H. (1977). Hue discrimination and light sources. *Lighting Research and Technology, 9*(3), 125–140.

Bridger, R. S. (2003). *Introduction to ergonomics* (2nd edition). London and New York: Taylor and Francis. Retrieved from http://dx.doi.org/10.4324/9780203426135

Dalke, H., Little, J., Niemann, E., Camgoz, N., Steadman, G., Hill, S., & Stott, L. (2006). Colour and lighting in hospital design. *Optics and Laser Technology, 38*(4-6), 343-365. Retrieved from http://dx.doi.org/10.1016/j.optlastec.2005.06.040

Fairchild, M. D., Rosen, M. R., & Johnson, G. M. (2001). Spectral and metameric color imaging, *MCSL Technical Report, 2001*.

Farnsworth, D. (1943). The Farnsworth-Munsell 100-Hue and dichotomous tests for color vision. *Journal of the Optical Society of America, 33*(10), 568. Retrieved from http://dx.doi.org/10.1364/JOSA.33.000568

Farnsworth, D. (1957). The Farnsworth-Munsell 100-Hue test for the examination of color discrimination - Manual.

Faulkner, T. W., & Murphy, T. J. (1973). Lighting for diff cult visual tasks. *Human Factors, 15*(2), 149–162. Retrieved from http://dx.doi.org/10.1177/001872087301500207

Fotios, S. (2001). Lamp colour properties and apparent brightness: a review. *Lighting Research and Technology, 33*(3), 163–178.

Hawes, B. K., Brunyé, T. T., Mahoney, C. R., Sullivan, J. M., & Aall, C. D. (2012). Effects of four workplace lighting technologies on perception, cognition and affective state. *International Journal of Industrial Ergonomics, 42*(1), 122–128. Retrieved from http://dx.doi.org/10.1016/j.ergon.2011.09.004

Kinnear, P. R. (1970). Proposals for scoring and assessing the 100-HUE test. *Vision Research, 10*(5), 423–433. Retrieved from http://dx.doi.org/10.1016/0042-6989(70)90123-9

Lakowski, R. (1971). The Farnsworth-Munsell 100 Hue Test*. *The Australian Journal of Optometry, 54*(10), 347–355. Retrieved from http://dx.doi.org/10.1111/j.1444-0938.1971.tb00013.x

Lennie, P., & D'Zmura, M. (1987). Mechanisms of color vision. *Critical Reviews in Neurobiology, 3*(4), 333–400.

Mann, M. (2011). The nervous system in action, Chapter 7, Vision.

Royer, M. P., Houser, K. W., & Wilkerson, A. M. (2012). Color discrimination capability under highly structured spectra, *37*(6), 441–449. Retrieved from http://dx.doi.org/10.1002/col.20702

Ryckaert, W. R., Smet, K. A. G., Roelandts, I. A. A., Van Gils, M., & Hanselaer, P. (2012). Linear LED tubes versus f uorescent lamps: An evaluation. *Energy and Buildings, 49*, 429–436. Retrieved from http://dx.doi.org/10.1016/j.enbuild.2012.02.042

Schanda, J. (2007). *Colorimetry: Understanding the CIE system.* New Jersey: John Wiley & Sons.

Schanda, J. (2015). CIE standard illuminants and sources. In R. Luo (Ed.) *Encyclopedia of Color Science and Technology* (pp. 125–129). New York: Springer. Retrieved from http://dx.doi.org/10.1007/978-3-642-27851-8_324-1

Schwartz, S. H. (2010). *Visual perception: A clinical orientation* (3rd edition). New York: McGraw-Hill. Retrieved from http://dx.doi.org/10.1036/0838594662

Shamsul, B. M. ., Sia, C. C., Ng, Y., & Karmegan, K. (2013). Effects of light's colour temperatures on visual comfort level, task performances, and alertness among students. *American Journal of Public Health Research, 1*(7), 159–165. Retrieved from http://dx.doi.org/10.12691/ajphr-1-7-3

SLL CIBSE. (2009). *The Society of Light and Lighting Handbook. The Society of Light and Lighting* (Vol. 44).

Taylor, A. E. F. (2000). *Illumination fundamental*. New York: Lighting Research Centre

The Society of Light and Lighting. (2012). *The SLL Code for Lighting The Society of Light and Lighting* (Vol. 44).

Verriest, G. (1963). Further studies on acquired def ciency of color discrimination. *Journal of the Optical Society of America, 53*(1), 185. Retrieved from http://dx.doi.org/10.1364/JOSA.53.000185

Wyszecki, G., & Stiles, W. S. (1982). Color science, 2nd. New York: Wiley.

Xu, H. (2012). Conf guring a spectral power distribution for effective colour rendering. *Lighting Research and Technology, 44*(3), 309–315. Retrieved from http://dx.doi.org/10.1177/1477153512439447

Zahiruddin, K., Banu, S., Dharmarajan, R., & Kulothungan, V. (2010). Effect of illumination on colour vision testing with Farnsworth-Munsell 100 Hue Test: Customized colour vision booth versus room illumination, *24*(3), 159–162. Retrieved from http://dx.doi.org/10.3341/kjo.2010.24.3.159

Developing a User-Friendly Procedure in Quantifying Interior Lighting

Amirul Ad-din Majid, Ahmad Mursyid Ahmad Rudin and Ai-Hong Chen*

Fakulti Sains Kesihatan, Universiti Teknologi MARA (UiTM) ,42300 Puncak Alam, Selangor, Malaysia

ABSTRACT

The purpose of this study was to develop a simple, economical but eff cient procedure to collect illuminance data in quantifying interior lighting. This study was carried out in 3.8 m × 2.9 m × 3.0 m controlled experimental room. Three approaches to measure illuminance level were examined: (1) row-to-row; (2) column-to-column; and (3) zig-zag direction. A pre-determined 34 measurement points was used for all the three approaches. The duration required to complete the illuminance data measurement was recorded in minutes. There was a statistically signif cant difference in the total time measured to complete the illuminance data measurement in three different approaches ($F(2, 4) = 23266.81$, $p < 0.05$). The f nding concluded that the zig-zag direction approach was the fastest and most eff cient way in quantifying interior lighting.

Keywords: Illuminance, interior lighting, lux meter, lighting quantif cation, zig-zag pattern

INTRODUCTION

Lighting field measurement is important to verify the performance of the lighting system installed in a specific space for both interior and exterior spaces (Boyce & Raynham, 2009). The development in lighting measurement and calculation has contributed to the invention of advanced lighting simulation tools (Cassol, Schneider, França, & Silva, 2011; Ferentinos & Albright, 2005; Kasprzyk, 2012; Kasprzyk, Nawrowski, & Tomczewski, 2008; Kim, Choi, & Jeong, 2013; Kocabey & Ekren, 2014; Pachamanov & Pachamanova, 2008; Rochakl, Peretta, Lima, Marques, & Yamanaka, 2016; Shikder, Mourshed, & Price, 2010; Villa & Labayrade, 2013; Yu, Su, & Chen, 2014). Complex mathematical formula was used to f nd the optimal location of luminaires in various applications such as plant lighting system,

off ce lighting system, street and tunnel lighting (Ferentinos & Albright, 2005; Kasprzyk, 2012; Kasprzyk, Nawrowski, & Tomczewski, 2008; Kim, Choi, & Jeong, 2013; Pachamanov & Pachamanova, 2008).

Illuminance is a parameter of lighting condition that was measured in a lighting f eld measurement. CIBSE & Society of Light and Lighting have outlined an international standard method for lighting field measurement (Boyce & Raynham, 2009). For interior space, the number of measurement points are based on the room index. The guideline states the minimum number of measurement points to be based on the room index which lends about 10% error (Boyce & Raynham, 2009). The error percentage drops by half when the number of measurement points doubles (Kocabey & Ekren, 2014). To measure illuminance diversity and uniformity, the measurement points are not dependent on the room index but covers the whole working plane (Boyce & Raynham, 2009).

Finite element method (FEM) was used in previous study which involved less measurement points to determine the average illuminance and light f ux distribution (Kocabey & Ekren, 2014). The reduced number of measurement points (36 points) determined with FEM was able to calculate the average illuminance in comparison to the average illuminance measured with full experimental measurement points (930 points). The average illuminance measured with FEM also reduced the error to 5.3% compared to the average illuminance obtained by using the minimum measurement points based on room index calculation (16 points).

However, the measurement procedure used to collect the illuminance data points was not specif ed. This study aimed to evaluate and compare the three illuminance data measurement approaches and f nd out whether the differences in duration has any impact in time eff ciency.

MATERIALS AND METHODS

An experimental room was set up at the Optometry & Visual Science Research Centre (iROViS), UiTM Puncak Alam, Selangor. The dimensions of the room were 3.8 m × 2.9 m × 3.0 m. The interference of daylight was eliminated by sealing the windows and closing the doors. The lights in the corridor were turned off. There were 44 pre-installed recessed luminaires in the room with 4 f uorescent lamps holders (Philips Lifemax TLD 18W/54-765 Cool Daylight, 6200K; CRI= 72; 1050 lm).

A pre-determined 34 illuminance measurement points was set up in the room (seven columns labelled 1–7 from left to right and f ve rows labelled A–I from top to bottom). Measurements were taken at 0.75 m height from the f oor surface. Illuminance measurement grid with 0.46 m × 0.47 m was used (Figure 1). The measurement points were positioned at 0.50 m from the walls and any obstructions (Boyce & Raynham, 2009). A mobile stand (Figure 2) with measurement point marking device (Figure 3) was used to position the lux meter accurately in each measurement point. The setup of the instrument was modif ed from previous study by Kocabey and Ekren (2014).
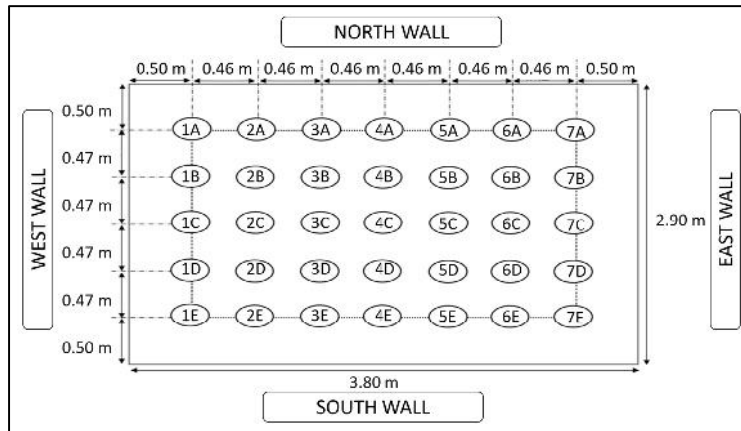
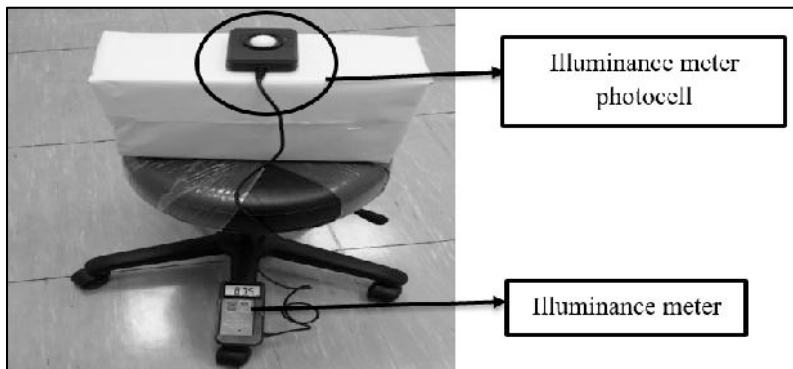*Figure 1.* Layout of the 34 measurement points
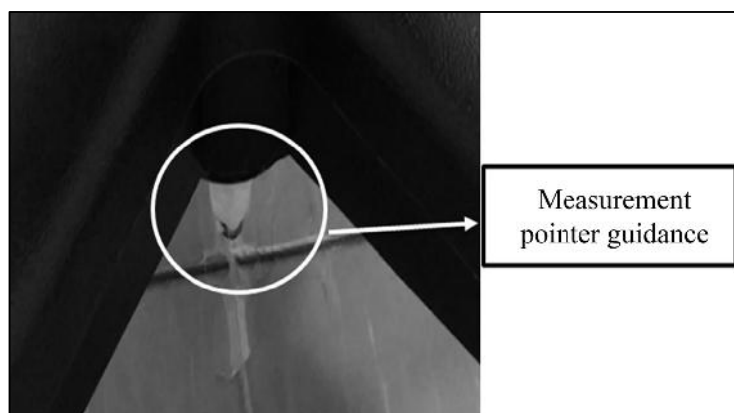

Figure 2. Lux meter on mobile stand

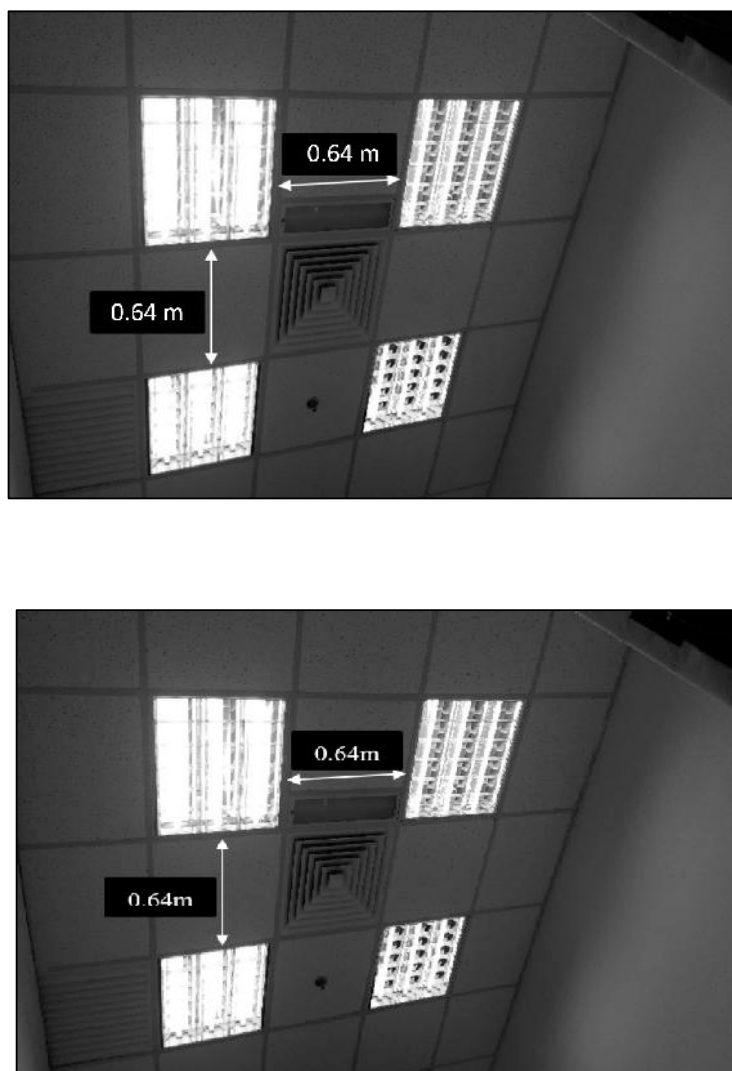*Figure 3.* Measurement point marking device

Figure 4. Positions of luminaires

The luminaires were turned on for one hour before any measurements was taken. It was recommended as the ideal time for f uorescent lamp to stabilise (Boyce & Raynham, 2009). A digital lux meter capable of measuring up to 20000 lux was used. The photocell was cleaned, zero calibrated and exposed to the light environment for about f ve minutes before any illuminance measurement was taken. This study aimed to compare the time or duration involved in three different approaches for illuminance data measurement; row-to-row, column-to-column, and zig-zag pattern. The time involved in each approach to complete the full measurement set was recorded in minutes. The f rst approach was row-to-row approach. The measurement in this approach started at row A (1A) and f nished at row E (7E). The exact f ow of all measurements was illustrated in Figure 5.
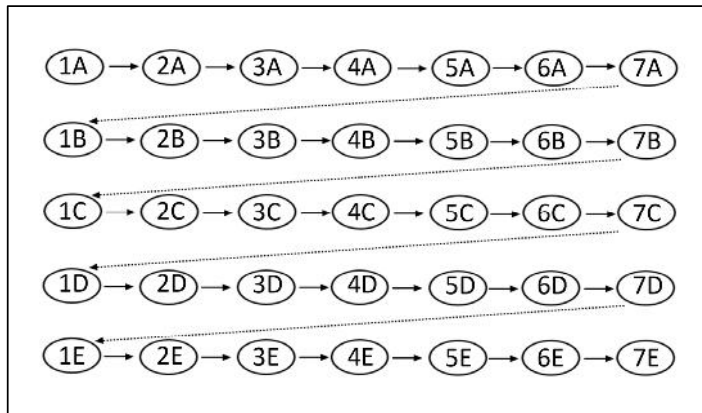
Figure 5. Row-to-row approach

The second approach tested was column-to-column approach. The measurement started at column 1 (1A) and f nished at column 7 (7E). The exact f ow of all measurements is illustrated in Figure 6.
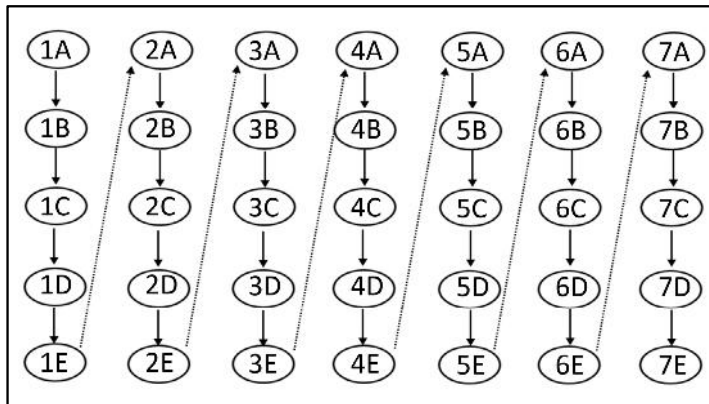

Figure 6. Column-to-column Approach

Lastly, the third approach tested was zig-zag pattern approach. The measurement started at point 1A and end at point 7E. The difference of this approach compared to row-to-row approach was after the measurement in a row was completed, the measurement for the next row was carried out in the opposite direction. The exact f ow of all measurements is illustrated in Figure 7.
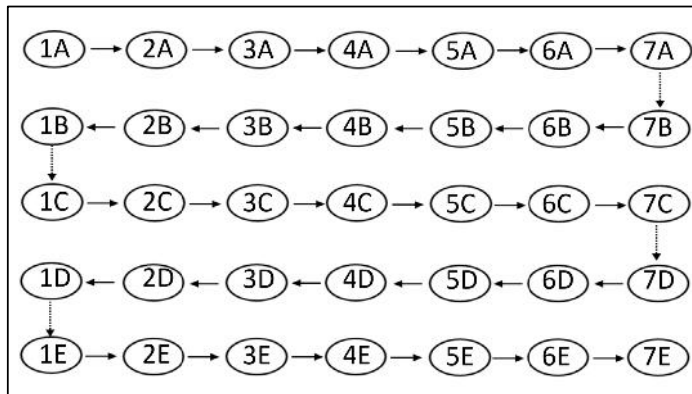
Figure 7. Zig-Zag pattern approach

Three measurements of illuminance were taken for each point. The average illuminance at each point was calculated. The range of the illuminance data measured for each approach was recorded and the time required to complete each approach was recorded in minutes.

RESULTS AND DISCUSSION

This study aimed to compare the total time required to collect the full illuminance data set for three different approaches (row-to-row approach, column-to-column approach and zig-zag pattern approach) in the same room at 34 pre-determined points. In previous study, a total of 930 experimental measurement points were used to compare the average illuminance with a proposed number of measurement points (36 points) while the number of measurement points according to room index for the room used was only 16 points (Kocabey & Ekren, 2014). They recorded the error percentage to become lesser as the number of measurement points increased.

The researchers could have also used room index equation to get the minimum number of measurement points required for the room but it only gave the minimum number of measurement points and it may be necessary to increase the number of measurement points according to the room size so as to reduce the errors (Boyce & Raynham, 2009). The calculation of the room index is as follows:

$$Room\ index = \frac{L\ x\ W}{H(L+W)} \tag{1}$$

Based on the calculation of room index in equation (1), the room index was 0.76 which is lower than 1. The minimum number of measurement points for the experimental room was 9 points with three rows and three columns (Table 1).

Table 1

Minimum number of measurement points to calculate average illuminance (Adapted from Boyce & Raynham, 2009)

Room index (RI)	Minimum number of measurement points
RI < 1	9
1 > RI < 2	16
2 > RI < 3	25
RI > 3	36

The recommended minimum number of measurement points required for calculating average illuminance for the room are nine points, but it is also recommended to increase the number of measurement points to get a better range of illuminance data, reducing errors and it also aids in further calculations such as illuminance uniformity and illuminance diversity (Boyce & Raynham, 2009). The measurement grid should be made of cells with the same size and must be made as square as possible (Boyce & Raynham, 2009). Illuminance level was measured at all points of the measurement grid except for 7A as there was a sink located at that particular point. Therefore, a total of 34 measurement points out of 35 were used to measure the illuminance level with point 7A being excluded.

The total time required for row-to-row approach to complete the measurement was 17.38 ± 0.25 minutes with illuminance reading ranging from 498.80 lux to 973.80 lux. Column-to-column approach had a total time of 14.25 ± 0.32 minutes with illuminance reading ranging from 497.00 lux to 972.40 lux. The zig-zag pattern approach measurement had recording in 11.51 ± 0.26 minutes with illuminance reading ranging from 499.40 lux to 977.40 lux. Since the absolute illuminance value was not the main objective of the measurements in our study, the variation of the illuminance measured was considered acceptable with a difference of less than 0.6% between each measurement. The variation of the illuminance measured could be from the light source itself because maintenance and light loss factor should be considered, or from the lux meter with uncertainty below 6% (Boyce & Raynham, 2009).

A one-way repeated measure ANOVA was conducted to determine whether there were statistically signif cant differences in total time required to complete illuminance measurement for the procedures tested. There were no outliers and the data was normally distributed, as assessed by Shapiro-Wilk's test ($p > 0.05$). There was statistically signif cant difference in total time needed to complete the measurement for each approach [$F_{(2,4)} = 23266.81$, $p < 0.05$].

Comparison of the time required to complete the measurements revealed that the row-to-row approach took the longest duration to complete (17.38 ± 0.25 min), followed by column-to-column approach (14.25 ± 0.32 min) and zig-zag approach (11.51 ± 0.26 min). Longer distance (2.84 m) was required to move the instrument to the next measurement point on the next row in the row-to-row approach which contributed to the differences. The column-to-column approach required to move the instrument for approximately 1.95 m to reach the next point in the next column while the zig-zag approach only required approximately 0.47 m to reach the next point in the next row. The zig-zag pattern approach was recommended as the

best approach in illuminance measurement study to enhance the process of illuminance data measurement.

In this study, an eff cient interior lighting f eld measurement approach that might reduce the illuminance measurement duration was introduced to quantify the illuminance data without compromising the standard measurement procedures specif ed by Society of Light and Lighting. Previous study on improving the lighting f eld measurement eff ciency was achieved using the numerical model (FEM) to improve the accuracy of the data taken without taking too many measurements (Kocabey & Ekren, 2014). Their recommended minimum points (36 points) were lower than their experimental measurement points (930 points), but produced low error percentage compared to the minimum 16 points based on the room index calculation (Boyce & Raynham, 2009; Kocabey & Ekren, 2014). Previous studies focused on reducing the number of total measurement points, but this study focused on reducing the duration to complete the same number of measurement points through transition strategy between measurement points. The f ndings provided both information for more eff cient illuminance measurement planning.

The instrument setup of this study consisted of a mobile stand with measurement pointer and illuminance meter. This setup was economic and user-friendly but had limitation of f xed height of 0.75 m. Therefore, a mobile stand with adjustable height would be recommended to overcome the limitation for future research.

The f nding is an important base to guide future research of large quantity and larger room size. The zig-zag approach managed to reduce the duration of the measurement signif cantly. The approaches used in this study did not involve specif c to specif c type of lighting. Hence, these approaches can be applied to any type of lighting condition because they are only used for illuminance in f eld measurement.

CONCLUSION

Three measurement approaches for lighting f eld measurement were introduced and tested. The approaches were row-to-row approach, column-to-column approach and zig-zag pattern approach. The time to complete the measurement was identif ed to have a signif cant difference between each approach. As a result, the most time-eff cient approach for illuminance data measurement in interior space was the zig-zag pattern approach.

ACKNOWLEDGEMENTS

REFERENCES

Boyce, P., & Raynham, P. (2009). *SLL lighting handbook*. (Boreham, S., & Hadley, P., Eds.) (9th ed.). London: The Society of Light and Lighting.

Cassol, F., Schneider, P. S., França, F. H. R., & Silva, A. J. (2011). Multi-objective optimization as a new approach to illumination design of interior spaces. *Building and Environment, 46*(2), 331–338. Retrieved from http://dx.doi.org/10.1016/j.buildenv.2010.07.028

CIBSE, The installer's guide to lighting design, Good practice guide 300 (2002). Retrieved from http://www.cibse.org/getmedia/0276ac78-dc41-4694-9378-8f984ef924f2/GPG300-The-Installers-Guide-to-Lighting-Design.pdf.aspx

Ferentinos, K. P., & Albright, L. D. (2005). Optimal design of plant lighting system by genetic algorithms. *Engineering Applications of Artif cial Intelligence, 18*(4), 473-484. Retrieved from http://dx.doi.org/10.1016/j.engappai.2004.11.005

Kasprzyk, L. (2012). Optimization of lighting systems with the use of the parallelized genetic algorithm on multi-core processors using the *NET Technology, 7*, 131–133.

Kasprzyk, L., Nawrowski, R., & Tomczewski, A. (2008). Optimization of Complex Lighting Systems in Interiors with the Use of Genetic Algorithm and Elements of Paralleling of the Computation Process. In *Intelligent Computer Techniques in Applied Electromagnetics* (pp. 21-29). Retrieved from http://dx.doi.org/10.1007/978-3-540-78490-6_3

Kim, Y. S., Choi, A. S., & Jeong, J. W. (2013). Applying micro genetic algorithm to numerical model for luminous intensity distribution of planar prism LED luminaire. *Optics Communications, 293*, 22–30. Retrieved from http://dx.doi.org/10.1016/j.optcom.2012.11.017

Kocabey, S., & Ekren, N. (2014). A new approach for examination of performance of interior lighting systems. *Energy and Buildings, 74*, 1–7. Retrieved from http://dx.doi.org/10.1016/j.enbuild.2014.01.014

Pachamanov, A., & Pachamanova, D. (2008). Optimization of the light distribution of luminaries for tunnel and street lighting. *Engineering Optimization, 40*(1), 47–65. Retrieved from http://dx.doi.org/10.1080/03052150701591160

Rocha, H., Peretta, I. S., Lima, G. F. M., Marques, L. G., & Yamanaka, K. (2016). Exterior lighting computer-automated design based on multi-criteria parallel evolutionary algorithm: Optimized designs for illumination quality and energy eff ciency. *Expert Systems with Applications, 45*, 208–222. Retrieved from http://dx.doi.org/10.1016/j.eswa.2015.09.046

Shikder, S. H., Mourshed, M. M., & Price, A. D. F. (2010). Luminaire position optimisation using radiance based simulation: A test case of a senior living room.

Villa, C., & Labayrade, R. (2013). Multi-objective optimisation of lighting installations taking into account user preferences – A pilot study. *Lighting Research and Technology, 45*(2), 176–196. Retrieved from http://dx.doi.org/10.1177/1477153511435629

Yu, X., Su, Y., & Chen, X. (2014). Application of RELUX simulation to investigate energy saving potential from daylighting in a new educational building in UK. *Energy and Buildings, 74*, 191–202. Retrieved from http://doi.org/10.1016/j.enbuild.2014.01.024

Early-Cleaving Embryos are Better Candidates for Vitrif cation: Patterns Associated with Mitochondria and Cytoskeleton

Wan Haf zah, W. J.[1,2], Nor Ashikin, M. N. K.[1]*, Rajikin, M. H.[1], Mutalip, S. S. M.[1,3], Nuraliza, A. S.[4], Nor Shahida, A. R.[1], Salina, O.[1], Norhazlin, J.[1], Razif, D.[1,5] and Fazirul, M.[1]

[1]*Maternofetal and Embryo Research Group (MatE), Faculty of Medicine, Universiti Teknologi MARA (UiTM) Selangor, Sungai Buloh Campus, 47000 Sungai Buloh, Selangor, Malaysia*
[2]*Faculty of Pharmacy and Health Sciences, Universiti Kuala Lumpur Royal College of Medicine Perak (UniKL RCMP), 30450 Ipoh, Perak, Malaysia*
[3]*Faculty of Pharmacy, Universiti Teknologi MARA (UiTM), Selangor, Puncak Alam Campus, 42300 Puncak Alam, Selangor, Malaysia*
[4]*Faculty of Medicine, Universiti Teknologi MARA (UiTM), Selangor, Sungai Buloh Campus, 47000 Sungai Buloh, Selangor, Malaysia*
[5]*Faculty of Health Sciences, Universiti Teknologi MARA (UiTM) Selangor, Puncak Alam Campus, 42300 Puncak Alam, Selangor, Malaysia*

ABSTRACT

This study was conducted to investigate mitochondrial, nuclear chromatin and cytoskeletal organisation of vitrif ed embryos based on timing of the f rst zygotic cleavage. Embryos were retrieved from superovulated ICR mice, 28 hours after hCG injection. Two-cell stage embryos were categorised as early-cleaving (EC), while zygotes with 2-pronuclei as late-cleaving (LC) embryos. Embryos were cultured overnight in M16 medium supplemented with 3% bovine serum albumin (BSA) in carbon dioxide incubator. After 20 hours, the embryos were vitrif ed for one hour and warmed to room temperature. They were then f xed and immunostained to visualise distribution and intensity of mitochondria, nuclear chromatin and cytoskeleton. Finally, the embryos were mounted on glass slides and examined under a Confocal Laser Scanning Microscope (CLSM). Fluorescence intensities were analysed using LAS-AF-Lite Software. Results showed that EC embryos had signif cantly higher mitochondria (39.22 ± 12.50 versus 35.42 ± 14.61 pixel, $p<0.05$) and actin f laments f uorescence intensities (11.43 ± 5.44 versus 5.23 ± 2.20 pixel) compared to LC embryos ($p<0.001$). There was no significant difference in nuclear chromatin and microtubules fluorescence intensities between EC and LC

embryos. These f ndings suggest that greater cryosurvivability of vitrif ed EC compared to LC embryos was contributed by higher densities of mitochondria and actin f laments. Thus, selection of embryos for IVF procedure should be made based on timing of the f rst zygotic cleavage.

Keywords: Actins, chromatin, cytoskeleton, early cleavage, embryo, microtubules, mitochondria, vitrif cation

INTRODUCTION

Timing of the f rst zygotic cleavage has become a common selection parameter in many in vitro fertilization (IVF) laboratories (Fancsovits et al., 2005; Fu et al., 2009; Nielsen & Ali, 2010). Embryos that cleaved early were selected for embryo transfer because of their good quality and higher developmental viability (Lundin, Bergh, & Hardarson, 2001; Salumets et al., 2003; Van Montfoort, Dumoulin, Kester, & Evers, 2004; Fu et al., 2009; Isom, Li, Whitworth, & Prather, 2012). However, the factors contributing to the superiority of early cleavers are still not clear. It is hypothesised that superiority may be related to the mitochondria, nucleus and cytoskeletal structures of embryos. Previous study conducted by the researchers reported higher abundance of actin f laments and nuclear chromatin in early cleaving embryos compared to their late counterparts (Wan Haf zah et al., 2015). Nonetheless, the effects of EC and LC status on vitrif cation outcomes, due to differences in actin, tubulin, nuclear chromatin and mitochondria have not been elucidated.

Vitrif cation of embryos has become a widely used method in embryology laboratories (Konc, Kanyo, Kriston, Somoskoi, & Cseh, 2014). However, the uses of high concentration of cryoprotectant and very low temperature during vitrif cation negatively impacts intracellular organelles and structures including mitochondria, cytoskeleton and nuclear chromatin (Jain & Paulson, 2006). In a study conducted to investigate embryo survivability and viability after vitrif cation based on timing of the f rst zygotic cleavage, EC embryos were found to produce higher survivability and developmental viability compared to EC embryos, after vitrif cation (Jusof, et al., 2015). It is not clear whether organisation of cytoskeleton and other organelles such as mitochondria and nucleus in vitrif ed EC embryos contribute to their higher survivability as reported in non-vitrif ed EC embryos (Wan Haf zah, et al., 2015). In a review paper, Lechniak, Pers-Kamcyc and Pawlak (2008) hypothesised that timing of the f rst zygotic cleavage was related to the number of mitochondria within the oocytes.

Mitochondria are the most abundant organelles at the early stages of embryonic development. They play an important role in energy production and thus contribute to embryo competence (Van Blerkom, Davis, & Alexander, 2000; Van Blerkom, 2004). Mitochondrial distribution and f uorescence intensities ref ect the amount of ATP generated, which correlate with embryo developmental competence (Van Blerkom et al., 2000). The nucleus controls protein synthesis and serves as a genetic blueprint during cell replication. It has been shown that nuclear chromatin morphology correlate with embryo developmental potential (Levy, Benchaib, Cordonier, Souchier, & Guerin, 1998). Most arrested or poor quality embryos display nuclear abnormalities such as chromatin condensation and fragmentation (Levy et al.,

1998). The cytoskeleton is an interconnected system of the cells that plays an important role during fertilisation and the preimplantation period (Chankitisakul, Tharasanit, Tasripoo, & Techakumphu, 2010; McKayed & Simpson, 2013). Based on the important roles of cytoskeleton during cell cleavage, it is hypothesised that they may be correlated with the timing of the f rst zygotic cleavage.

A previous study reported the effect of vitrification on mitochondrial distribution, mitochondrial activity and chromatin integrity of *in vivo* which produced mouse embryos (Martino et al., 2013). They found that vitrif cation changed the distribution pattern of mitochondria in early stage embryos, induced chromatin damage at the morula stage and reduced mitochondrial activity at the blastocyst stage (Martino et al., 2013). These f ndings leave open questions on whether vitrif cation has different effects on the mitochondria, cytoskeleton and nuclear chromatin of EC and LC embryos.

Thus, the present research was designed to study the effects of vitrification on the mitochondria, cytoskeleton (microtubules and actin f laments) as well as nuclear chromatin based on the timing of the f rst zygotic cleavage.

MATERIALS AND METHODS

Embryo Sources

All procedures involved were approved by the Institutional Animal Care and Use Committee (ACUC) (ACUC-7/11) of Universiti Teknologi MARA (UiTM). A total of 30 female ICR strain mice, six to eight weeks of age, weighing 25-35 g were used as embryo donors. The females were superovulated by intraperitoneal (i.p.) injections of 5 IU of Pregnant Mare Serum Gonadotrophin (PMSG: Folligon, Intervet International B.V, Holland), followed 48 hours later, by 5 IU of Human Chorionic Gonadotropin (hCG: Chorulon, Intervet International B.V, Holland). Immediately after hCG injection, the female mice were cohabited with a male stud for copulation. After 28 hours, plugged females were euthanised by cervical dislocation, and their oviducts excised. Embryos were f ushed out from the oviducts into M2 medium (Sigma, USA: M7167).

Timing of the First Sygotic Cleavage

Zygotes with 2 pronuclei and embryos at the 2-cell stage were considered to be fertilised. Only embryos that had even-sized blastomeres with no cytoplasmic fragments were collected. The embryos were then divided into two groups according to the timing of their f rst zygotic cleavage. Embryos at the 2-cell stage at 28-30 hours post hCG administration were categorised as EC embryos whereas the zygotes with the presence of the second polar body and two pronuclei were categorised as LC embryos. The embryo pools for the EC and LC groups comprised 48 and 45 embryos respectively. The zygotes and embryos were cultured overnight in M16 medium (Sigma, USA: M7292) supplemented with Bovine Serum Albumin (BSA) (Sigma, USA: A9418).

Wan Haf zah, W. J., Nor Ashikin, M. N. K., Rajikin, M. H., Mutalip, S. S. M., Nuraliza, A. S., Nor Shahida, A. R.,
Salina, O., Norhazlin, J., Razif, D. and Fazirul, M.

Vitrif cation

After 20 hours, embryos at the 2-cell stage were vitrif ed using the EFS20/40 vitrif cation method modif ed from Mochida, Hasegawa, Taguma, Yoshiki and Ogura (2011). The method uses EFS20 as an equilibration solution, and EFS40 as a vitrif cation solution. The EFS20 contained M2 medium with 20% v/v ethylene glycol, 24% w/v f coll 70 and 0.4 M sucrose, while EFS40 contained M2 medium with 40% v/v ethylene glycol, 18% w/v f coll 70 and 0.3 M sucrose. After vitrif cation, the embryos were warmed to room temperature and then cultured in M16 for 10 minutes before staining.

Embryo Fixation

Vitrif ed embryos were f xed with 4% paraformaldehyde (PFA, Sigma Aldrich: P6148) in Phosphate Buffer Saline (PBS) (Sigma, USA: P4417) at room temperature, until further processing. Following fixation, the embryos were washed in PBS for 30 minutes and immunof uorescent stained through serial incubations in dyes.

Immunof uorescence Staining

Embryos were f rst incubated with 4', 6'-diamino-2-phenylindole dihydrochloride (DAPI) (Molecular Probes, Life Technologies, USA: D3571) for 30 minutes to stain for DNA chromatin. Then, embryos were permeabilized with 0.1% Triton X-100 (Sigma, USA: X100) in Phosphate Buffer Saline (PBS) (Sigma, USA: P4417). After a 10-minute incubation in 0.1% Triton X-100, mitochondria were incubated with MitoTracker Red Probe [MitoTracker® Red (Invitrogen, USA: M7513)] for 40 minutes. The embryos were then washed twice with PBS for 10 minutes to remove excess MitoTracker from the cytoplasm. Finally, the embryos were counterstained with DAPI for 30 minutes.

To visualise the abundance and distribution of actin f laments and microtubules, embryos were f rst incubated with DAPI and permeabilized with 0.1% Triton X-100 in PBS as described above. Actin f laments were labelled with Alexa Fluor 635 Phalloidin (Molecular Probes, Life Technologies, USA: A34054) while microtubules structure were labelled with Monoclonal anti- -Tubulin conjugate with FITC (Sigma, USA: F2168) in PBS containing 1% BSA, for one hour. The embryos were then washed twice with PBS for 10 minutes. Finally, the embryos were counterstained with DAPI for 30 minutes.

The labelled embryos were mounted on glass microscope slides with an antifade medium (Pro Long Gold Antifading Agent) (Molecular Probes, Life Technologies, USA: P36934), and sealed under a coverslip. All slides were stored in the dark at 4°C prior to processing and imaging. Fluorescence signals were observed under a Confocal Laser Scanning Microscope (CLSM) (Leica TCS SP5 AOBS, Germany). The distribution pattern of actin f laments, microtubules, nuclear chromatin and mitochondria of vitrif ed EC and LC embryos were observed and recorded.

Quantif cation of Fluorescent Images

A software known as LAS AF Lite version 2.6 (Leica Microsystems CMS GmbH, Wetzlar, Germany) was used to quantify the f uorescence intensity of mitochondria, actin f laments, microtubules and nuclear chromatin in the immunof uorest images. Fluorescent intensities of mitochondria, actin f laments and microtubules were measured by manually outlining the blastomeres. Fluorescent intensities of nuclei were measured by manually outlining nuclei. Average f uorescent intensities per unit area within the region of interest (ROI) in the immunof uorescence images were measured after background subtraction.

Statistical Analysis

Statistical analysis was performed using the SPSS software for Windows version 19.0.1 (Statistical Package for Social Sciences, Inc., USA). All data were presented as the means ± standard deviation (SD). Independent T-test was performed to analyse differences in - immunof uorescent intensities among vitrif ed EC and LC embryos. Differences were considered signif cant when P-values were less than 0.05.

RESULTS

Mitochondria of Vitrif ed Embryos

Mitochondria of 48 vitrif ed EC and 45 LC embryos were observed at the 2-cell stage. Mitochondria of EC embryos were seen to be homogenously distributed in the cytoplasm of blastomeres (Figure 1A). Conversely, mitochondria of LC embryos were concentrated at the pericortical region (Figure 1B). There was generally no aggregation /clustering of mitochondria in EC and LC embryos, except in one LC embryo (representing 2.2% of samples) (Figure 1C). Most vitrif ed EC and LC embryos (83% and 82% respectively) showed symmetrical mitochondrial distribution patterns (Table 1). Mitochondrial f uorescent intensities of EC embryos were signif cantly higher compared to LC embryos (39.22 ± 12.50 vs 35.42 ± 14.61 pixel) ($p<0.001$) (Figure 2).
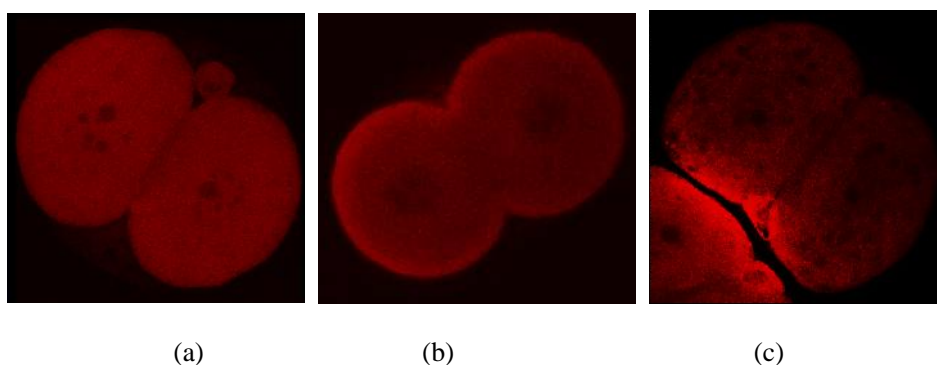

| (a) | (b) | (c) |

Figure 1. Vitrif ed embryos

There are three types of vitrif ed embryos in the f gure above. Figure 1(a) shows vitrif ed EC embryos, where mitochondria is distributed homogenously in the cytoplasmic region of blastomeres with higher f uorescence intensities. Figure 1(b) shows vitrif ed LC embryos where mitochondria is distributed homogenously in the cytoplasmic region of blastomeres with comparatively lower f uorescence intensities. Figure 1(c) is vitrif ed LC embryos. Here, mitochondria is distributed in cluster in the cytoplasmic region of blastomeres.

Table 1
Percentage of symmetrical mitochondrial distribution in blastomeres of vitrif ed EC and LC embryos

Group	Number of embryos	Percentage of embryos (%)	
		Symmetry	Asymmetry
EC embryos	48	40/48 (83%)	8/48 (17%)
LC embryos	45	37/45 (82%)	8/45 (18%)
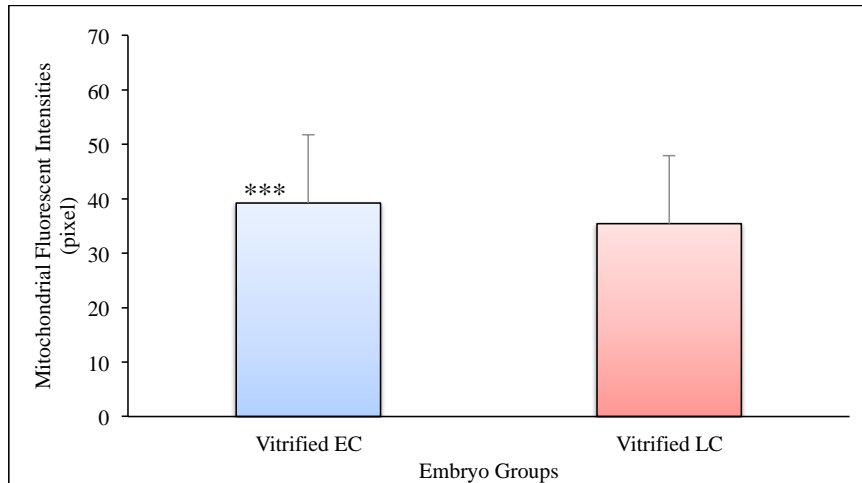
Figure 2. Mitochondrial Fluorescent Intensities in Vitrif ed EC vs LC Embryos (Mean ± SD)
*** vitrif ed EC versus LC embryos (p<0.001)

Cytoskeleton of Vitrif ed Embryos

A total of 44 vitrif ed EC embryos and 41 vitrif ed LC embryos at the 2-cell stage were processed for cytoskeletal analyses. Visual observation on cytoskeletal distributions revealed that actin f lament of vitrif ed EC and vitrif ed LC embryos were mostly located at the plasma cell membrane. Vitrif ed LC embryos were seen to have a relatively lower abundance of actin. Generally, actin f laments of EC embryos were concentrated at the intercellular space (Figure 3).
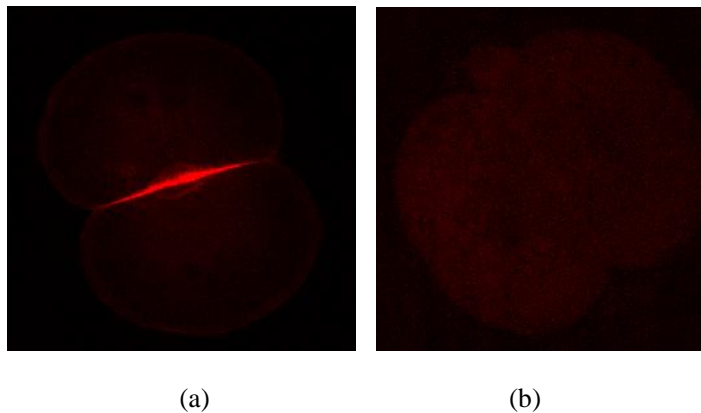
<center>(a)   (b)</center>

Figure 3. (a) Vitrif ed EC embryo; and (b) vitrif ed LC embryo stained with antibody to actin (Alexa Fluor 635-red)

Actin of vitrif ed EC and vitrif ed LC embryos were mostly located at the plasma cell membrane. Generally, actin of vitrif ed EC embryos was concentrated at the intercellular space, while actin of vitrif ed LC embryos had a relative weak cytoplasmic background.

Tubulin of EC and LC embryos were uniformly distributed in the cytoplasm of blastomeres. However, less tubulin was seen at cell contact areas. Figure 4 illustrates localisation of tubulin in EC and LC embryos. The cytoplasm of both EC and LC embryos was brightly stained for tubulin, especially in apical and central regions. Less f uorescence was observed in the basal region.

Table 2 shows f uorescent intensities of actin and tubulin in EC and LC embryos. Vitrif ed EC embryos had signif cantly higher actin f uorescence intensities compared to LC embryos (11.43 ± 5.44 vs 5.23 ± 2.20 pixel) ($p<0.001$). No signif cant difference was found between tubulin f uorescent intensities of EC and LC embryos.

<center>(a)   (b)</center>
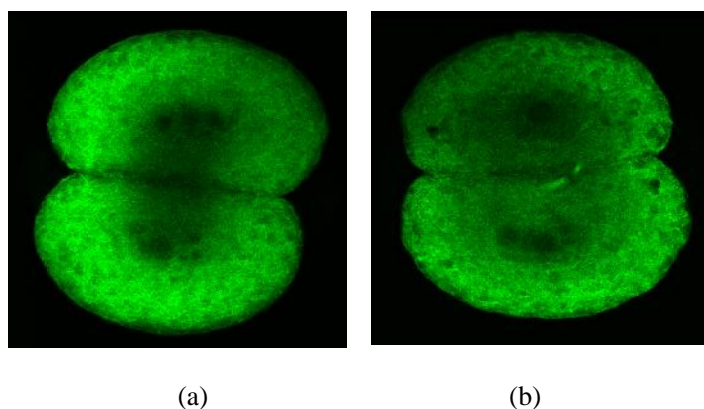
Figure 4. (a) Vitrif ed EC embryo; and (b) Vitrif ed LC embryo

Both the vitrif ed EC embryo and vitrif ed LC embryo were brightly stained with antibody to tubulin (Monoclonal anti -Tubulin conjugate with FITC - green). The distributions of tubulin in vitrif ed EC embryos were similar to vitrif ed LC embryos. They were distributed homogenously in the cytoplasmic region of blastomeres. Confocal images showed that the cytoplasm of the vitrif ed EC and vitrif ed LC embryos were strongly stained with anti -tubulin (green stain).

Table 2
Mean f uorescent intensities of actin and tubulin in vitrif ed EC and LC embryos (Mean ± SD)

Structure	Mean ± SD (pixel)		P value
	EC embryos	LC embryos	
Actin	11.43*** ± 5.44	5.23 ± 2.20	<0.001
Tubulin	29.77 ± 7.66	23.09 ± 8.38	0.084

*** vitrif ed EC versus LC embryos (p< 0.001)

Nuclear Chromatin of Vitrif ed Embryos

A total of 52 vitrif ed EC embryos and 40 vitrif ed LC embryos at the 2-cell stage were stained to study the impact of vitrif cation on nuclear chromatin. Nuclei of vitrif ed EC and LC embryos were centrally located in each blastomere (Figure 5). There was no signif cant difference between nuclear f uorescent intensities in vitrif ed EC and LC embryos (Table 3).

Table 3
Mean f uorescent intensities of nuclear chromatin of vitrif ed EC and LC Embryos (Mean ± SD)

Structure	Mean ± SD (pixel)		P value
	EC embryos	LC embryos	
Vitrif ed embryos	204.61 ± 41.66	213.15 ± 37.43	0.337

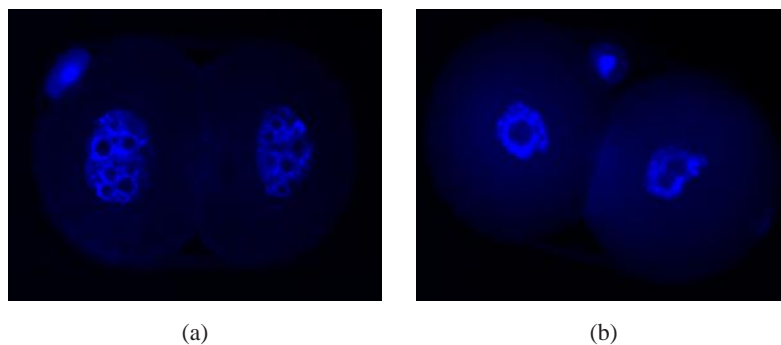(a)   (b)

Figure 5. (a) Vitrif ed EC embryo; and (b) vitrif ed LC embryo stained with antibody to chromatin (DAPI - blue). Nuclei of vitrif ed EC and vitrif ed LC embryos were centrally located with no fragmentation

DISCUSSION

This study examined the impact of vitrif cation on mitochondrial distribution, cytoskeletal organisation and nuclear chromatin conf gurations of mouse embryos based on timing of the f rst zygotic cleavage. The visualisation of morphology and quantif cation of immunof uoresence signals provide greater understanding of the differences controlling developmental competence in EC and LC embryos, after vitrif cation.

Mitochondria are important for energy production, and therefore indicate the quality and developmental potential of embryos. It has been shown that intracellular localisation of mitochondria is essential for successful development of embryos (Matsumoto, Shoji, Umezu, & Sato, 1998; Van Blerkom et al., 2000). In the present study, mitochondria of vitrif ed EC embryos were found to be homogenously distributed in the cytoplasm of blastomeres. Previous studies showed the same mitochondrial distribution pattern in inbred blocking strain and hybrid nonblocking strain mouse and rat embryos (Bavister & Squirrell, 2000). However, in outbred blocking strain mouse (Bavister & Squirrell, 2000; Bogolyubova, 2005), human (Van Blerkom et al., 2000) and hamster (Bavister & Squirrell, 2000; Kabashima, Matsuzaki, & Suzuki, 2007) embryos, mitochondria were concentrated at the perinuclear region. It has been proposed that the perinuclear mitochondrial localisation serves to supply energy for intranuclear processes and to protect nuclear structure against oxidative stress (Bavister and Squirrell, 2000; Ramalho-Santos, et al., 2009). In mouse embryos blocked at the two-cell stage or arrested embryos, no perinuclear concentration of mitochondria was observed. These mitochondria were found to aggregate into clusters (Bogolyubova, 2005).

In the present study, mitochondria of vitrif ed LC embryos were concentrated at the cortical region of blastomeres. These localisation patterns were also reported in a previous study on arrested mouse embryos (Muggleton-Harris & Brown, 1988). Localisation of mitochondria at the cortical region may be related to vitrif cation damage. This pattern of localisation may reduce energy supply to the nuclear region, thus increasing the risk of embryo arrest after subsequent culture. Homogenous distribution of mitochondria in the cytoplasm of vitrif ed EC embryos may be due to better recovery after vitrif cation. Mitochondria localised in the cortical region may be involved in the recovery process after vitrif cation. In other words, vitrif ed EC embryos may have good relocalisation of mitochondria to adjust to changes during vitrif cation. Generally, there was no aggregation of mitochondria in vitrif ed EC and vitrif ed LC embryos. Aggregation of mitochondria was only observed in one embryo, which increased the risk of its developmental arrest, as reported by a previous study (Bogolyubova, 2005).

In the present study, most mitochondria were distributed symmetrically between both blastomeres of vitrif ed EC and LC embryos. Previous study showed that embryos with unsymmetrical mitochondrial distribution between blastomeres remained undivided and often degenerated after subsequent culture (Van Blerkom et al., 2000). Observation on confocal images in the present study also revealed higher mitochondrial f uorescence signals in vitrif ed EC embryos compared to vitrif ed LC embryos. The signals differences were also supported by quantif cation analysis which showed signif cantly higher intensities of mitochondria in vitrif ed EC embryos compared to vitrif ed LC embryos. This indicates higher energy supply

for vitrif ed EC embryos to promote better survivability and developmental viability after vitrif cation, as reported earlier (Jusof et al., 2015).

Actin f laments of vitrif ed EC and LC embryos were primarily located at the cell membrane or in the cortical region of blastomeres, resulting in the presence of a ring-like f uorescence around each blastomere. This observation is largely in agreement with the results from previous studies which found the location of actin just beneath the cell membrane or in the cortical layer of blastomeres (Gallicano, 2001; Kabashima et al., 2007; Lehtonen & Badley, 1980). Although the localisation patterns of actin were similar in vitrif ed EC and LC embryos, higher signals of Alexa Flour 635 were detected at the intercellular contact points of EC embryos. Conversely, vitrif ed LC embryos showed a thinner layer of actin at the cortical layer of blastomeres and also at the intercellular contact points. The higher signals of actin in cortical region of vitrif ed EC embryos may contribute to the higher cleavage speed in vitrif ed EC embryos because actin f laments play an important role in the contractile system during the cytokinesis of blastomeres (Gallicano, 2001). During cytokinesis, actin f laments that are located at the pericellular space contract, tighten and pinch the cell into two (Nelson & Cox, 2008). For that reason, actin microf laments are concentrated in the intercellular space of dividing cells (Chankitisakul et al., 2010). Actin quality and distribution is important because it correlates with embryo viability. A normal actin content and distribution is required for embryos to undergo normal cell division (Zijlstra et al., 2008).

Actin f lament distribution differences were studied by Matsumoto et al. (1998). The authors compared distribution differences in non-blocked and blocked 2-cell stage rat embryos. In non-blocked embryos, they found that actin f laments were distributed adjacent to nuclei and along the cell membrane. However, in embryos blocked at the two-cell stage, actin f laments formed granules and were dispersed in the cytoplasm. Another study found actin abnormalities in embryos arrested at early stages of development and in cryopreserved embryos (Levy et al., 1998). Another study found a signif cant relationship between the osmotic levels and the chances of blastocysts exhibiting disrupted cellular actin f laments (Men, Agca, Mullen, Critser, & Critser, 2005). In the present study however, no actin f laments abnormalities were detected either in vitrif ed EC or LC embryos.

The distribution of actin f laments are clearly related to their function. Actin f laments provide support and structure to cell membrane. They regulate cell shape by interacting with integrin proteins at the cell membrane (Calderwood, Shattil, & Ginsberg, 2000). The concentration of actin f laments along the cell membrane in both vitrif ed EC and LC embryos in this study may therefore be attributed to their role of regulating cell shape via interaction with integrins.

Quantif cation of immunof uorescence images from the present study showed signif cantly higher actin f laments intensities in vitrif ed EC embryos compared to vitrif ed LC embryos. Higher intensities of actin in vitrif ed EC embryos ref ect higher abundance of actin f laments, thus conferring vitrif ed EC embryos with higher developmental viability compared to vitrif ed LC embryos (Isom et al., 2012; Lechniak et al., 2008; Lundin et al., 2001; Nielsen & Ali, 2010). Higher abundance of actin may also contribute to the maintenance of embryo shape after vitrif cation, thus increasing the survivability of vitrif ed ECs compared to LC embryos.

Another component of the cytoskeleton which demonstrates many important roles in cellular processes of preimplantation embryos are microtubules. Microtubules are involved in cell motility, cell division, control of cell shape and cytoplasmic organisation (De Brabander, 1982). They also organise the distribution of various cytoplasmic organelles including mitochondria (Heggeness, Simon, & Singer, 1978). While the function of microtubules are well known, little information is available regarding their roles during vitrif cation.

The distribution of microtubules is related to their function in a variety of cellular processes (Kavallaris, 2010). The present study found that microtubules of vitrif ed EC and LC embryos were distributed homogenously in the cytoplasm of blastomeres, especially in apical and central regions. In congruence, previous studies also found homogenous distribution of microtubules in the cytoplasm of developing two-cell stage mouse embryos (Kan et al., 2011; Matsumoto et al., 1998) with the highest density in apical cytoplasm (Van Blerkom et al., 2000). Microtubules were also found around nuclei as documented by previous studies (Kabashima et al., 2007; Van Blerkom et al., 2000), with a similar pattern in both vitrif ed EC and LC embryos. The present study also found less microtubules in the basal region or in the intercellular apposition of vitrif ed EC and LC embryos. This is in agreement with a previous study which found low abundance of microtubules in the intercellular contact of newly divided blastomeres (Van Blerkom et al., 2000). Another study however, reported a high abundance of microtubules in the area, with wide intercellular contact (Lehtonen & Badley, 1980).

In a study conducted to compare the distribution pattern in normal developing embryos and embryos exhibiting two-cell block by Matsumoto et al. (1998), the researchers found thicker f brous microtubules which distributed as rude meshwork structures in the cytoplasm of embryos exhibiting the two-cell block. Another study found low density of microtubules without perinuclear network in blocking two-cell embryos (Neganova, Sekirina, & Eichenlaub-Ritter, 2000). The present study found microtubules to be distributed homogenously in the cytoplasmic region of both vitrif ed EC and LC embryos. The nucleus is the largest organelle in the cell. The main function of the nucleus is to govern gene expression and facilitate DNA replication. Fluorescence microscopy of nuclear DNA is useful for the determination of exact functional stages of early embryo development (Mori, Hashimoto, & Hoshino, 1988). The rate of cell division, metabolism and development correlate with nuclear DNA content. Nuclear f uorescent intensity in confocal images is directly proportional to DNA content of the cells (Ljosa & Carpenter, 2009).

Vitrif cation was reported to increase DNA fragmentation and reduce developmental viability (Park et al., 2006). The present study showed that there is no signif cant difference between nuclear f uorescent intensity of vitrif ed EC embryos and LC embryos. The present study also showed the normal nuclei localisation and morphology with no fragmentation or chromatin condensation in both vitrif ed EC and LC embryos. A previous study reported that nuclear abnormalities such as chromatin condensation and fragmentation were found only in arrested embryos (Levy et al., 1998). Observation showed that mouse embryos were relatively tolerant to vitrif cation by EFS20/40 method. The recovery process was suff cient to allow for further development.

Wan Haf zah, W. J., Nor Ashikin, M. N. K., Rajikin, M. H., Mutalip, S. S. M., Nuraliza, A. S., Nor Shahida, A. R.,
Salina, O., Norhazlin, J., Razif, D. and Fazirul, M.

CONCLUSION

It can be concluded therefore that EC embryos are more cryo-tolerant due to higher densities of mitochondria and actin f laments which appear to result in more eff cient cell division, and therefore, greater developmental competence. Thus, selection of embryos for IVF procedure should be made based on timing of the f rst zygotic cleavage.

ACKNOWLEDGEMENTS

REFERENCES

Bavister, B. D., & Squirrell, J. M. (2000). Mitochondrial distribution and function in oocytes and early embryos. *Human Reproduction, 15*, 189-198.

Bogolyubova, N. A. (2005). Changes in the distribution of mitochondria in mouse embryos blocked at the two-cell stage. *Russian Journal of Developmental Biology, 36*(1), 43–50.

Calderwood, D. A., Shattil, S. J., & Ginsberg, M. H. (2000). Integrins and actin f laments: Reciprocal regulation of cell adhesion and signaling. *The Journal of Biological Chemistry, 275*(30), 22607-22610.

Chankitisakul, V., Tharasanit, T., Tasripoo, K., & Techakumphu, M. (2010). Chronological reorganization of microtubules, actin microf laments, and chromatin during the f rst cell cycle in swamp buffalo (Bubalus bubalis) embryos. *Veterinary medicine international, 2010.*

De Brabander, M. (1982). Microtubules, central elements of cellular organization. *Endeavour, 6*(3), 124-134.

Fancsovits, P., Toth, L., Takacs, Z. F., Murber, A., Papp, Z., & Urbancsek, J. (2005). Early pronuclear breakdown is a good indicator of embryo quality and viability. *Fertility and Sterility, 84*(4), 881-887.

Fu, J., Wang, X. J., Wang, Y. W., Sun, J., Gemzell-Danielsson, K., & Sun, X. X. (2009). The inf uence of early cleavage on embryo developmental potential and IVF/ICSI outcome. *Journal of Assisted Reproduction and Genetics, 26*(8), 437-441.

Gallicano, G. I. (2001). Composition, regulation, and function of the cytoskeleton in mammalian eggs and embryos. *Frontiers in Bioscience, 6*, 1089-1108.

Heggeness, M. H., Simon, M., & Singer, S. J. (1978). Association of mitochondria with microtubules in cultured cells. *Proceedings of the National Academy of Sciences of the United States of America, 75*(8), 3863-3866.

Isom, S. C., Li, R. F., Whitworth, K. M., & Prather, S. (2012). Timing of f rst embryonic cleavage is a positive indicator of the in vitro developmental potential of porcine embryos derived from in vitro fertilization. Somatic cell nuclear transfer and parthenogenesis. *Molecular Reproduction and Development, 79*(3), 197–207.

Jain, J. K., & Paulson, R. J. (2006). Oocyte cryopreservation. *Fertility and Sterility, 86*(3), 1037-1046.

Jusof, W. H. W., Khan, N. A. M. N., Rajikin, M. H., Satar, N. A., Mustafa, M. F., Jusoh, N., & Dasiman, R. (2015). Timing of the f rst zygotic cleavage affects post-vitrif cation viability of murine embryos produced *in vivo*. *International Journal of Fertility and Sterility, 9*(2), 221-229.

Kabashima, K., Matsuzaki, M., & Suzuki, H. (2007). Both microtubules and microf laments mutually control the distribution of mitochondria in two-cell embryos of golden hamsters. *Journal of Mammalian Ova Research, 24*(3), 120-125.

Kan, R., Yurttas, P., Kim, B., Jin, M., Wo, L., Lee, B., ... & Coonrod, S. A. (2011). Regulation of mouse oocyte microtubule and organelle dynamics by PADI6 and the cytoplasmic lattices. *Developmental Biology, 350*(2), 311-322.

Kavallaris, M. (2010). Microtubules and resistance to tubulin-binding agents. *Nature Reviews Cancer, 10*, 194-204.

Konc, J., Kanyo, K., Kriston, R., Somoskoi, B., & Cseh, S. (2014). Cryopreservation of embryos and oocytes in human assisted reproduction. *Biomed Research International*, 1-9.

Lechniak, D., Pers-Kamcyc, E., & Pawlak, P. (2008). Timing of f rst zygotic cleavage as a marker of developmental potential of mammalian embryo. *Reproductive Biology, 8*(1), 23–42.

Lehtonen, E., & Badley, R. A. (1980). Localization of cytoskeletal proteins in preimplantation mouse embryos. *Journal of Embryology and Experimental Morphology, 55*, 211-25.

Levy, R., Benchaib, M., Cordonier, H., Souchier, C., & Guerin, J. F. (1998). Laser scanning confocal imaging of abnormal or arrested human preimplantation embryos. *Journal of Assisted Reproduction and Genetics, 15*(8), 485-495.

Ljosa, V., & Carpenter, A. E. (2009). Introduction to the quantitative analysis of two-dimensional f uorescence microscopy images for cell-based screening. *PLoS Computational Biology, 5*, e1000603.

Lundin, K., Bergh, C., & Hardarson, T. (2001) Early embryo cleavage is a strong indicator of embryo quality in human IVF. *Human Reproduction,16*(12), 2652-2657.

Martino, N. A., Dell'aquila, M. E., Cardone, R. A., Somoskoi, B., Lacalandra, G. M., & Cseh, S. (2013). Vitrif cation preserves chromatin integrity, bioenergy potential and oxidative parameters in mouse embryos. *Reproductive Biology and Endocrinology, 11*(1), 27-38.

Matsumoto, H., Shoji, N., Umezu, M., & Sato, E. (1998). Microtubule and microf lament dynamics in rat embryos during the two-cell block *in vitro*. *The Journal of Experimental Zoology, 281*(2), 149–153.

McKayed, K., & Simpson, J. (2013). Actin in action: Imaging approaches to study cytoskeleton structure and function. *Cells, 2*(4), 715-731.

Men, H., Agca, Y., Mullen, S. F., Critser, E. S., & Critser, J. K. (2005). Osmotic tolerance of in vitro produced porcine blastocysts assessed by their morphological integrity and cellular actin f lament organization. *Cryobiology, 51*(2), 119-129.

Mochida, K., Hasegawa, A., Taguma, K., Yoshiki, A., & Ogura, A. (2011). Cryopreservation of mouse embryos by ethylene glycol-based vitrif cation. *Journal of Visualized Experiments, 57*, e3155.

Mori, C., Hashimoto, H., & Hoshino, K. (1988). Fluorescence microscopy of nuclear DNA in oocytes and zygotes during *in vitro* fertilization and development of early embryos in mice. *Biology of. Reproduction, 39*(3), 737– 742.

Muggleton-Harris, A. L., & Brown, J. J. (1988). Cytoplasmic factors influence mitochondrial reorganization and resumption of cleavage during culture of early mouse embryos. *Human Reproduction, 3*(8), 1020-1028.

Neganova, I. E., Sekirina, G. G., & Eichenlaub-Ritter, U. (2000). Surface-expressed E-cadherin, and mitochondrial and microtubule distribution in rescue of mouse embryos from 2-cell block by aggregation. *Molecular Human Reproduction, 6*(5), 454-464.

Nelson, D. L., & Cox, M. C. (2008). *Lehninger principles of Biochemistry*. (4th edition). United Kingdom: Palgrave Macmillan.

Nielsen, H. I., & Ali, J. (2010). Embryo culture media, culture techniques and embryo selection: A tribute to Wesley Kingston Whitten. *Journal of Reproductive and Stem Cell Biotechnology, 1*(1), 1-29.

Park, S. Y., Kim, E. Y., Cui, X. S., Tae, J. C., Lee, W. D., Kim, N. H., ... & Lim, J. H. (2006). Increase in DNA fragmentation and apoptosis-related gene expression in frozen-thawed bovine blastocysts. *Zygote, 14*(2), 125-131.

Ramalho-Santos, J., Varum, S., Amaral, S., Mota, P. C., Sousa, A. P., & Amaral, A. (2009). Mitochondrial functionality in reproduction: from gonads and gametes to embryos and embryonic stem cells. *Human Reproduction Update, 15*(5), 553-572.

Salumets, A., Hyden-Granskog, C., Makinen, S., Suikkari, A. M., Tiitinen, A., & Tuuri, T. (2003) Early cleavage predicts the viability of human embryos in elective single embryo transfer procedures. *Human Reproduction, 18*(4), 821-825.

Van Blerkom, J., Davis, P., & Alexander, S. (2000). Differential mitochondrial distribution in human pronuclear embryos leads to disproportionate inheritance between blastomeres: Relationship to microtubular organization, ATP content and competence. *Human Reproduction, 15*(12), 2621-2633.

Van Blerkom, J. (2004). Mitochondria in human oogenesis and preimplantation embryogenesis: engines of metabolism, ionic regulation and developmental competence. *Reproduction, 128*(3), 269-280.

Van Montfoort, A. P., Dumoulin, J. C., Kester, A. D., & Evers, J. L. (2004). Early cleavage is a valuable addition to existing embryo selection parameters: a study using single embryo transfers. *Human Reproduction, 19*(9), 2103–2108.

Wan Haf zah, W. J., Rajikin, M. H., Nuraliza, A. S., Zainuddin, H., Nur-Sakina, K. A., Nor-Shahida, A. R., ... & Nor-Ashikin, M. N. K. (2015). Organization of cytoskeleton and chromatin is related to the timing of the f rst zygotic cleavage or early development competence. *Biomedical Research, 26*(2), 286-292.

Zijlstra, C., Kidson, A., Schoevers, E. J., Daemen, A. J., Tharasanit, T., & Kuijk, E. W. (2008). Blastocyst morphology, actin cytoskeleton quality and chromosome content are correlated with embryo quality in the pig. *Theriogenology, 70*(6), 923-935.

Vitrif cation of Blastocyst Murine Embryos Affects PI3K Pathway by Modulating the Expression of XIAP and S6K1 Proteins

Mohd Fazirul, M.[1], Sharaniza, A. R.[2], Norhazlin, J. M. Y.[1,3], Wan Haf zah, W. J.[1,4], Razif, D.[1,5], Froemming, G. R. A.[2], Agarwal A.[6], Mastura, A. M.[1] and Nor Ashikin, M. N. K.[1]*

[1]*Maternofetal and Embryo Research Group (MatE), Faculty of Medicine, Universiti Teknologi MARA (UiTM) Selangor, Sungai Buloh Campus, 47000 Sungai Buloh, Selangor, Malaysia*
[2]*Faculty of Medicine, Universiti Teknologi MARA (UiTM) Selangor, Sungai Buloh Campus, 47000 Sungai Buloh, Selangor, Malaysia*
[3]*Faculty of Applied Sciences, Universiti Teknologi MARA (UiTM) Perak, Tapah Campus, 35400 Tapah Road, Tapah, Perak, Malaysia*
[4]*Faculty of Pharmacy and Health Sciences, Universiti Kuala Lumpur Royal College of Medicine Perak (UniKL RCMP), 30100 Ipoh, Perak, Malaysia*
[5]*Faculty of Health Sciences, Universiti Teknologi MARA (UiTM) Selangor, Puncak Alam Campus, 42300 Puncak Alam, Selangor, Malaysia*
[6]*Faculty of Medicine, Northern Border University, Kingdom of Saudi Arabia*

ABSTRACT

Cryopreservation by vitrif cation has been widely used in Assisted Reproductive Technology (ART) to preserve embryos for an extended period of time. However, the effect of vitrif cation on development of the embryos is lacking. Therefore, understanding on vitrif cation effects on embryonic proteins, especially those involved in preimplantation development is crucial to provide high quality embryos for further usage. In this study, XIAP and S6K1 protein expressions following vitrification was investigated, since they have been implicated in diverse cellular processes including cell growth, migration, proliferation, differentiation, survival and development of preimplantation embryos via the PI3K pathway. Embryos were obtained from superovulated female ICR mice which were mated with fertile males. The embryos were harvested at the 2-cell stage and cultured until blastocyst stage. Blastocysts were then vitrif ed in ESF40 cryoprotectant. Western blot was carried out to determine the expression of XIAP and S6K1 proteins. The results showed the expression of XIAP and S6K1 signif cantly decreased in vitrif ed

Mohd Fazirul, M., Sharaniza, A. R., Norhazlin, J. M. Y., Wan Haf zah, W. J., Razif, D., Froemming, G. R. A., Agarwal A., Mastura, A. M. and Nor Ashikin, M. N. K.

blastocyst compared to the control. This indicates that blastocyst vitrif cation may impact developmental competence through the activation of apoptotic pathways.

Keywords: Blastocyst, cryopreservation, embryo, PI3K, vitrif cation

---

INTRODUCTION

Studies of mammalian embryo development *in vitro*, especially in mice have provided insights into understanding the fundamental biological processes in early preimplantation development. This has enabled researchers to further understand the molecular basis of embryonic cellular differentiation and improve the quality of embryos produced in Assisted Reproductive Technologies (ART).

It is a common practice in ART today to limit transfer of embryos to maximum of two blastocysts at a time. Therefore, eff cient cryopreservation method for surplus blastocyst preservation is necessary to avoid waste and for future usage (Cutting et al., 2008; Sunde, 2007). Recent studies have favoured cryopreservation by vitrif cation, a technique which involves the solidif cation of water or water-based solutions into a glass-like amorphous liquid state (Fahy, MacFarlane, Angell, & Meryman, 1984; Rienzi et al., 2017; Vajta, Cobo, Conceicao, & Yovich, 2009) as it is quick and eff cient in maintaining viability of embryos.

However, the effect of vitrif cation on the intracellular signalling pathway is still poorly understood. Understanding of the vitrif cation effects on the embryos' biological processes and their regulation is important since their development depends on the signal generated by growth factors which are present in the maternal environment. These growth factors are known to regulate cell proliferation and differentiation during development of preimplantation embryos (Raff, 1992; Weil et al., 1996). A previous study by Dardik, Smith and Schultz (1992) has shown that embryos express many receptors for the ligands present in the maternal tract and those synthesised by the embryo itself.

The regulation of embryonic development during fertilisation and implantation is crucial for mammalian reproduction. Cell death occurs during preimplantation embryogenesis. Apoptosis may be involved in the embryonic arrest, producing cytoplasmic fragments. Most cells are programmed for apoptosis, with their protein components expressed and associated with inhibitors. Thus, any blockage of inhibitor synthesis will induce apoptosis. Gene expression will trigger depending on external factors, to either promote or inhibit cell death (Vinatier, Dufour, & Subtil, 1996). Deveraux et al. (1999) discovered a protein family of apoptosis inhibitor proteins (IAPs) which plays an important role in the inhibition of cell signalling apoptosis. X-linked IAP (XIAP) contains amino terminal baculoviral inhibitor of apoptosis repeat (BIR) domains and a carboxy terminal RING zinc f nger (Duckett et al., 1996; Listen et al., 1996; Rothe, Pan, Henzel, Ayres, & Goeddel, 1995; Uren, Pakusch, Hawkins, Puls, & Vaux, 1996) which leads to cell death suppression when induced by various apoptotic stimuli including TNF, Fas, growth factor/serum withdrawal, chemotherapeutic agents (etoposide, actinomycin D, taxol), menadione, and UV radiation (Ambrosini, Adida, & Altieri, 1997; Duckett et al., 1996; Li et al., 1998; Listen et al., 1996). Thus, XIAP appeared to be the most potent inhibitor

of caspases, a property that is most evident with its second BIR domain (BIR 2) (Takahashi et al., 1998). It can act as an inhibitor of apoptosis in a variety of systems.

The mammalian target of rapamycin (mTOR) integrates many cellular signals that coordinate cell growth and division in response to growth factors, nutrients and energy status of cell (Bozulic & Hemmings, 2009). mTOR is implicated in various human diseases such as cancer, diabetes and cardiovascular disease (Goberdhan & Boyd, 2009; Sabatini, 2006; Strimpakos, Karapanagiotou, Saif, & Syrigos, 2009). The predetermined coordinated cell growth is greatly inf uenced by mTOR downstream effector such as S6 kinase 1 (S6K1), as reported previously in studies in mice (Um et al., 2006). The ability of mTOR to phosphorylate and activate S6K1 depends on three associated protein type: (1) rapamycin-sensitive adaptor protein of mTOR (raptor); (2) the G protein -subunit-like protein (G L); and (3) the proline-rich protein kinase B substrate 40 kDa (PRAS40). S6K1 is an important factor as a downstream effector of mTORC1 in several cellular processes, including transcription, translation, autophagy, insulin resistance and tumorigenesis in regulating cell growth, metabolism and the oncogenic phenotype (Wullschleger, Loewith, & Hall, 2006).

These are the key factors for embryonic development and differentiation into the respective stages of preimplantation embryo. Reductions of these proteins could lead to serious consequences in early embryogenesis. Consequences such as decreased proliferation and survival of the embryos depend on protein-protein intracellular interaction. Although the effect of vitrif cation in oocytes and embryos has been reported (Chaves et al., 2017; Lavara, Baselga, Marco-Jiménez, & Vicente, 2015; Shirazi et al., 2016; Zhou et al., 2016), it remains unknown how cryopreservation modulates the expression of XIAP and S6K1proteins, which play signif cant roles in the preimplantation development.

MATERIALS AND METHOD

Animal Treatment

All procedures on the animals were approved by UiTM Animal Care & Use Committee (Approval code ACUC- 7/11). Female ICR mice (8 to 10-weeks old), of 35-40 g were used as embryo donors. The mice were housed in polyurethane cages at $22 \pm 2°C$, in a controlled light environment (12 hours light, 12 hours darkness) at Laboratory Animal Care Unit (LACU), Faculty of Medicine, UiTM and provided with water and standard rodents chow pellets *ad libitum*. For superovulation, the female mice were given 10 IU of pregnant mare serum gonadotrophin (PMSG), followed by 10 IU human chorionic gonadotropin (hCG) intraperitoneally, 48 hours apart. Females were then cohabited with fertile ICR males at a ratio of 1:1. Plugged embryo donors were euthanised at 23-25 hours post-HCG, by cervical dislocation, for the collection of embryos. Fallopian tubes were excised and embryos were f ushed using M2 medium, under a dissecting microscope (Leica Zoom 2000, Japan). Two pronuclear-stage (2PN) embryos were cultured at 37°C with 5% CO_2 in a humidif ed incubator until they developed into blastocysts.

Mohd Fazirul, M., Sharaniza, A. R., Norhazlin, J. M. Y., Wan Haf zah, W. J., Razif, D., Froemming, G. R. A.,
Agarwal A., Mastura, A. M. and Nor Ashikin, M. N. K.

Vitrif cation Protocol

Blastocysts were collected and transferred to M2 medium supplemented with 5mg/ml bovine serum albumin (BSA) and kept at room temperature. The straw for vitrif cation was loaded with 30 µL of EFS40 solution. A total of 10 blastocysts were aspirated into the straws, with a minimal volume of M2 medium. The straws were then sealed and their contents left to equilibrate for one minute. The straws were then placed on liquid nitrogen vapour (-180°C) for f ve minutes before being immersed into liquid nitrogen.

Warming Protocol

Blastocyst were warmed by holding straws on air at 22 ± 2°C for 10 seconds, followed by placing them in a water bath at 37°C for 20 seconds. Straw contents were then expelled into 0.5 M sucrose, and left there for two minutes. The blastocysts were then washed with M2 medium for two minutes followed by morphological evaluation. Blastocysts of excellent, good, and fair quality were considered to have survived. The surviving blastocysts were then transferred to KSOM medium before being subjected to western blot.

Protein Extraction and Western Blot

Pooled blastocysts were lysed using the Mammalian Protein Extraction Reagent (M-PER) (Thermo Fisher Scientif c, USA). A total of 100 µL of M-PER Reagent was added into 0.5 ml microcentrifuge tubes. One microlitre of Halt Protease Inhibitor Cocktail, EDTA free (Catalogue no: 87785, Thermo Fisher Scientif c, USA) was added to per 100 µL of lysis buffer. The blastocyst was then gently mixed for f ve minutes and centrifuged at 4°C with 17,000 rpm for 10 minutes. The pellet was discarded and the supernatant was collected and stored at -80°C until further use. Protein concentration was measured using Nanodrop ND-1000 (Thermo Fisher Scientif c, USA) followed by Bradford Assay Kit (Bio-Rad Laboratories, Hercules, California) for validation of protein concentration measurement. Protein samples (25 µg) were resolved by sodium dodecyl sulfate 12.5% gradient gel electrophoresis and then transferred to nitrocellulose membranes by electrophoretic blotting (Thermo Scientif c Pierce, USA). Blots were then incubated with the primary antibodies at 4°C overnight. After washing, membranes were incubated for two hours with anti-mouse or anti-rabbit horseradish peroxidase-conjugated IgG (1:1000). Immunoreactivity was detected using an enhanced SuperSignal West Pico Chemiluminescence reaction (Thermo Scientif c, Pierce, USA). Densitometric analysis employed Thermo Scientif c myImage Analysis Software (Thermo Scientif c, Pierce, USA). The following primary antibodies (Abcam, England) and dilutions were used: anti-S6K1 (ab32529, 1:100), anti-XIAP (ab28151, 1:100), and anti-b-actin (1:10000 dilution; Sigma–Aldrich).

Statistical Analysis

Data were analysed using the SPSS package programme (SPSS V. 19.0). Statistical analysis was performed using one-way ANOVA and paired sample t-test. A p value of <0.05 was considered statistically signif cant.

RESULTS AND DISCUSSION

Non-Vitrif ed Blastocyst

To investigate whether XIAP and S6K1 protein were expressed in blastocysts, western blot was performed on lysate protein of non-vitrif ed blastocysts. The results showed that XIAP and S6K1 protein were expressed in non-vitrif ed blastocyst, where the expression of XIAP proteins were signif cantly (P<0.05) higher than the S6K1 proteins (Figure 1).

Regulation of apoptosis played an important role at the blastocyst stage, since this is the last stage of preimplantation embryos where differentiation occurs. XIAP plays an important role in regulating this pathway as an inhibitor molecule. This was shown previously in which cells transfected with XIAP blocked programmed cell death in response to a variety of apoptotic stimuli (Duckett et al., 1996, 1998; Xu et al., 1999). In addition, recombinant XIAP was also demonstrated to specif cally block the activity of caspases 3, 7, and 9 (Datta et al., 2000; Deveraux et al., 1998). A study by Wu, Panakanti, Li and Mahato (2010) showed that increase of XIAP expression in INS-1E cells and human islets led to decrease in the activities of caspase proteins, hence reducing apoptotic cell death.

S6K1 protein is an important downstream target of mTOR and PI3K pathways in the regulation of cell growth. They ubiquitously express serine/threonine protein kinase which phosphorylates the 40S ribosomal protein S6 in response to mitogen stimulation (Dufner & Thomas, 1999). It was clearly identif ed that S6K1 is activated through mTOR phosphorylation on S6K1 at Thr389, a residue whose phosphorylation is rapamycin sensitive *in vivo* (Abraham & Wiederrecht, 1996; Brown et al., 1995; Burnett, Barrow, Cohen, Snyder, & Sabatini, 1998).

The presence of XIAP in non-vitrif ed blastocysts in this study (Figure 1) indicated inhibition of apoptosis during preimplantation embryonic development, via internal signaling PI3K pathway. The expression of S6K1 protein at the blastocyst stage is expected as the protein plays an important role in regulating cell cycle and development.
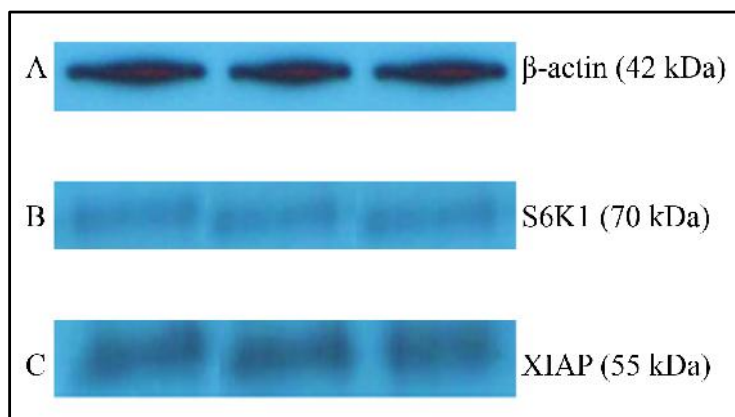
Figure 1. The expression of embryonic proteins of S6K1 and XIAP in non-vitrif ed blastocysts. Western blots analysis (triplicate) show expression of: (A) Positive control -actin (42 kDa); (B) S6K1 (70 kDa); and (C) XIAP (55 kDa)
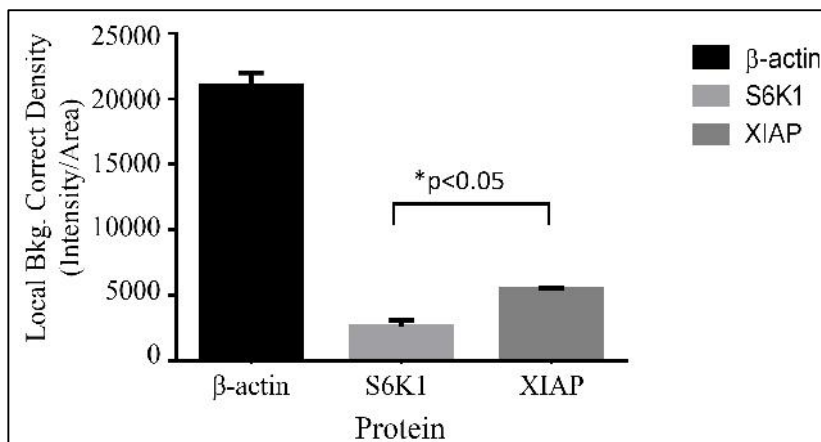
Vitrif ed Blastocysts

Western blot was also performed on lysate protein of vitrif ed blastocysts. The expression of S6K1 and XIAP proteins in vitrif ed blastocyst was similar to patterns in non-vitrif ed blastocysts (Figure 2). The expression level of XIAP was higher than S6K1. This was further conf rmed by quantif cation of band intensity using image analysis, which showed that the expression of XIAP was signif cantly (P<0.05) higher than S6K1 (Figure 3). This shows that the expression of S6K1 is affected in vitrif cation, and therefore, may impair cell cycle progression of vitrif ed embryos. The interruption of cell cycle in vitrif ed blastocysts could have a negative impact on the development of the embryos. This is supported by a previous study, which showed that germline disruption of mTOR in mice caused embryonic lethality at or around implantation (Gangloff et al., 2004; Murakami et al., 2004).
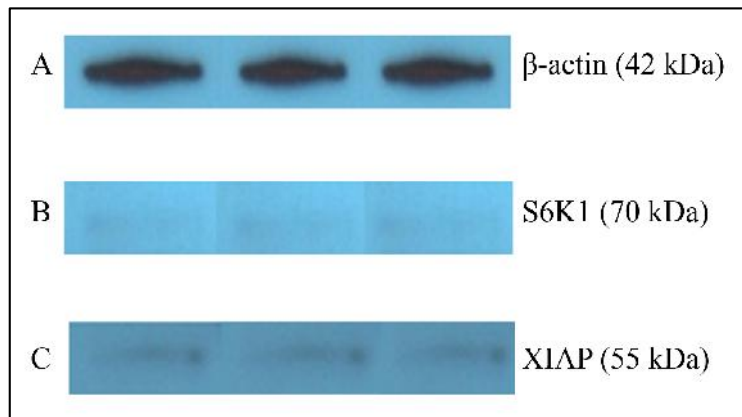
Figure 2. The expression of embryonic proteins of S6K1 and XIAP in vitrif ed blastocysts. Western blots analysis (triplicate) show expression of: (A) Positive control -actin (42 kDa); (B) S6K1 (70 kDa); and (C) XIAP (55 kDa)

Figure 3. Protein quantif cations for the expression of -actin, S6K1 and XIAP proteins in vitrif ed blastocysts. The results represent the mean ± S.E.M. for three replicates. Bars indicate signif cant differences (one-way ANOVA, P < 0.05).

In addition, a comparison of the proteins expressed was made between non-vitrif ed and vitrif ed blastocyst and the data was analysed using paired t-test. From the statistical analysis, the expression of both XIAP and S6K1 was signif cantly higher in non-vitrif ed, compared to vitrif ed blastocysts (Figure 4). The presence of S6K1 protein in preimplantation embryos at blastocyst stages in both non-vitrif ed and vitrif ed blastocysts has been demonstrated in this study. However, the expressions of these proteins are signif cantly lower in vitrif ed embryos (Figure 4). A previous study on S6K1 knockout mice resulted in reduced size and developmental delay (Shima et al., 1998). On the other hand, S6K1 overexpression induces larger cell size (Fingar et al., 2002), and skeletal muscle cell hypertrophy (Marabita et al., 2016; Rommel et al., 2001). These studies clearly indicate the involvement of S6K1 in cellular development. In addition, Lane, Fernandez, Lamb and Thomas (1993) demonstrated that S6K1 acts as a mediator for the G1/S transition of the cell cycle. Another study showed that S6K1 catalytic activity is high during G0–G1 transition of synchronised mouse 3T3 f broblasts, decreasing as it progressed through the cell cycle G1-M, and is activated again when cells progress from M into G1 (Edelmann, Kühne, Petritsch, & Ballou, 1996). Another study by Xu et al. (2009) showed that S6K1 was active throughout the cell cycle, with higher activity in G2 and M phases. These data suggest the importance of S6K1 in early development. In this study, it shows that the expression of S6K1 is affected in vitrif ed embryos.
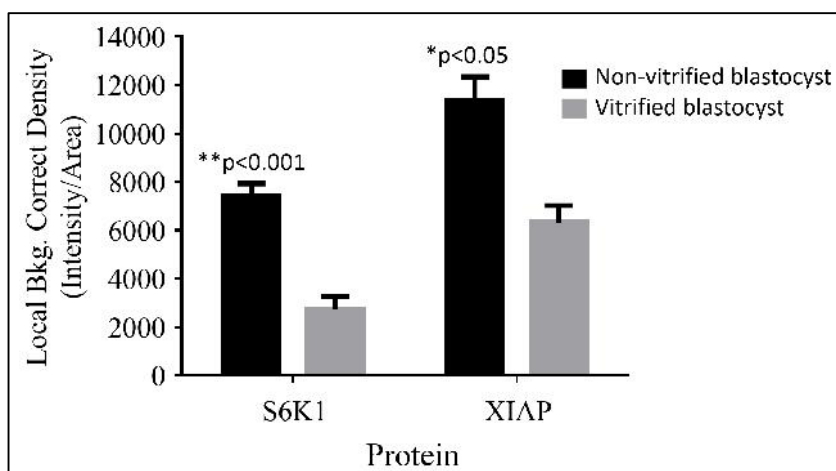
Figure 4. Protein quantif cations for the expression of -actin, S6K1 and XIAP proteins in non-vitrif ed and vitrif ed blastocyst. The results represent the mean ± S.E.M. for three replicates. Bars indicate signif cant differences (paired sample t-test, P < 0.05).

Overall, vitrif ed blastocyst showed a decrease in S6K1 and XIAP protein expressions compared to non-vitrif ed blastocysts. This indicates that vitrif cation negatively affected S6K1 and XIAP proteins in the PI3K pathway. The decrease in protein expression may be the result of embryos responding to signif cant stress and may consequently compromise embryonic development. Vitrif cation-warming procedures often results in cell loss and damage. It is likely that such

damage could result in alterations of autocrine secretion of growth factors and therefore heighten the impact of the post-vitrif cation culture environment.

During vitrif cation, blastocysts undergo considerable stress due to cold shock and osmotic stress (de Oliveira Leme et al., 2016) during the vitrif cation-warming procedure, causing morphological abnormality and functional damage. This is ref ected by the lower expression of S6K1 and XIAP in vitrif ed blastocysts compared to non-vitrif ed blastocysts. Inhibition of the PI3K pathway in blastocysts may have resulted in an increase in blastocyst apoptosis and def ciencies in glucose uptake and metabolism. Further, inhibition of this pathway during this stage may result in a striking increase of pregnancy loss.

CONCLUSION

Data presented in this study showed that vitrif cation of murine blastocysts induced signif cant expression changes in the proteins involved in PI3K signalling pathways.

ACKNOWLEDGEMENTS

REFERENCES

Abraham, R. T., & Wiederrecht, G. J. (1996). Immunopharmacology of Rapamycin. *Annual Review of Immunology, 14*(1), 483–510.

Ambrosini, G., Adida, C., & Altieri, D. C. (1997). A novel anti-apoptosis gene, survivin, expressed in cancer and lymphoma. *Nature Medicine, 3*(8), 917–921.

Bozulic, L., & Hemmings, B. A. (2009). PIKKing on PKB: Regulation of PKB activity by phosphorylation. *Current Opinion in Cell Biology, 21*(2), 256-261.

Brown, E. J., Beal, P. A., Keith, C. T., Chen, J., Shin, T. B., & Schreiber, S. L. (1995). Control of p70 s6 kinase by kinase activity of FRAP *in vivo*. *Nature, 377*(6548), 441-6

Burnett, P. E., Barrow, R. K., Cohen, N. A., Snyder, S. H., & Sabatini, D. M. (1998). RAFT1 phosphorylation of the translational regulators p70 S6 kinase and 4E-BP1. *Proceedings of the National Academy of Sciences, 95*(4), 1432–7.

Chaves, D. F., Corbin, E., Almiñana, C., Locatelli, Y., Souza-Fabjan, J. M., Bhat, M. H., ... & Mermillod, P. (2017). Vitrif cation of immature and *in vitro* matured bovine cumulus-oocyte complexes: Effects on oocyte structure and embryo development. *Livestock Science, 199*, 50-56.

Cutting, R., Morroll, D., Roberts, S. A., Pickering, S., Rutherford, A., & on behalf of the BFS and ACE. (2008). Elective single embryo transfer: Guidelines for practice British Fertility Society and Association of Clinical Embryologists. *Human Fertility, 11*(3), 131–146.

Dardik, A., Smith, R. M., & Schultz, R. M. (1992). Colocalization of transforming growth factor- and a functional epidermal growth factor receptor (EGFR) to the inner cell mass and preferential localization of the EGFR on the basolateral surface of the trophectoderm in the mouse blastocyst. *Developmental Biology, 154*(2), 396–409.

Datta, S. R., Katsov, A., Hu, L., Petros, A., Fesik, S. W., Yaffe, M. B., & Greenberg, M. E. (2000). 14-3-3 proteins and survival kinases cooperate to inactivate BAD by BH3 domain phosphorylation. *Molecular Cell, 6*(1), 41-51.

de Oliveira Leme, L., Dufort, I., Spricigo, J. F. W., Braga, T. F., Sirard, M. A., Franco, M. M., & Dode, M. A. N. (2016). Effect of vitrif cation using the Cryotop method on the gene expression prof le of in vitro–produced bovine embryos. *Theriogenology, 85*(4), 724-733.

Deveraux, Q. L., Leo, E., Stennicke, H. R., Welsh, K., Salvesen, G. S., & Reed, J. C. (1999). Cleavage of human inhibitor of apoptosis protein XIAP results in fragments with distinct specif cities for caspases. *EMBO Journal, 18*(19), 5242–5251.

Deveraux, Q. L., Roy, N., Stennicke, H. R., Van Arsdale, T., Zhou, Q., Srinivasula, S. M., ... & Reed, J. C. (1998). IAPs block apoptotic events induced by caspase-8 and cytochrome c by direct inhibition of distinct caspases. *The EMBO Journal, 17*(8), 2215-2223.

Duckett, C. S., Li, F., Wang, Y., Tomaselli, K. J., Thompson, C. B., & Armstrong, R. C. (1998). Human IAP-like protein regulates programmed cell death downstream of Bcl-xL and cytochrome c. *Molecular and Cellular Biology, 18*(1), 608–615.

Duckett, C. S., Nava, V. E., Gedrich, R. W., Clem, R. J., Van Dongen, J. L., Gilf llan, M. C., ... & Thompson, C. B. (1996). A conserved family of cellular genes related to the baculovirus iap gene and encoding apoptosis inhibitors. *The EMBO Journal, 15*(11), 2685-2694.

Dufner, A., & Thomas, G. (1999). Ribosomal S6 Kinase signaling and the control of translation. *Experimental Cell Research, 253*, 100–109.

Edelmann, H. M. L., Kühne, C., Petritsch, C., & Ballou, L. M. (1996). Cell cycle regulation of p70 S6 kinase and p42/p44 mitogen-activated protein kinases in Swiss mouse 3T3 f broblasts. *Journal of Biological Chemistry, 271*(2), 963–971.

Fahy, G. M., MacFarlane, D. R., Angell, C. A., & Meryman, H. T. (1984). Vitrif cation as an approach to cryopreservation. *Cryobiology, 21*(4), 407–426.

Fingar, D. C., Salama, S., Tsou, C., Harlow, E., & Blenis, J. (2002). Mammalian cell size is controlled by mTOR and its downstream targets S6K1 and 4EBP1/eIF4E. *Genes and Development, 16*(12), 1472–1487.

Gangloff, Y. G., Mueller, M., Dann, S. G., Svoboda, P., Sticker, M., Spetz, J. F., ... & Kozma, S. C. (2004). Disruption of the mouse mTOR gene leads to early postimplantation lethality and prohibits embryonic stem cell development. *Molecular and Cellular Biology, 24*(21), 9508-9516.

Goberdhan, D. C. I., & Boyd, C. A. (2009). mTOR: Dissecting regulation and mechanism of action to understand human disease. *Biochemical Society Transactions, 37*(1), 213–216.

Lane, H. A., Fernandez, A., Lamb, N. J., & Thomas, G. (1993). p70s6k function is essential for G1 progression. *Nature, 363*(6425), 170–172.

Lavara, R., Baselga, M., Marco-Jiménez, F., & Vicente, J. S. (2015). Embryo vitrif cation in rabbits: Consequences for progeny growth. *Theriogenology, 84*(5), 674–680.

Li, F., Ambrosini, G., Chu, E. Y., Plescia, J., Tognin, S., Marchisio, P. C., & Altieri, D. C. (1998). Control of apoptosis and mitotic spindle checkpoint by survivin. *Nature, 396*(6711), 580-584.

Listen, P., Roy, N., Tamai, K., Lefebvre, C., Baird, S., Cherton-Horvat, G., ... & Korneluk, R. G. (1996). Suppression of apoptosis in mammalian cells by NAIP and a related family of IAP genes. *Nature, 379*(6563), 349-353.

Marabita, M., Baraldo, M., Solagna, F., Ceelen, J. J. M., Sartori, R., Nolte, H., ... & Blaauw, B. (2016). S6K1 is required for increasing skeletal muscle force during hypertrophy. *Cell Reports, 17*(2), 501-513.

Murakami, M., Ichisaka, T., Maeda, M., Oshiro, N., Hara, K., Edenhofer, F., ... & Yamanaka, S. (2004). mTOR is essential for growth and proliferation in early mouse embryos and embryonic stem cells. *Molecular and Cellular Biology, 24*(15), 6710-6718.

Raff, M. C. (1992). Social controls on cell survival and cell death. *Nature, 356*(6368), 397–400.

Rienzi, L., Gracia, C., Maggiulli, R., LaBarbera, A. R., Kaser, D. J., Ubaldi, F. M., ... & Racowsky, C. (2017). Oocyte, embryo and blastocyst cryopreservation in ART: systematic review and meta-analysis comparing slow-freezing versus vitrif cation to produce evidence for the development of global guidance. *Human Reproduction Update, 23*(2), 139-155.

Rommel, C., Bodine, S. C., Clarke, B. A., Rossman, R., Nunez, L., Stitt, T. N., ... & Glass, D. J. (2001). Mediation of IGF-1-induced skeletal myotube hypertrophy by PI (3) K/Akt/mTOR and PI (3) K/Akt/GSK3 pathways. *Nature Cell Biology, 3*(11), 1009-1013.

Rothe, M., Pan, M. G., Henzel, W. J., Ayres, T. M., & Goeddel, D. V. (1995). The TNFR2-TRAF signaling complex contains two novel proteins related to baculoviral inhibitor of apoptosis proteins. *Cell, 83*(7), 1243–1252.

Sabatini, D. M. (2006). mTOR and cancer: insights into a complex relationship. *Nature Reviews Cancer, 6*(9), 729–734.

Shima, H., Pende, M., Chen, Y., Fumagalli, S., Thomas, G., & Kozma, S. C. (1998). Disruption of the p70(s6k)/p85(s6k) gene reveals a small mouse phenotype and a new functional S6 kinase. *The EMBO Journal, 17*(22), 6649–59.

Shirazi, A., Naderi, M. M., Hassanpour, H., Heidari, M., Borjian, S., Sarvari, A., & Akhondi, M. M. (2016). The effect of ovine oocyte vitrif cation on expression of subset of genes involved in epigenetic modif cations during oocyte maturation and early embryo development. *Theriogenology, 86*(9), 2136-2146.

Strimpakos, A. S., Karapanagiotou, E. M., Saif, M. W., & Syrigos, K. N. (2009). The role of mTOR in the management of solid tumors: An overview. *Cancer Treatment Reviews*.

Sunde, A. (2007). Signif cant reduction of twins with single embryo transfer in IVF. *Reproductive BioMedicine Online, 15*, 28–34.

Takahashi, R., Deveraux, Q., Tamm, I., Welsh, K., Assa-Munt, N., Salvesen, G. S., & Reed, J. C. (1998). A single BIR domain of XIAP suff cient for inhibiting caspases. *Journal of Biological Chemistry, 273*(14), 7787-7790.

Um, S. H., D'Alessio, D., & Thomas, G. (2006). Nutrient overload, insulin resistance, and ribosomal protein S6 kinase 1, S6K1. *Cell Metab, 3*(6), 393-402.

Uren, A. G., Pakusch, M., Hawkins, C. J., Puls, K. L., & Vaux, D. L. (1996). Cloning and expression of apoptosis inhibitory protein homologs that function to inhibit apoptosis and/or bind tumor necrosis factor receptor-associated factors. *Proc Natl Acad Sci U S A, 93*(10), 4974–4978.

Vajta, G., Nagy, Z. P., Cobo, A., Conceicao, J., & Yovich, J. (2009). Vitrif cation in assisted reproduction: Myths, mistakes, disbeliefs and confusion. *Reproductive BioMedicine Online, 19*, (Suppl:3), 1–7.

Vinatier, D., Dufour, P., & Subtil, D. (1996). Apoptosis: A programmed cell death involved in ovarian and uterine physiology. *European Journal of Obstetrics Gynecology and Reproductive Biology, 67*, 85-102.

Weil, M., Jacobson, M. D., Coles, H. S. R., Davies, T. J., Gardner, R. L., Raff, K. D., & Raff, M. C. (1996). Constitutive expression of the machinery for programmed cell death. *The Journal of Cell Biology, 133*(5), 1053-1059.

Wu, H., Panakanti, R., Li, F., & Mahato, R. I. (2010). XIAP gene expression protects -cells and human islets from apoptotic cell death. *Molecular Pharmaceutics, 7*(5), 1655–66.

Wullschleger, S., Loewith, R., & Hall, M. N. (2006). TOR signaling in growth and metabolism. *Cell, 124*(3), 471–484.

Xu, D., Bureau, Y., McIntyre, D. C., Nicholson, D. W., Liston, P., Zhu, Y., ... & Robertson, G. S. (1999). Attenuation of ischemia-induced cellular and behavioral def cits by X chromosome-linked inhibitor of apoptosis protein overexpression in the rat hippocampus. *Journal of Neuroscience, 19*(12), 5026-5033.

Xu, X. Y., Zhang, Z., Su, W. H., Zhang, Y., Yu, Y. Q., Li, Y. X., ... & Yu, B. Z. (2009). Characterization of p70 S6 kinase 1 in early development of mouse embryos. *Developmental Dynamics, 238*(12), 3025-3034.

Zhou, G., Zeng, Y., Guo, J., Meng, Q., Meng, Q., Jia, G., ... & Zhu, S. E. (2016). Vitrif cation transiently alters Oct-4, Bcl2 and P53 expression in mouse morulae but does not affect embryo development in vitro. *Cryobiology, 73*(2), 120-125.

Mechanical Properties Study on Different Types of Kenaf PVC Wall Panel Product

Zuraidah Salleh[1]*, Nik Rozlin Nik Masdek[1], Koay Mei Hyie[2] and Syarifah Yunus[1]

[1]*Faculty of Mechanical Engineering, Universiti Teknologi MARA (UiTM), 40450 Shah Alam, Selangor, Malaysia*
[2]*Faculty of Mechanical Engineering, Universiti Teknologi MARA (UiTM) Pulau Pinang, 13500 Permatang Pauh, Pulau Pinang, Malaysia*

ABSTRACT

Kenaf f bre is one of the natural f bers that has received much attention of many researchers because of its good properties and f exible use. Kenaf f bre composites have been proposed as interior building materials. In this study, the recycling effect on the kenaf PVC wall panel is focused. The main objective of this study is to determine the mechanical properties of different types of kenaf PVC wall panels. The samples were formulated based on the f rst and third recycling process. The specimens were subjected to several types of tests, namely, tensile, izod impact, f exural and hardness based on ASTM D3039, ASTM D256, ASTM D7264 and ASTM D785, respectively. The results indicate that the mechanical properties of the third recycled kenaf PVC wall panel product is better than the virgin and f rst recycled specimen. This shows that the recycling process enhances the mechanical properties of the product. On the other hand, the hardness of the specimen decreases after f rst recycling due to the reheating effect.

Keywords: Kenaf f ber, kenaf PVC wall panel, mechanical properties, recycling

INTRODUCTION

The demand for using natural resources in engineering products in the building structure has increased in recent years due to global environmental issues. Natural resources such as natural f bre composites used in engineering application are hence, encouraged as these are environmental friendly and can provide good properties compared to synthetic f bres. The natural f bre composite offers tailorable durability, good fatigue performance and is of low cost (Humpreys, 2003). It also has

high specif c strength and specif c stiffness but is much cheaper than glass f bre (Bledzki & Gassan, 1999; Salleh et al., 2014). Moreover, natural f bre has low density, availability and biodegradability which makes natural f bre favourable as reinforcing material for composite products (Nishino, Hirao, Kotera, Nakamae, & Inagi, 2003).

The potential of natural f bre such as kenaf has attracted many researchers. The exploitation of kenaf f bre for building material has been extremely widespread due to its ability to grow faster than any other natural f ber. The kenaf tree can grow in only three months (after sowing). It is also able to grow under a wide range of weather conditions, to a height of more than 3 m and a base diameter of 3 to 5 cm (Aziz, Ansell, Clarke, & Panteny, 2005). The growing speed of kenaf may reach up to 10 cm/day under optimum ambient conditions (Nishino, 2004). Thus, it can be harvested and be used regularly for many applications. The kenaf tree has three types of f bres showing its versatility in engineering application. The type of f bre strongly inf uences the tensile properties of a composite (Salleh et al., 2012). Kenaf is scientif cally known as *Hibiscus cannabinus*, has 65.7% cellulose and 15.7% lignin. Fibre reinforced composite as a building material has been widely applied for a long time. The applications include compound curved roofs (Hollaway, 2002), pedestrian and vehicle bridges, bridge decks (Federal Hyway Administration, 2002), energy absorbing roadside guardrails (Bank & Gentry, 2000), modular rooftop cooling towers (Barbero & Ganga Rao, 1991), access platforms for industrial, chemical and offshore (Hale, 1997), electricity transmission towers, power poles and marine structures such as seawalls and fenders (Nishino et al., 2003).

One of the kenaf f bre composites in building material industry is the Kenaf Plastic Composite (KPC) product. KPC product such as wall panel, decking, fences and skirting are examples of popular building materials. KPC has good properties such as being lightweight, eco-friendly, and has high strength and rigidity. This unique characteristic has made KPC product to be one of the most highly potential building materials.

However, KPC product itself is still a new building material and not much study has been done especially on recycled products. The recyclability of the product itself, although has been considered as an advantage for reducing and wasting natural resources, is yet to be explored. Hence, the study is aimed to focus on the mechanical properties of virgin and recycled kenaf PVC panels.

MATERIALS AND METHODS

Specimen Preparation

The specimen used in this work is kenaf PVC wall panels. The panels can be used as wall panels or ceiling panels (interior design building materials). The panels were obtained directly from the manufacturer, Everise Crimson (M) Sdn. Bhd. which is located in Kelantan, Malaysia. There are three different types of samples used in this research, that is, virgin, f rst recycled and third recycled. Figure 1 shows the kenaf PVC wall panel specimens. The product was made from 40 mesh kenaf powders.
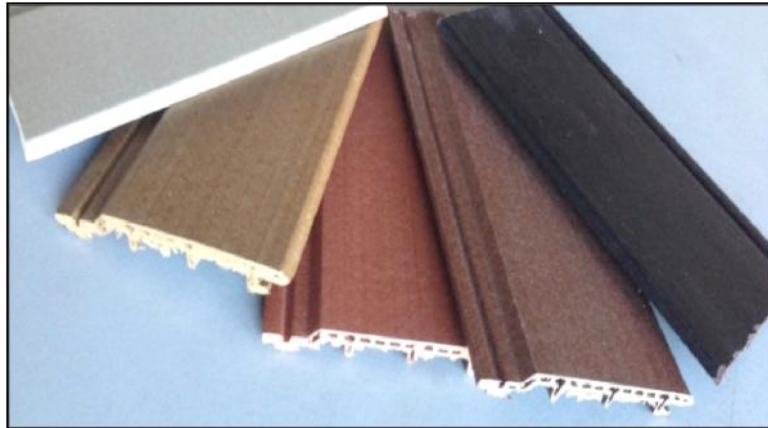
Figure 1. Kenaf PVC wall panel products

The fabrication process of the three different types of samples is as follows:

i.   Virgin - The original product was produced from extrusion molding process.

ii. 1st Recycled - The specimen was made from the excess or unused virgin product. The virgin product was crushed into powders form and was named as the 1st recycled material.

iii. 3rd Recycled - The specimen was made from the 2nd recycling. The 2nd recycled specimen was crushed into powders form and was termed as the 3rd recycled material.

In every recycling process, chemicals designated as LX 551, Chlorinated Polyethylene (CPE), PE Wax and Calcium Zinc were added into the crushed materials.The purpose of adding the chemicals is to maintain the original properties of the product during the extrusion molding process.

Mechanical Testing

The tensile properties of the specimen were tested according to ASTM D3039, using the model 3382 of Uniaxial INSTRON Tensile Machine. The recommended dimension of the specimen according to the ASTM D3039 was 250 mm × 25 mm × 5.5 mm. The specimen was pulled at the speed of 2 mm per minute.

The f exural test was conducted based on three points bending conf guration where the specimen was supported on both ends while the force was applied at the center of the specimen. The test was conducted according to the ASTM D7264. The dimension of the specimen was 88 mm × 13 mm × 5.5 mm. The speed used in the test was 2 mm per minute and the support span size was 48 mm. The testing equipment was the model 3382 of Uniaxial INSTRON Tensile Machine.

Izod impact test was conducted on the sample using India model International Equipment (IE) computerised Izod impact tester, according to the ASTM D256. The recommended dimension according to the standard was 60 mm × 10 mm × 5.5 mm. The notch used for this type of specimen was V-notch. The hardness of the specimen was conducted according to ASTM

D785 using the Rockwell Hardness Test Machine. The hardness of the test was determined by the indention depth of the specimen.

The surface fracture of the specimen after the mechanical properties testing was observed under Hitachi model TM3030Plus SEM machine.

RESULTS AND DISCUSSION

Tensile Properties

Five samples for each type of wall panel products was subjected to tensile test. The data obtained was analysed and the mean value was calculated. The best set of data was selected according to the mean values. The data is summarised in Table 1.

Table 1
The modulus, tensile stress and tensile strain of kenaf PVC panel products

Types of product	Tensile modulus (MPa)	Ultimate tensile strength (MPa)	Ultimate tensile strain (mm/mm)
Virgin	495.08	7.4587	0.0149
1st Recycled	598.75	8.9601	0.0134
3rd Recycled	683.93	10.5973	0.0124

Indeed, the results shown in Table 1 indicate that the recycling process strongly affects the tensile properties of the samples. Tensile modulus lies between 495.08 MPa to 683.93 MPa, which is considered low to be applied in many engineering applications. Hence, the product is currently recommended for interior use only. The modulus of the virgin sample is 495.08 MPa. The modulus increased after 1st recycled product, that is, about 21% compared to the virgin product. The modulus of the 3rd recycled product was recorded as the highest, which is 683.93 MPa, a noticeable increase of about 38% compared to the virgin sample.
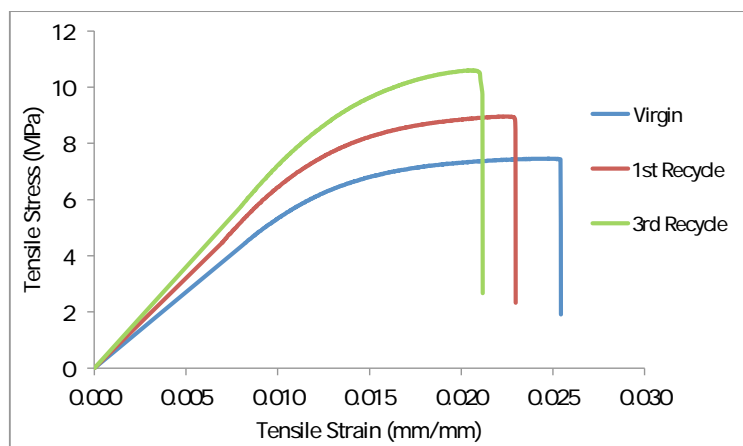
Figure 2. Typical stress-strain curve of kenaf PVC panel products

According to the stress-strain curve as shown in Figure 2, it is clearly seen that the 3rd recycled wall panel yielded a higher tensile strength and modulus but lower ductility as compared to the other samples. However, the ultimate tensile strain of the virgin sample is the highest, which is 0.0149 before failure, indicating better ductility than others. Although the tensile and modulus of the products were improved by the recycling process, the loss of ductility limited the product from its ability to deform further under the load.

Flexural Properties

In the f exural test, f ve specimens from each type of samples were prepared and tested. The best set of data was chosen from the f ve samples according to the mean values as tabulated in Table 2.

Table 2
The modulus, f exure stress and f exure strain of kenaf PVC panel products

Types of product	Modulus (MPa)	At maximum loading	
		Flexure stress (MPa)	Flexure strain (mm/mm)
Virgin	587.28	16.821	0.041
1st Recycled	665.87	21.137	0.044
3rd Recycled	753.00	23.438	0.049

From the data obtained, it is evident that the recycling process changed the f exure properties of the material. At 1st recycling, the modulus obtained shows an increase of about 13.38%, compared to the virgin sample. The modulus increased to 753 MPa for the 3rd recycled specimen, which is 28.22% higher than the virgin sample.
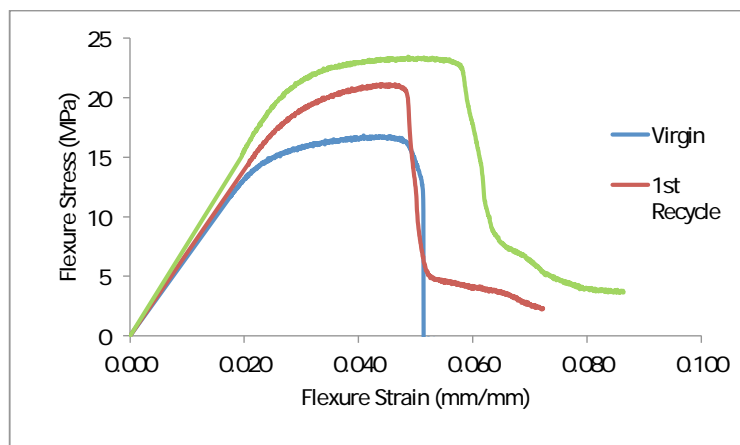
Figure 3. Typical f exure stress-strain curve of kenaf PVC products

In Figure 3, it is clearly revealed that the 3rd recycled specimen exhibited better f exure performance compared to other specimens. It shows that the virgin sample has the lowest yielding. The low f exure strain of the virgin sample indicates the brittle failure phenomenon.

The cellulose content of the kenaf f bre is believed to decrease after each recycling process, thus, it improves the f exure strain of the sample. The diminishing of cellulose in the f bre enhances the f exibility of the kenaf f bre because of plasticization effect (Ghani et al., 2012). The increase in modulus also indicates that the stiffness and rigidity of the product increase was proportionate to the recycling process.

Izod Impact Properties

Izod impact test was conducted at room temperature to obtain the comparative impact energy and impact strength of the kenaf PVC panel products. Five specimens of each type of sample were prepared according to ASTM D256. The weight of the hammer used was 0.452 kg, which produced a maximum impact energy of 0.271 joules. The impact energy absorbed by the material was recorded via the machine data logger. The average impact strength was calculated based on the impact energy per net cross-sectional area of the specimen as summarised in Table 3.

Table 3
Impact energy and the impact strength of kenaf PVC panel products

Type of product	Average Impact energy (J)	Percentage of impact absorbed from R1 hammer (%)	Average impact strength (kJ/m^2)	Changes in impact strength for each type of products compared to virgin (%)
Virgin	0.068	25.09	1.2364 (*SD=0.39)	-
1st Recycled	0.066	24.35	1.2000 (SD=0.10)	-2.94
3rd Recycled	0.106	39.11	1.9273 (SD=0.35)	55.87

*SD = Standard Deviation

According to the data in Table 3, the virgin and 1st recycled products absorbed 25.09% and 24.35% of the impact energy respectively from the hammer prior to fracture. However, the highest impact energy absorbed was obtained by the 3rd recycled product, which was 0.106J, and about 39.11% of energy impacted. This proves that the 3rd recycled sample has the highest impact toughness compared to other samples (Nielsen & Landel, 2003).

Similar results of the impact strength are presented in Table 3. The 3rd recycled sample recorded the highest average impact strength which is more than 55 % as compared to the virgin sample. As for the 1st recycled products, there was a slight drop of about 3 %, compared to the virgin sample.

Hardness

Hardness is def ned as the ability of a material to resist scratching, abrasion or cutting (Bernard et al., 2011). From the result tabulated in Table 4, it is clearly seen that the hardness of the

virgin sample is the lowest among all the specimens. The hardness of virgin sample is recorded as 21.28 RH. On the other hand, the hardest specimen is the 1st recycled product, which shows a reading of 48.80 RH.

Table 4
Hardness of kenaf PVC panel products

Type of product	Hardness value (Average)	Standard deviation
Virgin	21.28	5.185
1st Recycled	48.80	5.006
3rd Recycled	33.18	3.506

Microstructure of Fractured Surface

The SEM micrograph of the fracture surface is shown in Figure 4. A few fracture elements were identified in the SEM micrograph. The fracture elements are fibre matrix debonding, fibre fracture, fibre pull-out and the matrix fracture. The complex nature of the fracture mechanism in composite system is similar as reported in previous findings (Salleh et al., 2014).
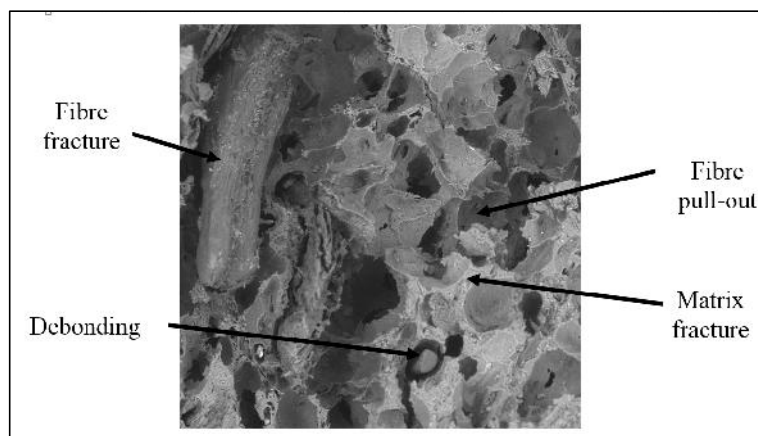
Figure 4. The microstructure of fracture surface of kenaf PVC wall panel product

In fact, the 3rd recycled product showed better properties than the virgin and the previous recycled specimen. This is because the tensile stress, flexure stress, modulus and the impact strength of the specimen was higher (Paul, Jan, & Ignaas, 2001).

CONCLUSION

Based on the results obtained, the recycling process of the kenaf PVC wall panel product modified the mechanical and physical properties of the composite. The tensile properties, impact strength and flexure properties of the samples increased due to the chemical addition during each recycling process. The 3rd recycled product performed better tensile, impact and

f exure properties compared to the virgin and the previous recycled specimens. However, the specimen appeared to be brittle but with a slightly elastic behavior, causing the hardness of the 3rd recycled specimen to decrease. Anyway, the hardness of the 3rd recycled specimen performed better than the virgin product. Furthermore, like all other natural f bre products, the properties of kenaf f bre vary according to the conditions of growth and harvest. The degree of maturity at the time of harvest has a direct effect on the strength of the f bers obtained. It is recommended that the product be manufactured by using long kenaf f bre instead of kenaf powder. The addition of long kenaf f bre in kenaf PVC panel products in future studies will seek signif cant improvement in properties, particularly the impact strength, tensile strength and modulus.

ACKNOWLEDGEMENTS

REFERENCES

Aziz, S. H., Ansell, M. P., Clarke, S. J., & Panteny, S. R. (2005). Modif ed polyester resins for natural f ber composites. *Composite Science Technology, 65*, 525–35.

Bledzki, A. K., & Gassan, J. (1999). Composites reinforced with cellulose base f bres. *Progress in Polymer Science, 24*, 21-274.

Barbero, E., & Ganga Rao, H. V. S. (1991). Structural applications of composites in Infrastructure.

Federal Hyway Administration (2000). *Fibre reinforced polymer composites bridge technology, US Department of Transport Federal Hyway Administration.* Retrieved from http://www.fhwa.dot.gov/bridge/frp/index.htm

Hale, J. M. (1997). Strength reduction of GRP composites exposed to high temperature marine environments, *Proceedings of ICCM11 International Conference on Composite Materials*. Australian Composites Structures Society, Australia.

Hollaway, L. C. (2002). 1.1 The development and the future of advanced polymer composites in the civil infrastructure. In *Advanced polymer composites for structural applications in construction: Proceedings of the f rst international conference, held at Southampton University, UK, on 15–17 April 2002* (pp. 1-21). Thomas Telford Publishing.

Ghani M. A. A., Salleh, Z., Koay, M. H., Berhan, M. N., Taib, Y. M. D., & Bakri, M. A. I. (2012). Mechanical properties of kenaf / f berglass polyster hybrid composite. *Procedia Engineering, 41*, 1654-1659.

Bernard, M., Khalina, A., Ali, A., Janius, R., Faizal, M., Hasnah, K. S., & Sanuddin, A. B. (2011). The effect of processing parameters on the mechanical properties of kenaf f bre plastic composite. *Materials and Design, 32*(2), 1039-1043.

Humpreys, M. F. (2003). The use of polymer composite in construction. Retrieved from http://eprints. qut.edu.au/139/1/Humphreys-polymercomposites.PDF

Nielsen, L. E., & Landel, R. F. (2003). *The mechanical and physical properties of polymers and composites (2nd Edition)*. New York: Marcel Dekker Inc.

Nishino T. (2004). Composites: Polymer composites and the environment, United Kingdom. *Green Composite, 49.*

Nishino T., Hirao K., Kotera M., Nakamae K., & Inagi H. (2003). Kenaf reinforced biodegradable composite. *Composite Science Technology, 63*, 1281–1286.

Salleh, Z., Koay M. H., Berhan, M. N., Taib, Y. M. D., Latip, E. N. A., & Kalam, A. (2014). Residual tensile stress of kenaf polyester and kenaf hybrid under post impact and open hole tensile. P*rocedia Technology, 15*, 856-861.

Salleh, Z., Koay M. H., Berhan, M. N., Talib, Y. M., Hassan, M. K., & Isaac, D. H. (2012). Effect of low impact energy on kenaf composite and kenaf / f breglass hybrid composite material. *Applied Mechanics and Materials, 393,* 228-233.

Pertanika Journals

Our goal is to bring high quality research to the widest possible audience

INSTRUCTIONS TO AUTHORS
(Manuscript Preparation & Submission Guide)

Revised: June 2016

Please read the Pertanika guidelines and follow these instructions carefully. Manuscripts not adhering to the instructions will be returned for revision without review. The Chief Executive Editor reserves the right to return manuscripts that are not prepared in accordance with these guidelines.

MANUSCRIPT PREPARATION

Manuscript Types

Pertanika accepts submission of mainly **four** types of manuscripts for peer-review.

1. **REGULAR ARTICLE**

   Regular articles are full-length original empirical investigations, consisting of introduction, materials and methods, results and discussion, conclusions. Original work must provide references and an explanation on research findings that contain new and significant findings.

   Size: Generally, these are expected to be between 6 and 12 journal pages (excluding the abstract, references, tables and/or figures), a maximum of 80 references, and an abstract of 100–200 words.

2. **REVIEW ARTICLE**

   These report critical evaluation of materials about current research that has already been published by organizing, integrating, and evaluating previously published materials. It summarizes the status of knowledge and outline future directions of research within the journal scope. Review articles should aim to provide systemic overviews, evaluations and interpretations of research in a given field. Re-analyses as meta-analysis and systemic reviews are encouraged. The manuscript title must start with "Review Article:".

   Size: These articles do not have an expected page limit or maximum number of references, should include appropriate figures and/or tables, and an abstract of 100–200 words. Ideally, a review article should be of 7 to 8 printed pages.

3. **SHORT COMMUNICATIONS**

   They are timely, peer-reviewed and brief. These are suitable for the publication of significant technical advances and may be used to:

   (a) report new developments, significant advances and novel aspects of experimental and theoretical methods and techniques which are relevant for scientific investigations within the journal scope;

   (b) report/discuss on significant matters of policy and perspective related to the science of the journal, including 'personal' commentary;

   (c) disseminate information and data on topical events of significant scientific and/or social interest within the scope of the journal.

   The manuscript title must start with "*Brief Communication*:".

   Size: These are usually between 2 and 4 journal pages and have a maximum of three figures and/or tables, from 8 to 20 references, and an abstract length not exceeding 100 words. Information must be in short but complete form and it is not intended to publish preliminary results or to be a reduced version of Regular or Rapid Papers.

4. **Others**

Brief reports, case studies, comments, concept papers, Letters to the Editor, and replies on previously published articles may be considered.

PLEASE NOTE: NO EXCEPTIONS WILL BE MADE FOR PAGE LENGTH.

Language Accuracy

Pertanika **emphasizes** on the linguistic accuracy of every manuscript published. Articles must be in **English** and they must be competently written and argued in clear and concise grammatical English. Contributors are strongly advised to have the manuscript checked by a colleague with ample experience in writing English manuscripts or a competent English language editor.

Author(s) **must provide a certif cate** conf rming that their manuscripts have been adequately edited. A proof from a recognised editing service should be submitted together with the cover letter at the time of submitting a manuscript to Pertanika**. All editing costs must be borne by the author(s)**. This step, taken by authors before submission, will greatly facilitate reviewing, and thus publication if the content is acceptable.

Linguistically hopeless manuscripts will be rejected straightaway (e.g., when the language is so poor that one cannot be sure of what the authors really mean). This process, taken by authors before submission, will greatly facilitate reviewing, and thus publication if the content is acceptable.

MANUSCRIPT FORMAT

The paper should be submitted in one column format with at least 4cm margins and 1.5 line spacing throughout. Authors are advised to use Times New Roman 12-point font and *MS Word* format.

1. *Manuscript Structure*

Manuscripts in general should be organised in the following order:

Page 1: *Running title*

This page should **only** contain the running title of your paper. The running title is an abbreviated title used as the running head on every page of the manuscript. The running title should not exceed 60 characters, counting letters and spaces.

Page 2: *Author(s) and Corresponding author information.*

This page should contain the **full title** of your paper not exceeding 25 words, with name(s) of all the authors, institutions and corresponding author's name, institution and full address (Street address, telephone number (including extension), hand phone number, and e-mail address) for editorial correspondence. First and corresponding authors must be clearly indicated.

The names of the authors may be abbreviated following the international naming convention. e.g. Salleh, A.B.[1], Tan, S.G[2]*., and Sapuan, S.M[3].

Authors' addresses. Multiple authors with different addresses must indicate their respective addresses separately by superscript numbers:

George Swan[1] and Nayan Kanwal[2]

[1]Department of Biology, Faculty of Science, Duke University, Durham, North Carolina, USA.,
[2]Off ce of the Deputy Vice Chancellor (R&I), Universiti Putra Malaysia, Serdang, Malaysia.

A **list** of number of **black and white / colour f gures and tables** should also be indicated on this page**.** Figures submitted in color will be printed in colour. See "*5. Figures & Photographs"* for details.

Page 3: *Abstract*

This page should **repeat** the **full title** of your paper with only the **Abstract** (the abstract should be less than 250 words for a Regular Paper and up to 100 words for a Short Communication), and **Keywords**.

Keywords: Not more than eight keywords in alphabetical order must be provided to describe the contents of the manuscript.

Page 4: *Introduction*

This page should begin with the **Introduction** of your article and followed by the rest of your paper.

2. Text

Regular Papers should be prepared with the headings *Introduction, Materials and Methods, Results and Discussion, Conclusions, Acknowledgements, References, and Supplementary data* (if avavailble) in this order.

| Title |
| Abstract |
| Keywords |
| |
| **(IMRAD)** |
| **I**ntroduction |
| **M**ethods |
| **R**esults |
| **A**nd |
| **D**iscussions |
| |
| Conclusions |
| Acknowledgements |
| References |
| Supplementary data |

MAKE YOUR ARTICLES AS CONCISE AS POSSIBLE

Most scientific papers are prepared according to a format called IMRAD. The term represents the first letters of the words Introduction, Materials and Methods, Results, And, Discussion. It indicates a pattern or format rather than a complete list of headings or components of research papers; the missing parts of a paper are: Title, Authors, Keywords, Abstract, Conclusions, and References. Additionally, some papers include Acknowledgments and Appendices.

The Introduction explains the scope and objective of the study in the light of current knowledge on the subject; the Materials and Methods describes how the study was conducted; the Results section reports what was found in the study; and the Discussion section explains meaning and significance of the results and provides suggestions for future directions of research. The manuscript must be prepared according to the Journal's instructions to authors.

3. Equations and Formulae

These must be set up clearly and should be typed double spaced. Numbers identifying equations should be in square brackets and placed on the right margin of the text.

4. Tables

All tables should be prepared in a form consistent with recent issues of Pertanika and should be numbered consecutively with Roman numerals. Explanatory material should be given in the table legends and footnotes. Each table should be prepared on a new page, embedded in the manuscript.

When a manuscript is submitted for publication, tables must also be submitted separately as data - .doc, .rtf, Excel or PowerPoint f les- because tables submitted as image data cannot be edited for publication and are usually in low-resolution.

5. Figures & Photographs

Submit an **original** f gure or photograph. Line drawings must be clear, with high black and white contrast. Each f gure or photograph should be prepared on a new page, embedded in the manuscript for reviewing to keep the f le of the manuscript under 5 MB. These should be numbered consecutively with Roman numerals.

Figures or photographs must also be submitted separately as TIFF, JPEG, or Excel f les- because f gures or photographs submitted in low-resolution embedded in the manuscript cannot be accepted for publication. For electronic f gures, create your f gures using applications that are capable of preparing high resolution TIFF f les. In general, we require **300 dpi** or higher resolution for **coloured and half-tone artwork**, and **1200 dpi or higher** for **line drawings** are required.

Failure to comply with these specif cations will require new f gures and delay in publication.
NOTE: Illustrations may be produced in colour at no extra cost at the discretion of the Publisher; the author could be charged Malaysian Ringgit 50 for each colour page.

6. References

References begin on their own page and are listed in alphabetical order by the f rst author's last name. Only references cited within the text should be included. All references should be in 12-point font and double-spaced.

NOTE: When formatting your references, please follow the **APA reference style** (6th Edition). Ensure that the references are strictly in the journal's prescribed style, failing which your article will **not be accepted for peer-review**. You may refer to the *Publication Manual of the American Psychological Association* for further details (http://www.apastyle.org/).

7. General Guidelines

Abbreviations: Defne alphabetically, other than abbreviations that can be used without defnition. Words or phrases that are abbreviated in the introduction and following text should be written out in full the frst time that they appear in the text, with each abbreviated form in parenthesis. Include the common name or scientifc name, or both, of animal and plant materials.

Acknowledgements: Individuals and entities that have provided essential support such as research grants and fellowships and other sources of funding should be acknowledged. Contributions that do not involve researching (clerical assistance or personal acknowledgements) should **not** appear in acknowledgements.

Authors' Affliation: The primary affliation for each author should be the institution where the majority of their work was done. If an author has subsequently moved to another institution, the current address may also be stated in the footer.

Co-Authors: The commonly accepted guideline for authorship is that one must have substantially contributed to the development of the paper and share accountability for the results. Researchers should decide who will be an author and what order they will be listed depending upon their order of importance to the study. Other contributions should be cited in the manuscript's Acknowledgements.

Copyright Permissions: Authors should seek necessary permissions for quotations, artwork, boxes or tables taken from other publications or from other freely available sources on the Internet before submission to Pertanika. Acknowledgement must be given to the original source in the illustration legend, in a table footnote, or at the end of the quotation.

Footnotes: Current addresses of authors if different from heading may be inserted here.

Page Numbering: Every page of the manuscript, including the title page, references, tables, etc. should be numbered.

Spelling: The journal uses American or British spelling and authors may follow the latest edition of the Oxford Advanced Learner's Dictionary for British spellings.

SUBMISSION OF MANUSCRIPTS

Owing to the volume of manuscripts we receive, we must insist that all submissions be made electronically using the **online submission system ScholarOne™**, a web-based portal by Thomson Reuters. For more information, go to our web page and click "**Online Submission**".

Submission Checklist

1. **MANUSCRIPT**: Ensure your MS has followed the Pertanika style particularly the frst four pages as explained earlier. The article should be written in a good academic style and provide an accurate and succinct description of the contents ensuring that grammar and spelling errors have been corrected before submission. It should also not exceed the suggested length.

   COVER LETTER: All submissions must be accompanied by a cover letter detailing what you are submitting. Papers are accepted for publication in the journal on the understanding that the article is **original** and the content has **not been published** either **in English** or **any other language(s)** or **submitted for publication elsewhere**. The letter should also briefy describe the research you are reporting, why it is important, and why you think the readers of the journal would be interested in it. The cover letter must also contain an acknowledgement that all authors have contributed signifcantly, and that all authors have approved the paper for release and are in agreement with its content.

   The cover letter of the paper should contain (i) the title; (ii) the full names of the authors; (iii) the addresses of the institutions at which the work was carried out together with (iv) the full postal and email address, plus telephone numbers and emails of all the authors. The current address of any author, if different from that where the work was carried out, should be supplied in a footnote.

   The above must be stated in the cover letter. Submission of your manuscript will not be accepted until a cover letter has been received.

2. **COPYRIGHT**: Authors publishing the Journal will be asked to sign a copyright form. In signing the form, it is assumed that authors have obtained permission to use any copyrighted or previously published material. All authors must read and agree to the conditions outlined in the form, and must sign the form or agree that the corresponding author can sign on their behalf. Articles cannot be published until a signed form *(original pen-to-paper signature)* has been received.

Please do **not** submit manuscripts to the editor-in-chief or to any other off ce directly. Any queries must be directed to the **Chief Executive Editor's** off ce via email to nayan@upm.my.

Visit our Journal's website for more details at [ht p://www.pertanika.upm.edu.my/home.php](http://www.pertanika.upm.edu.my/home.php).

HARDCOPIES OF THE JOURNALS AND OFF PRINTS

Under the Journal's open access initiative, authors can choose to download free material (via PDF link) from any of the journal issues from Pertanika's website. Under "**Browse Journals**" you will see a link, "*Current Issues*" or "*Archives*". Here you will get access to all current and back-issues from 1978 onwards.

The **corresponding author** for all articles will receive one complimentary hardcopy of the journal in which his/her articles is published. In addition, 20 off prints of the full text of their article will also be provided. Additional copies of the journals may be purchased by writing to the Chief Executive Editor.

Why should you publish in *Pertanika?*

BENEFITS TO AUTHORS

PROFILE: Our journals are circulated in large numbers all over Malaysia, and beyond in Southeast Asia. Our circulation covers other overseas countries as well. We ensure that your work reaches the widest possible audience in print and online, through our wide publicity campaigns held frequently, and through our constantly developing electronic initiatives such as Web of Science Author Connect backed by Thomson Reuters.

QUALITY: Our journals' reputation for quality is unsurpassed ensuring that the originality, authority and accuracy of your work are fully recognised. Each manuscript submitted to Pertanika undergoes a rigid originality check. Our double-blind peer refereeing procedures are fair and open, and we aim to help authors develop and improve their scientific work. Pertanika is now over 38 years old; this accumulated knowledge has resulted in our journals being indexed in SCOPUS (Elsevier), **Thomson (ISI) Web of Science™ Core Collection, Emerging Sources Citation Index (ESCI)**, Web of Knowledge [BIOSIS & CAB Abstracts], EBSCO, DOAJ, ERA, AGRICOLA, Google Scholar, ISC, TIB, Journal Guide, Citefactor, Cabell's Directories and MyCite.

AUTHOR SERVICES: We provide a rapid response service to all our authors, with dedicated support staff for each journal, and a point of contact throughout the refereeing and production processes. Our aim is to ensure that the production process is as smooth as possible, is borne out by the high number of authors who prefer to publish with us.

CODE OF ETHICS: Our Journal has adopted a Code of Ethics to ensure that its commitment to integrity is recognized and adhered to by contributors, editors and reviewers. It warns against plagiarism and self-plagiarism, and provides guidelines on authorship, copyright and submission, among others.

PRESS RELEASES: Landmark academic papers that are published in Pertanika journals are converted into press-releases as a unique strategy for increasing visibility of the journal as well as to make major findings accessible to non-specialist readers. These press releases are then featured in the university's UK and Australian based research portal, ResearchSEA, for the perusal of journalists all over the world.

LAG TIME: The elapsed time from submission to publication for the articles averages 3 to 4 months. A decision on acceptance of a manuscript is reached in 3 to 4 months (average 14 weeks).

Address your submissions to:
The Chief Executive Editor
Tel: +603 8947 1622
nayan@upm.my

PERTANIKA
J O U R N A L S

Journal's Profile: www.pertanika.upm.edu.my/

Call for Papers 2017-18
now accepting submissions...

Pertanika invites you to explore frontiers from all key areas of agriculture, science and technology to social sciences and humanities.

Original research and review articles are invited from scholars, scientists, professors, post-docs, and university students who are seeking publishing opportunities for their research papers through the Journal's three titles; JTAS, JST & JSSH. Preference is given to the work on leading and innovative research approaches.

Pertanika is a fast track peer-reviewed and open-access academic journal published by Universiti Putra Malaysia. To date, Pertanika Journals have been indexed by many important databases. Authors may contribute their scientific work by publishing in UPM's hallmark SCOPUS & ISI indexed journals.

Our journals are open access - international journals. Researchers worldwide will have full access to all the articles published online and be able to download them with zero subscription fee.

Pertanika uses online article submission, review and tracking system for quality and quick review processing backed by Thomson Reuter's ScholarOne™. Journals provide rapid publication of research articles through this system.

For details on the Guide to Online Submissions, please visit http://www.pertanika.upm.edu.my/guide_online_submission.php

About the Journal

Pertanika is an international multidisciplinary peer-reviewed leading journal in Malaysia which began publication in 1978. The journal publishes in three different areas — Journal of Tropical Agricultural Science (JTAS); Journal of Science and Technology (JST); and Journal of Social Sciences and Humanities (JSSH). All journals are published in English.

JTAS is devoted to the publication of original papers that serves as a forum for practical approaches to improving quality in issues pertaining to tropical agricultural research- or related fields of study. It is published four times a year in *February, May, August* and *November.*

JST caters for science and engineering research- or related fields of study. It is published twice a year in *January* and *July.*

JSSH deals in research or theories in social sciences and humanities research. It aims to develop as a flagship journal with a focus on emerging issues pertaining to the social and behavioural sciences as well as the humanities, particularly in the Asia Pacific region. It is published four times a year in *March, June, September* and *December.*

An **Award-winning** International-Malaysian Journal — **CREAM AWARD**, MoHE –Sept 2015

Contents

Advances in Science & Technology Research